

AD-A065 267

NAVAL RESEARCH LAB WASHINGTON D C
THE EOMET CRUISE OF THE USNS HAYES: MAY - JUNE 1977.(U)
JAN 79 S G GATHMAN, B G JULIAN

F/G 4/2

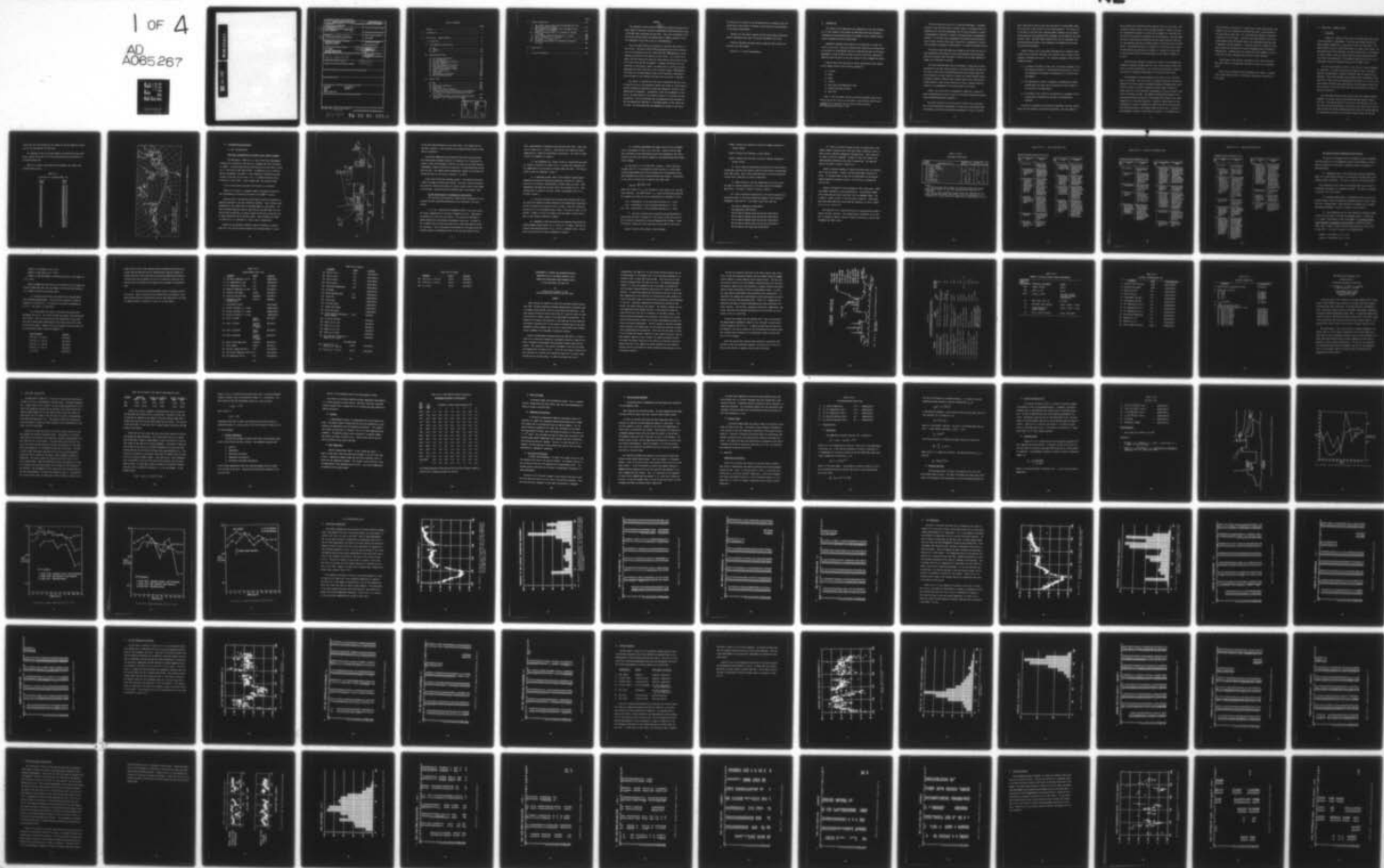
UNCLASSIFIED

NRL-MR-3924

NL

1 OF 4

AD
A065267



DDC FILE COPY

AD A0 65267

SECURITY CLASSIFICATION OF THIS PAGE (When Data Entered)

REPORT DOCUMENTATION PAGE		READ INSTRUCTIONS BEFORE COMPLETING FORM
1. REPORT NUMBER NRL Memorandum Report 3924 ✓	2. GOVT ACCESSION NO.	3. RECIPIENT'S CATALOG NUMBER
4. TITLE (and Subtitle) THE EOMET CRUISE OF THE USNS HAYES: MAY - JUNE 1977 ,		5. TYPE OF REPORT & PERIOD COVERED
7. AUTHOR(s) Stuart G. Gathman and Ben G. Julian, Editors		6. PERFORMING ORG. REPORT NUMBER
9. PERFORMING ORGANIZATION NAME AND ADDRESS Naval Research Laboratory Washington, D.C. 20375		8. CONTRACT OR GRANT NUMBER(s) NOSC 62759N
11. CONTROLLING OFFICE NAME AND ADDRESS Dr. J. Richter Naval Ocean Systems Center San Diego, California 92152		10. PROGRAM ELEMENT, PROJECT, TASK AREA & WORK UNIT NUMBERS NRL Problem A03-14A
14. MONITORING AGENCY NAME & ADDRESS (if different from Controlling Office) NRL-MR-3924		12. REPORT DATE January 31, 1979
		13. NUMBER OF PAGES 320
		15. SECURITY CLASS. (of this report) UNCLASSIFIED
		15a. DECLASSIFICATION/DOWNGRADING SCHEDULE
16. DISTRIBUTION STATEMENT (of this Report) Approved for public release; distribution unlimited.		
17. DISTRIBUTION STATEMENT (of the abstract entered in Block 20, if different from Report)		
18. SUPPLEMENTARY NOTES		
19. KEY WORDS (Continue on reverse side if necessary and identify by block number) Meteorology Air temperature Aerosol Dewpoint Lidar Marine boundary layer		
20. ABSTRACT (Continue on reverse side if necessary and identify by block number)		

DD FORM 1473 1 JAN 73

EDITION OF 1 NOV 65 IS OBSOLETE
S/N 0102-014-6601

SECURITY CLASSIFICATION OF THIS PAGE (When Data Entered)

251 950

79 03 01 058 LB

Table of Contents

	Page
Preface	v
A. Introduction	1
B. Cruise Data: General Results	6
I. Cruise Map	6
II. Instrumentation Description	9
a) NRL	9
b) Calspan	26
c) NPS	34
III. Meteorological Data	52
a) Sea Surface Temperature	52
b) Air Temperature	58
c) Air-Sea Temperature Difference	64
d) Relative Humidity	69
e) Real Wind Speed and Direction	77
f) Turbulence-Friction Velocity	87
g) Stability-Richardson's Number	92
h) Radon Concentration	97
i) Visibility	102
j) Meteorological Soundings	108
K) Sea State Observations	128
IV. Aerosol Data	132
a) CN	134
b) CCN	141
c) Scattering Coefficient	145
d) Royco Data	152
e) Electrical Aerosol Analyzer	172
f) "Particulate Aerosol Size Spectra, as measured by the PMS Axially Scattering Spectrometer Probe". R. K. Jeck	185
g) "Aerosol Measurements for Optical Extinction Pre- dictions". G. L. Trusty & T. H. Cosden.	205

DATE					
TIME					
LOCATION					
NAME					
UNIT					
SECTION					
TYPE					
REMARKS					
SIGNATURE					
DATE					
TIME					
LOCATION					
NAME					
UNIT					
SECTION					
TYPE					
REMARKS					
SIGNATURE					
DATE					
TIME					
LOCATION					
NAME					
UNIT					
SECTION					
TYPE					
REMARKS					
SIGNATURE					
DATE					
TIME					
LOCATION					
NAME					
UNIT					
SECTION					
TYPE					
REMARKS					
SIGNATURE					
DATE					
TIME					
LOCATION					
NAME					
UNIT					
SECTION					
TYPE					
REMARKS					
SIGNATURE					
DATE					
TIME					
LOCATION					
NAME					
UNIT					
SECTION					
TYPE					
REMARKS					
SIGNATURE					
DATE					
TIME					
LOCATION					
NAME					
UNIT					
SECTION					
TYPE					
REMARKS					
SIGNATURE					
DATE					
TIME					
LOCATION					
NAME					
UNIT					
SECTION					
TYPE					
REMARKS					
SIGNATURE					
DATE					
TIME					
LOCATION					
NAME					
UNIT					
SECTION					
TYPE					
REMARKS					
SIGNATURE					
DATE					
TIME					
LOCATION					
NAME					
UNIT					
SECTION					
TYPE					
REMARKS					
SIGNATURE					
DATE					
TIME					
LOCATION					
NAME					
UNIT					
SECTION					
TYPE					
REMARKS					
SIGNATURE					
DATE					
TIME					
LOCATION					
NAME					
UNIT					

	Page
C. Special Experiments	211
I. NRL--Marine Observations with the NRL Mobility Size Spectrometer--W. A. Hoppel	211
II. NRL--Shipboard Measurements with a Portable Transmissometer-- H. E. Gerber	217
III. Raman Scattering Lidar--D. A. Leonard, B. Caputo, S. Gathman	228
IV. Ship Induced Condensation Nuclei--J. N. Hayes	239
V. "Salt Load Data". D. J. Bressan	248
VI. SRI Report. E. Uthe et al	252
VII. "Satellite Observations of Atmospheric Aerosols". M. Griggs	291
D. Data Archive	302
E. Cruise Participants	314

PREFACE

✓
(NRL's)
The Atmospheric Physics Branch of the Ocean Sciences Division, of the Naval Research Laboratory organized and executed a multidisciplined cruise of the USNS Hayes during May and June 1977. The cruise was devoted to observing the electro-optical and meteorological (EOMET) properties of marine atmosphere using state of the art instrumentation.

The aim of this report is to organize in one place the results of this cruise. The data of most of the investigators were sent to the editor to be incorporated into this report and thus it encompasses a fairly complete description of the results of this cruise. In an effort to organize the data archive this data was transferred by various means to the disc files of the NRL PDP-10 computer. Although considerable care was exercised in this process, there is no doubt that in an effort of this magnitude that errors were made in this transfer process. Consequently, the credit for the measurements belong to the individual investigators but the blame for any erroneous data must be on the editor's shoulders.

This report is organized with the view of presenting the data to be of particular use to the atmospheric modeler who wishes to relate electro-optical transmission parameters produced by atmospheric aerosols to the meteorological parameters. Consequently, after the introduction in Section A, the data portion of this report, Section B, is divided into four subsections. The first describes the instrumentations and locations of the instrumentations reported in a continuous manner in this report and its data. The second describes the geographical aspects of the cruise.

The third part is devoted to the key meteorological parameters while the fourth part of the section is devoted to describing the various aspects of the aerosol measurements.

Section C of this report contains various signed papers describing special experiments which were carried out throughout the cruise.

Section D describes the data archive system and what products are available from this system.

Section E is a list of participants.

A. INTRODUCTION

This report is the compilation and condensation of the data obtained on a 21 day research cruise aboard the USNS Hayes which was designed to investigate the relationships which are thought to exist between electro-optical phenomenon and marine meteorology.

Atmospheric boundary layer research on the high seas is always difficult to carry out. There are relatively few alternative platforms which are available to investigators who wish to make measurements on the marine atmosphere in order to have real data on which to base their theoretical deductions and with which to test the results of their mathematical models.

Platforms which have been used to obtain representative data samples can be roughly placed in the following categories:

- a) aircraft
- b) ships
- c) buoys
- d) islands
- e) shore based instrumentation sites
- f) offshore man-made platforms
- g) satellites

Both in situ and remote sensing of the marine boundary layer can be carried out by the first six of the vehicle types whereas satellite measurements are by necessity strictly done by remote sensing.

Note: Manuscript submitted December 14, 1978.

There are pros and cons to all of these platform types. Instrumentation of fixed locations such as islands, buoys, or platforms offer the opportunity for long term measurements but are very inflexible in obtaining geographical variations or physical variations based on geographical location. On the other hand, measurements made aboard moving platforms such as ships, aircraft offer great flexibility in geographical location but the length of endurance of measurements is limited by economic factors.

The cruise of the USNS Hayes was designed to skirt the east coast of the continental United States to obtain representative aerosol measurements and to monitor their evolution in time as the air mass proceeds to change from continental to oceanic.

The cruise obtained EOMET data with extremes in stability not often encountered in the open ocean but which is very much present off shore in the areas of Nova Scotia and Newfoundland where cold coastal waters and warm continental air mass combine to produce very stable boundary layers. A hundred kilometers south and east of these stable areas, the warm Gulf Stream produces a high surface instability on the air masses which have started to be accommodated to cold areas closer to the shore.

Finally, the cruise offers a geographical comparison in which the same instrumentation was used to look for differences between mid-Atlantic Ocean and Mediterranean Sea situations.

The overall mission of this cruise was to obtain from a wide data base various simultaneous measurements of electro-optics parameters made simultaneously with marine meteorology measurements in order to provide

both a data base on which to base the construction of needed EOMET models and a test set of data on which to test existing models. This latter use of the data is such that both a measured EOMET parameter and the simultaneously measured input meteorological parameters are recorded for the same period of time. The EOMET model prediction can then be calculated from the measured meteorological input parameters and compared with the measured predicted parameter.

Several similar sets of data made simultaneously by different investigators using different techniques were routinely taken of many critical parameters throughout the cruise. This apparent redundancy serves several valuable purposes.

- 1) It reduces the number of times that a particular parameter is not being measured because of instrumentation malfunction (a not too rare phenomenon for shipboard instrumentation in a hostile salt environment).
- 2) The observation of several independent instrumentation systems reading nearly the same values simultaneously adds credence to the validity of the measurement.
- 3) It provides a set of data for the detection of systematic errors in particular instrumentation systems or instrumentation locations.

As with all experiments which have been undertaken with many investigators and with automatic data processing machines, the total amount of

data collected and stored during this research cruise is very large. The printing of reams of paper filled with many columns of numbers, each number representing the data of a particular instrument at a particular second of the cruise would be completely out of the question. Not only would the cost of publishing be prohibitive but the results would be difficult for any potential data user to handle because of the great bulk of printed matter. The theoretician who it is hoped will utilize this data in both the construction and testing of his models is in danger of losing sight of the proverbial forest of meaning because of the trees of numbers in his way.

There have been attempts at obtaining a solution to this modern day dilemma of seemingly too much data but in our opinion none of these solutions is entirely satisfactory. Our solution to this problem is based on the access of interested investigators to the data on three levels.

Our philosophy for the presentation of the data for the scientific user is as follows. The first level is a general overview of the best estimates of the various physical parameters measured throughout the cruise which are present in terms of graphical displays found in Section B. These curves will allow individual investigators to select portions of the cruise of interest to them. The graphical presentations however do not give the precision which exists in the original data either in the values themselves or in the time resolution. Therefore a second level of data presentation or access is necessary to enable the data to be utilized to the extent envisioned in the original plans of the cruise. Listings of key parameters are given in the tables of Section B. In addition all of

the cruise data is available on a second level of data access which is designed to give the investigator individualized access to any portions of the data which he might need. This individualized approach is described in Section D of this report. The data in the data archive of the cruise contain hourly values recorded by each of the instruments when they were in apparently working operation. In addition there are a number of files which contain the calculations of certain parameters which are based on measured data. Software exists for putting this data together in any desired order so that customized data sorting is easily achieved.

Finally most of the original investigators have copies of the raw data which they will probably make available to others on an individual basis.

Data files are referred to often throughout this report. The meanings of these names and how to find them are described in Section D of this report.

B. CRUISE DATA: GENERAL RESULTS

I. Cruise Map:

Figure B-I-1 shows the ships track of the USNS Hayes while carrying out the EOMET 77 experiments. The cruise was divided into two non equal segments separated by a 2 day period in port at Rota, Spain. The North Atlantic leg was a slight modification to a great circle route. The modification was a short deviation into Nova Scotian waters in an endeavor to repeat certain of the fog studies that were obtained during the 1975 fog cruise of the USNS Hayes. Unfortunately conditions were such that no appreciable fogs were encountered during the 1977 EOMET cruise.

The cruise was planned to provide a wide variety of marine atmospheric conditions. The ships track lead up the eastern coast of the North American continent where a strongly continental type of aerosol was encountered. Very stable boundary layer conditions were encountered in the waters off of Nova Scotia and Newfoundland during May 18, 19, and 20, 1977. Very unstable conditions were experienced as the ship passed rapidly from the cold waters of the Grand Banks area into the warm waters of the Gulf Stream on 23 May 1977.

One unfortunate feature of the track was that the strongly eastward component of the ships direction paralleled the main westerly winds of this area. Thus during periods of strong real wind conditions, the relative wind direction experienced at the ship was from time to time from the stern and thus the aerosol sampling apparatus located for optimum sampling for normal head winds would give erroneous results unless the ship was

turned into the wind periodically to produce the desired sampling orientation of the ship heading into the wind.

The remainder of the cruise gave samples of mid-Atlantic Ocean conditions, coastal conditions off of the Iberian Peninsula and conditions in the Mediterranean Sea.

Table B-I-1 relates Julian dates used throughout this report with calendar month and day.

TABLE B-I-1

Julian Date vs. Calendar Month, Day

<u>Julian Date</u>	<u>Month Day</u>
134	May 14
135	May 15
136	May 16
137	May 17
138	May 18
139	May 19
140	May 20
141	May 21
142	May 22
143	May 23
144	May 24
145	May 25
146	May 26
147	May 27
148	May 28
149	May 29
150	May 30
151	May 31
152	June 1
153	June 2
154	June 3
155	June 4
156	June 5
157	June 6
158	June 7

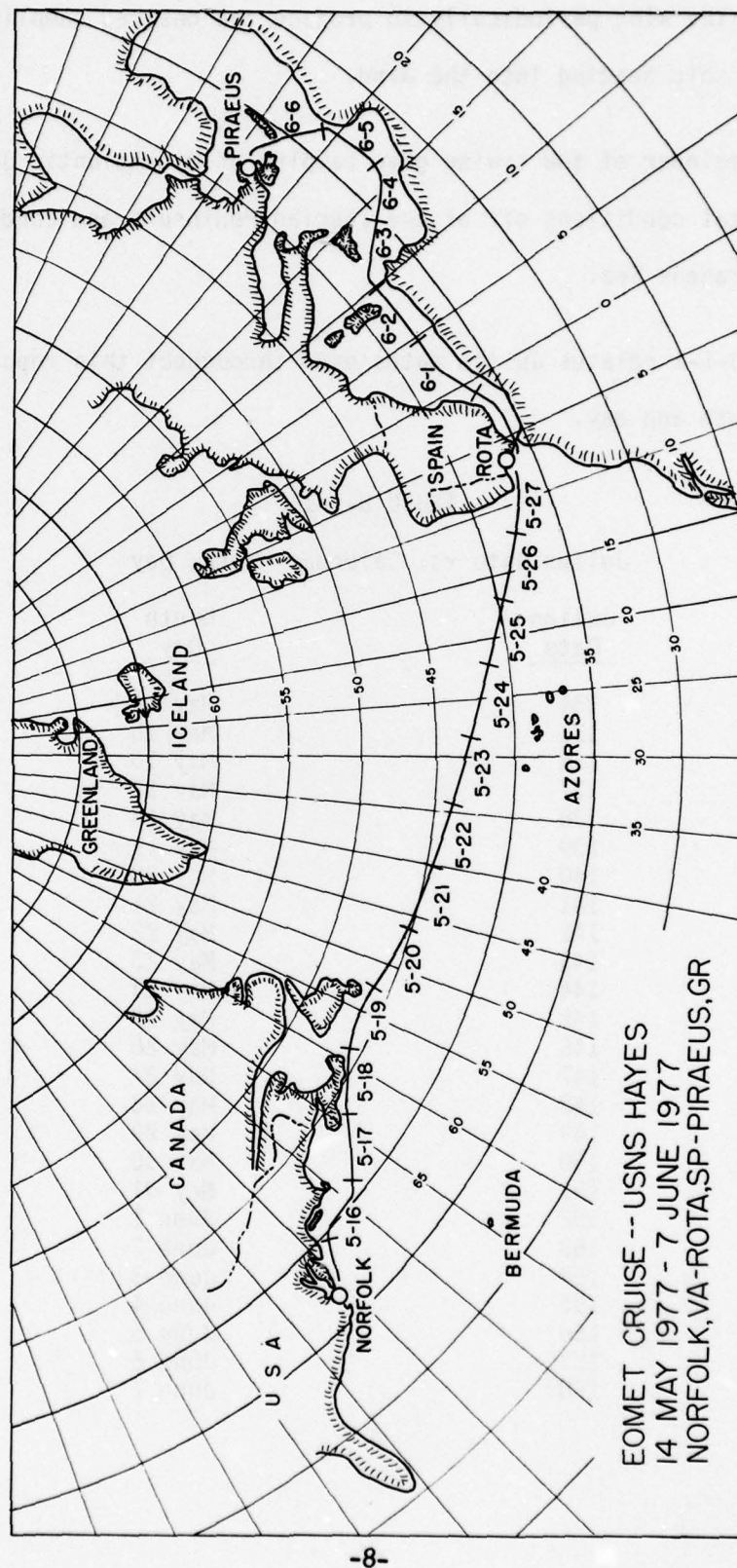


Fig. (B-I-1) Ships track of the 1977 EOMET Cruise.

II. Instrumentation Description

a) NRL Instrumentation

USNS Hayes Instrumentation for EOMET Cruise--General Comments

The USNS Hayes (T-ACOR 16) is a large (3180 tons) oceanographic research ship configured in the form of a catamaran 246 feet (75 meters) in length. A detailed description of the ship and its facilities is given by A. T. McClinton in NRL Report #7370. In addition to its 11 officers and 34 crew members, the EOMET 77 cruise berthed 31 scientists and technicians in two legs of the cruise. Dr. L. H. Ruhnke of NRL was Senior Scientist on board (SSOB). Stuart Gathman, NRL, was Assistant SSOB.

A list of participants and their affiliations is in Section E.

Figure B-II-1 shows in a schematic manner, the general location of the instrumentation installed on the ship for the EOMET 77 cruise.

Care was taken in placing the various sensors which are sensitive to sampling techniques to the most favorable locations. These locations were determined by scale model tests of the USNS Hayes in a wind tunnel. The least disturbed sampling areas for head winds on the USNS Hayes are locations on the forward mast, on towers located on the bows of the ship, and on towers mounted on top of the pilot house. These locations are shown in Figure B-II-1, as locations A, C and D, and B, respectively.

Because of the potential problem of aerosol diffusion to sampling tube walls, the various aerosol analyzers were located either in situ or

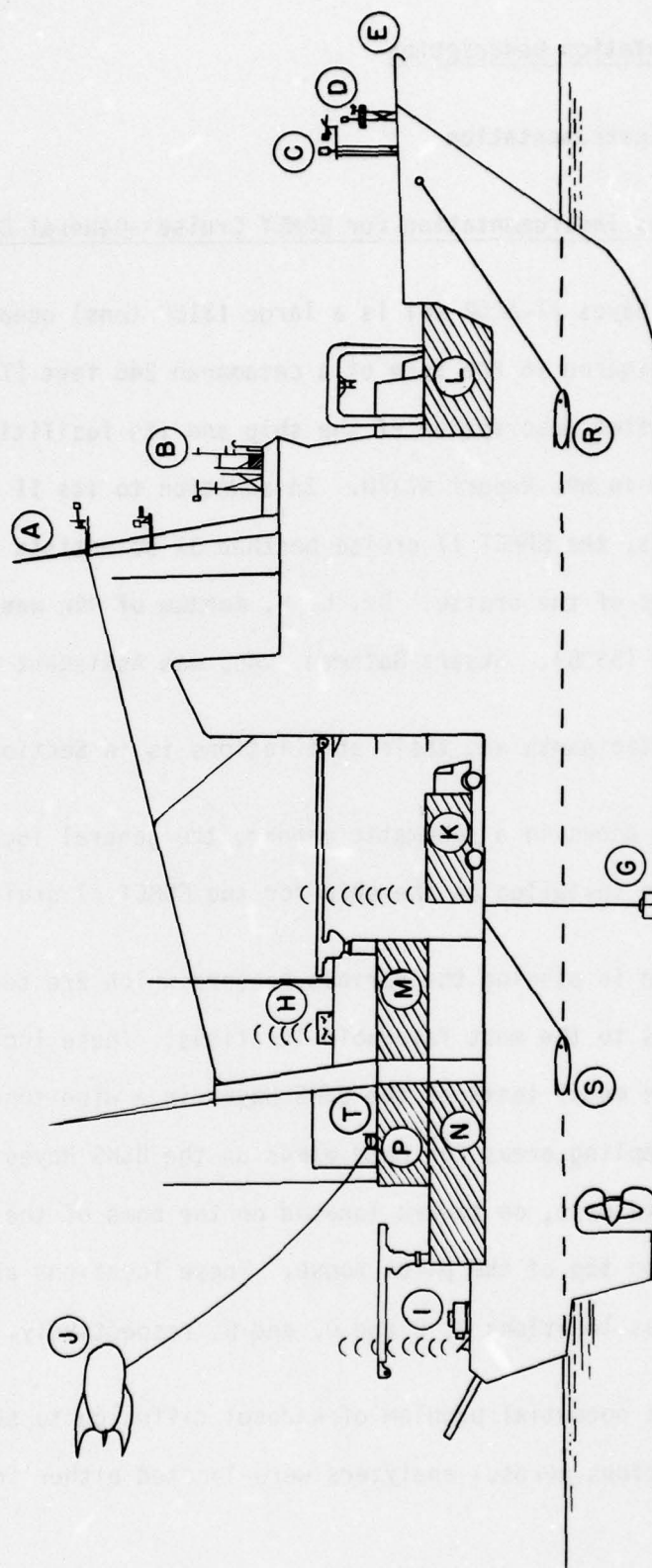


Fig. (B-II-1) Schematic location of sensors and laboratories aboard the USNS HAYES.

on the areas described above or just below deck in the forward part of the ship, location L, with relatively short sampling tubes going to input ports at location E.

Sea surface temperatures were obtained from probes pulled through the surface waters between the hulls at locations R & S, from probes located in a well at the bottom of the hull at location G and from infrared thermometers located at point B but focused at the undisturbed sea surface near the ship. The remote sensing systems were located in the center and towards the stern of the ship at locations I, H, and K.

Finally the kite balloon sounding system, J, was operated from point T where its hangar and winch were located. This device could be operated only when the relative wind vector was within certain limits in both speed and direction. Location M was main recorder room; P was computer room.

The NRL Meteorological Instrumentation Descriptions

This section of the report will describe the instrumentation used to obtain the NRL Code 8320 meteorological data contained in the data archive.

1) A Y.S.I. Scanning Tele-Thermometer model 47 was used to monitor several temperatures at locations throughout the ship. Temperatures are measured to $1/10^{\circ}\text{C}$ with this device. This device was developed to sample sequentially seven matched thermometers every hour. Included in the 7 samples were two fixed resistors used as calibration monitor points for the device. Two of the sensors were mounted on a carriage inside the starboard midship instrumentation well of the ship and lowered to keel

level, approximately 2 centimeters from the water flow lines. Their location in Figure B-II-1 is point G. These devices thus sample sea water temperature at a depth of approximately seven meters. This data is found in data file THERM.DAT in column 2.

2) One thermometer was located inside of a ventilated sun shield on a tower at location B in Figure B-II-1. Its data thus represents the air temperature at an altitude of 19 meters above sea level. This data is found in data file THERM.DAT, column 3.

3) A Cambridge Systems, model 110S-M automatic meteorological temperature and dew point measuring system was installed on a tower at point B at an altitude of approximately 19 meters above sea level. Both temperatures and dewpoints with this device are accurate to 0.1°C. Temperature data is stored in FILE.DAT, column 2 and dewpoint data is in FILE.DAT, column 3.

4) Relative wind speed and directions were obtained with a Bendix type F/60 windspeed indicator mounted on the forward mast (radar mast) giving wind speed to an accuracy of plus or minus 1 knot and a direction accuracy of $\pm 2^\circ$ at wind speeds above 5 knots. This data is found in file ASC.DAT. Column 2 of this file contains the wind speed in knots and column 3 is the relative direction in degrees.

5) Atmospheric radon concentration was obtained from the NRL designed Automatic Radon Counter (R. E. Larson, B. J. Bressan, "ARC for Continental Unattended Operations" R.S.I., 49 (7), p 965-969, July). Hourly data from this device is found in RADON2.DAT, column 2.

6) Turbidity measurements were made with the Voltz sun photometer at wavelengths of 0.88μ , 0.5μ , and 0.94μ . Values of the air mass were calculated at each observational point from knowledge of the ship's position and time using various programs in the Hewlett-Packard-65 navigational package.

Air mass data is in file VOLTZ.DAT, column 2. The air mass has a minimum value of 1.0 for situations in which the sun is at the zenith. Turbidity measurements made with calibrated Voltz sun photometers were made throughout the cruise at three different wave lengths. Calculations of the optical thickness due to aerosols were made using:

$$\tau_{\text{aerosol}} = \frac{1}{m} \ln \frac{I_0}{I} - 0.157$$

where the air mass is m , I_0 the calibration of the device, and I the measured intensity. The other effects, i.e., ozone and Rayleigh scattering, are assumed to be constant and are represented by a thickness of 0.157.

File: Turbid.DAT(2) is the calculated thickness at $\lambda = 0.88\mu$

File: Turbid.DAT(3) is the calculated thickness at $\lambda = 0.5\mu$

and File: Turbid.DAT(4) is the calculated thickness at $\lambda = 0.94\mu$

7) The ship's positions were constantly being pinpointed by a professional scientific navigator Mr. Tony Zuccaro of NRL who relied in part on satellite observations using the Magnavox 706C systems. A data file NAV.DAT relates the ship's positions for each hour of the cruise.

Column 2 contains the latitude in whole degrees.

Column 3 contains the additional fraction of degrees expressed in decimal minutes

Column 4 contains the longitude in whole degrees

Column 5 contains the additional fraction of degrees expressed in decimal minutes

8) Ship's speed and heading were calculated from the scientific navigational log which was based on satellite observations using the Magnavox 706C system. Ship's course made good data is stored in NAV.DAT(6) and the ship's speed data is stored in NAV.DAT(7).

9) Remote sensing of the skin temperature of the sea surface was done by a Barnes Engineering Co. Precision Radiation Thermometer model PRT-5. This data is found in FILE.DAT, column 4.

10) Hourly radiational observations of the marine boundary were obtained by means of the Barnes Engineering Company's Field Radiation Thermometer, model PRT-10. Files which contain this data are:

Sea Surface Temperature--PRT10.DAT(2)

Sky Temperature--PRT10.DAT(3)

PRT-10 aimed 10 degrees below the horizon--PRT10.DAT(4)

PRT-10 aimed 10 degrees above the horizon--PRT10.DAT(5)

PRT-10 aimed 30 degrees above the horizon--PRT10.DAT(6)

PRT-10 aimed 60 degrees above the horizon--PRT10.DAT(7)

PRT-10 aimed at the cloud base--PRT10.DAT(8)

11) There are several subjective types of observations of the general weather conditions which have been coded to numerical values to depict various important atmospheric characteristics. These codes are all found in the file CLOUD.DAT. Column 2 of this file contains the coded seastate conditions at the time of observation. The numerical code of this data is given in Table B-II-1.

Column 3 contains estimates of foam and whitecap cover as a percentage of the sea surface. Column 4 includes approximate visibility in miles. In instances where no haze was distinguishable at the horizon, making subjective estimates difficult, this clarity is assigned the value of 100.

Column 5 corresponds to the percentage to total cloud cover. Again, this number represents a visual approximation. The following columns (6-8) break down the total cloud cover into its component types: low (column 6), middle (column 7) and high clouds (column 8). These types have been coded numerically based upon WMO standards, as seen in Tables B-II-2, B-II-3, and B-II-4.

The CLOUD.DAT file is comprised entirely of eye observations made at regular daylight intervals. This meteorological information can be useful in conveying a general picture of weather conditions as they existed throughout the EOMET cruise.

Table B-II-1
SEASTATE CONDITIONS

Code Figure	Description of sea	Height of waves in feet	Height of waves in meters
00	Calm (glassy) - - - - -	0	0
01	Calm (rippled) - - - - -	0 - 1/3	0 - 0.1
02	Smooth (wavelets) - - - - -	1/3 - 1-2/3	0.1 - 0.5
03	Slight - - - - -	1-2/3 - 4	0.5 - 1.25
04	Moderate - - - - -	4 - 8	1.25 - 2.5
05	Rough - - - - -	8 - 13	2.5 - 4
06	Very rough - - - - -	13 - 20	4 - 6
07	High - - - - -	20 - 30	6 - 9
08	Very high - - - - -	35 - 45	9 - 14
09	Phenomenal - - - - -	Over 45	Over 14

Notes:

(1) The average wave height as obtained from the larger well-formed waves of the wave system being observed is reported.

(2) If an exact boundary height could be reported by two code figures the lower code figure will be reported; e.g., a height of 13 feet would be reported by code figure 5 or 05.

Table B-II-2. Low Cloud-WMO Code

Symbol C_L=Clouds of Genera Sc, St, Cu, Cb

Code Figure	Technical Specifications	Nontechnical Specifications	Code Figure	Technical Specifications	Nontechnical Specifications
0	No C _L clouds-----	No Stratocumulus, Stratus, Cumulus, or Cumulonimbus.	6	Stratus nebulosus or Stratus fractus other than of bad weather, ¹ or both.	Stratus in a more or less continuous sheet or layer, or in ragged shreds, or both, but no Stratus fractus of bad weather. ¹
1	Cumulus humilis or Cumulus fractus other than of bad weather, or both.	Cumulus with little vertical extent and seemingly flattened, or ragged Cumulus other than of bad weather, ¹ or both.	7	Stratus fractus or Cumulus fractus of bad weather, ¹ or both (pannus), usually below Altostratus or Nimbostratus.	Stratus fractus of bad weather ¹ or Cumulus fractus of bad weather, ¹ or both (pannus), usually below Altostratus or Nimbostratus.
2	Cumulus mediocris or congestus, with or without Cumulus of species fractus or humilis, or Stratocumulus, all having their bases at the same level.	Cumulus of moderate or strong vertical extent generally with protuberances in the form of domes or towers, either accompanied or not by other Cumulus or by Stratocumulus; all having their bases at the same level.	8	Cumulus and Stratocumulus other than Stratocumulus cumulogenitus, with bases at different levels.	Cumulus and Stratocumulus other than that formed from the spreading out of Cumulus; the base of the Cumulus is at a different level from that of the Stratocumulus.
3	Cumulonimbus calvus, with or without Cumulus, Stratocumulus or Stratus.	Cumulonimbus, the summits of which, at least partially, lack sharp outlines, but are neither clearly fibrous (cirriform) nor in the form of an anvil; Cumulus, Stratocumulus or Stratus may also be present.	9	Cumulonimbus capillatus (often with an anvil), with or without Cumulonimbus calvus, Cumulus, Stratocumulus, Stratus or pannus.	Cumulonimbus, the upper part of which is clearly fibrous (cirriform), often in the form of an anvil, either accompanied or not by Cumulonimbus without anvil or fibrous upper part, by Cumulus, Stratocumulus, Stratus or pannus
4	Stratocumulus cumulogenitus.	Stratocumulus formed by the spreading out of Cumulus; Cumulus may also be present.			
5	Stratocumulus other than Stratocumulus cumulogenitus.	Stratocumulus not resulting from the spreading out of Cumulus.			

Table B-II-3. Middle Cloud-WMO Code

Symbol C_M =Clouds of Genera Ac, As, Ns

Code Figure	Technical Specifications	Nontechnical Specifications
0	No C_M clouds.....	No Altopcumulus, Altostratus or Nimbostratus.
1	Altostratus translucidus.	Altostratus, the greater part of which is semitransparent; through this part the sun or moon may be weakly visible as through ground glass.
2	Altostratus opacus or Nimbostratus.	Altostratus, the greater part of which is sufficiently dense to hide the sun or moon, or Nimbostratus.
3	Altopcumulus translucidus at a single level.	Altopcumulus, the greater part of which is semitransparent, the various elements of the cloud change only slowly and are all at a single level.
4	Patches (often lenticular) of Altopcumulus translucidus, continually changing and occurring at one or more levels.	Patches (often in the form of almonds or fishes) of Altopcumulus, the greater part of which is semitransparent; the clouds occur at one or more levels and the elements are continually changing in appearance.

Code Figure	Technical Specifications	Nontechnical Specifications
5	Altopcumulus translucidus in bands, or one or more layers of Altopcumulus translucidus or opacus, progressively invading the sky; these Altopcumulus clouds generally thicken as a whole.	Semitransparent Altopcumulus in bands, or Altopcumulus in one or more fairly continuous layers (semitransparent or opaque), progressively invading the sky; these Altopcumulus clouds generally thicken as a whole.
6	Altopcumulus cumulogenitus (or cumulonimbo-genitus).	Altopcumulus resulting from the spreading out of Cumulus (or Cumulonimbus).
7	Altopcumulus translucidus or opacus in two or more layers, or Altopcumulus opacus in a single layer not progressively invading the sky, or Altopcumulus with Altostratus or Nimbostratus.	Altopcumulus in two or more layers, usually opaque in places, and not progressively invading the sky; or opaque layer of Altopcumulus, not progressively invading the sky; or Altopcumulus together with Altostratus or Nimbostratus.
8	Altopcumulus castellanus or floccus.	Altopcumulus with sproutings in the form of small towers or battlements, or Altopcumulus having the appearance of cumuliform tufts.
9	Altopcumulus of a chaotic sky, generally at several levels.	Altopcumulus of a chaotic sky, generally at several levels.

Table B-II-4. High Cloud-WMO Code

Symbol C_H=Clouds of Genera Ci, Cc, Cs

Code Figure	Technical Specifications	Nontechnical Specifications	Code Figure	Technical Specifications	Nontechnical Specifications
0	No C _H clouds-----	No Cirrus, Cirrocumulus, or Cirrostratus.	6	Cirrus (often in bands) and Cirrostratus, or Cirrostratus alone, progressively invading the sky; they generally thicken as a whole; the continuous veil extends more than 45° above the horizon, without the sky being totally covered.	Cirrus (often in bands converging towards one or two opposite points of the horizon) and Cirrostratus, or Cirrostratus alone; in either case, they are progressively invading the sky, and generally growing denser as a whole; the continuous veil extends more than 45° above the horizon, without the sky being totally covered.
1	Cirrus fibratus, sometimes uncinus, not progressively invading the sky.	Cirrus in the form of filaments, strands or hooks, not progressively invading the sky.	7	Cirrostratus covering the whole sky	Veil of Cirrostratus covering the celestial dome.
2	Cirrus spissatus, in patches or entangled sheaves, which usually do not increase and sometimes seem to be the remains of the upper part of a Cumulonimbus; or Cirrus castellanus or floccus.	Dense Cirrus in patches or entangled sheaves, which usually do not increase and sometimes seem to be the remains of the upper part of a Cumulonimbus; or Cirrus with sproutings in the form of small turrets or battlements, or Cirrus having the appearance of cumuliform tufts.	8	Cirrostratus not progressively invading the sky and not entirely covering it.	Cirrostratus not progressively invading the sky and not completely covering the celestial dome.
3	Cirrus spissatus cumulonimbogenitus.	Dense Cirrus, often in the form of an anvil, being the remains of the upper parts of Cumulonimbus.	9	Cirrocumulus alone, or Cirrocumulus predominant among the C _H clouds.	Cirrocumulus alone, or Cirrocumulus accompanied by Cirrus or Cirrostratus, or both, but Cirrocumulus is predominant.
4	Cirrus uncinus or fibratus, or both, progressively invading the sky; they generally thicken as a whole.	Cirrus in the form of hooks or of filaments or both, progressively invading the sky; they generally become denser as a whole.			
5	Cirrus (often in bands) and Cirrostratus, or Cirrostratus alone, progressively invading the sky; they generally thicken as a whole, but the continuous veil does not reach 45° above the horizon.	Cirrus (often in bands converging towards one or two opposite points of the horizon) and Cirrostratus, or Cirrostratus alone; in either case, they are progressively invading the sky, and generally growing denser as a whole, but the continuous veil does not reach 45° above the horizon.			

NRL Aerosol Related Instrumentation Descriptions

The suite of instruments which was assembled by NRL to determine the characteristics of the atmosphere by means of measurement of various physical parameters of the natural atmospheric aerosol constituency is described below:

1) Condensation nuclei (CN) density were precisely obtained by means of a Pollak Counter which has its calibration traceable back to the Pollak original calibration. This data is found in file CN.DAT column 2.

The condensation nuclei density distribution about the ship was obtained with a portable G.E. condensation counter. This work is presented in section C-IV of this report.

2) Continuous observations of condensation nuclei were also obtained by means of the Environment One Condensation Nuclei Monitor, model Rich 100. Although there is some question as to whether this instrument was operating properly, its data is stored in file ASC.DAT(7).

3) Cloud Condensation Nuclei (CCN) counts were obtained throughout the cruise by means of the NRL CCN equipment (see R. E. Ruskin and J. E. Dinger, "Descriptions of NRL CCN Equipment in The Second International Workshop on Condensation and Ice Nuclei," compiled by Lewis O. Grant, Dept. of Atmos. Science, Colorado State University, Fort Collins, CO, May 1971). This data is stored in file CCN.DAT where:

Column 2 is the CCN/cc at $\Delta T = 2.0^{\circ}\text{C}$

Column 3 is the CCN/cc at $\Delta T = 3.0^{\circ}\text{C}$

Column 4 is the CCN/cc at $\Delta T = 4.3^{\circ}\text{C}$

Column 5 is the CCN/cc at $\Delta T = 5.0^{\circ}\text{C}$

Column 6 is the percentage of involatile particles in the sample at
a $\Delta T = 4.3^{\circ}\text{C}$.

Values of 88888 mean that data was not available for this number and
values of 99999 mean that very high numbers of particles were observed,
i.e., numbers too high to accurately count.

4) Scattering coefficients were measured with the MRI Model
1567 Integrating Nephelometer. This device was located on a tower at
location B in Figure B-II-1. The units of this data are expressed as
 10^{-4} m^{-1} . This data is in ASC.DAT(4).

5) A Royco model 225 aerosol sizing device was used by NRL
throughout the cruise. This device divides the aerosol size distribution
into 5 parts. Thus, for every hour we have represented in these data
files the 10 minute mean concentrations of particles which fall within
the five size classes. Numbers used are the number of particles per cm^3
in the following ranges of particle diameter, d:

<u>Size of Channel</u>	<u>Location</u>
$0.45 \text{ } \mu\text{m} \leq d < 0.60 \text{ } \mu\text{m}$	ROY.DAT(2)
$0.60 \text{ } \mu\text{m} \leq d < 1.50 \text{ } \mu\text{m}$	ROY.DAT(3)
$1.50 \text{ } \mu\text{m} \leq d < 2.50 \text{ } \mu\text{m}$	ROY.DAT(4)
$2.50 \text{ } \mu\text{m} \leq d < 4.0 \text{ } \mu\text{m}$	ROY.DAT(5)
$d \geq 4.0 \text{ } \mu\text{m}$	ROY.DAT(6)

These values are the "true" ambient particle concentrations and were obtained from the measured particle concentrations using the formula of Balyaev and Levin (1972) which gives the particle sampling efficiency of a tube facing into the ambient air flow as a function of particle size and the ratio of the ambient wind speed to the airspeed in the sampling tube.

6) There were two new experimental aerosol instruments used on this cruise. These principles are not widely known and therefore a more detailed description of these devices and the data obtained will be found in separate reports in Sections C-I and C-II of this report.

TABLE B-II-5
Meteorological Data Files

<u>Parameter</u>	<u>Units</u>	<u>Location</u>
1) Sea Water Temperature at 7m	(°C)	THERM.DAT(2)
2) Air Temperature at 19m	(°C)	THERM.DAT(3)
3) Air Temperature at 19m	(°C)	FILE.DAT(2)
4) Dewpoint Temperature at 19m	(°C)	FILE.DAT(3)
5) Relative Wind Speed	(knots)	ASC.DAT(2)
6) Relative Wind Direction	(degrees)	ASC.DAT(3)
7) Atmospheric Radon Concentration	(pCi/cc)	RADON2(2)
8) Calculated Air Mass		VOLTZ.DAT(2)
9) Aerosol Thickness ($\lambda = 0.88\mu$)		TURBID.DAT(2)
10) Aerosol Thickness ($\lambda = 0.50\mu$)		TURBID.DAT(3)
11) Aerosol Thickness ($\lambda = 0.94\mu$)		TURBID.DAT(4)
12) Ship's Latitude	(whole degrees)	NAV.DAT(2)
13) Ship's Latitude	(decimal fraction of degree)	NAV.DAT(3)
14) Ship's Longitude	(whole degree)	NAV.DAT(4)
15) Ship's Longitude	(decimal fraction of degree)	NAV.DAT(5)
16) Ship's Course Made Good	(degrees)	NAV.DAT(6)
17) Ship's Speed	(knots)	NAV.DAT(7)
18) Sea Skin Temperature PRT-5	(°C)	FILE.DAT(4)
19) Sea Surface Temperature PRT-10	(°C)	PRT10.DAT(2)
20) Sky Temperature PRT-10	(°C)	PRT10.DAT(3)

TABLE B-II-5 (Contd)

<u>Parameter</u>	<u>Units</u>	<u>Location</u>
21) PRT-10 (-10°)	(°C)	PRT10.DAT(4)
22) PRT-10 (+10°)	(°C)	PRT10.DAT(5)
23) PRT-10 (+30°)	(°C)	PRT10.DAT(6)
24) PRT-10 (+60°)	(°C)	PRT10.DAT(7)
25) Cloud Base Temperature	(°C)	PRT10.DAT(8)
26) Sea State		CLOUD.DAT(2)
27) White Cap/Foam Cover	(%)	CLOUD.DAT(3)
28) Visibility	(mi)	CLOUD.DAT(4)
29) Cloud Cover		CLOUD.DAT(5)
30) Low Cloud Types		CLOUD.DAT(6)
31) Middle Cloud Types		CLOUD.DAT(7)
32) High Cloud Types		CLOUD.DAT(8)
33) Pollak Counter Condensation Nuclei Density	(#/cc)	CN.DAT(2)
34) E.O.C.N.M.-CN Data		ASC.DAT(7)
35) CCN/cc at ΔT 2.0°C		CCN.DAT(2)
36) CCN/cc at ΔT 3.0°C		CCN.DAT(3)
37) CCN/cc at ΔT 4.3°C		CCN.DAT(4)
38) CCN/cc at ΔT 5.0°C		CCN.DAT(5)
39) (%) Involatile Particles in Sample at $\Delta T = 4.3^\circ\text{C}$		CCN.DAT(6)
NRL ROYCO DATA		
40) Channel Size = d, $0.45 \mu\text{m} \leq d < 0.60 \mu\text{m}$	(#/cc)	ROY.DAT(2)
41) $0.60 \mu\text{m} \leq d < 1.50 \mu\text{m}$	(#/cc)	ROY.DAT(3)

TABLE B-II-5 (Contd)

<u>Parameter</u>	<u>Units</u>	<u>Location</u>
42) $1.50 \mu\text{m} \leq d < 2.50 \mu\text{m}$	(#/cc)	ROY.DAT(4)
43) $2.50 \mu\text{m} \leq d < 4.0 \mu\text{m}$	(#/cc)	ROY.DAT(5)
44) $d \geq 4.0 \mu\text{m}$	(#/cc)	ROY.DAT(6)

MEASUREMENTS OF AEROSOL AND MICROMETEOROLOGICAL
CHARACTERISTICS OF THE MARINE BOUNDARY LAYER
DURING THE TRANSATLANTIC/MEDITERRANEAN CRUISE
OF THE USNS HAYES, MAY-JUNE 1977

by

Ulrich Katz and Eugene J. Mack
Calspan Corporation, Buffalo, New York 14221

SUMMARY

Under contract no. N00173-77-C-0126 with the Naval Research Laboratory (NRL), Calspan Corporation provided meteorological and aerosol physics support during the NRL cruise 77-16-04 aboard the USNS HAYES. Data were acquired during the period from 14 May to 7 June 1977 while en route from Virginia to Athens, Greece via the Grand Banks and Gibraltar. The objective of Calspan's participation in the study was to record physical and chemical characteristics of the aerosol (including fog) in the lower atmospheric marine boundary layer as well as the pertinent basic meteorological parameters for subsequent interpretive analyses.

Calspan instrumentation deployed aboard the USNS HAYES is listed in Table B-II-6 along with information on parameters measured, range of variables, frequency of measurements and measurement heights above the sea surface. The locations of the various instruments on the ship are depicted schematically in Figure B-II-2. The first five items in Table B-II-6 were installed in a shelter which formed the lower half of a small tower erected atop the flying bridge. In order to minimize the risk of

contamination, the sample air for the various particle monitors was aspirated through a 5 cm diameter (ID), 2.5 m long tube extending to 2 m forward of and 2 m above the flying bridge. (Flow rate was such that aerosol residence within the tube was 2 sec.) Fog sampling equipment (items 6, 7, and 8) was mounted on top of the tower to minimize the ship's thermal influence when the wind direction is within the forward quadrant. A second drop sampler was positioned on the top of one of the bows (depending on wind direction) for collecting sea spray droplets as close to the water surface as possible while escaping any spray generated by the ship. Continuous temperature recordings were obtained at four levels, the lowest being the sea surface. (By towing an armored sea surface temperature probe between the bows, it was possible to make the probe follow within the top 10 centimeters of the water surface.) Continuous humidity measurements were obtained at two levels with lithium chloride based dew point sensors while manual psychrometry provided calibration and backup measurements. The main purpose of the wind instrumentation mounted on the antenna mast was the convenient detection of potentially contaminating wind conditions. While the last two items in Table B-II-6 provided bulk aerosol samples for later chemical analysis, the cascade impactor samples are most suitable for combined scanning electron microscopy and energy dispersive X-ray analysis of individual particles, whereas the bulk filter samples are partly earmarked for wet chemical analyses and partly designed for atomic absorption spectroscopy or X-ray fluorescence analysis.

The data are presently available in the form of hourly logs, strip chart records and unprocessed samples from the thermal diffusion chamber, droplet impactor, cascade impactor and hi-volume filters. The logs comprise hourly values of all the parameters measured except CCN, sea spray and chemical samples which were obtained at irregular intervals and which require further processing to arrive at quantitative values. In total, the logs comprise approximately 400 successful hourly observations. An additional 100 readings were contaminated (aerosol data mainly) by ship's exhaust resulting from unfavorable winds. Table B-II-7 summarizes the quantities and types of aerosol measurements which were obtained at discrete intervals. Visibilities, scattering coefficient, temperatures, dew points, and winds were recorded continuously and are available on strip charts as well as in the logs.

The data are grouped into two separate hourly logs, one containing the meteorological parameters (Table B-II-8), the other listing aerosol-related readings (Table B-II-9). It should be noted that the Royco values entered in the log are counts for the 10-minute period centered about the indicated time; printouts of five additional counts for every hour are on file at Calspan.

Since the raw EAA data required some processing, the aerosol data archived in the data system and presented in Section B-IV-d of this report are the results of computer analysis done at Calspan.

USNS HAYES

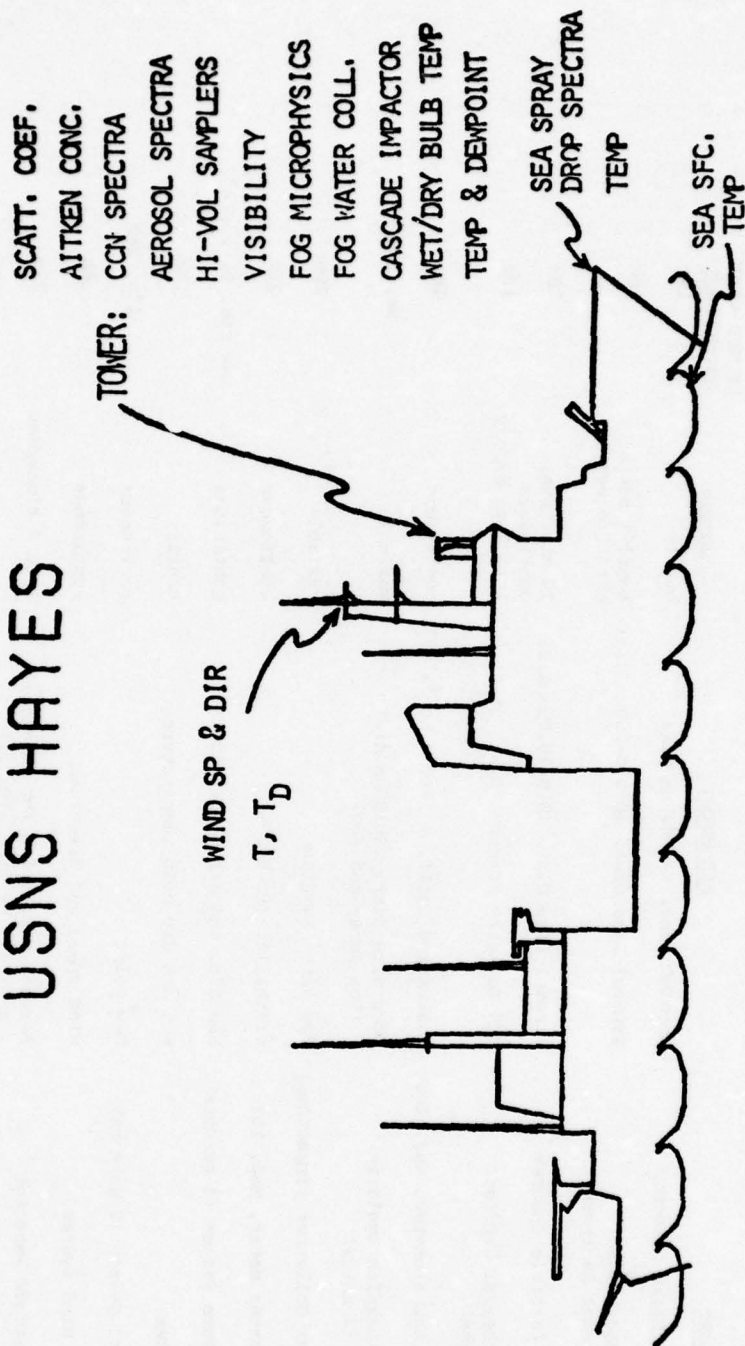


Fig. (B-II-2) Deployment of Calspan Instrumentation on the USNS HAYES.

Table B-II-6

CALSPAN INSTRUMENTATION INSTALLED ON THE USNS HAYES
NORTH ATLANTIC/MEDITERRANEAN EOMET CRUISE MAY-JUNE 1977

INSTRUMENT	PARAMETER	RECORD	HEIGHT ABOVE SEA SURFACE
1. Gardner Small Particle Detector	Aerosol Conc. ($> .0025\mu\text{m}$ dia)	hourly	18m
2. Thermo Systems Model 3030 Electrical Aerosol Analyzer	Aerosol Size Dist. ($0.003-1.0\mu\text{m}$ dia)	hourly; occ'n'ly more frequently	18m
3. Royco Model 225 Particle Counter	Aerosol Size Dist. ($0.3-10.0\mu\text{m}$ dia)	10 min. avg. continuous	18m
4. Calspan Static Thermal Gradient Diffusion Chamber	CCN Activity Spectra ($0.2-3.0\%$ S)	2 to 7 times/day	18m
5. MRI Integrating Nephelometer, Mod. 2050	Scattering Coeff. ($.1-40 \times 10^{-4}\text{m}^{-1}$)	continuous	18m
6. Calspan Droplet Sampler (gelatin replication) (2 units)	Drop size dist. ($3-100\mu\text{m}$ dia) (Sea spray and fog)	variable	9m, 20m
7. Calspan Fog Water Collector (impaction)	Fog water samples	variable	20m
8. EG&G Forward Scatter Meter, Mod. 107	Visibility ($60-6000\text{m}$)	continuous	21m
9. Foxboro Temperature System (4 sensors)	Sea Sfc. and air temperatures	continuous	sea sfc, 9, 17, 28
10. Sling Psychrometer	Wet and dry bulb temperatures	hourly	17m
11. Foxboro Dew Point System (2 sensors)	Dew point	continuous	17m, 28m
12. Beckman-Whitley Wind System	Wind speed and direction	continuous	28m
13. Battelle-type Cascade Impactor	Aerosol separation for chemical analysis by size ($>0.5\mu\text{m}$)	1 to 4 times/day	17m
14. Hi-Vol Aerosol Samplers (3 systems)	Chemical analysis of bulk aerosol samples on 3 diff. filter types: Teflon, quartz and cellulose	daily	18m

TABLE B-II-7
SUMMARY OF CALSPAN DISCRETE AEROSOL MEASUREMENTS

<u>Approximate Number of Measurements</u>	<u>Particles, Instruments</u>	<u>Period</u>
420	Aitken, Gardner	Hourly
390	Small p., EAA	Hourly
1600	Large p., Royco	10 minute averages. Some gaps (printer malfunction)
90	CCN, Therm. Diff. Ch.	3-4 hours
20	Sea spray, Drop Impactor	Irreg., 25 May - 6 June
35	Large and giant p., Cascade Impactor	Irreg., 17 May - 7 June
12	All p., Hi-Vol filters	Irreg., 8-20 hours

TABLE B-II-8

CALSPAN'S METEOROLOGICAL LOG

<u>Parameter</u>	<u>Units</u>	<u>File/Column No.</u>
1) Relative Wind Direction	(deg) :	CALVIS.DAT(2)
2) Relative Wind Speed	(mph) :	CALVIS.DAT(3)
3) EG&G Visibility	(m) :	CALVIS.DAT(4)
4) MRI Visibility	(mi) :	CALVIS.DAT(5)
5) Psychrometer Dry Bulb	(°F) :	CALVIS.DAT(6)
6) Psychrometer Wet Bulb	(°F) :	CALVIS.DAT(7)
7) Air Temperature at 27 m	(°C) :	CALTMP.DAT(2)
8) Air Temperature at 15 m	(°C) :	CALTMP.DAT(3)
9) Air Temperature at 9 m	(°C) :	CALTMP.DAT(4)
10) Sea Surface Temperature	(°C) :	CALTMP.DAT(5)
11) Dewpoint at 27 m	(°C) :	CALTMP.DAT(6)
12) Dewpoint at 15 m	(°C) :	CALTMP.DAT(7)
13) Ship's Magnetic Heading	(deg) :	CALTMP.DAT(8)

TABLE B-II-9
CALSPAN'S AEROSOL LOG

<u>Parameter</u>	<u>File(Column No.)</u>
1) Aitken Nuclei Concentration (#/cc) :	OUT.AER(2)
2) Royco Data in #/2.8 μ	
a) >0.3 μ :	OUT.AER(3)
b) >0.6 μ :	OUT.AER(4)
c) >1.2 μ :	OUT.AER(5)
d) >3. μ :	OUT.AER(6)
e) >5. μ :	OUT.AER(7)
3) $b_{\text{scat}} (10^{-4} \text{ m}^{-1})$:	OUT.AER(8)
4) Thermo Systems Model 3030 Electrical Aerosol Analyzer N = #/cc	
a) Log N ($r > .0032 \mu$)	WHIT2.DAT(2)
b) Log N ($r > .0056 \mu$)	WHIT2.DAT(3)
c) Log N ($r > .01 \mu$)	WHIT2.DAT(4)
d) Log N ($r > .0178 \mu$)	WHIT2.DAT(5)
e) Log N ($r > .0316 \mu$)	WHIT2.DAT(6)
f) Log N ($r > .0562 \mu$)	WHIT2.DAT(7)
g) Log N ($r > .1 \mu$)	WHIT2.DAT(8)
h) Log N ($r > .178 \mu$)	WHIT2.DAT(9)
i) Log N ($r > .360 \mu$)	WHIT2.DAT(10)
j) Log N ($r > .560 \mu$)	WHIT2.DAT(11)

USNS HAYES Marine Boundary Layer

Research Cruise:

Preliminary Evaluation of NPS Data

C. W. Fairall, L. F. May, K. L. Davidson
T. Houlihan and G. E. Schacher

Environmental Physics Group
Naval Postgraduate School
Monterey, CA 93940

In May and June of 1977 the Naval Air Systems Command (AIR 370) sponsored a marine boundary layer research cruise aboard the Naval Research Laboratory (NRL) ship, USNS HAYES, in the North Atlantic and Mediterranean. The cruise involved scientific personnel from several laboratories including the Naval Postgraduate School (NPS). We departed Chatham Annex, Virginia on May 15, paralleled the Coast to Nova Scotia, then took a great circle route across the Atlantic arriving in Rota, Spain on May 27. We departed Rota, Spain on May 30 and arrived in Piraeus, Greece on June 7.

NPS participated in the cruise primarily to gather atmospheric turbulence data for a wide range of atmospheric and sea state conditions. These data are used to determine turbulent fluxes of heat, momentum, and water vapor and turbulent mixing of other atmospheric scalars such as aerosols, electric charge and pollutants. The data are also important for characterizing the optical propagation qualities of the atmosphere. This is a preliminary report on the basic mean and turbulence data gathered by the NPS personnel.

II. USNS HAYES INSTALLATION

The USNS HAYES (T-AGOR 16) is a twin hull ship that was constructed for NRL for use as an oceanographic research vessel. Pertinent dimensions are: length overall 246 ft, beam 75 ft, and distance between hulls 27 ft. Due to the catamaran construction the ship has a very broad forward wall beginning approximately 50 ft back from the bows of the ship, which extends nearly the full width of the ship and to a height of approximately 56 ft above the mean water line. The presence of this wall greatly perturbs the natural airflow and causes problems in the interpretation of our data, as will be described.

Figure B-II-3 shows the profile of the ship and the location of the two stations at which NPS installed sensors. We welded a 12 ft tubular steel tower as far forward on the port bow as possible (approximately 2 ft back from the tip of the bulwark). The mean sensors were placed at the top of this tower and the turbulence sensors were mounted on a wind vane, which was mounted on a 4 ft extension at the top of the tower. The vane is used to keep the sensors pointing into the wind, and the extension places the sensors forward of the tower so that shipboard influence is eliminated. The second station was located on the first level of the ship's forward mast. Again the turbulence sensors were mounted on a vane on an extension to keep these sensors as far forward of the platform as was feasible. The arrangement at this station was such that the mean sensors were approximately 2 ft below the turbulence sensors. The heights of the various sensors above the mean water level are found in Table B-II-10.

TABLE B-II-10 Height of NPS Sensors Above Mean Sea Level

STATION	SENSOR ht.		EFFECT. ht. (tunnel)		EFFECT. ht (meas.)	
	Mean	Turb	Mean	Turb	Mean	Turb
BOW	12.1m	12.1m	11.3m	11.3m	11.0m	11.0m
MAST	23.8m	24.5m	17.6m	18.5m	19.6m	20.5m

Figure B-II-3 shows a schematic representation of the air flow over the ship when the relative wind is from the bow. The effect of the flow is that the air sampled by the sensors at the mast station comes from a height lower than their actual height above the sea surface. The location of the bow station is such that the air sampled comes from nearly the same height as the sensors.

Before the 1975 fog cruise, NRL had a wind tunnel analysis of the air flow around the Hayes performed. Also, during that cruise, Dr. Richard Jeck of NRL made a number of measurements of the wind velocity in the forward region of the ship with a bivane anemometer. Evaluation of these two sets of data do not give us as accurate information as we need, but they do show that the air arriving at the mast rises approximately 20 ft. This correction is applied to the height, giving the air height listed in Table B-II-10 as effective height (tunnel). Note that the air flow information that is available is only for the relative wind directly from the bow at about 10 knots. We have made a better estimate of the effective heights from the ratio of turbulent dissipation, ϵ , at the two heights. In the boundary layer,

$$Z_1/Z_2 = (\epsilon_2/\epsilon_1) f_\epsilon (Z_1/L)/f_\epsilon (Z_2/L)$$

where $f_\epsilon (Z/L)$ is a stability correcting factor and L is the Monin-Obukhov length (a typical value for the Northern oceans if $L = 100$ meters). For this cruise we have 230 simultaneous values of ϵ_1 and ϵ_2 giving

$$\langle \epsilon_1/\epsilon_2 \rangle = 1.97$$

which results in

$$Z_2/Z_1 = 1.86.$$

Assuming the bow level is much less affected than the mast we have assigned the values of Z_1 and Z_2 given in the third column of Table B-II-10.

III. NPS Equipment

1) General Information

We installed equipment to measure both mean and turbulence parameters at both the bow and mast stations. The parameters measured were:

- a. humidity
- b. temperature
- c. horizontal wind speed
- d. temperature fluctuations
- e. horizontal wind speed fluctuations

A sea surface temperature sensor was installed between the hulls about 75 ft forward of the stern. Relative wind direction was measured at the port bow level.

Details of the equipment used for the measurements follows.

The sensors for both mean humidity and mean temperature were mounted in a single aspirator at each station. They were, therefore, protected from the weather while a steady flow of air insured that they remained at ambient conditions.

2) Humidity

A Hygro Dynamics Digital II system employing 15-1818 sensors was used. The sensors contain lithium chloride cells and thermistors so that humidity and temperature were both measured continuously. This temperature sensor was used only as a monitor, not for our mean temperature measurements. The humidity sensors were calibrated in a humidity chamber, the results are shown in Table B-II-11. Sensor #2 was used on the bow level and Sensor #6 was used on the mast.

3) Mean Temperature

Hewlett Packard Model 2801A. In this system the sensor is a quartz crystal which forms the capacitive element in an oscillator tank circuit. Temperature changes change the oscillator frequency, which is sensed for the temperature readout. This system is quite accurate, allowing temperatures to be determined within 0.03°C . Sea surface temperature is measured with the same system.

Table B-II-11 NPS Humidity Sensor Calibration

Hydrodynamics Digital II Calibration

Wet-Dry Bulb %RH	Ave Hygro %RH	Deviation of Sensor from Ave Hygro % RH							
		1	2	3	4	5	6	7	8
33.0	31.6	1.4	-1.4	-0.6	1.5	-0.2	-1.6	-0.9	1.8
36.0	37.2	-0.5	-0.8	-0.3	1.6	0.5	-1.4	-0.1	1.2
44.0	41.2	-0.8	-0.4	-0.3	0.6	0.9	0.4	-0.1	0.3
NA	41.5	-0.5	-0.4	-0.3	0.5	0.9	-0.4	-0.1	-0.1
NA	42.6	-1.2	-0.5	-0.5	-0.9	1.8	-0.4	-0.2	0.1
NA	65.8	-0.2	-1.4	-2.5	0.8	1.8	-0.3	1.3	0.3
74.8	73.6	0.2	0.2	-1.3	0.5	-0.2	0.4	-0.4	0.8
88.3	85.0	-0.7	0.9	-0.4	0.1	-0.6	0.0	0.4	0.2
82.6	86.7	-1.4	-0.6	-0.5	0.1	-0.2	0.3	0.7	0.3
82.6	87.0	-1.0	0.5	-0.7	0.0	0.3	0.7	0.0	0.2
85.0	88.0	-0.4	1.1	-0.1	0.1	-1.8	1.1	-0.6	-0.1
93.9	89.6	0.1	0.8	-0.2	0.3	-2.2	2.1	-1.5	0.4
94.4	92.3	-0.6	1.1	-0.5	-0.3	-0.4	1.2	-0.5	0.4
94.4	93.6	-0.8	1.0	-0.8	-0.3	0.4	-0.2	0.8	-0.4
Ave Deviat		-0.5	-0.0	-0.6	0.3	0.1	0.1	-0.1	0.4
σ		0.7	0.9	0.6	0.7	1.1	1.0	0.7	0.6

The average deviation of the wet-dry bulb from the Ave Hygro reading is 0.4% RH with a standard deviation of 2.9% RH.

4) Mean Wind Speed

Thorntwaite Model 101 Wind Register System. This is a photo-electric system with very light plastic cups that allow measurements of winds as slight as one half knot.

5) Temperature Fluctuations

A low power ac Wheatstone bridge was constructed using a GTE Sylvania, Inc. Model 140 Lightweight Thermo-sonde System with TSI Model 1210 probes with P 8 platinum wire used as sensing elements. The low power bridge was operated at 100 μ Amp, the resistances of the probes were approximately 40 Ohms, thus, the energy dissipation in the sensor is 5×10^{-7} Watts. Very low power was used to insure that the sensor is not elevated above ambient temperature which prevents velocity fluctuations from influencing the wire response. The wire is 1.2mm long and 2.5μ in diameter, and the probe has a time constant much shorter than the times encountered in atmospheric turbulence.

6) Wind Speed Fluctuations

TSI Model 1054B Anemometer, TSI Model 1210 probes with 6 mil. hot film elements were used as the sensing elements. An overheat ratio of 1.2 was utilized so that the wire temperature was approximately 150°C. The overheat greatly diminishes the influence of temperature fluctuations on these measurements.

The axes of the films were aligned in the vertical direction so that the wires were not sensitive to air flow in the vertical direction. Thus, only the horizontal component of wind speed fluctuations is detected.

7) Data Recording Equipment

Fluctuation data for temperature and wind speed were recorded on 1/4 inch magnetic tape.

Mean wind data was recorded by hand. The mean temperature and humidity were printed on paper tape with a Hewlett Packard 562AR printer.

In order to correctly understand the mean temperature data, it is necessary to describe the data gathering sequence in some detail. There are five signals to record: humidity at two levels and temperature at three levels, including the sea surface. These signals are processed by a homemade sequencer which sorts and sends the signals to the printer. The sequencer steps cyclically from level to level in the sequence: sea surface to bow to mast, and the temperature and humidity at a given level are printed simultaneously. When the sequencer is at the sea surface step, zeros are printed for the humidity and this allows us to identify the levels on the print tape.

The interfacing between the sequencer and the Hewlett Packard temperature readout posed some problems. Since the readout is a frequency counter, it has its own count cycle, the timing of which is set by a front panel control. It was not possible to control the readout timing by a command from the sequencer and we did not construct the sequencer to accept a command from the readout. Thus, it is possible for the sequencer to issue a print command when the counter is in a read cycle, leading to an error. We set the readout timer in a way so that such errors are very infrequent and they are normally easily identified.

The three mean temperatures and the two mean humidities were read and recorded every 2.5 minutes throughout the cruise except when a malfunction occurred. Fluctuation data was recorded at hourly intervals, as conditions warranted. The fluctuating signals were also continually processed by filtering and RMS units and recorded on strip chart units for real time averages of C_T and e .

8) Acoustic Radar

An Aeroenvironment Model 300 acoustic radar was installed on the upper aft deck of the ship. The acoustic radar provides an information cross section of the lower atmosphere by emitting a brief pulse of sound upward ($f = 1600$ HZ), listening to the echoes which are reflected by temperature variations aloft, and displaying the height of the echoes on a chart. This device has been used successfully on shipboard in the Pacific to measure the height of the marine inversion up to 1 km. No inversions were observed during the entire trip.

IV. MEAN DATA

Temperature and Humidity

Table B-II-12 contains the location in the data archive system of mean values of temperatures and humidity obtained from the NPS equipment during the trip. Level 1 is the bow station, level 2 is the radar mast station and T_s is the sea "surface" temperature. Since the sea temperature sensor was between the hulls in a very turbulent region, it is assumed that it is more of a "bucket" temperature than an actual surface temperature.

Table B-II-12

NPS Meteorological Data Files

1)	T_s , Surface Temperature	(°C) :	NAVPGS.DAT(2)
2)	T_1 , Air Temperature level 1	(°C) :	NAVPGS.DAT(3)
3)	T_2 , Air Temperature level 2	(°C) :	NAVPGS.DAT(4)
4)	H_1 , Relative Humidity level 1	(%) :	NAVPGS.DAT(5)
5)	H_2 , Relative Humidity level 2	(%) :	NAVPGS.DAT(6)

V. TURBULENCE DATA

1) Definitions

The temperature structure function, C_T^2 , is defined as

$$C_T^2 = \langle [T(x) - T(x+d)]^2 \rangle d^{-2/3}$$

where $T(x)$ is the temperature at position x and $T(x+d)$ is the temperature at position $x+d$. In the inertial subrange of isotropic turbulence, C_T^2 is independent of d and can be related to the one dimensional power spectrum of temperature fluctuations, ϕ_T , by

$$\phi_T(k) = .25 C_T^2 k^{-5/3}$$

where k is the wave number. The parameter of optical interest is the index of refraction structure function, C_N^2 , which is given approximately by (at sea level),

$$C_N^2 = (9.8 \times 10^{-7} \text{ } ^\circ\text{C}^{-1})^2 C_T^2$$

The rate of dissipation of turbulent energy, ϵ , is related to the one dimensional power spectrum of velocity fluctuations, ϕ_u , by

$$\phi_u(k) = .5 \epsilon^{2/3} k^{-5/3}$$

in the inertial subrange. In the constant stress surface layer, the friction velocity, U_* , is related to ϵ by

$$\epsilon K Z = U_*^3 f_\epsilon(Z/L),$$

where K is von Karmon's constant = .35 and Z is the height above the surface. In near neutral conditions, $f_\epsilon(Z/L) = 1$ and

$$U_* = (\epsilon K Z)^{1/3}$$

The friction velocity is related to the mean velocity (u) profile by

$$\frac{\delta u}{\delta z} = \frac{U_*}{K Z} f_u(Z/L),$$

where $f_u(Z/L)$ is a stability correction. The eddy diffusivity, K_m , is given by

$$K_m = K Z U_* f_u^{-1}(Z/L).$$

2) Atlantic Crossing

Daily average values of C_T^2 and T are shown in Fig. B-II-4 for the Atlantic Ocean crossing. This data illustrates the large values of C_T^2 found at the boundary of the warm waters of the Gulf Stream around May 22.

3) Diurnal Variation of C_T^2

The diurnal variation of C_T^2 is of interest to optical propagation modelers as well as micrometeorologists. In general, the marine boundary layer is considerably less variable than its overland counterpart. We have divided the data into three separate geographical locations: the Atlantic coast of the U.S. and Canada (May 15-21), the warm waters of the Mid-Atlantic (May 22-27) and the Mediterranean Sea (May 30-June 6). Figure B-II-5 is the bow level data ($Z = 11$ meters), Figure B-II-6 is the radar mast level ($Z = 20.5$ meters) and Figure B-II-7 shows both levels for all three regions combined.

4) Turbulence Data

Table B-II-13 is a compilation of the fluctuation parameters C_T^2 and ϵ measured during the cruise. In addition, we have the friction velocity U_* which is related to the eddy diffusivity and λ_0 , the microscale of turbulence. The atmospheric stability is given in terms of Richardson number, R_i .

$$R_i = \frac{g}{T} \frac{(\delta \theta_v / \delta Z)}{(\delta U / \delta Z)^2}$$

where g is the gravitational acceleration and θ_v is the virtual potential temperature.

Table B-II-13

NPS Data Files

1)	$C_{T1}^2 (10^{-3} \text{C/m}^{2/3})$ level 1	:	NAVPGS.DAT(7)
2)	$C_{T2}^2 (10^{-3} \text{C/m}^{2/3})$ level 2	:	NAVPGS.DAT(8)
3)	$\epsilon_1 (10^{-3} \text{m}^2/\text{sec}^3)$ level 1	:	NAVPGS.DAT(9)
4)	$\epsilon_2 (10^{-3} \text{m}^2/\text{sec}^3)$ level 2	:	NAVPGS.DAT(10)
5)	U_* (m/sec)	:	NAVPGS.DAT(11)
6)	Richardson's Number	:	NAVPGS.DAT(12)

Acknowledgements

Work supported by NAVAIR 370 and NRL.

REFERENCES

1. Businger, J. A., Wyngaard, J. C., Izumi, Y. and Bradley, E. F., J. Atmos. Sci. 28, 181 (1971).
2. Lumley, J. L. and Panofsky, H. A., The Structure of Atmospheric Turbulence, New York, Interscience 1964.

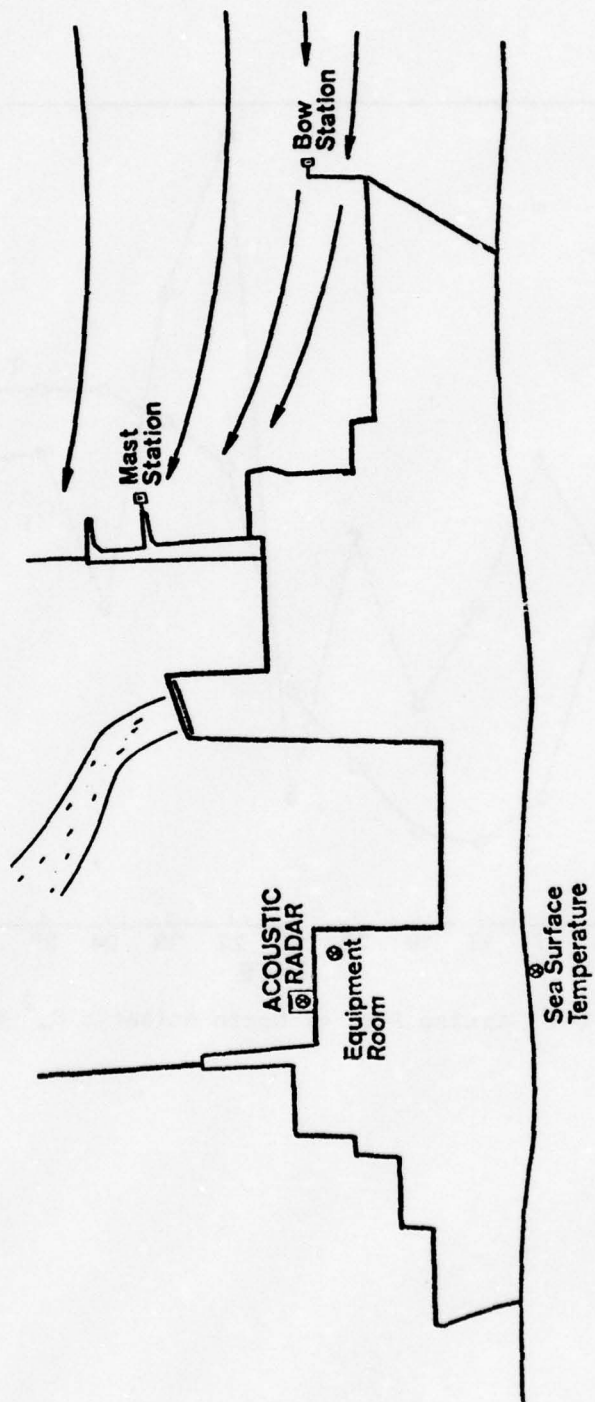


Fig. (B-II-3) Location of the Naval Postgraduate School instrumentation.

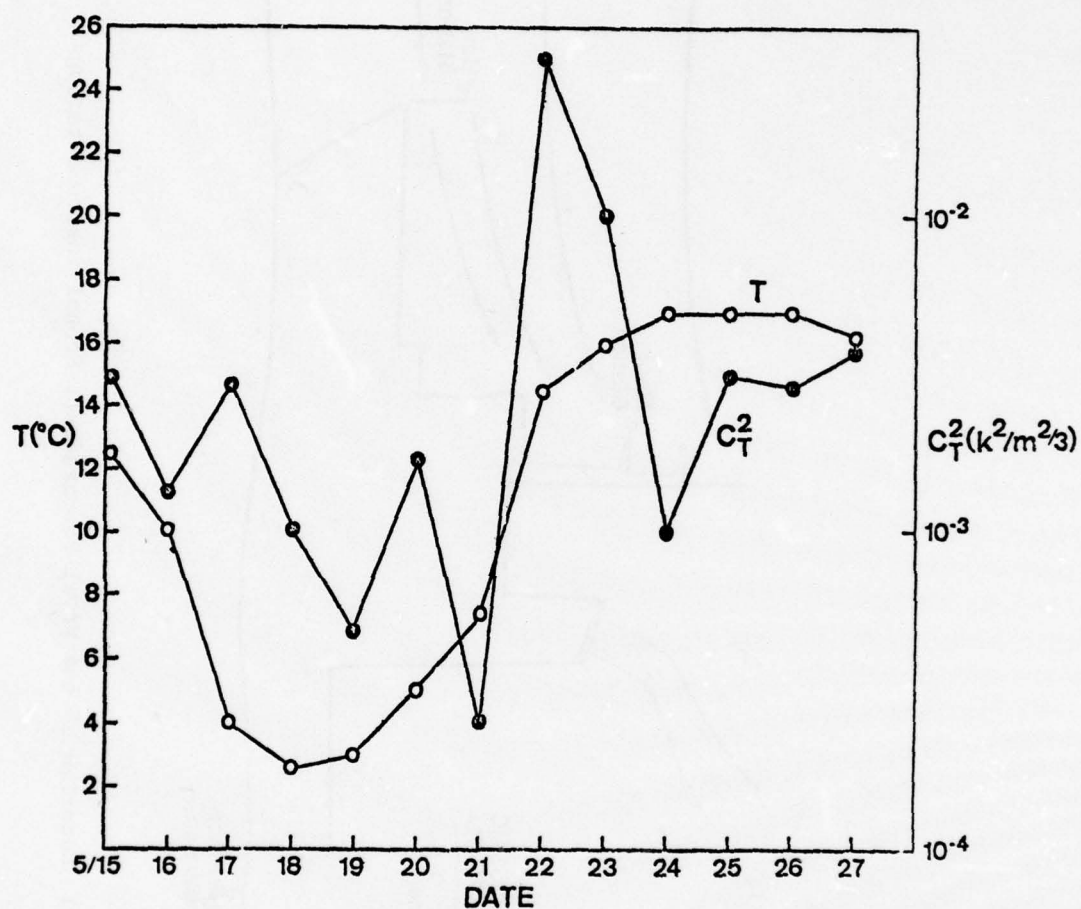


Fig. (B-II-4) Cruise Plot of North Atlantic C_T^2 and T Measurements

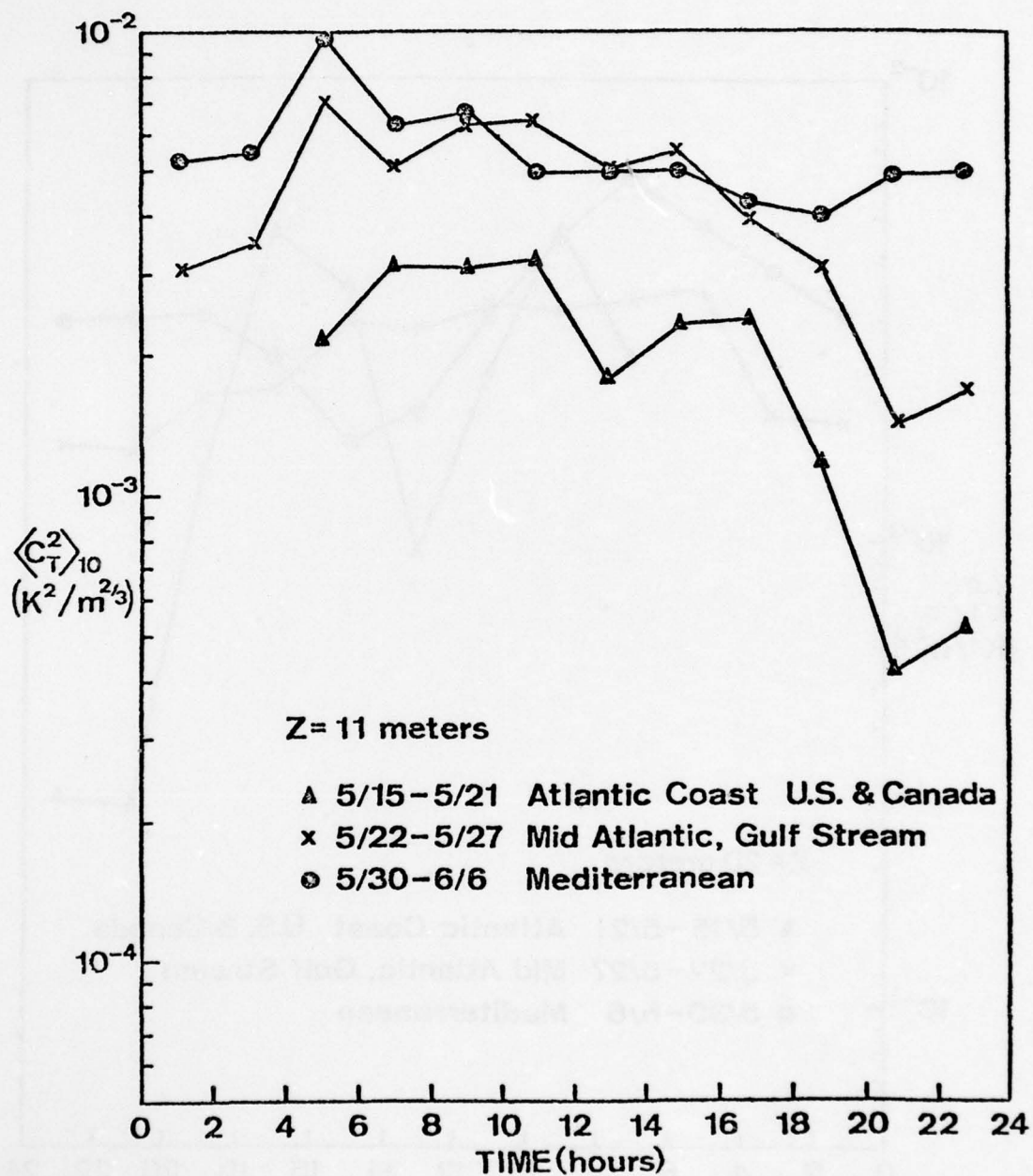


Fig. (B-II-5) Diurnal variations of C_T^2 at $Z = 11 \text{ m}$.

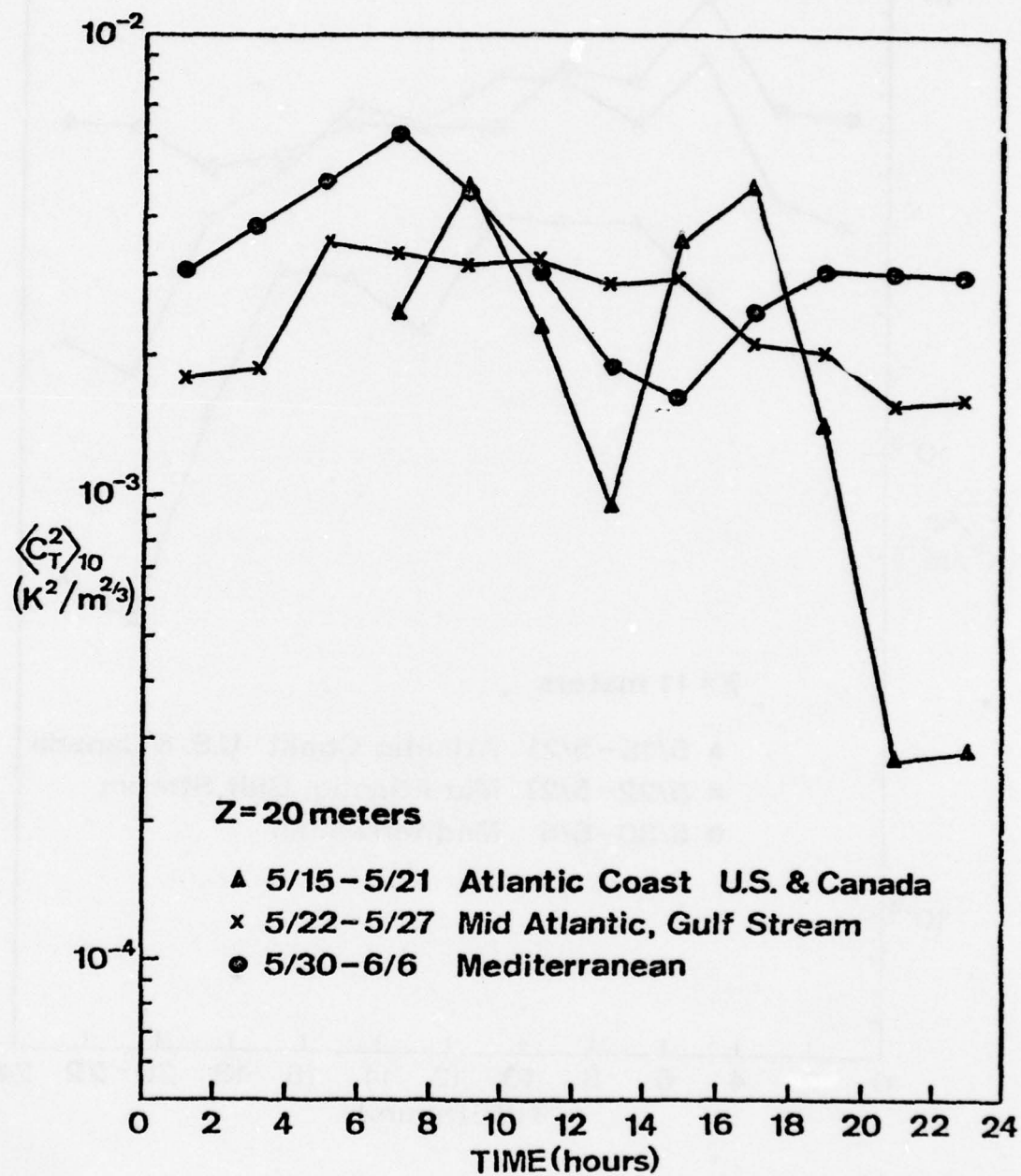


Fig. (B-II-6) Diurnal variations of C_T^2 at $Z = 20$ m.

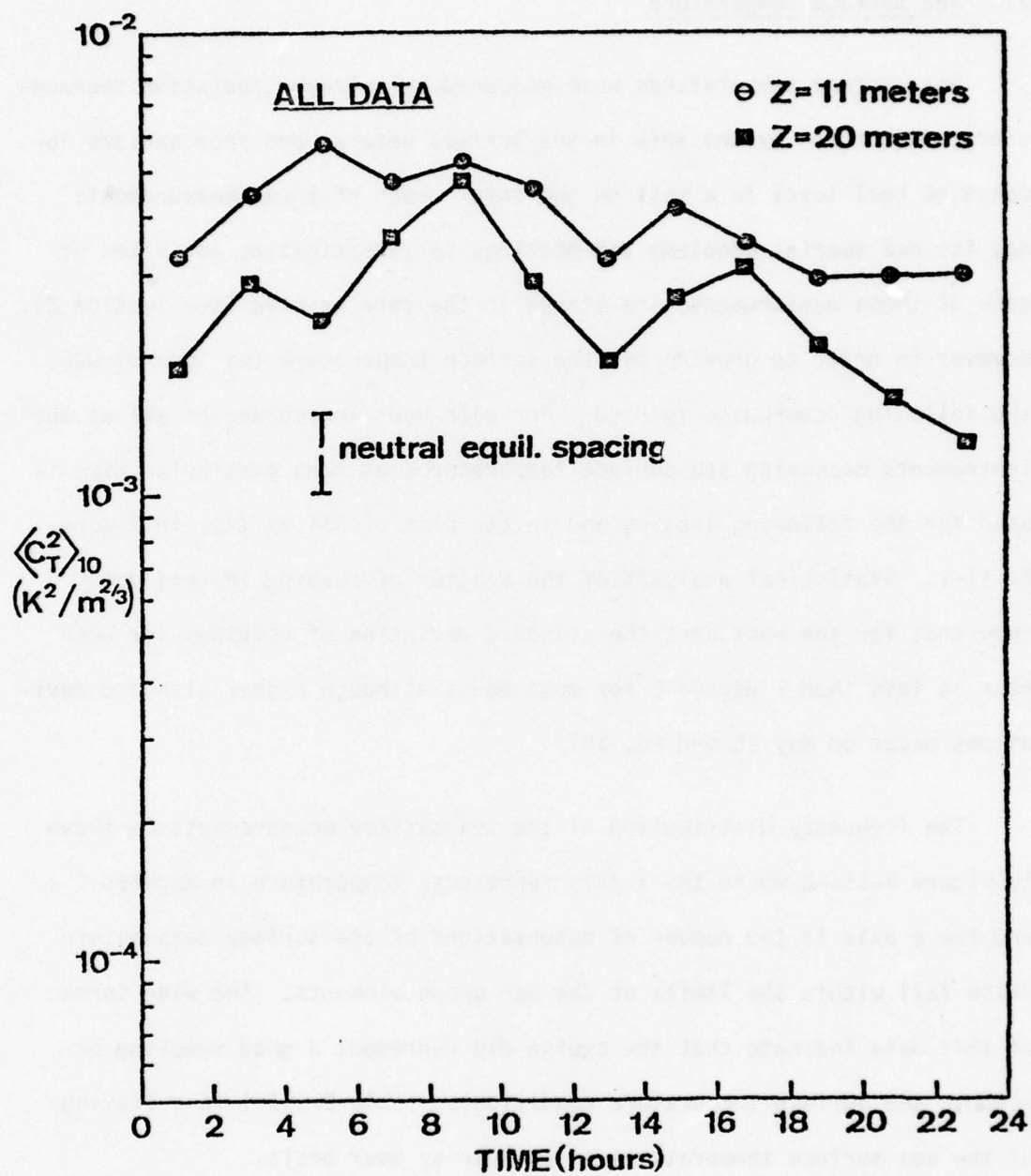


Fig. (B-II-7) Diurnal variations of C_T^2 for all data.

B-III METEOROLOGICAL DATA

a) Sea Surface Temperature

Sea surface temperatures were measured by infrared radiation thermometers, fish towed by the ship in the surface waters, and from sensors located at keel level in a well on the ship. Each of these measurements has its own special problems and meanings to investigators and files of each of these measurements are stored in the data archive (see Section D). However in order to provide one sea surface temperature for general use, the following compromise is used. For each hour an average of all of the instruments measuring sea surface temperatures at that particular time is used for the following listing and in the plot of SST vs time in Figure B-III-1. Statistical analysis of the scatter of reading in this data show that for the most part the standard deviation of readings for each hour is less than 1 degree C for most hours although higher standard deviations occur on May 15 and 20, 1977.

The frequency distribution of the sea surface measurements is shown in Figure B-III-2 where the x axis represents temperature in degrees C and the y axis is the number of observations of sea surface temperature which fall within the limits of the bar graph elements. The wide spread of this data indicate that the cruise did represent a good sampling of oceanic sea surface temperature conditions. Table B-III-1 is a listing of the sea surface temperatures on an hour by hour basis.

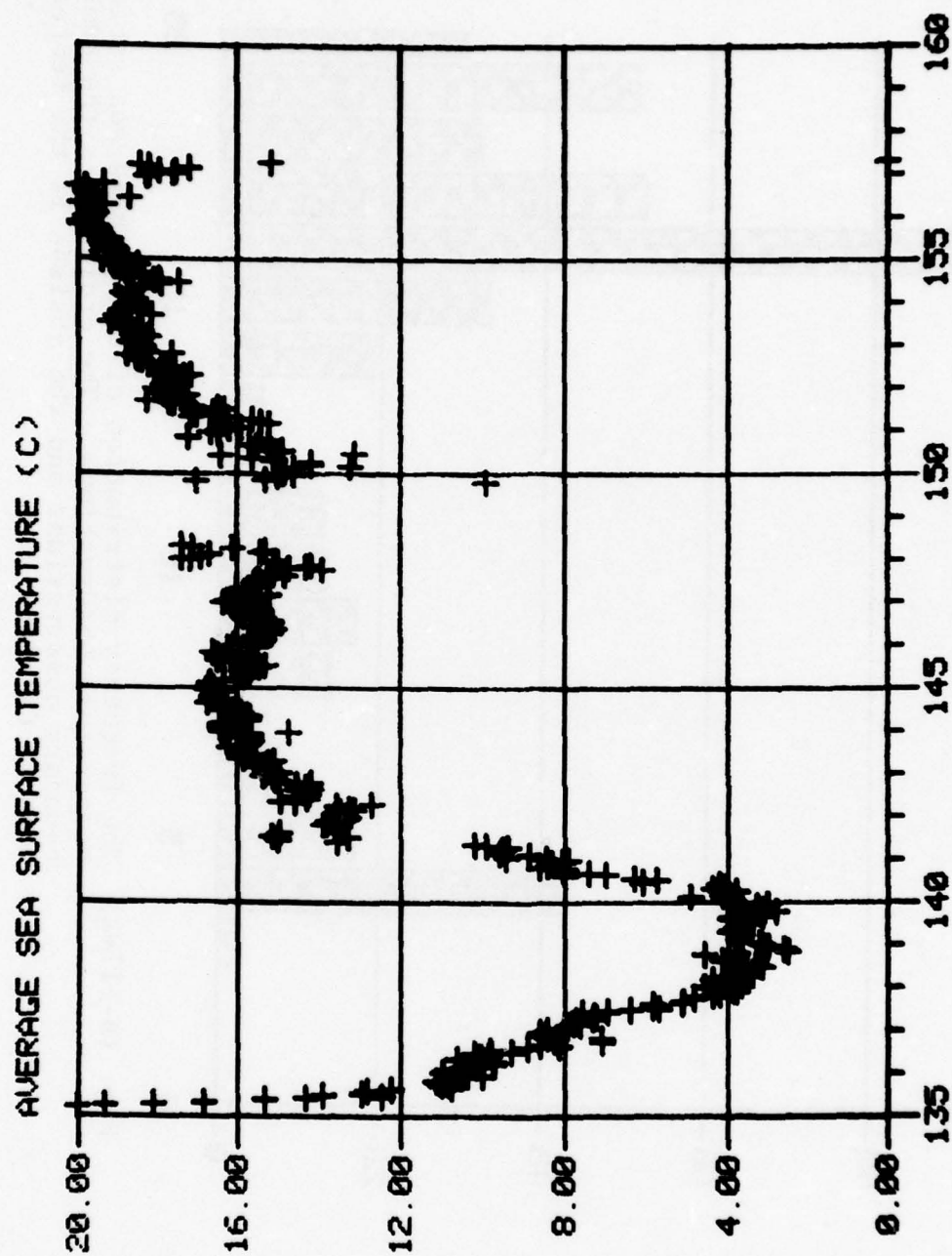


Fig. (B-III-1) Cruise plot of the average sea surface temperature vs. Julian date. The "y" axis is the temperature value expressed in degrees Celsius and the X axis is the GMT Julian date.

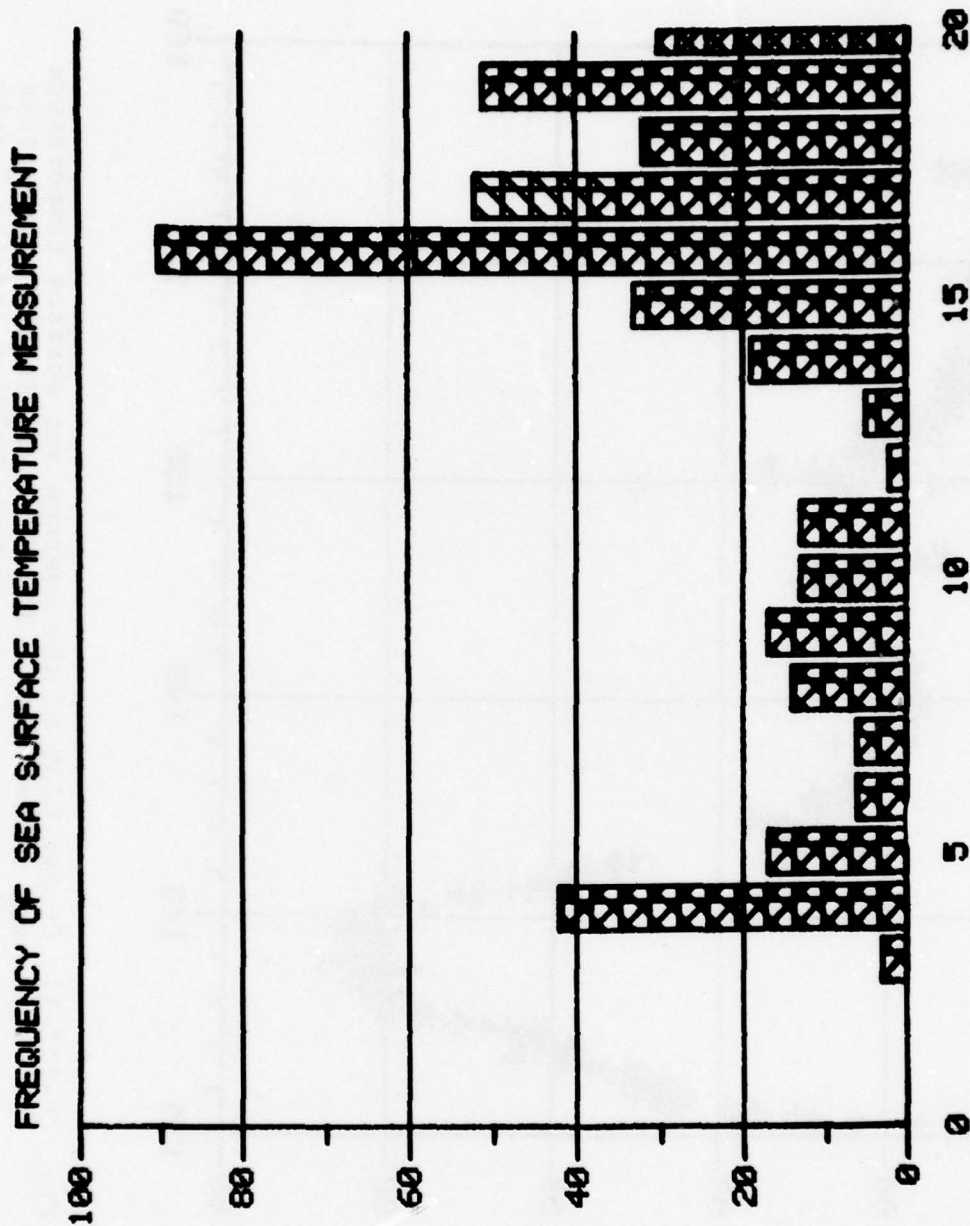


Fig. (B-III-2) The frequency distribution of the average sea surface temperature observations. The ordinate is the number boundary observations and the abscissa is the temperature in Celsius.

* HOUR	SEA SURFACE TEMPERATURE (C)									
	5/15/77	5/16/77	5/17/77	5/18/77	5/19/77	5/20/77	5/21/77	5/22/77	5/23/77	5/24/77
0		10.4	8.6	4.3	3.0	3.7	7.9	13.3		
1		10.5	8.4	4.6	3.3	3.9	8.5	13.4		
2		11.0	8.7	5.7	3.5	4.4	8.6	13.5		
3		10.6	8.9	5.7	3.5	4.4	8.6	13.5		
4	23.5	10.5	7.7	5.4	3.5	4.4	8.6	13.5		
5	20.0	10.2	7.7	4.4	3.5	4.4	8.6	13.5		
6	20.5	9.7	7.7	4.1	3.5	4.4	8.6	13.5		
7	19.5	9.7	7.7	4.5	3.5	4.4	8.6	13.5		
8	18.1	9.0	7.7	5.5	3.5	4.4	8.6	13.5		
9	16.8	10.6	7.7	5.5	3.5	4.4	8.6	13.5		
10	15.5	10.1	7.7	5.5	3.5	4.4	8.6	13.5		
11	14.5	9.9	7.7	5.5	3.5	4.4	8.6	13.5		
12	12.5	9.2	7.7	5.5	3.5	4.4	8.6	13.5		
13	13.5	9.3	7.7	5.5	3.5	4.4	8.6	13.5		
14	12.5	9.3	7.7	5.5	3.5	4.4	8.6	13.5		
15	12.5	9.3	7.7	5.5	3.5	4.4	8.6	13.5		
16	12.5	9.3	7.7	5.5	3.5	4.4	8.6	13.5		
17	12.5	9.3	7.7	5.5	3.5	4.4	8.6	13.5		
18	10.8	8.1	7.7	5.5	3.5	4.4	8.6	13.5		
19	11.0	8.7	7.7	5.5	3.5	4.4	8.6	13.5		
20	10.9	8.7	7.7	5.5	3.5	4.4	8.6	13.5		
21	11.0	8.7	7.7	5.5	3.5	4.4	8.6	13.5		
22	11.1	8.7	7.7	5.5	3.5	4.4	8.6	13.5		
23	10.7	8.6	7.7	5.5	3.5	4.4	8.6	13.5		

Table B-III-1. Average Sea Surface Temperature

* HOUR	SEA SURFACE TEMPERATURE (C)									
	5/23/77	5/24/77	5/25/77	5/26/77	5/27/77	5/28/77	5/29/77	5/30/77		
0		16.4	16.6	16.1	16.3	17.2		14.9		
1	15.0	16.3	16.6	15.6	16.3	17.4		14.8		
2	15.1	16.4	16.7	15.7	16.1	16.9		14.8		
3	15.2	16.4	16.7	15.7	15.7	16.7		14.6		
4	15.5	16.4	16.3	15.5	15.2	15.4		13.2		
5	15.4	16.3	16.3	15.5	15.2	15.3		14.2		
6	15.3	15.7	15.8	15.2	15.8	15.1		14.2		
7	15.1	15.8	15.8	15.3	15.0	16.1		14.1		
8	15.5	15.7	15.8	15.3	15.7	17.1		15.1		
9	15.8	15.8	15.7	15.1	15.5	17.4		15.6		
10	15.7	15.9	15.7	15.5	15.5			16.4		
11	15.8	16.1	15.7	15.3	15.5			13.1		
12	16.0	16.3	15.5	15.2	15.4			15.0		
13	16.0	16.4	15.8	15.1	15.5			14.9		
14	15.9	16.3	15.3	15.2	15.3			15.2		
15	16.2	16.4	16.2	15.8	14.8			15.5		
16	15.8	16.7	16.5	15.8	15.1			15.7		
17	15.7	16.3	16.3	15.9	15.2			15.2		
18	15.7	16.6	16.5	15.4	13.9			15.2		
19	15.7	16.6	16.1	16.0	14.7		9.9	15.4		
20	15.7	16.6	16.6	15.4	14.3		17.0	17.2		
21	15.9	16.6	16.2	16.0	14.2		15.3	17.2		
22	15.7	16.4	16.2	15.6	15.0		15.0	16.5		
23	14.7	16.8	15.5	16.0	15.1		14.6	16.7		

Table B-III-1. Average Sea Surface Temperature (cont'd)

* HOUR	5/31/77	6/1/77	6/2/77	6/3/77	6/4/77	6/5/77	6/6/77	6/7/77
0		17.7	18.4	18.7	19.2	19.7	17.6	
1	16.9	17.7	18.7	18.6	19.0	19.7	17.5	
2	15.3	17.8	18.7	18.5	19.0	19.5	18.0	
3	16.3	17.5	18.4	18.7	19.4	19.7	17.2	
4	15.2	17.5	18.4	18.8	19.2	19.7	18.2	
5	15.4	17.5	18.2	18.9	19.0	19.7	18.4	
6	15.6	17.3	18.4	18.6	19.1	19.7	15.2	
7	16.3	17.2	18.5	18.8	19.3	19.7	0.	
8	17.2	17.8	18.4	18.4	19.3	19.7		
9	17.0	18.0	18.8	18.8	19.3	20.1		
10	16.6	17.6	18.8	17.9	19.2	18.7		
11	17.1	17.9	18.9	17.5	19.2	19.0		
12	16.3	17.9	18.8	18.1	19.5	19.8		
13	16.5	18.2	19.2	18.8	19.7	19.8		
14	17.1	18.2	18.9	18.8	19.4	19.8		
15	17.6	18.4	19.0	18.8	19.7	20.0		
16	17.7	18.5	19.1	18.3	19.6	19.8		
17	18.3	18.5	18.2	18.7	19.7	20.0		
18	17.4	18.8	18.7	18.6	19.5	19.3		
19	17.8	17.6	18.5	18.6	19.9	20.4		
20	17.3	18.3	18.8	19.1	19.7	20.3		
21	17.8	18.4	18.7	18.5	20.0	20.4		
22	17.9	18.4	18.5	19.2	19.7	18.3		
23	18.1	18.4	18.7	19.4	19.8	18.2		

Table B-III-1. Average Sea Surface Temperature (cont'd)

b) Air Temperature

Each hour of the data from which the air temperature plot shown in Figure B-III-3 was made up from is the average value of up to seven simultaneous measurements of air temperature. This is our method of providing one standard air temperature value for various calculation purposes. The data is made up of data taken on the ship's bow, on towers mounted above the pilot house and from thermometers located on the forward mast. These instruments were operated by NRL, the Naval Postgraduate School and Calspan Corporation. These instruments and their locations are described in Section B-II of this report. The standard deviation of the measured temperature for a typical hour was less than 1 degree Centigrade but on occasion standard deviations on the order of 4 degrees C were observed. Such an average value for air temperature of course masks all real effects of sensor location and of observing techniques. All of the individual specialized data is of course available in the data archive system, the use of which is described in Section D of this report. Table B-III-2 is a printed record of each of the average value of air temperature data that is available for the cruise.

Figure B-III-4 is the frequency distribution of this data in which the y axis is the number of observations of average air temperature within the indicated band and the x axis is the air temperature in degrees C. This curve like that of the sea surface temperature in Figure B-III-2 shows that indeed a broad sampling of thermal conditions were encountered on the EOMET 77 cruise.

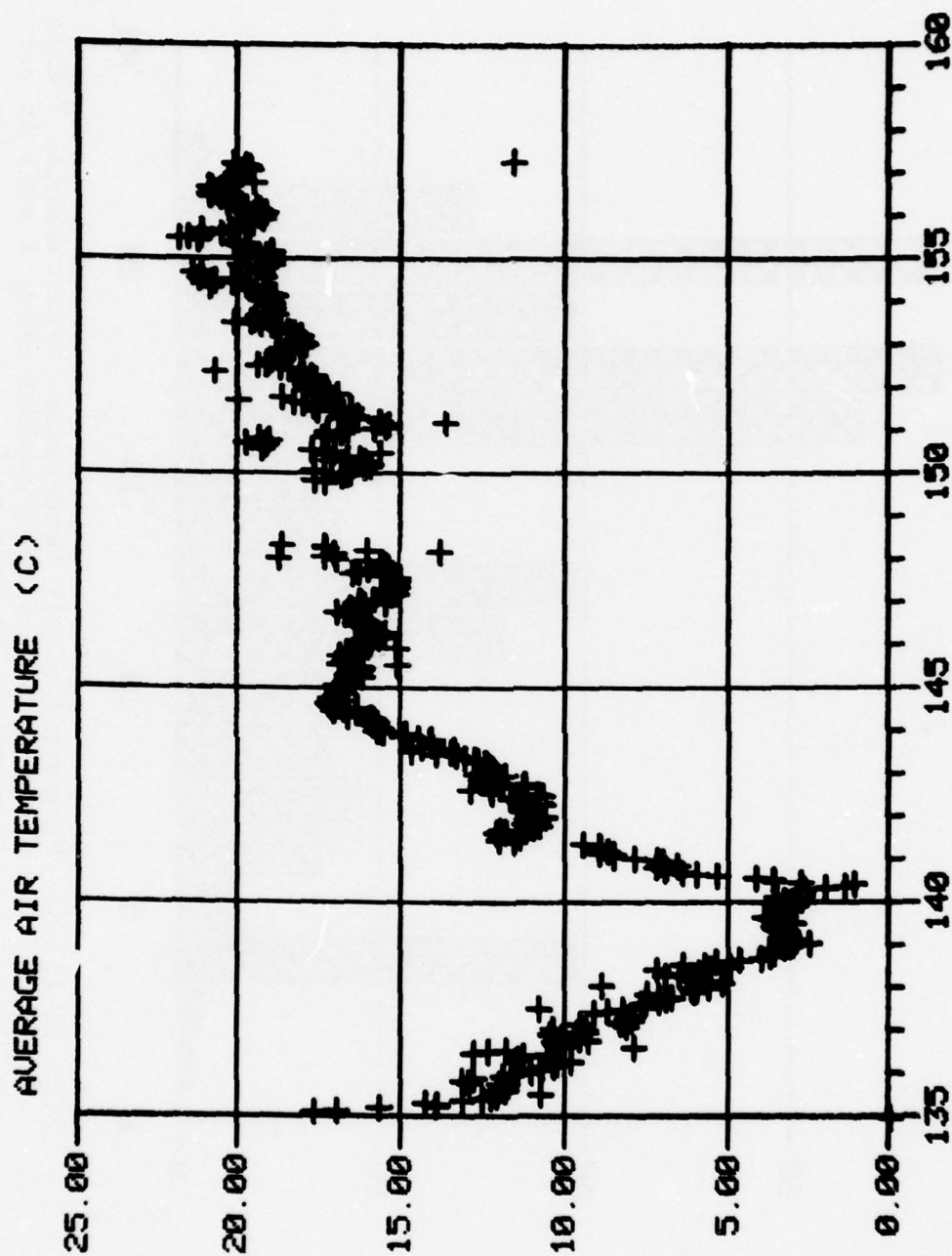


Fig. (B-III-3) Cruise plot of the average air temperature expressed in Celsius vs. time expressed in GMT Julian days.

FREQUENCY OF AIR TEMPERATURE MEASUREMENTS

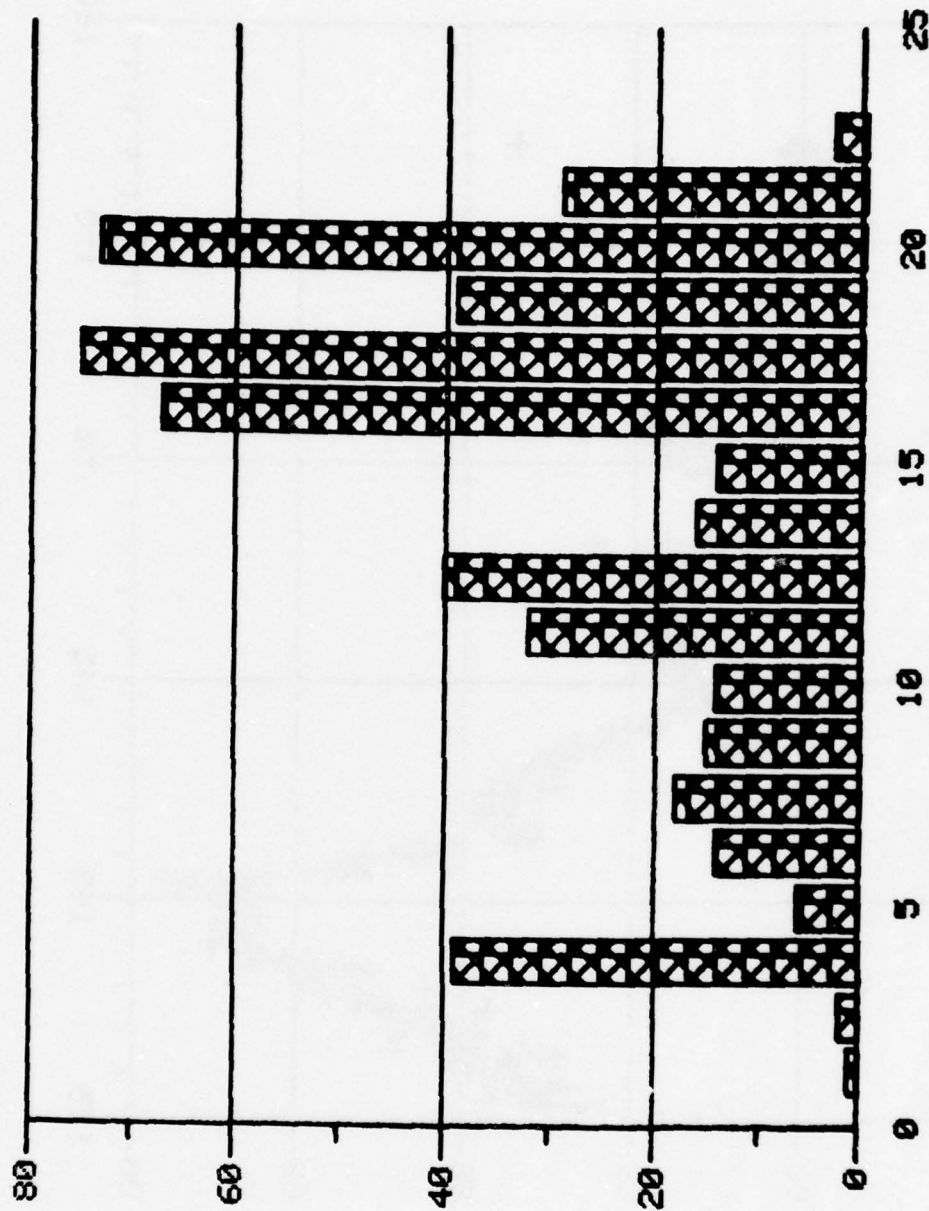


Fig. (B-III-4) Frequency of air temperature measurements; Y axis shows number of observations made; X axis is air temperature in degrees C.

* HOUR	AVERAGE AIR TEMPERATURE (C)									
	5/15/77	5/16/77	5/17/77	5/18/77	5/19/77	5/20/77	5/21/77	5/22/77	5/23/77	5/24/77
0		11.6	9.4	6.1	3.1	3.3	7.2	10.6		
1		11.4	9.4	5.6	3.0	3.3	7.9	11.0		
2		11.0	10.3	5.9	3.2	3.8	8.5	11.1		
3		10.7	8.1	5.2	3.5	5.7	9.0	11.3		
4	17.6	10.7	9.5	5.0	3.2	7.8	8.7	11.1		
5	16.9	10.3	8.8	5.0	3.2	7.7	8.9	11.0		
6	15.6	10.2	8.8	5.0	3.2	7.7	8.9	10.6		
7	13.9	9.9	8.8	5.0	3.2	7.0	9.0	10.7		
8	13.9	10.4	8.7	5.0	3.2	1.4	9.5	11.4		
9	14.2	11.4	9.1	5.2	3.4	1.1	11.5	11.6		
10	13.1	11.3	9.1	5.2	3.5	1.8	12.0	11.5		
11	12.5	10.5	8.7	5.0	3.5	2.3	12.4	10.7		
12	12.3	12.4	8.2	5.0	3.5	3.6	11.4	11.7		
13	12.1	11.8	7.6	5.0	3.5	4.2	11.4	10.8		
14	10.7	7.9	7.7	4.4	3.5	5.0	12.1	12.9		
15	12.0	10.1	7.5	4.7	3.5	6.0	12.8	12.3		
16	11.8	10.3	7.1	4.4	3.5	6.5	12.0	11.2		
17	11.9	10.3	6.6	4.3	3.5	7.0	11.0	12.0		
18	11.8	9.9	6.6	4.3	3.5	7.6	10.8	12.5		
19	12.0	9.9	7.1	4.6	3.5	8.2	11.1	12.1		
20	12.9	10.1	7.5	4.7	3.5	9.2	11.2	12.1		
21	13.2	10.4	7.6	4.7	3.5	7.1	10.8	12.1		
22	12.8	10.4	7.6	4.7	3.5	7.7	11.1	11.8		
23	11.9	9.6	6.6	4.3	3.5	7.0	11.1	11.8		

Table B-III-2. Average Air Temperature

* HOUR	AVERAGE AIR TEMPERATURE (C)									
	5/23/77	5/24/77	5/25/77	5/26/77	5/27/77	5/28/77	5/29/77	5/30/77		
0		15.7	16.9	16.1	16.2	17.0		16.5		
1		15.6	16.9	15.9	16.2	18.7		16.5		
2	12.2	15.6	16.9	15.9	15.8	17.3		17.6		
3	12.2	15.8	16.7	15.9	15.5	17.0		16.1		
4	12.3	15.9	16.6	15.7	15.3	13.8		15.9		
5	12.3	15.7	16.5	15.6	15.1	16.0		15.9		
6	12.4	15.8	16.1	15.5	15.3	17.3		16.1		
7	12.7	15.9	16.3	15.7	15.5	17.3		17.1		
8	12.7	16.6	16.3	15.8	15.2	18.6		16.2		
9	13.0	16.6	16.2	15.9	15.1			16.6		
10	13.3	16.3	16.2	15.9	15.1			17.3		
11	13.9	17.0	16.1	16.3	15.1			15.6		
12	13.5	16.7	16.2	16.3	15.1			17.0		
13	14.6	16.3	15.1	16.0	15.2			17.2		
14	13.4	17.1	16.8	16.2	15.1			19.2		
15	14.4	17.2	16.7	16.2	15.6			19.2		
16	14.0	17.1	16.6	16.4	16.5			19.1		
17	14.1	16.6	16.5	16.7	16.3			19.7		
18	14.1	17.1	16.8	16.9	16.0			19.0		
19	14.1	17.0	16.4	16.4	15.4			19.3		
20	14.4	16.9	16.6	16.3	15.4			17.2		
21	15.0	16.7	16.5	16.1	15.6		17.6			
22	14.8	16.7	15.1	16.1	15.6		17.3			
23	15.5	16.9	16.0	15.4	16.0		16.6			

Table B-III-2. Average Air Temperature (cont'd)

* HOUR	AVERAGE AIR TEMPERATURE (C)									
	5/31/77	6/1/77	6/2/77	6/3/77	6/4/77	6/5/77	6/6/77	6/7/77		
0		17.3	17.9	19.1	18.9	19.6	19.9			
1	15.5	17.7	18.0	19.0	19.1	19.5	19.8			
2	15.4	17.9	18.1	19.0	19.1	19.1	19.6			
3	15.6	17.8	18.1	18.8	18.9	19.3	19.6			
4	15.6	17.9	18.1	19.0	19.0	19.4	19.7			
5	16.5	17.6	18.1	19.2	19.7	19.7	19.9			
6	16.8	17.7	18.2	19.5	19.7	19.3	20.1			
7	16.3	18.0	18.4	19.6	20.0	20.3	20.1			
8	16.5	18.0	18.7	20.8	19.7	20.3	20.3			
9	16.8	20.7	18.7	19.7	20.1	20.5	20.9			
10	16.8	18.4	18.9	20.1	21.2	20.7	20.7			
11	17.5	18.7	19.2	20.7	21.8	20.9	20.7			
12	16.5	19.3	20.1	20.1	21.5	20.7	20.5			
13	17.1	19.1	19.6	21.2	21.1	20.7	20.8			
14	17.6	19.0	19.5	19.2	20.0	20.8	20.9			
15	17.9	19.0	19.2	19.7	20.0	20.3	20.3			
16	18.2	18.6	19.4	21.4	21.1	20.9	20.5			
17	20.0	18.7	18.8	21.1	20.2	20.3	19.5			
18	18.6	18.8	19.2	19.4	19.6	20.2	20.1			
19	17.3	18.5	19.2	19.1	19.5	20.0	20.9			
20	16.9	18.5	18.9	19.9	19.7	20.1	20.1			
21	17.2	18.4	19.0	18.9	19.7	20.9	20.9			
22	17.9	18.0	18.9	19.0	19.2	20.9	20.9			
23	17.3	18.0	18.9	18.9	19.2	19.9	19.9			

Table B-III-2. Average Air Temperature (cont'd)

c) Air-Sea Temperature Difference

The data that is present in Figure B-III-5 is the calculated difference between the air temperature and the sea surface temperature plotted against time throughout the cruise. Each hour of the data from which this plot was obtained represents the arithmetical difference between the average air temperature and the average sea surface temperature for that hour. The average air temperature and the average sea surface temperature data are discussed in Sections B-III-a and B-III-b of this report. This plot shows in a graphic way the areas where the atmospheric boundary layer and the surface waters are not in thermal equilibrium. The cold Nova Scotian coastal waters and the Gulf Stream stand out as significantly affecting the chemical stability of the boundary layer as is seen by large deviations both positively and negatively in this presentation. This same behavior is observable in the plot of Richardson's number in Section B-III-g of this report. The printed version of this calculated data for each hour is presented in Table B-III-3.

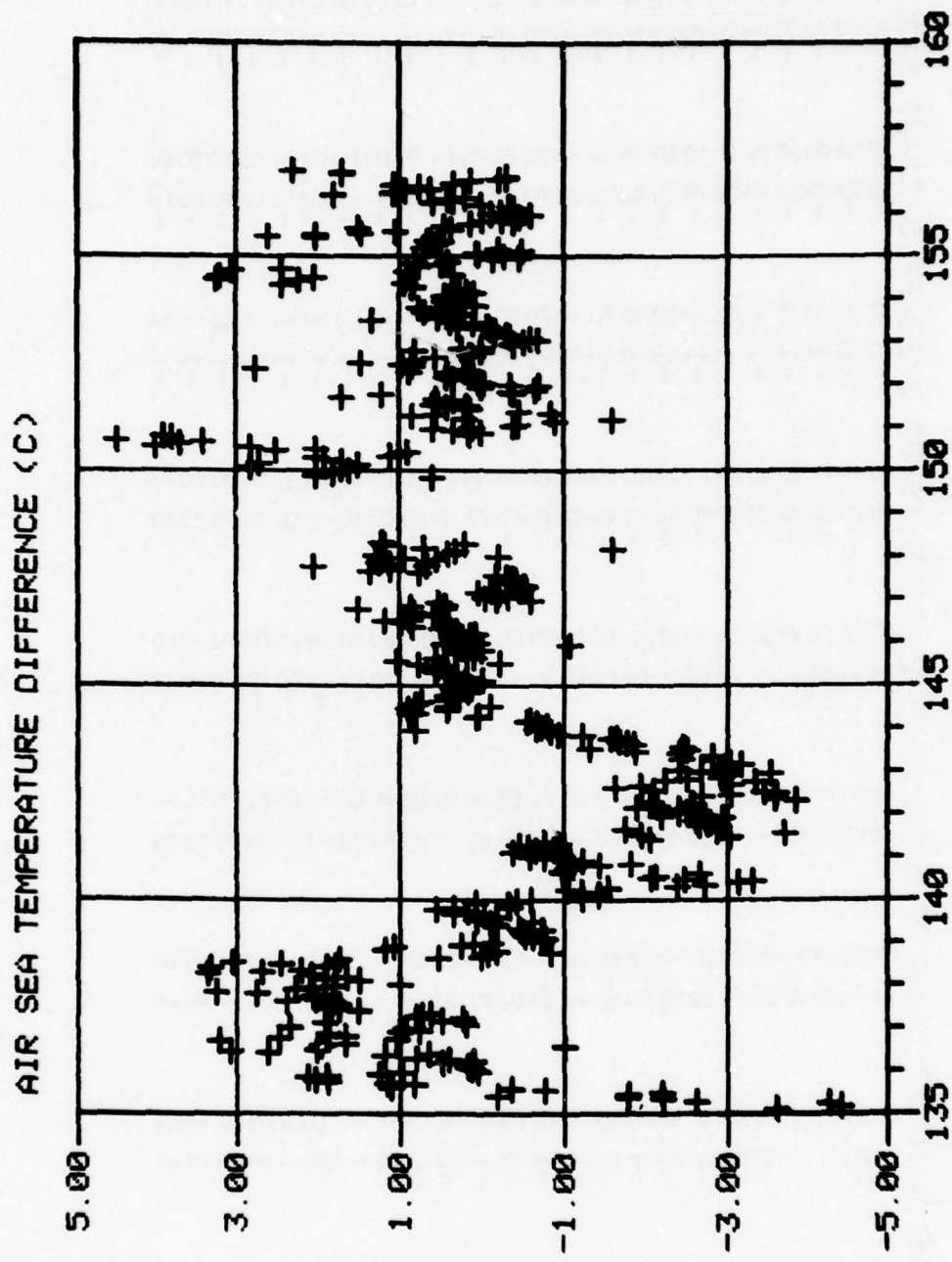


Fig. (B-III-5) Air-sea temperature difference.
Time in Julian day, temperature in degrees C.

* AIR SEA TEMPERATURE DIFFERENCE (C)											
HOUR	5/15/77	5/16/77	5/17/77	5/18/77	5/19/77	5/20/77	5/21/77	5/22/77			
0		1.3	0.8	1.8	0.1	-0.4	-0.8	-2.7			
1	-8.3	1.0	0.9	1.0	-0.1	-0.6	-0.6	-2.4			
2		0.1	2.3	5.2	-0.7	-1.2	-0.9	-2.5			
3		0.1	0.2	1.5	-0.8	-1.4	-0.4	-2.4			
4		0.2	0.9	1.9	-0.6	-1.4	-0.7	-1.9			
5		0.5	0.5	1.7	-0.5	-1.2	-0.9	-2.1			
6		0.5	0.0	2.3	-0.5	-1.1	-0.6	-2.2			
7		0.1	0.0	3.2	-0.5	-1.5	-0.5	-2.3			
8		0.4	0.0	2.7	-0.7	-2.4	-0.8	-3.3			
9		0.8	0.6	2.3	-0.5	-2.7	-2.1	-3.6			
10		1.2	1.5	3.9	-0.2	-3.1	-3.0	-3.7			
11		0.7	1.7	1.8	-0.1	-3.3	-3.0	-3.6			
12		2.6	1.8	5.0	-0.6	-2.1	-1.9	-3.4			
13		3.1	1.8	3.7	-0.1	-2.2	-2.7	-2.1			
14		2.0	1.8	3.0	0.1	-2.7	-2.9	-1.6			
15		-1.0	2.4	0.5	-0.2	-1.7	-1.8	-3.0			
16		1.9	2.0	0.7	0.3	-1.0	1.2	-3.3			
17		1.7	2.2	0.5	0.3	-1.0	2.3	-3.2			
18		3.2	2.1	0.1	0.5	-1.1	3.6	-2.5			
19		1.1	1.9	0.2	0.3	-1.1	2.7	-2.5			
20		2.5	2.3	0.2	0.3	-1.4	2.8	-2.3			
21		1.7	3.3	1.1	-0.3	-1.8	2.6	-2.3			
22		1.9	2.2	1.1	-0.3	-1.2	2.9	-3.3			
23		1.0	2.1	0.3	0.1	-1.1	2.2	-3.5			

Table B-III-3. Air-Sea Temperature Differences

* AIR SEA TEMPERATURE DIFFERENCE (C)									
HOUR	5/23/77	5/24/77	5/25/77	5/26/77	5/27/77	5/28/77	5/29/77	5/30/77	
0	4.0	-0.7	0.3	0.1	-0.2	-0.2		1.6	
1	-2.5	-0.7	0.3	0.3	-0.0	1.3		1.7	
2	-3.5	-0.8	0.2	0.2	-0.3	0.3		1.2	
3	-3.5	-0.7	0.3	0.2	-0.0	0.4		1.2	
4	-3.5	-0.6	0.3	0.1	-0.1	0.5		1.2	
5	-3.2	-0.6	0.2	0.1	-0.1	0.7		1.1	
6	-2.2	0.1	0.3	0.3	-0.5	0.9		1.2	
7	-2.2	0.1	0.4	0.4	-0.5	1.0		1.0	
8	-2.2	0.0	0.6	0.5	-0.4	0.9		1.0	
9	-2.2	0.0	0.6	0.4	-0.4	0.5		0.9	
10	-2.2	0.0	0.5	0.4	-0.4	0.5		0.9	
11	-1.2	0.0	0.5	0.4	-0.4	0.5		0.9	
12	-1.2	0.0	0.5	0.4	-0.4	0.5		0.9	
13	-1.2	0.0	0.5	0.4	-0.4	0.5		0.9	
14	-1.2	0.0	0.5	0.4	-0.4	0.5		0.9	
15	-1.2	0.0	0.5	0.4	-0.4	0.5		0.9	
16	-1.2	0.0	0.5	0.4	-0.4	0.5		0.9	
17	-1.2	0.0	0.5	0.4	-0.4	0.5		0.9	
18	-1.2	0.0	0.5	0.4	-0.4	0.5		0.9	
19	-1.2	0.0	0.5	0.4	-0.4	0.5		0.9	
20	-1.2	0.0	0.5	0.4	-0.4	0.5		0.9	
21	-1.2	0.0	0.5	0.4	-0.4	0.5		0.9	
22	-1.2	0.0	0.5	0.4	-0.4	0.5		0.9	
23	-1.2	0.0	0.5	0.4	-0.4	0.5		0.9	

7.4
0.6
2.0
1.0
2.0

Table B-III-3. Air-Sea Temperature Differences (cont'd)

* HOUR	AIR SEA TEMPERATURE DIFFERENCE (C)						
	5/31/77	6/1/77	6/2/77	6/3/77	6/4/77	6/5/77	6/6/77 6/7/77
0		-0.4	-0.5	0.4	-0.3	-0.1	2.3
1	-0.4	-0.0	-0.7	0.4	-0.1	-0.2	
2	-0.5	-0.0	-0.6	0.5	0.1	-0.4	
3	-0.9	0.3	-0.3	0.1	0.5	-0.4	
4	-1.6	0.4	-0.3	0.2	0.2	-0.5	
5	0.2	0.1	-0.2	0.3	0.7	0.6	
6	0.9	0.4	-0.2	0.0	0.6	0.4	
7	0.6	0.9	-0.1	0.4	0.6	0.4	
8	-0.9	0.2	-0.3	0.2	0.5	0.2	
9	-0.5	0.0	-0.1	0.3	0.7	0.0	
10	0.2	0.2	-0.0	0.2	0.2	1.1	
11	0.4	0.5	0.0	0.3	0.5	1.1	
12	0.2	0.5	0.4	0.2	0.5	0.6	
13	0.6	0.0	0.4	0.2	1.4	0.0	
14	0.5	0.0	0.5	0.4	0.5	0.0	
15	0.3	0.6	0.0	0.1	0.5	1.3	
16	0.5	0.1	0.0	0.5	0.5	1.2	
17	0.5	0.1	0.0	0.0	0.5	0.5	
18	1.2	0.0	0.0	0.0	0.0	0.0	
19	2.4	0.0	0.0	0.0	0.0	0.0	
20	4.4	0.0	0.0	0.0	0.0	0.0	
21	7.0	-0.0	0.0	0.0	0.0	0.0	
22	0.7	-0.0	0.0	0.0	0.0	0.0	
23		-0.0	0.0	0.0	0.0	0.0	

Table B-III-3. Air-Sea Temperature Differences (cont'd)

d) Relative Humidity

The data shown in Figure B-III-6 represents average values of relative humidity obtained by the various methods and presented here as the representative relative humidity data for the cruise. This data is calculated from 7 different measurements that were made throughout the cruise. The various measurements of relative humidity are listed below:

	<u>ORGANIZATION</u>	<u>METHOD</u>	<u>DATA FORMAT IN ARCHIVE</u>
1)	NRL (tower)	Dewpoint	Dewpoint, temperature
2)	Calspan (bow)	Lithium Chloride	Dewpoint, temperature
3)	Calspan (mast)	Lithium Chloride	Dewpoint, temperature
4)	Calspan (tower)	Sling Psychrometer	Dry bulb temperature, wet bulb temperature
5)	NRL (deck)	Psychrometer	Dry bulb temperature, wet bulb temperature
6)	NPS (bow)	Lithium Chloride	Relative humidity
7)	NPS (mast)	Lithium Chloride	Relative humidity

Each set of humidity measurements were converted into relative humidity values for comparison purposes and then for each hour, up to seven calculations of relative humidity are available. The average value of these calculations is then presented as the representative relative humidity for that particular hour on the cruise. The error between the simultaneous measurements of relative humidity is shown in Figure B-III-7 by the frequency distribution of the standard deviation of these values for each hour. It shows that for most cases, the calculations had a standard

deviation of about 6 to 7% relative humidity. On special occasions however the standard deviation went up to 20% relative humidity. The individual measurements of the particular instruments are available in the data archive.

Figure B-III-8 is the frequency distribution of the relative humidity measurements from the EOMET 77 cruise. It shows that the relative humidities are quite sharply centered about 85%. The printed version of the hourly representative relative humidity data is presented in Table B-III-4.

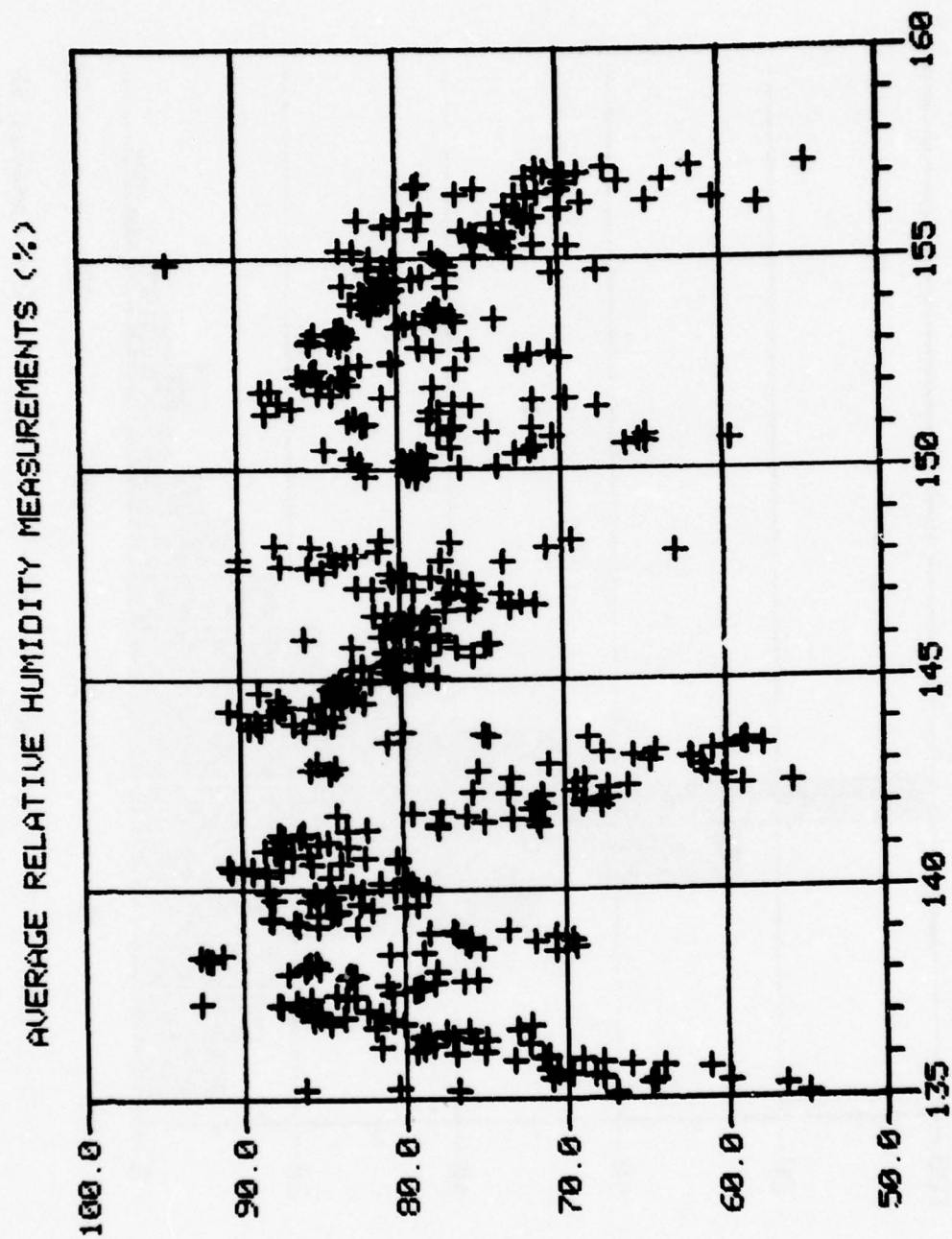


Fig. (B-III-6) Average relative humidity measurements.
Julian date vs. RH (%).

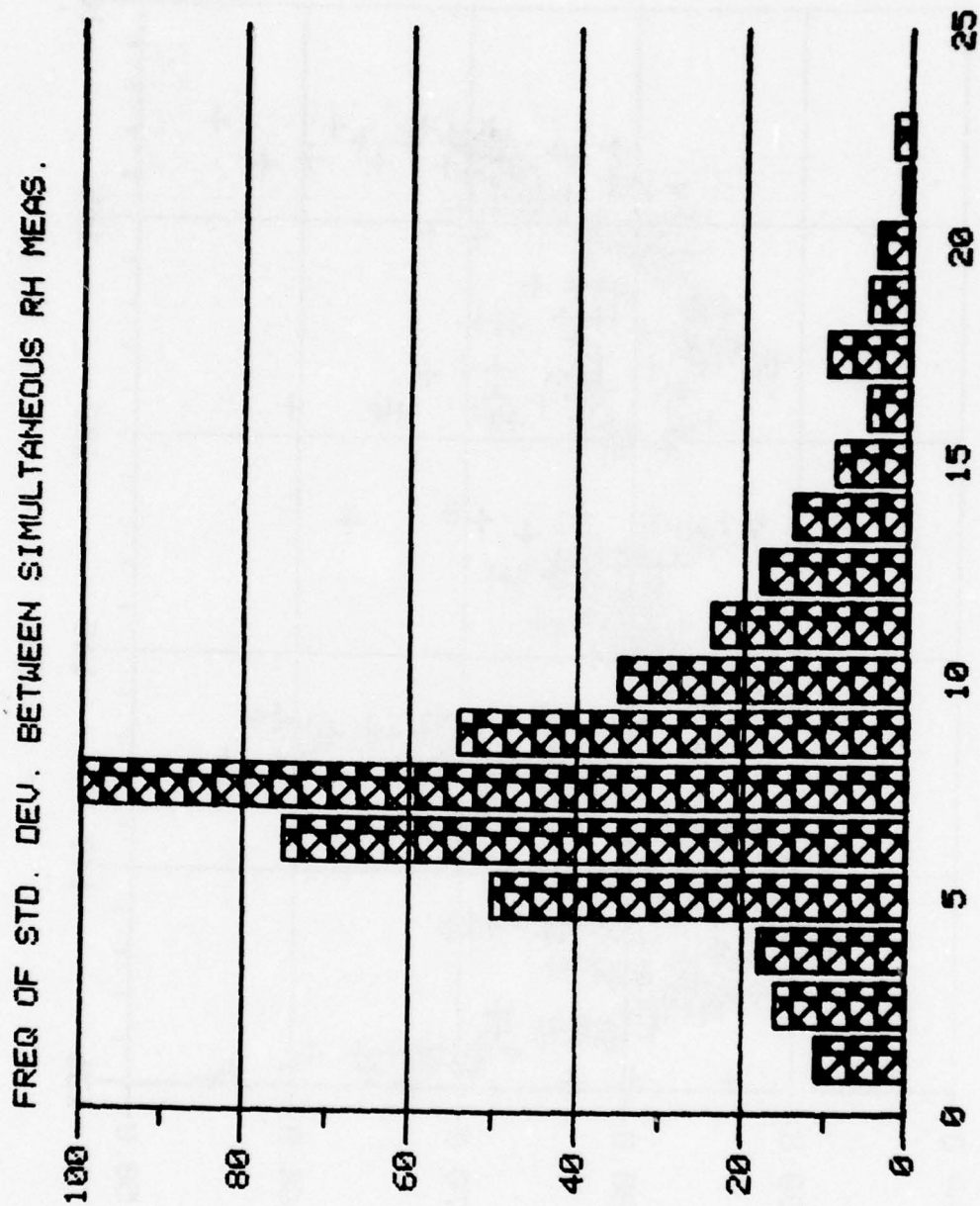


Fig. (B-III-7) Frequency of std. dev. between simultaneous RH measurements.

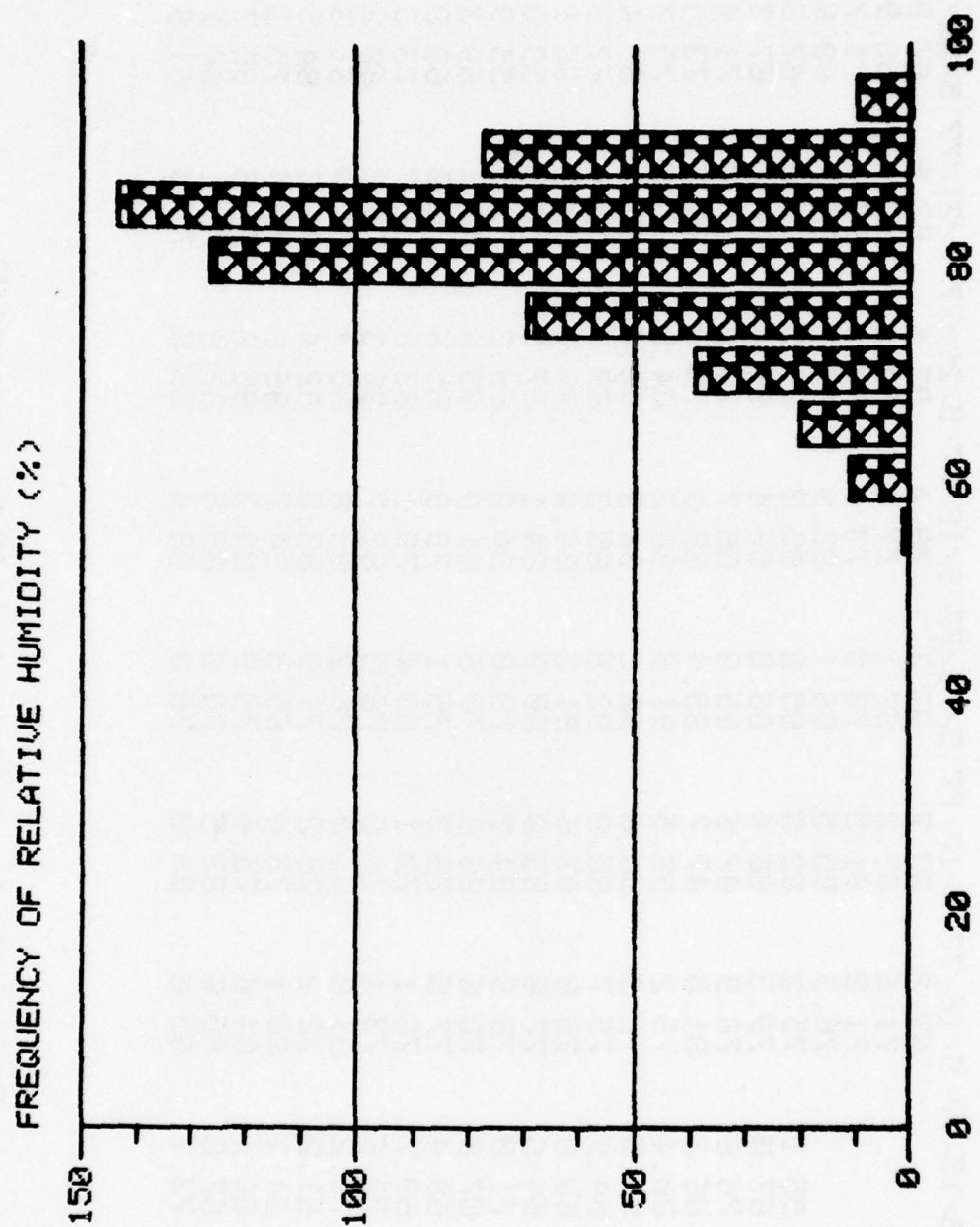


Fig. (B-III-8) Frequency of relative humidity.

* HOUR	AVERAGE RELATIVE HUMIDITY (PERCENT)										
	5/15/77	5/16/77	5/17/77	5/18/77	5/19/77	5/20/77	5/21/77	5/22/77			
0		69.2	83.7	83.3	78.4	82.6	87.9	67.8			
1		71.6	85.2	87.1	77.0	80.5	87.5	68.9			
2		71.2	81.5	78.0	73.6	78.5	83.4	71.7			
3		76.9	85.5	86.1	82.9	83.3	85.2	68.8			
4	55.1	75.2	82.3	85.2	85.3	79.5	84.6	67.8			
5	67.0	79.3	86.4	86.0	86.4	81.4	87.4	67.3			
6	76.8	78.9	87.6	85.8	86.7	79.9	87.3	71.4			
7	86.2	81.5	87.7	85.4	86.7	79.9	86.3	73.5			
8	80.4	78.2	92.5	91.9	88.1	84.5	87.5	75.7			
9	56.5	72.3	86.6	92.2	88.2	88.4	86.1	69.4			
10	64.9	75.7	85.8	92.6	85.3	89.3	83.4	67.3			
11	60.0	75.0	83.6	91.2	84.4	90.7	82.2	66.1			
12	64.6	77.0	83.0	89.9	84.1	87.5	77.8	59.0			
13	71.0	78.9	84.2	78.8	84.0	89.3	71.5	55.9			
14	67.8	78.6	80.8	79.6	81.9	90.8	77.8	69.3			
15	68.4	77.5	79.3	75.1	79.9	85.6	75.0	68.8			
16	69.7	76.1	79.1	69.4	79.1	83.8	71.7	69.3			
17	70.6	73.1	79.0	76.0	82.7	89.3	73.2	69.2			
18	71.2	81.8	81.0	76.2	85.8	89.4	76.0	61.3			
19	61.2	72.2	78.2	71.9	88.0	82.4	84.0	84.5			
20	64.1	80.1	76.4	69.5	84.7	86.8	79.4	75.3			
21	66.1	84.6	75.4	75.9	84.3	85.8	77.6	85.7			
22	67.8	80.8	83.5	70.6	85.5	87.9	72.1	84.1			
23	73.3	85.6	83.0	76.8	88.4	88.5	71.3	61.6			

Table B-III-4. Average Hourly RH Measurement (%)

* HOUR	AVERAGE RELATIVE HUMIDITY (PERCENT)									
	5/23/77	5/24/77	5/25/77	5/26/77	5/27/77	5/28/77	5/29/77	5/30/77	5/31/77	
0		89.0	80.4	78.6	75.8	84.3		78.2		
1	85.2	84.8	80.1	81.1	73.8	63.0		76.2		
2	64.7	85.1	77.8	77.5	77.0	81.3		73.9		
3	62.2	84.2	78.7	79.3	79.1	71.0		82.4		
4	62.3	88.1	80.4	80.4	81.7	85.5		79.2		
5	65.8	90.0	80.8	80.1	82.6	87.6		79.7		
6	67.7	90.7	82.9	80.0	75.6	76.8		82.9		
7	64.3	87.6	82.3	80.9	76.5	69.4		78.3		
8	60.9	85.6	82.3	79.8	76.9	81.2		78.7		
9	60.1	87.2	80.9	78.5	80.5			72.8		
10	57.7	84.8	80.7	79.3	78.1			71.9		
11	58.8	82.3	80.5	78.3	79.8			84.5		
12	59.0	83.6	79.1	79.2	79.7			76.8		
13	80.9	87.6	80.4	81.5	80.6			71.5		
14	58.8	83.0	75.5	80.7	84.7			66.0		
15	68.5	83.8	78.3	77.2	89.9			64.7		
16	74.7	83.4	80.9	75.7	85.7			65.1		
17	74.9	88.8	79.4	73.2	87.3			59.5		
18	79.9	83.4	76.5	71.7	83.9		78.9	70.4		
19	86.0	84.4	82.9	73.3	73.6		82.0	64.7		
20	88.7	83.2	74.7	72.5	77.5		79.4	77.4		
21	89.4	84.1	74.5	75.4	89.9		78.8	74.5		
22	84.3	83.7	77.6	77.3	83.3		79.3	76.7		
23	86.6	81.8	85.9	75.7	82.7			71.8		

Table B-III-4. Average Hourly RH Measurement (%)

* HOUR	AVERAGE RELATIVE HUMIDITY < PERCENT >							
	5/31/77	6/1/77	6/2/77	6/3/77	6/4/77	6/5/77	6/6/77	6/7/77
0		83.0	84.1	80.6	81.6	71.5	69.6	
1	82.2	85.8	85.4	80.7	72.9	72.4	68.8	
2	81.9	84.7	83.4	81.4	75.1	78.5	70.8	
3	83.0	83.3	83.0	82.0	77.7	72.6	71.3	
4	78.1	83.5	83.7	82.2	82.6	70.0	67.1	
5	82.6	86.1	85.2	80.5	83.5	69.8	61.8	
6		85.3	83.8	73.3	73.3	54.6		
7	88.2	85.2	83.8	81.5	69.4	57.7		
8	77.5	85.0	83.4	76.9	71.5	68.5		
9	77.9	76.4	79.9	83.3	73.6	64.6		
10	86.5	83.1	79.5	80.9	75.2	60.5		
11	67.6	82.3	78.9	80.6	74.0	72.0		
12	75.5	80.3	76.4	79.0	73.3	72.6		
13	76.6	80.4	77.7	80.5	75.0	76.3		
14	87.3	72.6	74.0	78.9	75.3	71.2		
15	71.6	70.0	76.6	76.9	73.3	69.9		
16	69.6	72.6	77.9	70.4	75.9	75.2		
17	80.9	71.8	81.7	67.7	78.7	78.9		
18	84.1	70.6	77.4	81.7	80.7	78.6		
19	84.9	77.9	77.6	80.7	80.7	69.7		
20	88.4	75.6	81.5	77.0	74.1	66.3		
21	87.8	78.7	82.0	94.4	72.1	72.0		
22	77.9	83.5	82.8	77.3	82.4	69.9		
23	84.0	85.5	81.7	80.1	79.8			

Table B-III-4. Average Hourly RH Measurement (%)

e) Real Wind (Speed and Direction)

The calculation of the real wind speed and direction from measurements aboard a moving ship requires the simultaneous knowledge of four shipboard measurements. They are the relative wind speed as measured from an anemometer located on the moving ship, the direction of the apparent wind relative to the bow of the ship, the true speed of the ship and the heading of the ship. While direct measurements of the relative wind speed and direction and the ships heading are easily and accurately obtained, the speed of the ship relative to a fixed reference point is difficult to make because of the problems of ocean currents and other effects on the ship. Consequently the data on ships speed used for this cruise was obtained by means of calculating it from accurately obtained ships positions. This approach assumes that the average speed of the ship between two nearby positions as obtained by dividing the distance between the two points by the elapsed time required to traverse the distance between the points is a good approximation of what the ship was actually doing as it traversed the track between the two points. This assumption is adequate if the ship maintained a constant heading and propeller rpm between the two measurement points.

Figure B-III-9 shows in two plots the values of the true wind and its direction as a function of time for the cruise. The upper plot shows calculated values of real wind direction. In this curve winds from the north have a value of either 0 or 360 degrees as measured along the ordinate of the plot while east winds have a value of 90 degrees. The lower curve is a plot of wind speed as measured in meters per second along the ordinate

and time along the x axis is measured in Julian days. A periodic fluctuation in this parameter is indicative of large scale air mass structures moving across the North Atlantic. Figure B-III-10 is the frequency distribution of the real wind speed calculations. Tables B-III-5 and B-III-6 contain the hourly calculations of real wind speed and real wind direction respectively.

EOMET 77 WNDPLOT JULIAN DAY 135=15 MAY 1977

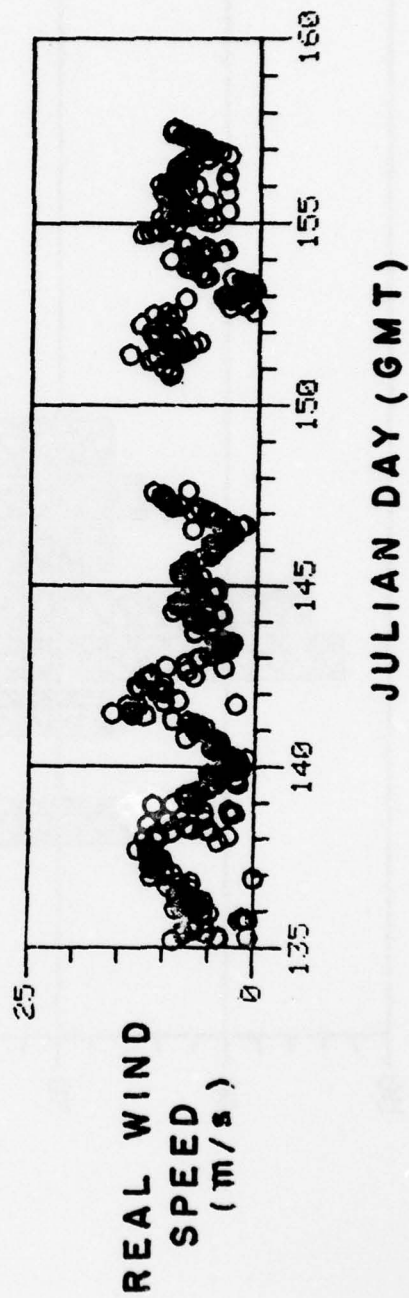
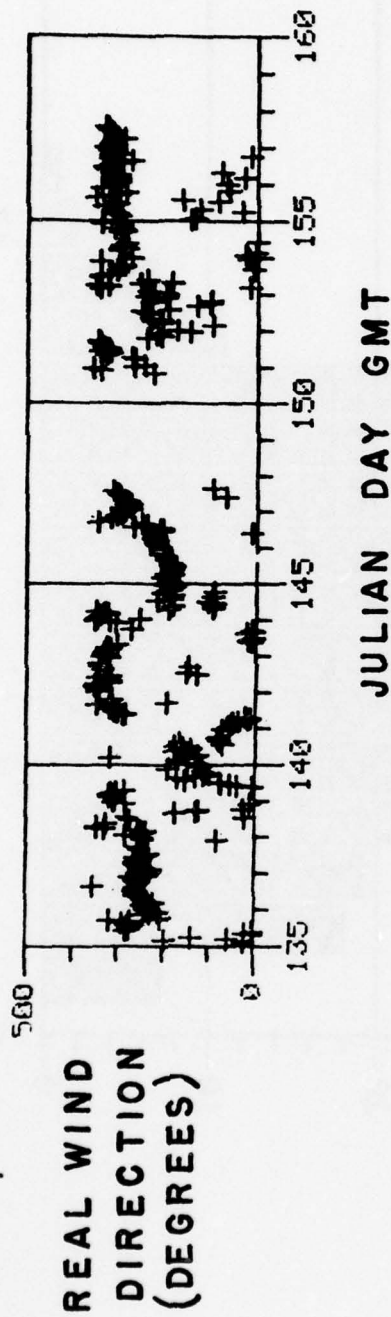


Fig. (B-III-9) Real wind direction and real wind speed.

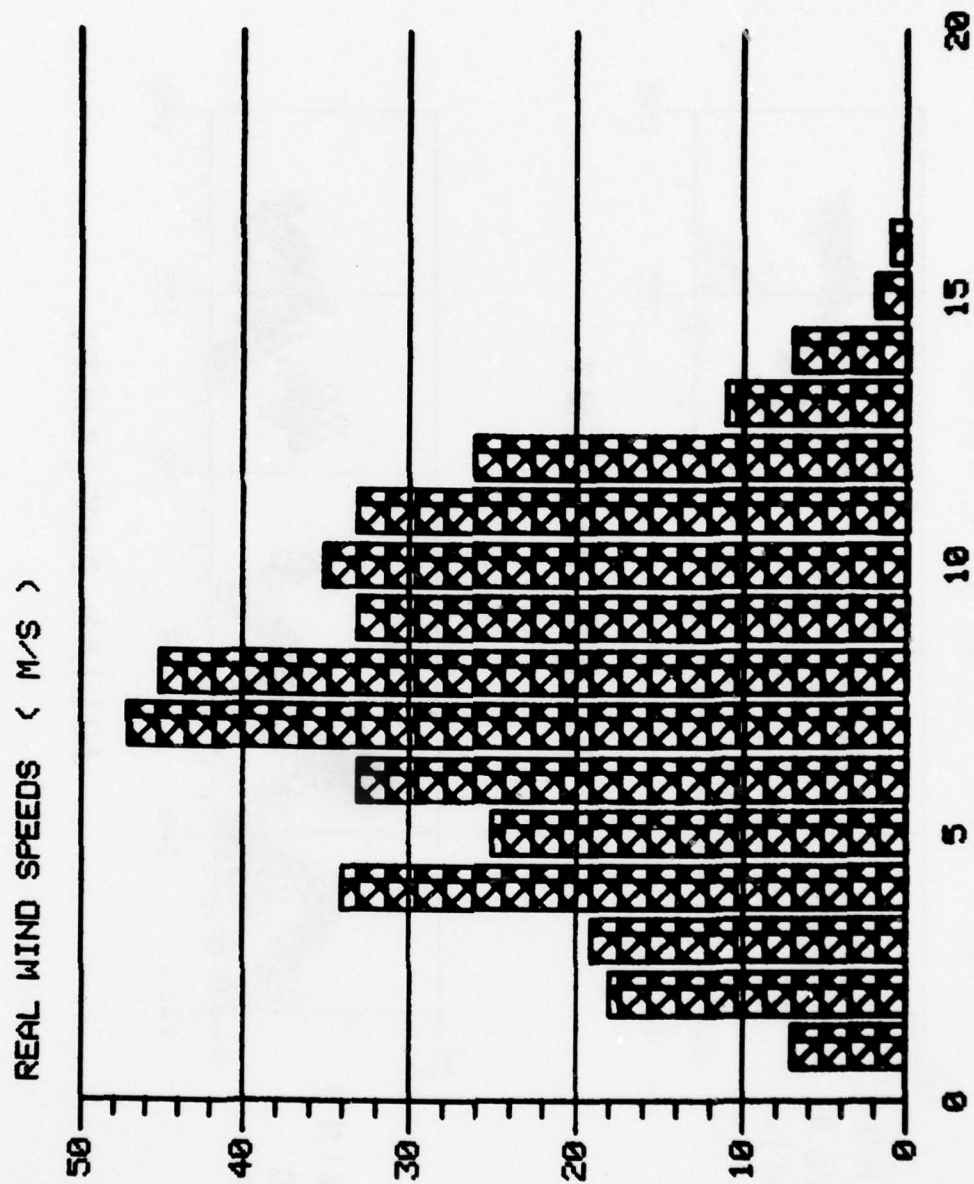


Fig. (B-III-10) Frequency distribution of real wind speeds (m/s).

* REAL WIND SPEED CALCULATIONS (M/S)											
HOUR	5/15/77	5/16/77	5/17/77	5/18/77	5/19/77	5/20/77	5/21/77	5/22/77			
0		5.5	9.8	12.1	6.7	2.0	6.1	11.8			
1		7.4	8.9	10.6	6.4	1.9	6.7	10.2			
2		8.7	9.9	2.9		2.0	5.6	11.0			
3		8.1	9.9	10.5	7.2	1.7	6.8	10.5			
4		7.6	11.2	9.3	7.7		6.4	12.9			
5	8.9	6.7	11.3	4.8	7.7	1.0	7.6	12.8			
6	4.0	6.1	11.4	5.3	7.1	2.4	7.4	13.1			
7	3.7	5.5	11.0	6.8	6.4	3.6	9.2	10.3			
8	0.5	6.8	10.9	7.5	6.4	3.0					
9	7.7	8.5	10.5	11.7	5.2	4.0	12.2	11.9			
10	5.1	7.7	10.1		5.3	3.7	13.5	12.4			
11	7.7	7.2	10.9		4.7	4.5	13.8	12.0			
12	6.6		11.4	9.5	4.3	4.8	13.8	12.7			
13	6.8		11.1	5.2	4.9	3.9	13.5				
14	6.6	7.7	11.3	8.8	2.0	4.5	5.5	7.7			
15	6.9	7.0	11.7	7.2	2.1	4.2	13.0				
16		9.4		7.2	4.1	3.8	14.1	10.8			
17	5.4		12.8	5.7	4.6		2.1	11.0			
18	1.5	8.1	11.7		5.2	4.7	10.3				
19	0.5	6.8		2.7	5.1		8.5	7.9			
20	1.2				2.1						
21				11.1	1.6	6.5	11.2	6.5			
22	5.8	0.0	4.0	9.0							
23	4.8	11.3	10.8								

Table B-III-5. Average Wind Speed (hourly)

* REAL WIND SPEED CALCULATIONS	< M/S >									
HOUR	5/23/77	5/24/77	5/25/77	5/26/77	5/27/77	5/28/77	5/29/77	5/30/77		
0		6.7	6.7	4.6	5.6					
1		7.1	7.4		7.1					
2	5.1	6.2	7.0	4.6	5.6					
3	3.8	3.9	7.0	5.1	6.4					
4	3.8	4.2	7.4	3.9	9.4					
5	3.5	5.5	6.1		8.7					
6	3.9	4.0	7.1	5						
7		9.3	7.9	3.8	9.9					
8	3.8	7.3	8.5	3.8	10.2					
9	2.5	7.4	8.5	2.8	10.2					
10	4.4	7.7	8.6	3.6	13.8					
11	3.9	8.9	8.4	2.5	13.8					
12		8.3	7.9	3.7	10.4					
13		8.9		3.8						
14		8.1	7.9	7.1	11.4					
15	4.9	8.0		1.8						
16	4.9	7.6	7.5	1.4						
17	6.8		6.6	3.2						
18		6.6	6.6							
19		5.0		3.9						9.8
20		4.4	5.2	5.1						9.7
21	5.1	4.5	5.2	4.6						
22	6.4	4.4	5.2							
23		6.3								9.7

Table B-III-5. Average Wind Speed - Hourly (cont'd)

* REAL WIND SPEED CALCULATIONS	(M/S)								
HOUR	5/31/77	6/1/77	6/2/77	6/3/77	6/4/77	6/5/77	6/6/77	6/7/77	
0		11.9	3.5	9.9	10.3	7.0	5.7		
1	10.5		2.4		5.2	11.0	6.3		
2			2.1	8.0	6.0	10.3	6.5		
3		10.6	1.2	6.4	11.0	9.6	6.3		
4		10.9	0.6	5.4	8.5	3.7	6.3		
5	12.0	13.0	0.9	4.1	7.6	8.1	7.5		
6	11.9	10.5	1.8	3.7	8.0	9.0	6.4		
7			1.2	5.9	10.6	3.5	7.0		
8	11.3	9.9	0.9	6.4	8.5	8.0	7.9		
9	14.1		2.0	8.0	9.1	9.7	8.3		
10	9.4				10.3	9.3	9.7		
11	8.4	11.5	3.0		10.1	8.5	9.4		
12	8.1	9.3	6.1			9.1	9.4		
13	9.1	10.1	5.7			7.4	9.0		
14		0.6							
15	7.4	3.3	6.3		5.4	8.1			
16			6.3		9.2	8.4			
17	6.6			12.2	9.7				
18		1.7	7.5	11.0	9.5	5.9			
19	9.4	1.5	8.1	11.6	10.7	3.4			
20	11.4	1.4		9.6	8.2	7.0			
21	10.5	3.1	7.2	11.9	10.1	4.4			
22	11.7	8.2		9.5	9.6	5.2			
23	11.1	4.0	7.5		10.1	5.2			

Table B-III-5. Average Wind Speed - Hourly (cont'd)

* HOUR	REAL WIND DIRECTIONS (DEGREES)									
	5/15/77	5/16/77	5/17/77	5/18/77	5/19/77	5/20/77	5/21/77	5/22/77	5/23/77	5/24/77
0		210	245	247	309	131	71			
1		232	253	256	305	148	59	345		
2		236	229	284		172	57	343		
3		241	227	246	317	170	52	347		
4		246	239	238	312		49	350		
5	20	235	247	255	319	316	38	350		
6	194	220	254	329	314	132	18	348		
7	58	230	260	347	302	125	11	317		
8	136	242	262	347	286	150				
9	4	250	254	326	7	178	288	327		
10	21	261	250		40	167	283	345		
11	2	260	259		54	141	300	318		
12	279		244	272	73	156	309	151		
13	271		236	24	77	178				
14	270	262	232	279	154	72	317	333		
15	276	261			172	166	310			
16		353	250	175	131	80	345	147		
17	289		251	129	114		194	339		
18	271		255	124		82				
19	316	254		27	109	79	320	339		
20	205	261			115		313			
21					191					
22	242	270	84	11	119	57		320		
23	228	235	244	283						

Table B-III-6. Average Wind Direction (hourly)

* HOUR	5/23/77	5/24/77	5/25/77	5/26/77	5/27/77	5/28/77	5/29/77	5/30/77
0		350	193	208	290			
1		254	187		289			
2	331	348	190	217	275			
3	328	341	190	220	276			
4	323	324	205	216	286			
5	317	332	191		273			
6	325	349	184	227				
7		192	198	221	280			
8	304	94	186	224	286			
9		183	187	10	66			
10	16	91	183	210	296			
11	12	94	188	205	299			
12	7	106	181	205	304			
13		218		210				
14		186	187	268	312			
15	19	93		240	95			
16	6	183	196	250				
17	9			345				
18	270	206	197					
19		92						
20		189	210	317				227
21		185	208	306				341
22	307	180	211	297				
23	321	197		295				357

Table B-III-6. Average Wind Direction - Hourly (cont'd)

* HOUR	5/31/77	6/1/77	6/2/77	6/3/77	6/4/77	6/5/77	6/6/77	6/7/77
0		175	198	274	299	66	334	
1	246		228		146	313	324	
2			236	27	137	299	324	
3		97	343	4	299	300	317	
4		211	16	300	306	29	313	
5	266	208	326	300	309		315	
6	270	211	351	284	35	304	288	
7			253	296	317	319	311	
8	328	231	187	294	126	76	312	
9	319		241	285	338	330	314	
10	343			1	316		316	
11	327	237	342		305	336	324	
12	322	240	342		311	322		
13	334	252	323			317		
14		195				295	326	
15	342		305		162	274	331	
16		131	9	299	352	322	0	
17	345			288	301			
18		103	302	292	302	15		
19	239	231	292	312	287	324		
20	208	100		298	61	305		
21	221	199	342	296	339	327		
22	216	244		341	315	310		
23	147	199	21		316	312		

Table B-III-6. Average Wind Direction - Hourly (cont'd)

f) Friction Velocity

One micrometeorological parameter of interest to boundary layer studies is the friction velocity. The friction velocity is a parameter which is related to the mean velocity profile and to the eddy diffusivity of momentum. The values shown plotted in Figure B-III-11 are those calculated from measurements by the NPS during the EOMET cruise of the USNS Hayes. A description of the instrumentation and some definition of terms and relationships are discussed in Section B-II-c of this report. In the figure, the ordinate scale of the friction velocity values is meters per second. The X axis is of course the time of the measurement expressed in Julian days. Table B-III-7 is an hourly listing of the NPS calculations of friction velocity.

NAVAL POSTGRADUATE SCHOOL FRICTION VELOCITY

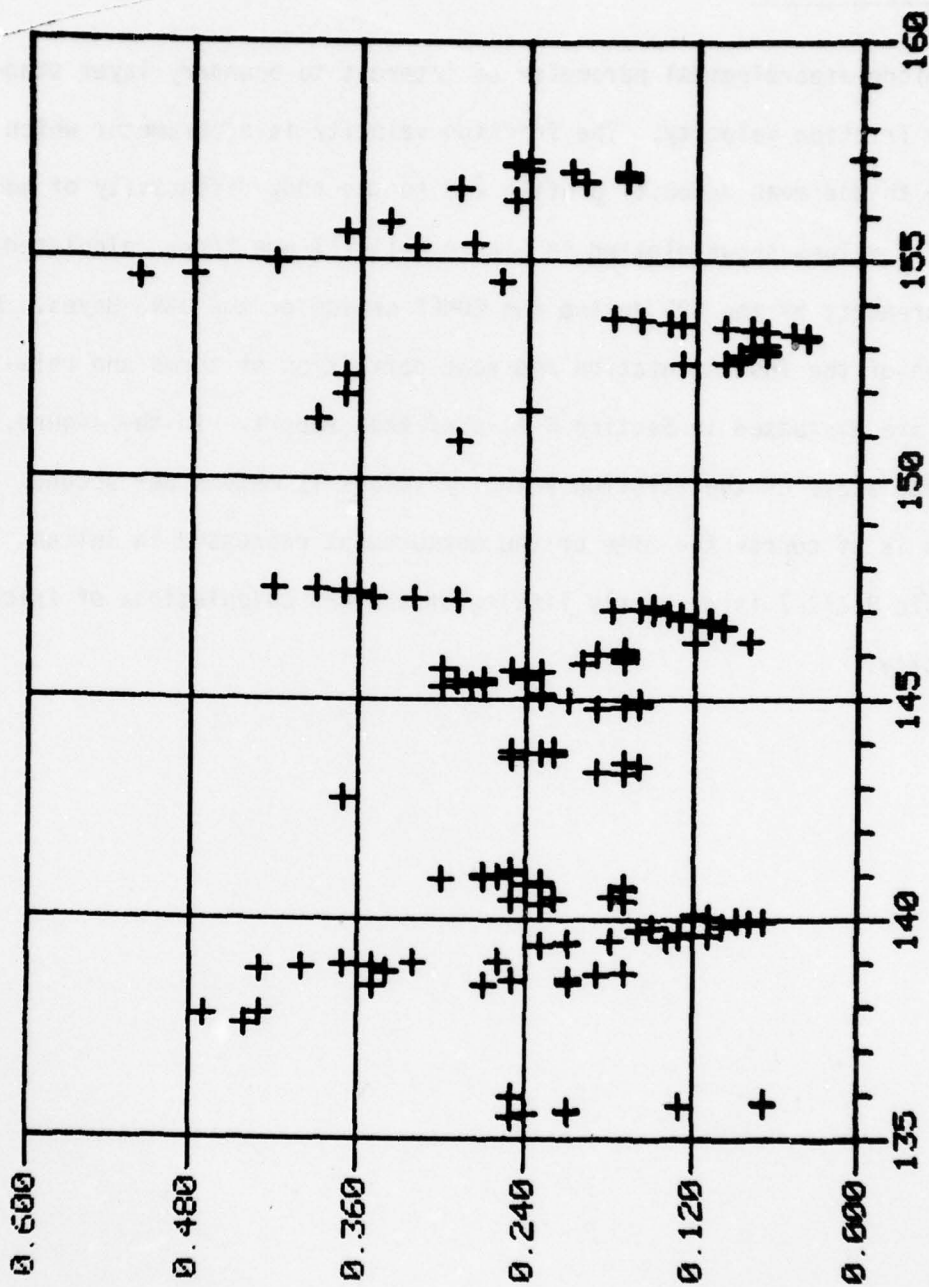


Fig. (B-III-11) Friction velocity; X axis-Julian days; Y axis is meters/sec.

* NAVAL POSTGRADUATE SCHOOL	FRICTION VELOCITY (M/S)			
HOUR	5/15/77	5/16/77	5/17/77	5/18/77
0	0.25	0.37	0.09	0.26
1		0.32	0.11	0.27
2		0.26	0.11	0.25
3			0.12	0.25
4				
5				
6				
7				
8				
9				
10		0.23	0.23	0.17
11		0.21	0.17	0.25
12		0.21	0.22	0.18
13		0.18		
14		0.14		
15	0.25	0.13		
16	0.24	0.11		
17	0.21	0.13		
18	0.21	0.16	0.17	0.37
19	0.13		0.17	
20	0.07	0.15	0.23	
21	0.07	0.10	0.24	
22		0.08	0.23	
23		0.07	0.30	

Table B-III-7. Friction Velocity Hourly Listing

* HOUR	5/23/77	5/24/77	5/25/77	5/26/77	5/27/77	5/28/77	5/29/77	5/30/77
0			0.21	0.17	0.15			
1			0.24	0.19	0.18			
2			0.23	0.17	0.16			
3			0.23	0.17	0.15			
4								
5								
6								
7								
8								
9	0.19		0.30	0.12	0.29			
10			0.28	0.08	0.32			
11			0.27		0.35			
12	0.16		0.29		0.36			
13			0.27		0.37			
14	0.17		0.24		0.39			
15					0.42			
16			0.24					
17			0.23	0.10				
18			0.25	0.10				
19			0.30	0.11				
20	0.25	0.19		0.11				
21	0.22	0.17	0.20	0.13				
22	0.23	0.16	0.17	0.13				
23	0.22	0.16	0.17	0.13				
		0.16		0.14				
								0.29

Table B-III-7. Friction Velocity Hourly Listing (cont'd)

AD-A065 267

NAVAL RESEARCH LAB WASHINGTON D C
THE EOMET CRUISE OF THE USNS HAYES: MAY - JUNE 1977.(U)
JAN 79 S G GATHMAN, B G JULIAN
NRL-MR-3924

F/G 4/2

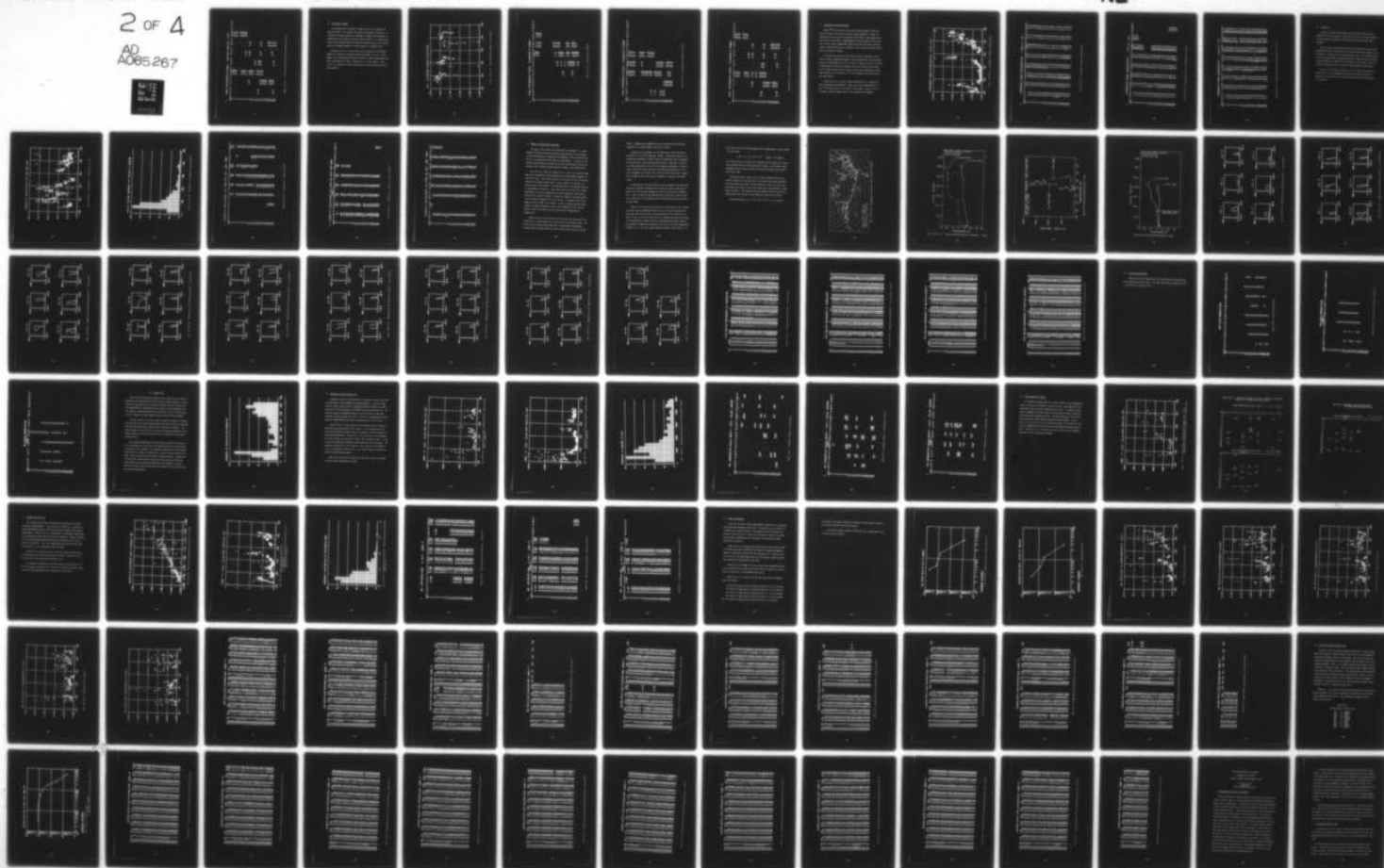
UNCLASSIFIED

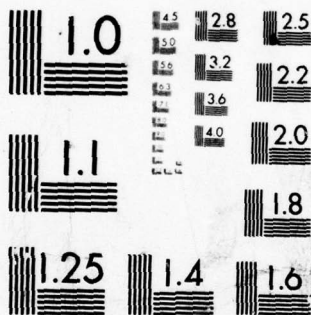
2 OF 4

AD
A065 267



NL





MICROCOPY RESOLUTION TEST CHART
NATIONAL BUREAU OF STANDARDS-1963-A

* NAVAL POSTGRADUATE SCHOOL	FRICTION VELOCITY (M/S)						
HOUR	5/31/77	6/1/77	6/2/77	6/3/77	6/4/77	6/5/77	6/6/77 6/7/77
0			0.08				0.17
1			0.08				0.21
2			0.07				0.24
3							
4							
5			0.04				0.25
6			0.04				0.25
7			0.05		0.32		0.24
8							0.00
9		0.37	0.07		0.28	0.25	
10			0.08				
11			0.10				
12				0.26			
13			0.13				
14	0.24		0.14				
15		0.13	0.16	0.52	0.37	0.29	
16		0.10	0.18	0.48			
17		0.09					
18		0.09					
19							
20		0.09				0.20	
21		0.07			0.34	0.17	
22	0.37	0.07		0.42		0.17	
23						0.17	

Table B-III-7. Friction Velocity Hourly Listing (cont'd)

g) Richardson's Number

The dimensionless Richardson's number serves as an estimate for energy transfer in a turbulent flow under non adiabatic conditions. It indicates the energy supplied or consumed by thermal stratification as compared with the energy furnished by eddy stresses. It is positive for stable stratifications where the turbulent stresses have to work against gravity and becomes negative in super adiabatic or unstable cases.

Figure B-III-12 is a cruise plot of the variation of Richardson's number as a function of time/place during the EOMET 77 cruise. These numbers were calculated by the NPS and details of their measurements and their calculation are found in Section B-II-c of this report. Table B-III-8 is an hourly listing of these data as they were reported by NPS during EOMET 77.

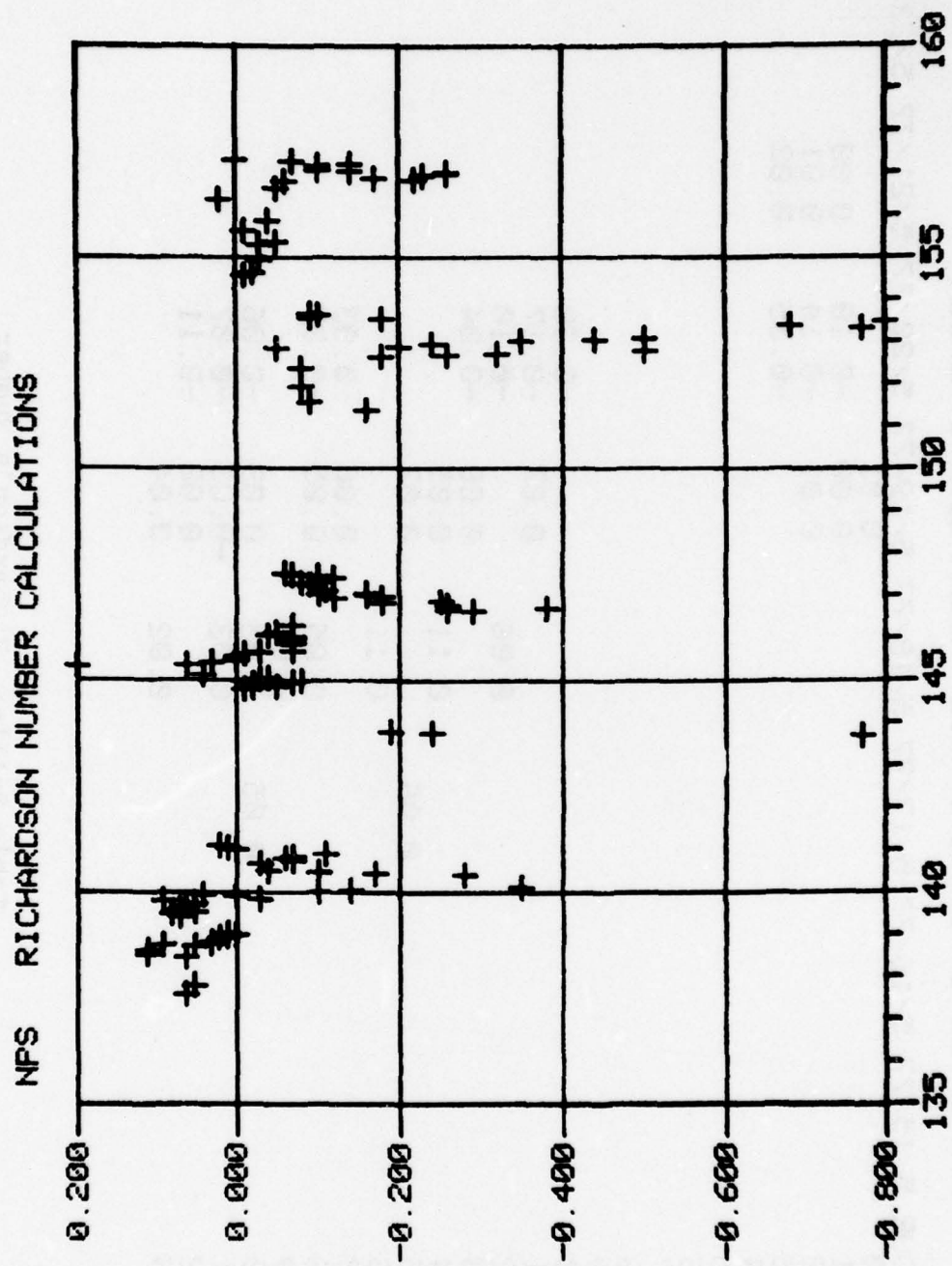


Fig. (B-III-12) NPS Richardson number calculations.

* HOUR	5/15/77	5/16/77	5/17/77	5/18/77	5/19/77	5/20/77	5/21/77	5/22/77
0					0.01	-0.10	0.00	
1					0.00	-0.14	0.01	
2					0.01	-0.35	0.02	
3								
4								
5								
6								
7								
8								
9								
10						-0.28		
11					0.07	-0.17		
12				0.06		-0.10		
13				0.11	0.08	-0.04		
14					0.05			
15			0.06		0.07			
16				0.11				
17					0.06	-0.03		
18				0.05	0.05	-0.07		
19				0.09				
20			0.05	0.03	0.09	-0.06		
21				0.03	-0.03	-0.07		
22				0.03	0.00	-0.11		
23				0.02	0.04			

Table B-III-8 Richardson's Number

* HOUR	5/23/77	5/24/77	5/25/77	5/26/77	5/27/77	5/28/77	5/29/77	5/30/77
0			-0.08	-0.07	-0.16			
1			-0.03	-0.07	-0.10			
2			-0.04	-0.04	-0.16			
3			0.04	-0.05	-0.11			
4								
5								
6								
7			0.22	-0.07	-0.09			
8			0.20		-0.08			
9			0.06		-0.10			
10			0.03		-0.12			
11			0.00		-0.10			
12	-1.49		0.00		-0.07			
13					-0.06			
14	-1.25		0.00					
15			-0.01	-0.29				
16			-0.03	-0.26				
17	-0.77		-0.07	-0.38				
18	-0.24			-0.26				
19	-0.19							
20		-0.01						
21		-0.02		-0.18				
22		-0.05	-0.07	-0.25				
23		-0.02	-0.07	-0.12				
		-0.07		-0.18				

Table B-III-8 Richardson's Number (cont'd)

* HOUR	5/31/77	6/1/77	6/2/77	6/3/77	6/4/77	6/5/77	6/6/77	6/7/77
0			-0.35				-0.26	
1			-0.44				-0.14	
2			-0.50				-0.10	
3								
4								
5			-1.00				-0.10	
6			-0.86				-0.14	
7			-0.77		-0.03		-0.07	
8								
9		-0.08	-0.68		-0.05	0.02		
10								
11			-0.80					
12								
13			-0.18					
14	-0.09		-0.09	-0.01				
15		-0.18	-0.10	-0.02	-0.01	-0.05		
16		-0.26	-0.09					
17		-0.32						
18		-0.50						
19							-0.06	
20		-0.05					-0.22	
21		-0.20					-0.17	
22	-0.08	-0.24		-0.03	-0.04		-0.23	
23							-0.26	

Table B-III-8 Richardson's Number (cont'd)

h) Atmospheric Radon Calculation

Radon (^{222}Rn) has proven to be an excellent indicator of the continental nature of over ocean air and air mass boundaries. Radon is a radioactive rare gas with a 3.8 day half life which is continuously emanated from all land areas. Radon emanates from the oceans but at a rate two or three orders of magnitude smaller than from land areas, and this enables radon to be used as an indicator of any recent continental contribution to marine air masses.

The transition from pure "continental" to pure "maritime" air produces an order of magnitude change in radon concentration from a few picocuries per cubic meters (pCi m^{-3}) or more to a tenth of a pCi m^{-3} or less. In many areas over the North Atlantic and Pacific Oceans, two or three pCi m^{-3} radon is about as low as one can anticipate encountering, while radon levels of a few tenths pCi m^{-3} can be expected over some areas of the South Pacific.

Figure B-III-13 is a plot of radon concentration as a function of time as measured during EOMET 77. The Y axis is the concentration in pCi m^{-3} while the X axis is the time in Julian days. Table B-III-9 is an hourly listing of radon data as it was obtained and recorded.

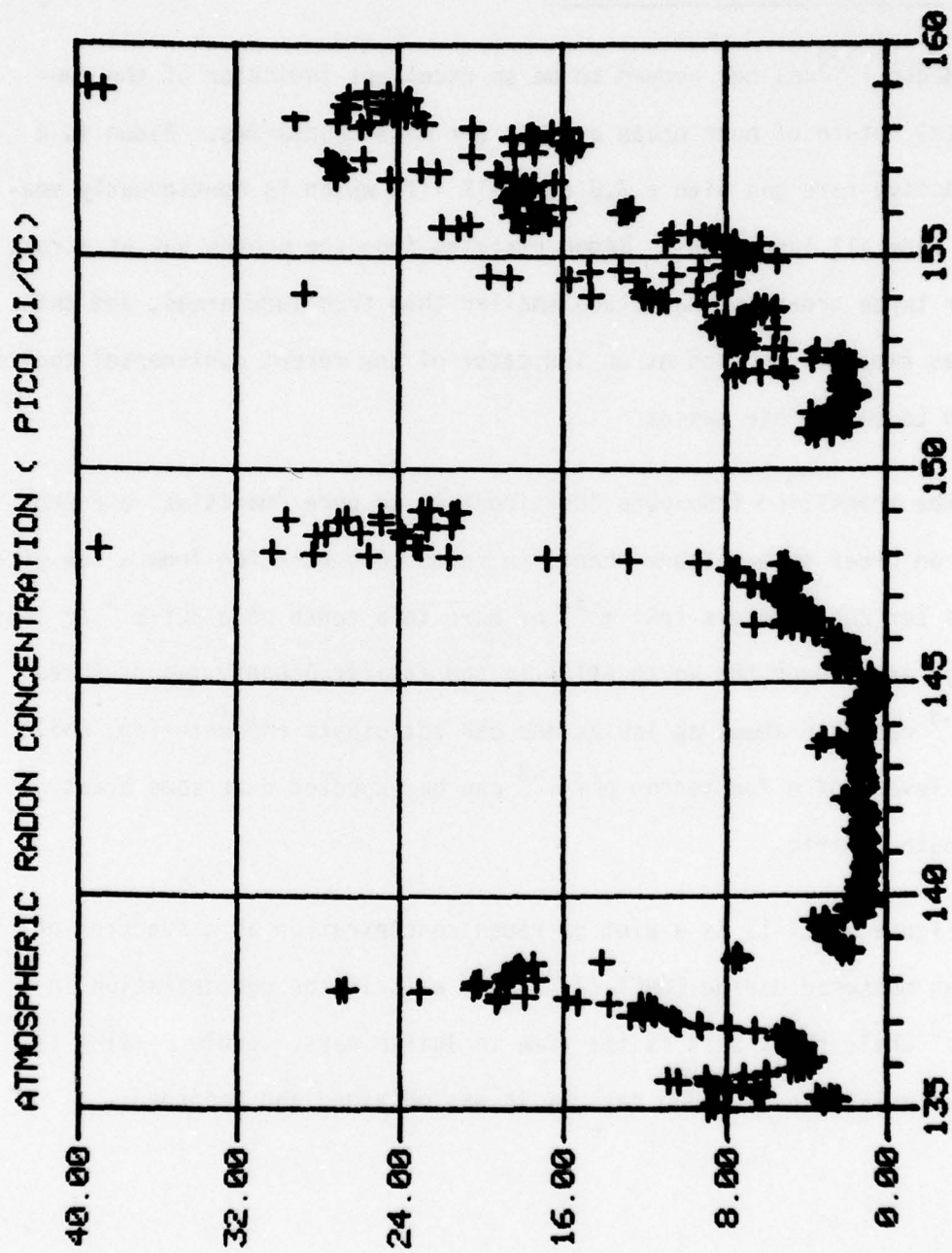


Fig. (B-III-13) Atmospheric Radon concentration.

* ATMOSPHERIC RADON CONCENTRATION (PICO CI / CC)									
HOUR	5/15/77	5/16/77	5/17/77	5/18/77	5/19/77	5/20/77	5/21/77	5/22/77	
0		4.3	9.4	20.1	3.0	0.9	1.0	1.2	1
1	8.1	3.9	10.4	18.7	3.1	1.0	1.1	1.2	1
2	8.9	4.4	10.6	17.3	3.1	1.0	1.1	1.2	1
3	8.7	4.3	10.7	18.8	3.1	1.2	1.3	1.3	1
4	8.7	3.7	12.1	18.8	3.1	1.5	1.3	1.8	1
5	3.3	3.8	12.7	18.5	3.1	1.5	1.3	2.1	1
6	2.6	4.5	11.6	18.0	3.4	1.0	1.3	2.2	1
7	3.6	4.8	11.6	18.4	3.1	1.2	0.9	1.7	1
8	3.6	4.8	12.2	18.3	3.1	1.4	1.2	1.5	1
9	6.3	4.9	11.5	18.2	3.7	1.2	1.1	1.3	1
10	6.6	4.6	11.9	17.5	3.2	1.1	1.2	1.3	1
11	6.5	4.7	12.2	14.2	3.2	1.1	1.2	1.2	1
12	8.2	4.6	13.8	17.2	2.2	1.1	1.4	1.0	1
13	7.9	4.2	15.3	7.7	1.2	0.9	1.6	1.1	1
14	7.4	4.7	15.9	7.3	1.4	1.1	1.4	1.1	1
15	9.4	4.8	15.9	7.5	1.6	1.2	1.5	1.2	1
16	10.4	4.9	17.9	2.3	1.2	1.1	1.2	1.1	1
17	10.9	5.5	19.2	1.9	1.1	1.1	1.1	1.1	1
18	9.0	5.8	23.0	1.8	1.9	1.0	1.2	1.1	1
19	7.2	5.5	27.0	2.3	0.8	0.9	0.9	1.4	1
20	6.0	5.2	26.6	2.5	0.8	0.9	1.1	1.4	1
21	6.1	6.7	20.4	2.5	0.8	0.9	1.0	1.2	1
22	4.4	7.9	20.2	2.2	0.8	1.1	1.0	1.2	1
23	4.6	9.3	20.3	7.8	0.8	1.0	1.1	1.3	1

Table B-III-9 Atmospheric Radon Concentration

* HOUR	5/31/77	6/1/77	6/2/77	6/3/77	6/4/77	6/5/77	6/6/77	6/7/77
0		2.4	7.2	11.7	7.4	18.1	22.0	15.7
1	1.0	2.2	6.9	12.1	7.4	13.2	22.9	20.4
2	2.0	2.2	7.2	14.6	7.5	12.9	26.7	25.8
3	5.0	3.0	7.5	28.6	7.5	12.6	27.0	22.8
4	5.0	5.7	7.1	12.1	7.6	15.9	27.1	25.4
5	2.2	5.3	7.9	9.4	7.6	17.0	27.2	27.0
6	2.2	5.3	8.3	8.4	6.3	17.6	27.5	29.1
7	2.2	5.1	8.5	8.3	8.5	18.3	25.7	23.7
8	2.2	5.2	8.7	8.0	7.6	18.7	23.1	23.1
9	5.0	5.5	8.8	7.8	11.0	18.3	4.3	24.3
10	5.0	6.5	8.8	12.4	8.7	18.4	18.3	24.6
11	5.0	6.5	8.8	15.6	8.4	18.4	17.3	24.8
12	5.0	6.5	8.8	18.6	9.1	18.3	15.6	24.1
13	5.0	6.5	8.8	19.6	10.7	18.3	15.7	26.1
14	5.0	6.5	8.8	19.6	10.8	17.9	15.7	26.7
15	5.0	6.5	8.8	14.7	18.0	17.0	15.7	24.7
16	5.0	6.5	8.8	13.2	21.1	17.4	15.7	23.6
17	5.0	6.5	8.8	9.0	21.9	17.4	15.7	23.5
18	5.0	6.5	8.8	7.6	20.5	16.4	17.3	26.5
19	5.0	6.5	8.8	7.6	16.6	18.3	18.4	25.5
20	5.0	6.5	8.8	7.7	17.5	24.4	17.6	24.5
21	5.0	6.5	8.8	7.5	17.2	27.0	17.4	25.6
22	5.0	6.5	8.8	6.7	16.9	19.0	16.5	28.5
23	5.0	6.5	8.8	7.0	18.5	19.2	15.7	29.5

Table B-III-9 Atmospheric Radon Concentration (cont'd)

i) Visibility

Accurate visibility measurements from on board a ship at sea are normally difficult to obtain. Estimates of visibility are made routinely at sea by observers who have only the horizon on which to base their estimates.

The visibility values given here were calculated from the well-known Koschmieder formula. According to this formula visibility is equal to the constant 3.91 divided by the scattering coefficient. The required values of the scattering coefficient were obtained by adding a molecular scattering contribution of $1.65 \times 10^{-5} \text{ m}^{-1}$ to the values of the aerosol scattering coefficient measured with the MRI model 1567 integrating nephelometer.

Figure B-III-14 is the cruise plot of the visibility calculations. Figure B-III-15 is the frequency distribution of these calculations. Table B-III-10 lists all of the valid calculated visibilities obtained for the cruise.

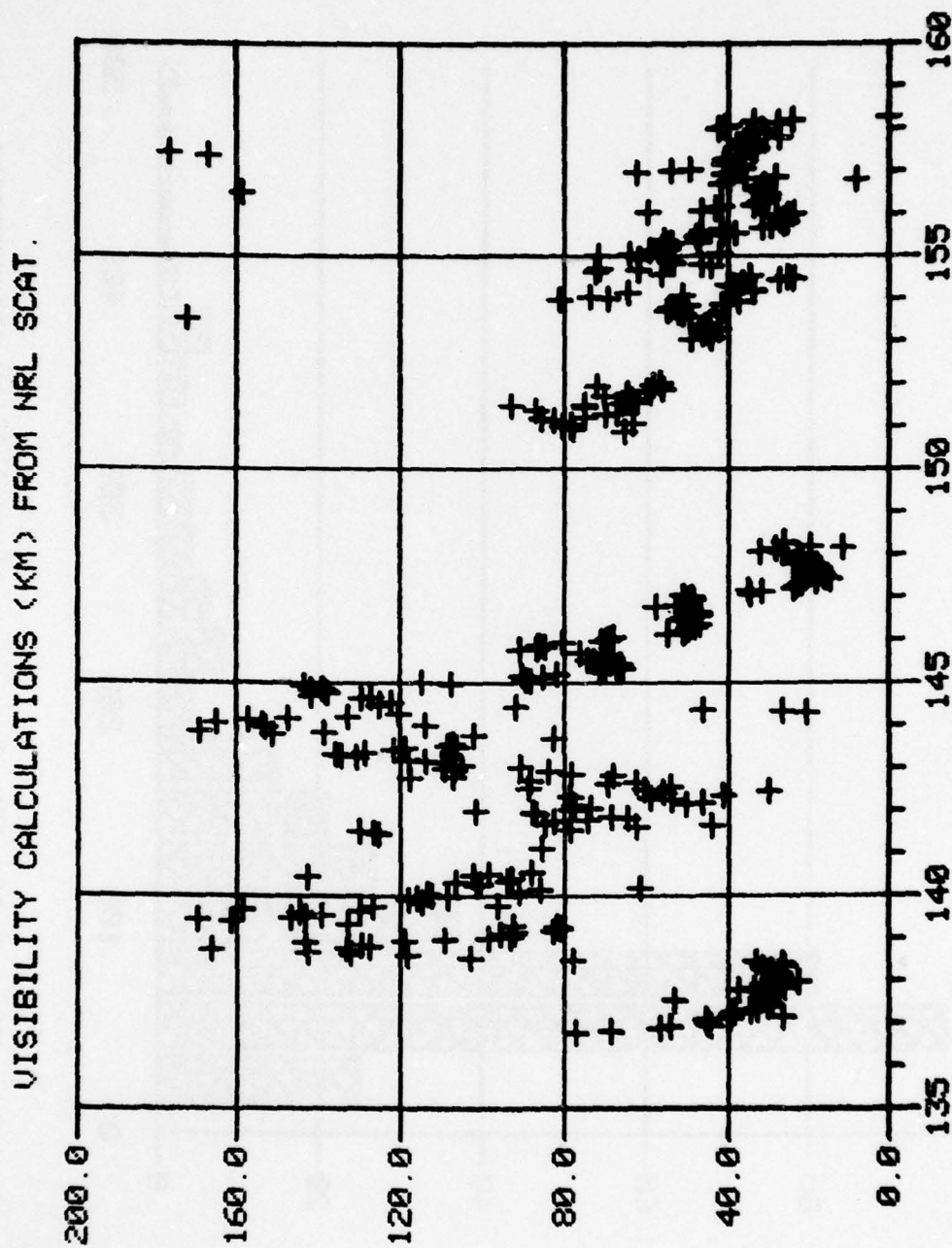


Fig. (B-III-14) Visibility - Julian day vs. KM.

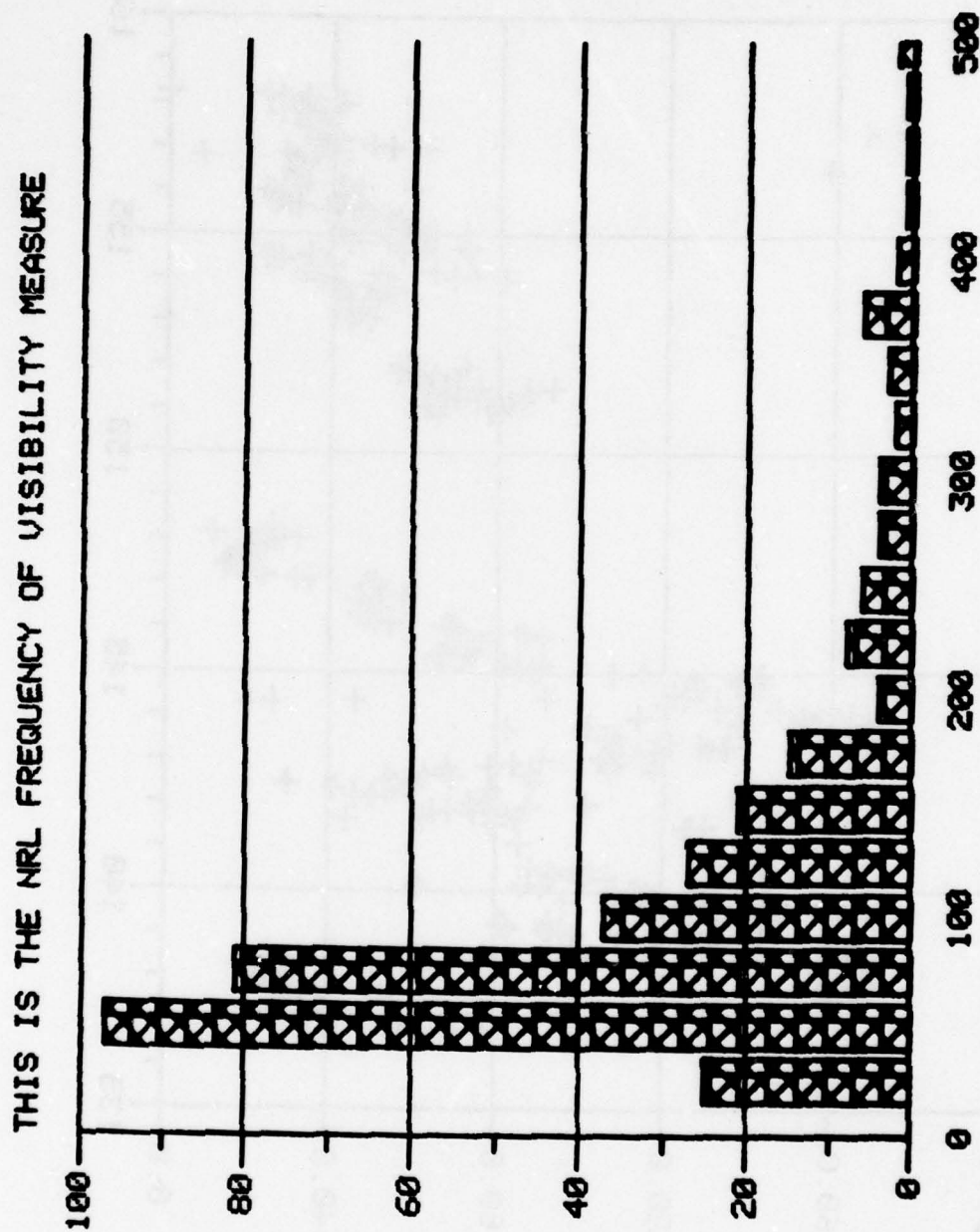


Fig. (B-III-15) Frequence of visibility measurements.

* VISIBILITY CALCULATIONS (KM) FROM NRL SCAT. COEF. MEAS.

HOUR	5/15/77	5/16/77	5/17/77	5/18/77	5/19/77	5/20/77	5/21/77	5/22/77
0			44	22	109	108		101
1			45	26	98	112		78
2							85	
3			45	29	95	91		77
4			39	27	92	86		50
5			26	27	82	61		46
6			39	29	81	101		53
7			38	31	81	100		59
8			34	31	92	106		78
9			32	26	132	94		41
10			30	26	161	92		55
11			29	33	169	142	125	30
12			30	78	146	102	126	60
13			30		143	98	129	88
14			53	103	139	87	78	54
15			31	118	144		62	69
16			30	131	129		44	62
17			31	142	158		84	88
18			32	166	126		82	117
19		77	37	132	96		74	107
20		68	33	127	211		64	68
21		56	26	129	114		68	78
22		54	31	142	118		86	83
23			27	118	115		87	106

Table B-III-10. Visibility - Hourly Listing

* VISIBILITY CALCULATIONS (KM) FROM NRL SCAT. COEF. MEAS.

PAGE 2

HOUR	5/23/77	5/24/77	5/25/77	5/26/77	5/27/77	5/28/77	5/29/77	5/30/77
0	113	114	69	48	23			
1	153	88	68	51	26			
2								
3	109	85	54	32	28			
4	113	90	51	35	11			
5	118	81	50	24	19			
6	130	71	49	23	26			
7	134	70	48	22				
8	135	65	48	22				
9	128	67	47	18				
10	121	66	49	15				
11	118	69	52	16				
12	106	72	51	16				
13	108	74	49	19				
14	107	243	47	16				
15	213	70	46	19				
16	211	70	49	20				
17	82	76	49	19				
18	101	90	57	18				
19	150	86	52	24				
20	138	84	50	22				
21	169	86	49	22				
22	206	80	48	20				
23	152	71	49	22				

65778

Table B-III-10 Visibility - Hourly Listing (cont'd)

VISIBILITY CALCULATIONS (KM) FROM NRL SCAT. COEF. MEAS.									
HOUR	5/31/77	6/1/77	6/2/77	6/3/77	6/4/77	6/5/77	6/6/77	6/7/77	
0		56		69	71	23	53	42	
1	78		49	73	64	59	49	41	
2	63		44	51	42	46	36	40	
3	82		44	64	59	43	37	27	
4	85		46	33	54	41	41	33	
5	75		45	34	56	33	40	24	
6	69		42	37	54	32	40		
7	67		43	39	53	31	39		
8	216		45	39	47	30	38		
9	87		45	36	55	30	167		
10	75		44	27	47	31	176		
11	92		43	24	47	30	34		
12	75	172	43	25	41	158	33		
13	65		43	34	38	31	33		
14	62	49		56	46	33	34		
15	63	51		72	41	31	36		
16	64	52		61	31	31	35		
17	70	55		71	29	41	36		
18	64	54		44	26	39	35		
19	59	52		46	25	8	27		
20	59	50		53	27	35	31		
21	56	41		54	26	28	35		
22	71	37		61	28	41	31		
23	58	81		55	25	62	32		

Table B-III-10 Visibility - Hourly Listing (cont'd)

j) EOMET 77 Meteorological Soundings

The data in this section were obtained by two methods. Dr. Ralph Markson of Airborne Research Associates supported the cruise by making aircraft measurements of temperature and dewpoint in the vicinity of the ship as it proceeded along the coast of North America. A series of kite balloon soundings were also made with the NRL microprocessor controlled boundary layer sounding system described in detail in NRL Report #8271.

Figure B-III-16 shows the location of all of the kite balloon flights which are indicated by circles containing the flight numbers adjacent to the cruise track. Each flight consists of one ascent of the kite balloon system to a maximum altitude where it can no longer rise and then its descent again to the surface. The time required for one complete sounding is approximately 40 minutes. Every minute during the flight the current measurement of dry bulb temperature, wet bulb temperature, and pressure altitude are digitally recorded. Consecutive flights in the same general area are shown by adjacent circles on the map. In actuality the flight numbers show the order of the flights. There are several missing flight numbers and these correspond to real flight attempts but which for one reason or other the flights were aborted without an adequate data accumulation.

Figures B-III-17, B-III-18 and B-III-19 are the aircraft profiles obtained on 15, 17 and 18 May 1977 in the vicinity of the ship's track. The aircraft used in these measurements was a single engine turbocharged Bellanca which has been flown to as low as 3 meters and as high as 10,000

meters. Temperature and dewpoint data are recorded along with other parameters on an eight channel strip chart recorder.

Figures B-III-20 through B-III-28 show plots of the kite balloon soundings for all of the successful flights. These plots show the kite balloon data expressed in terms of dry air temperature and its dewpoint. On the plots the Y axes show altitude of from 0 to 800 meters and the X axis shows temperature of from -10 to 25 degrees centigrade. On each of these flights the actual data points have been approximated by a third order polynomial least square fits of the discrete flight data. Temperature is shown by the solid curves and dewpoint is shown by the dashed curves.

A calibration of the kite balloon system instruments was obtained by flying the instrument package at mast height and comparing the measurements of the kite balloon package with the precision ships instrumentation. Such a calibration was made before and after each flight to watch for a possibility of instrumentation drift which might have occurred during the flight.

Tables B-III-11 and B-III-12 contain the coefficients of the fitting curves for the air temperature data and for the relative humidity data. The actual data that was used in the calculation of the coefficient in Table B-III-11 are the kite balloon dry air temperatures and the altitude of the measurements together with the simultaneously measured shipboard mast height air temperature weighted by 10 and the sea surface temperature weighted by 10. The least squares analysis produces coefficients A, B, C

and D which show the relation between dry air temperature, T and altitude z by the formula:

$$T(C^{\circ}) = A + B^*z + C^*z^2 + D^*z^3 \quad \text{where } z \text{ is in meters.}$$

This fitted curve is only good for altitudes from the surface to the maximum altitude obtained on that particular flight. As with other fitted polynomials gross errors can occur outside the area where the original points were taken.

The coefficients in Table B-III-12 contain numbers which fit the relative humidity at each data point to a similar third order polynomial. At each discrete data point, relative humidity in terms of percent was calculated from the dry and wet bulb temperatures using the usual psychrometric formulas. The resultant relative humidity profile can be represented between the surface and the maximum altitude by the formula:

$$\text{Relative Humidity (5)} = A + B^*z + C^*z^2 + D^*z^3 \quad (z \text{ is in meters}).$$

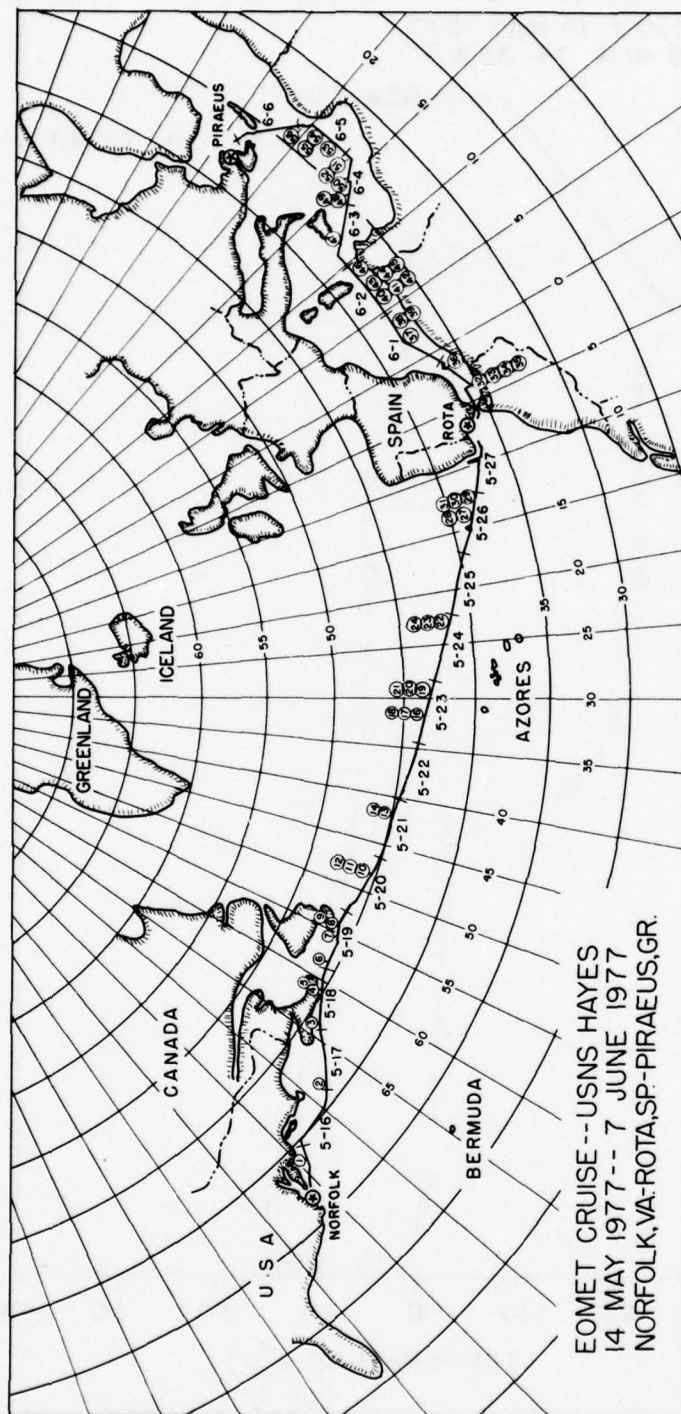


Fig. (B-III-16) Geographic location of kite balloon flights.

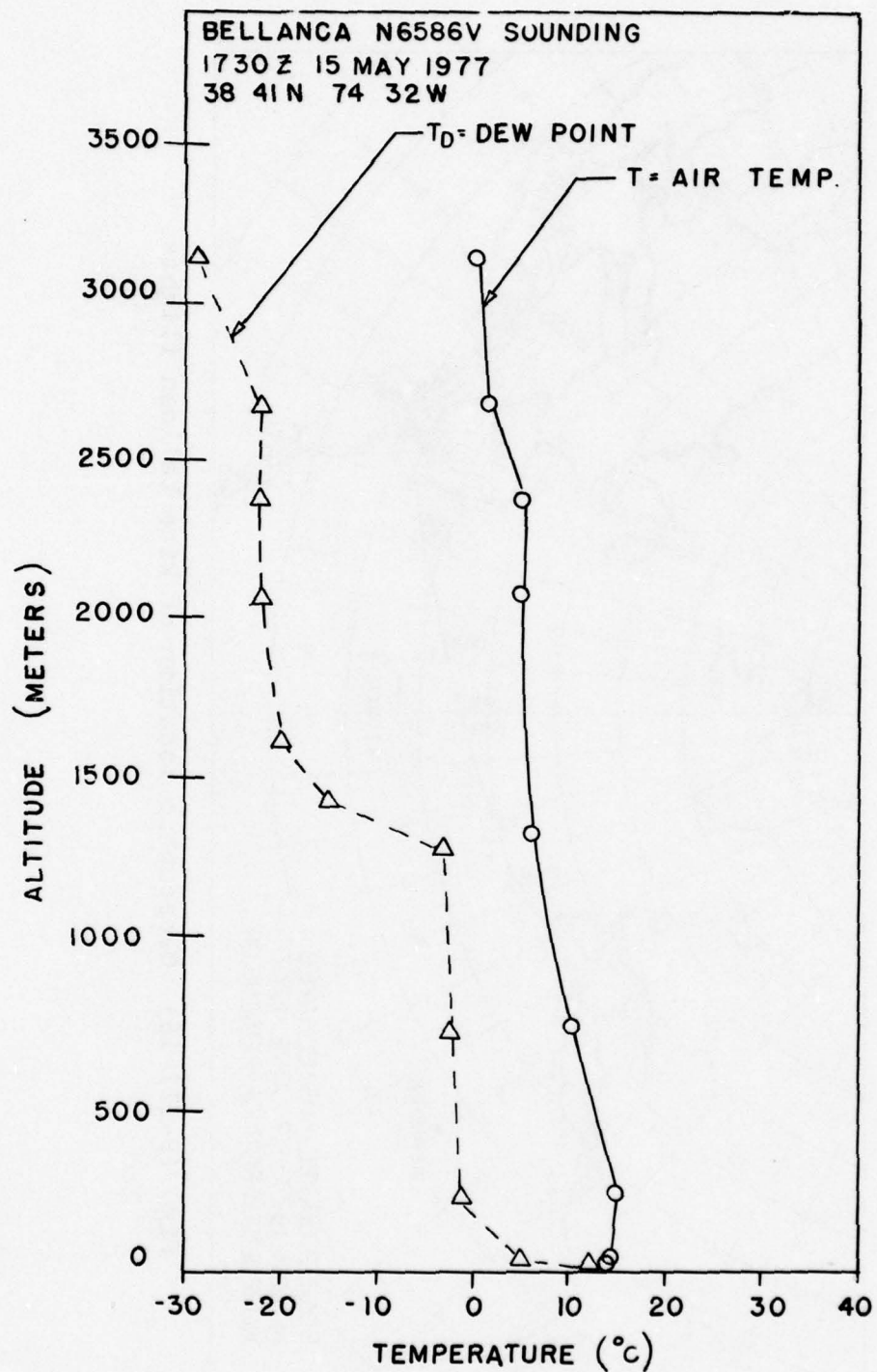


Fig. (B-III-17) Aircraft meteorological sounding - 15 May

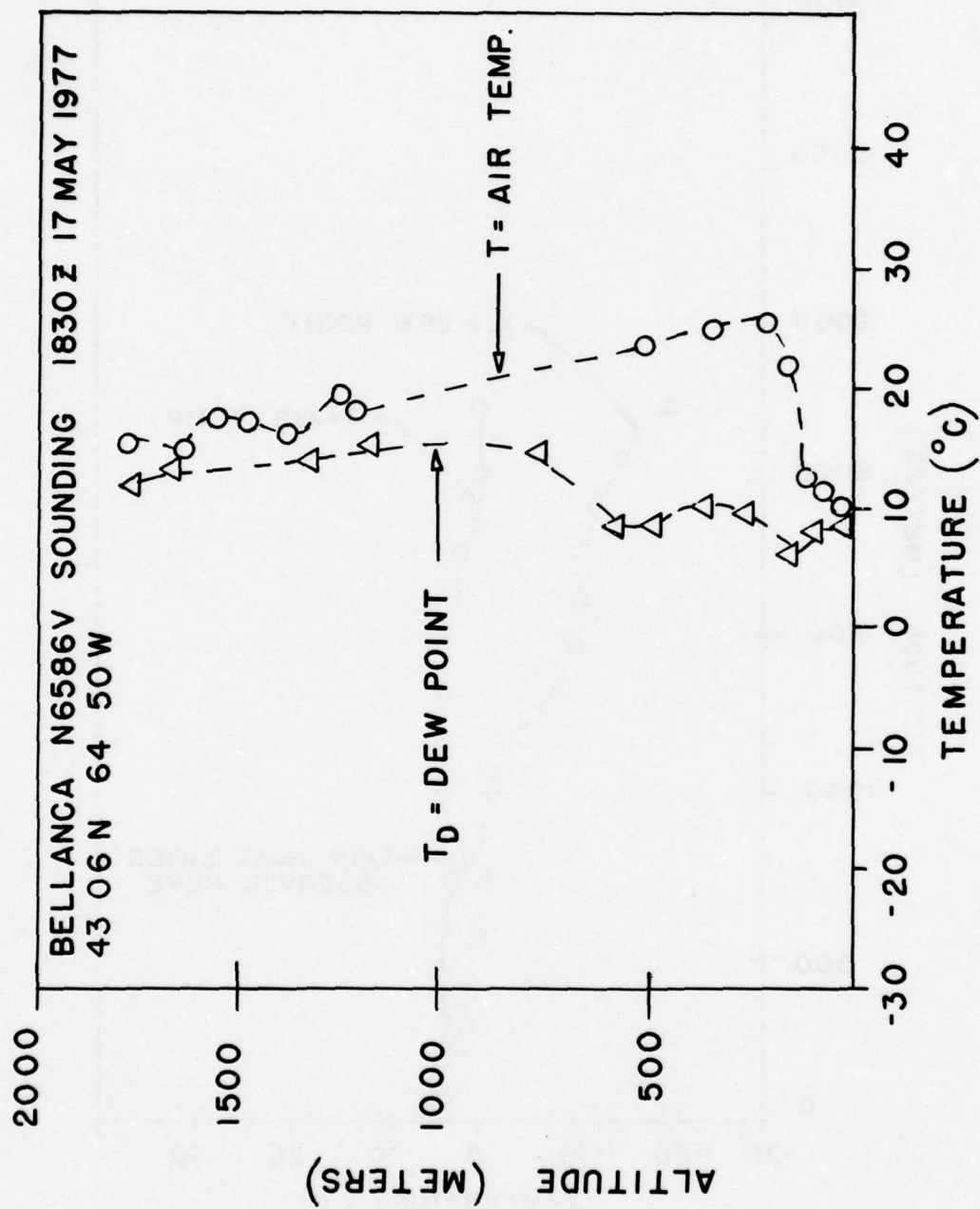


Fig. (B-III-18) Aircraft meteorological sounding - 17 May

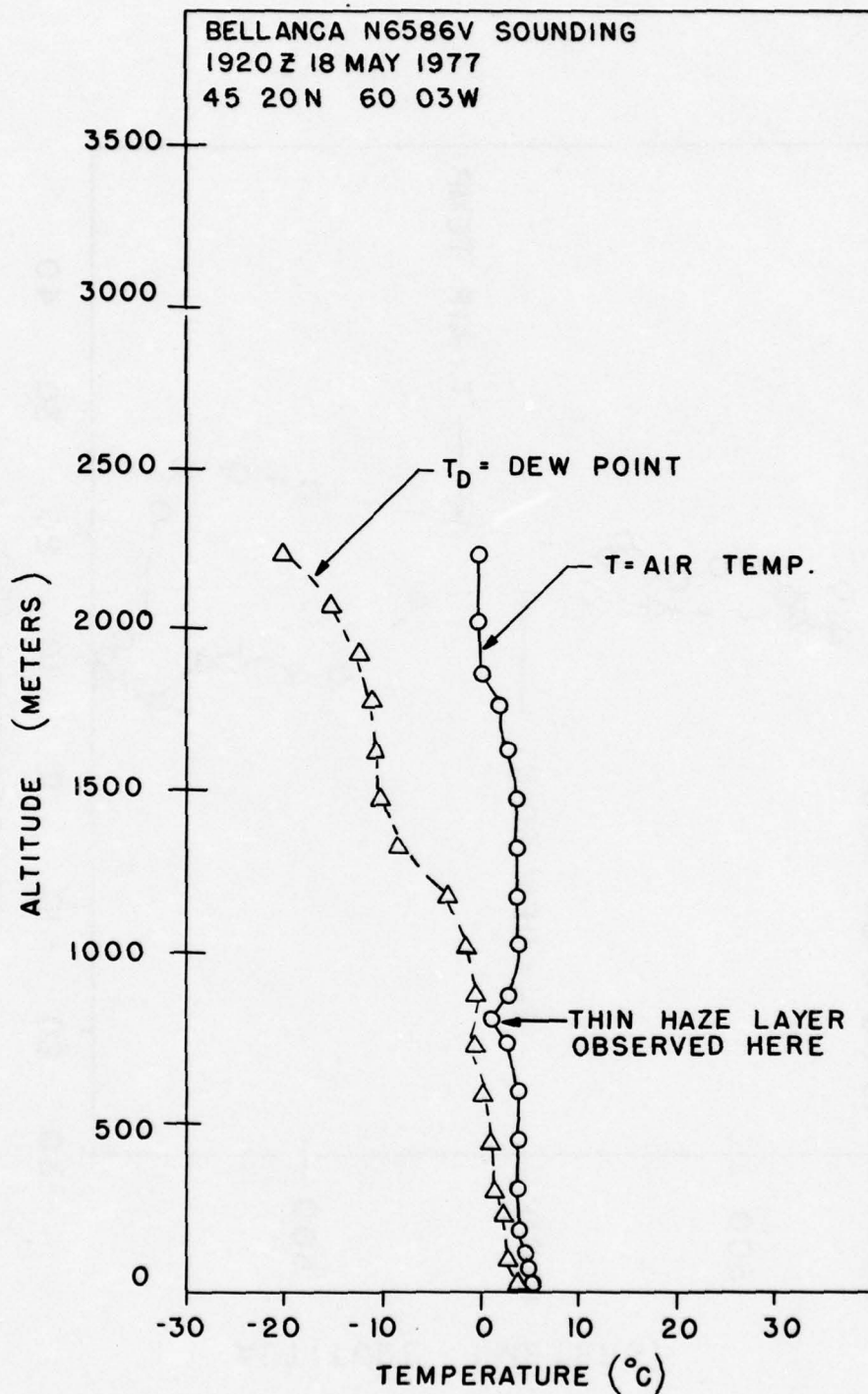


Fig. (B-III-19) Aircraft meteorological sounding — 18 May

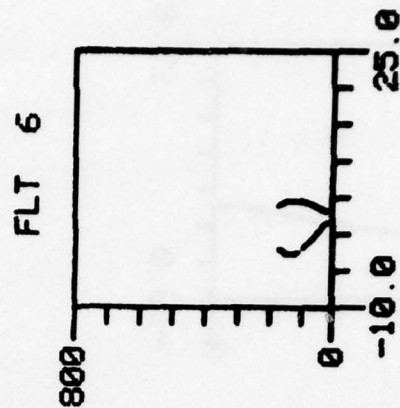
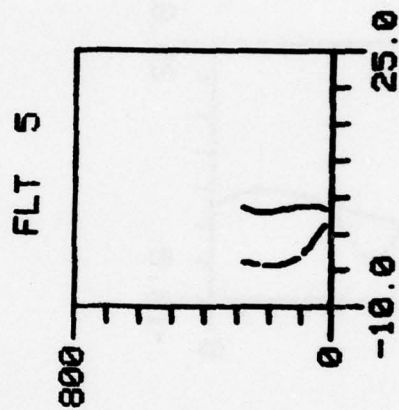
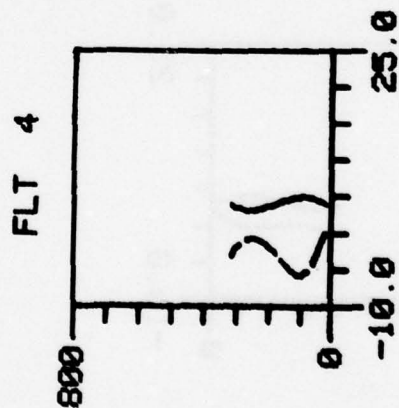
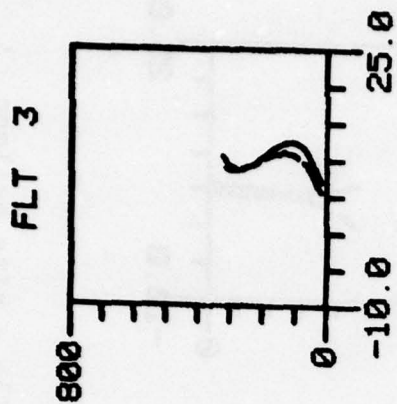
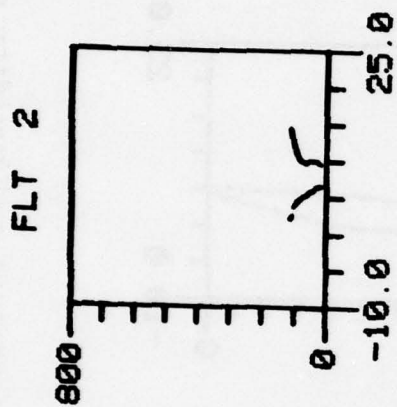
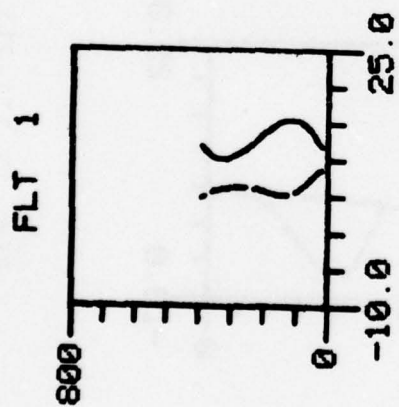


Fig. (B-III-20) Temperature and humidity profile - kite balloon.

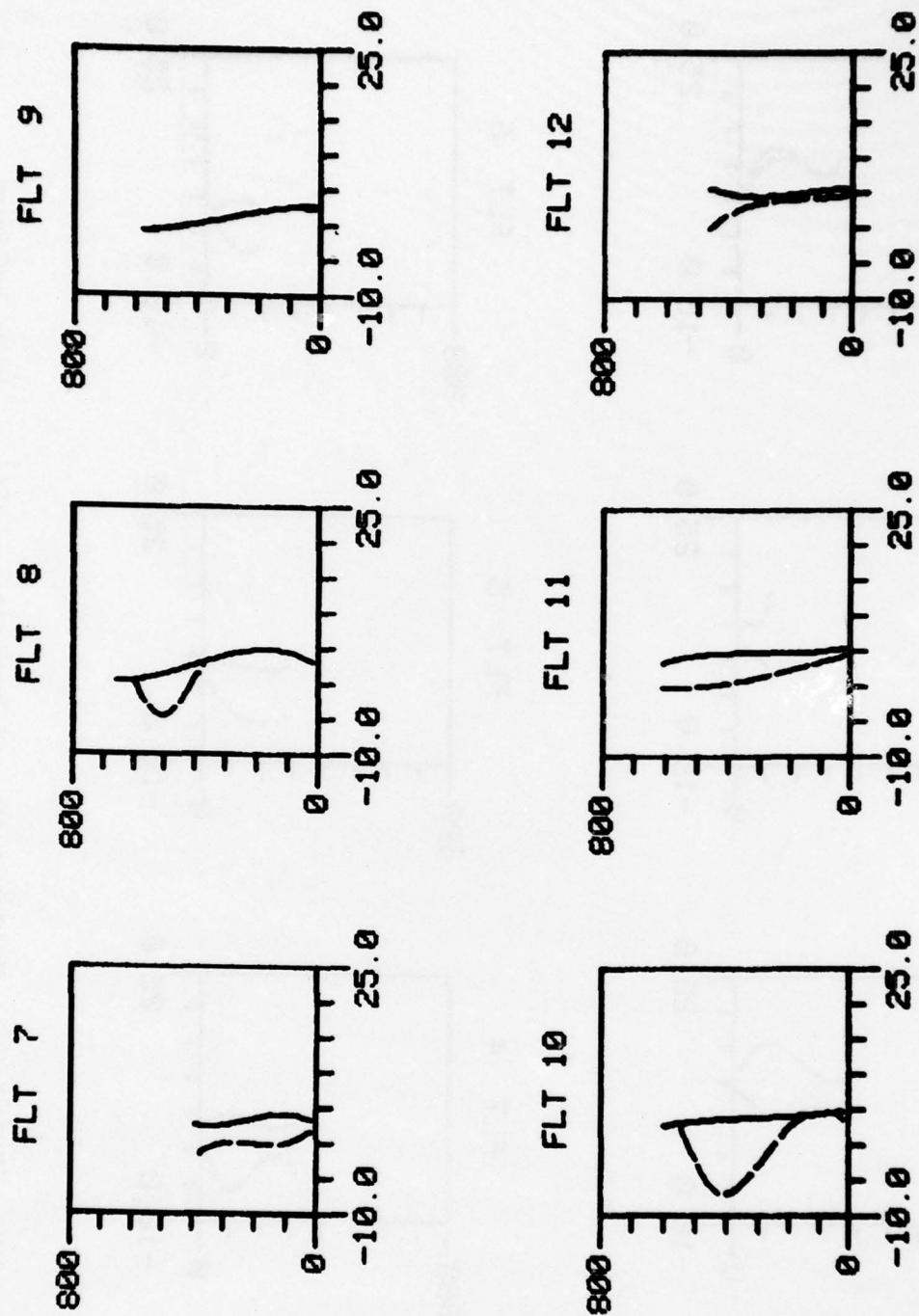


Fig. (B-III-21) Temperature and humidity profile - kite balloon.

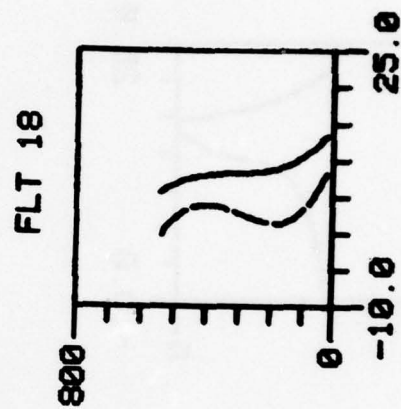
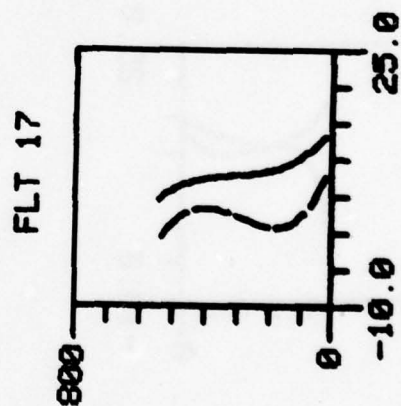
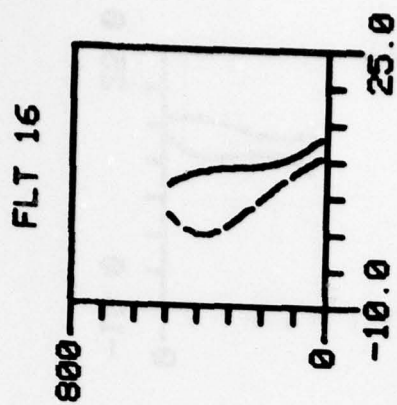
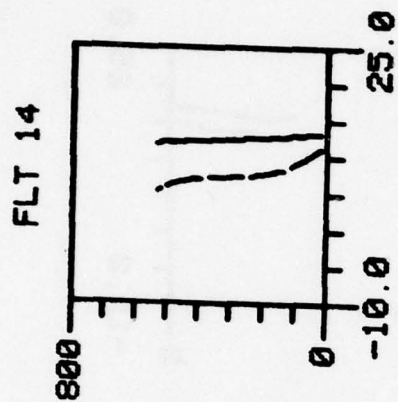
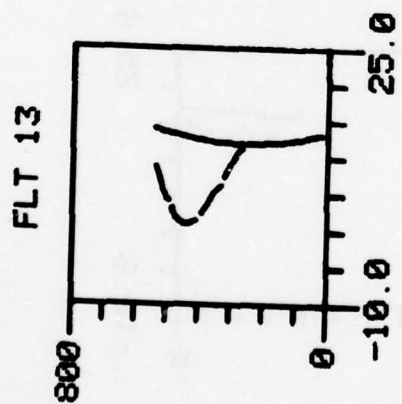


Fig. (B-III-22) Temperature and humidity profile - kite balloon.

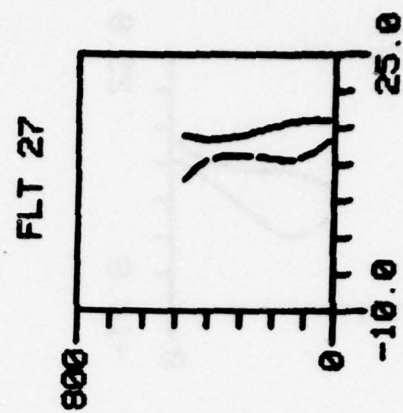
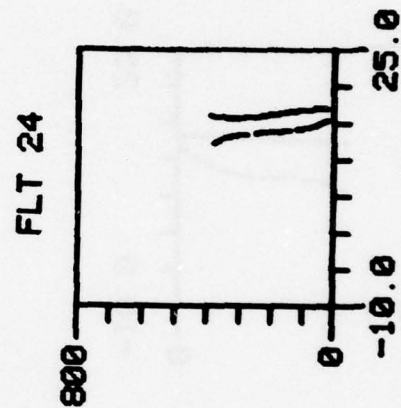
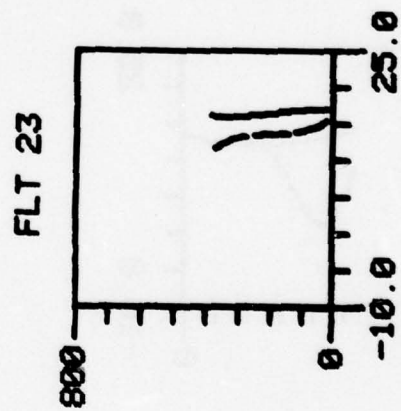
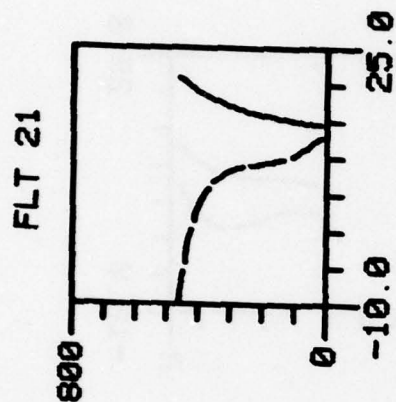
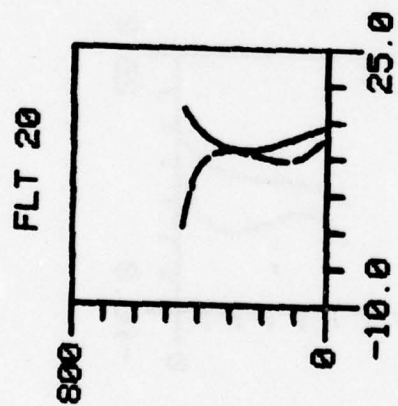


Fig. (B-III-23) Temperature and humidity profile - kite balloon.

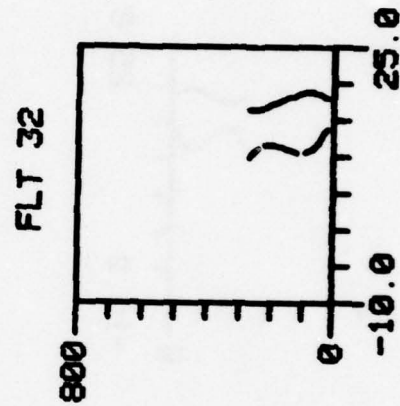
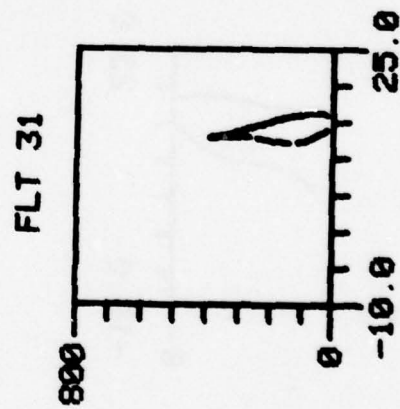
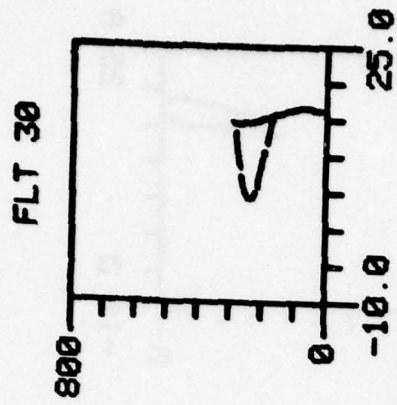
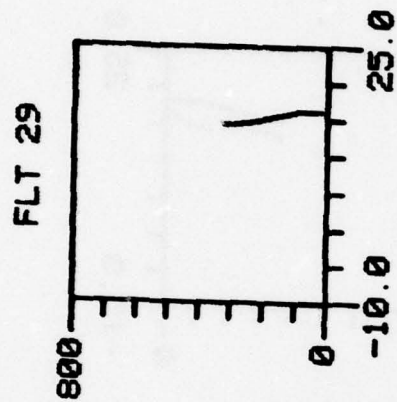
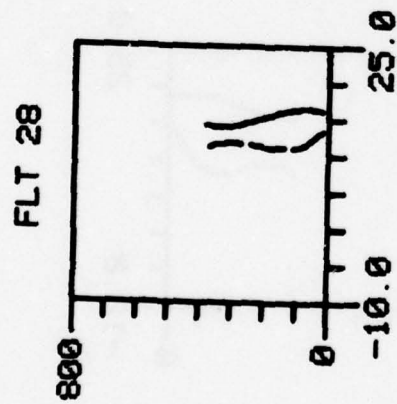


Fig. (B-III-24) Temperature and humidity profile - kite balloon.

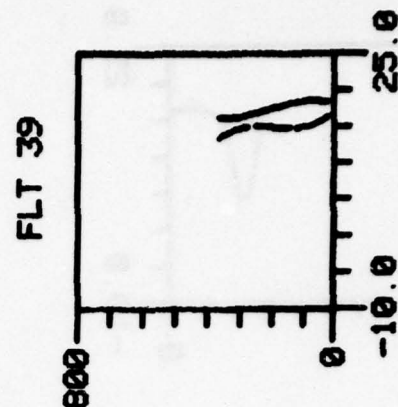
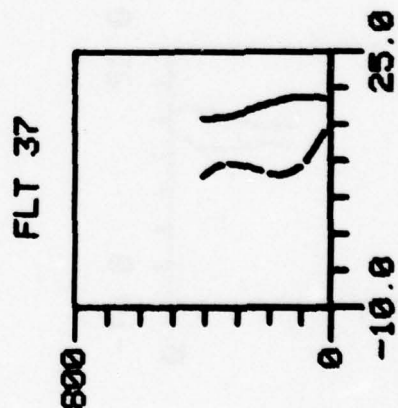
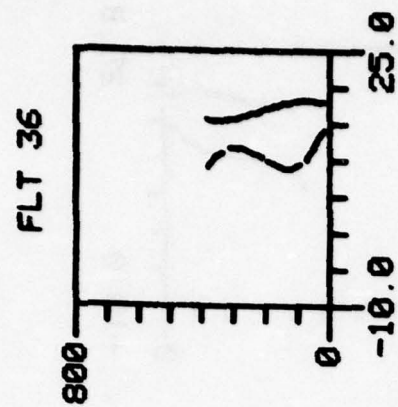
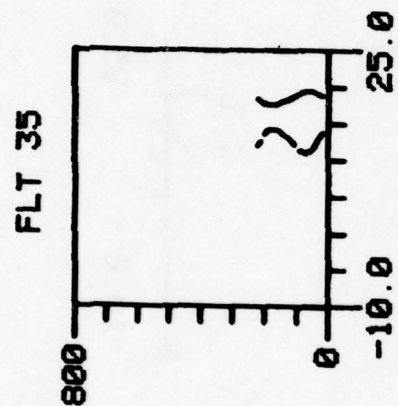
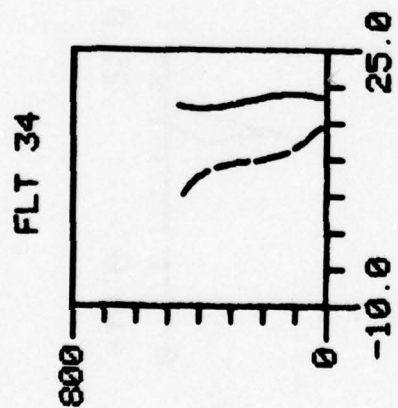


Fig. (B-III-25) Temperature and humidity profile - kite balloon.

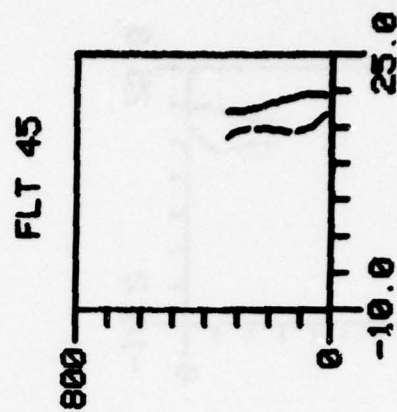
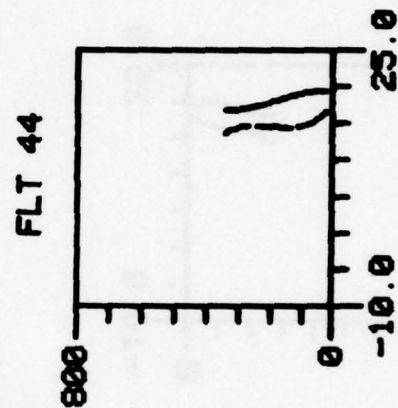
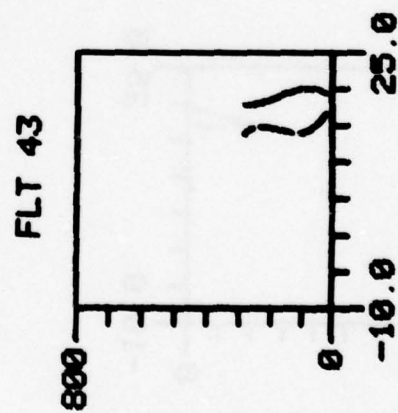
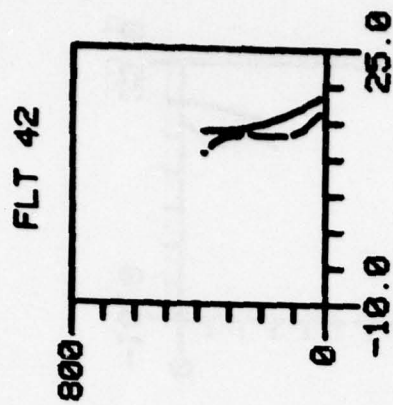
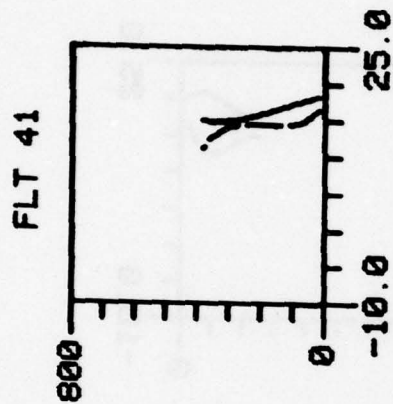
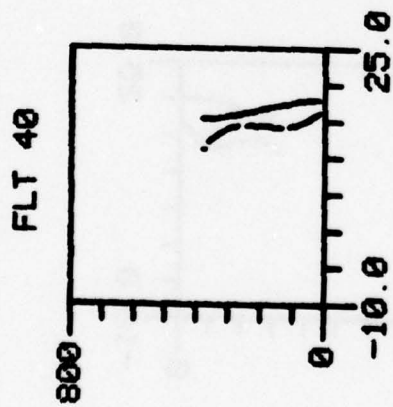


Fig. (B-III-26) Temperature and humidity profile - kite balloon.

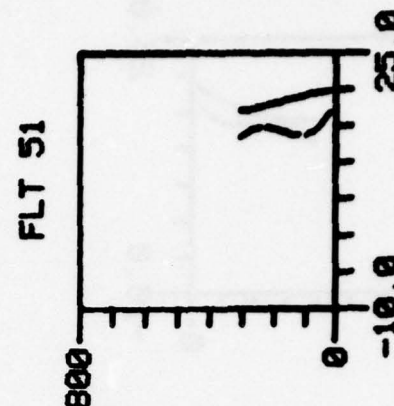
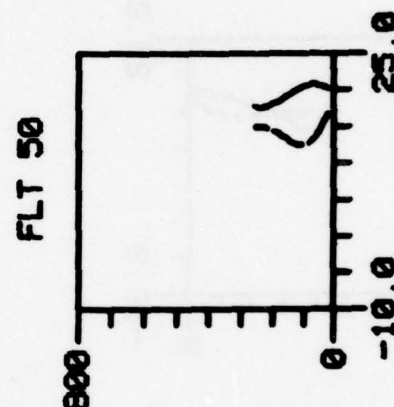
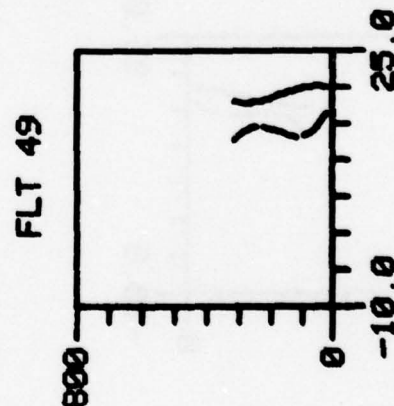
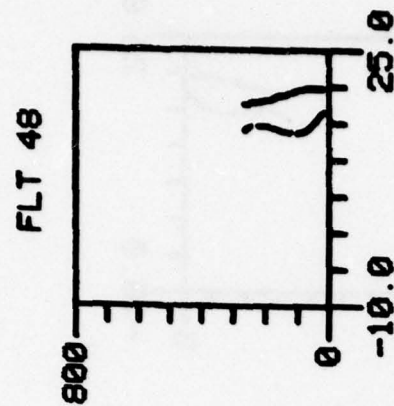
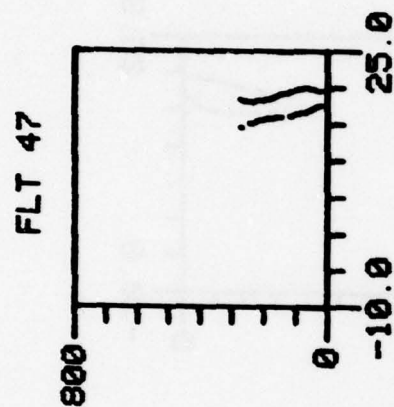
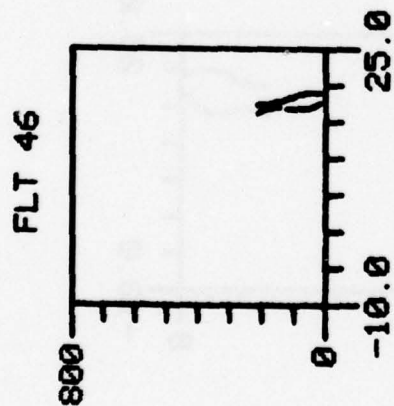


Fig. (B-III-27) Temperature and humidity profile - kite balloon.

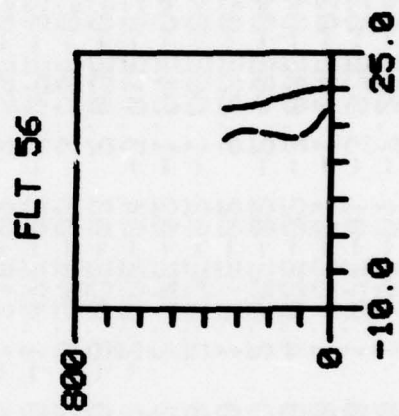
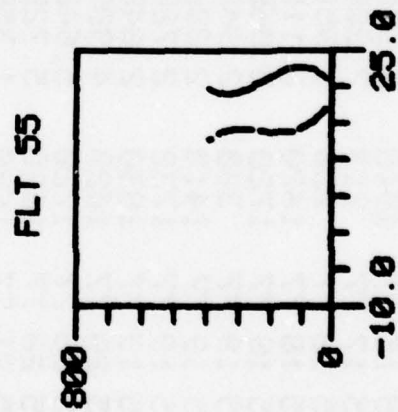
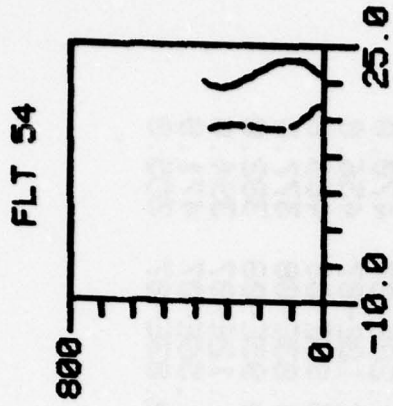
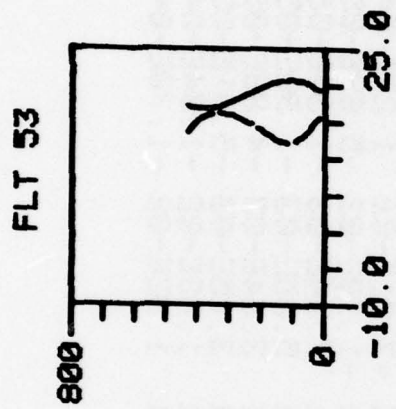
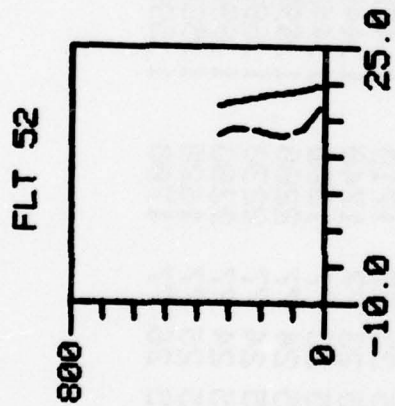


Fig. (B-III-28) Temperature and humidity profile - kite balloon.

KITE BALLOON MEASUREMENT OF TEMPERATURE

FLT	DATE	TIME	A	B	C	D	MAX ALT
1	5 15 77	1940	9.90E+00	1.19E-01	-7.28E-04	1.12E-06	392.0
2	5 17 77	213	7.20E+00	1.87E-01	-3.92E-03	2.56E-05	116.0
3	5 18 77	220	3.95E+00	1.78E-01	-1.14E-03	2.02E-06	324.0
4	5 18 77	1620	3.11E+00	4.83E-02	-3.80E-04	7.44E-07	310.0
5	5 18 77	1720	3.06E+00	2.65E-02	-2.48E-04	5.76E-07	284.0
6	5 19 77	300	2.94E+00	1.61E-02	9.22E-05	-8.82E-07	174.0
7	5 19 77	1410	2.88E+00	2.63E-02	-1.66E-04	2.48E-07	392.0
8	5 19 77	1732	2.72E+00	2.77E-02	-1.04E-04	8.61E-08	668.0
9	5 19 77	1830	2.84E+00	-2.68E-04	-3.01E-05	3.37E-08	577.0
10	5 20 77	1620	4.98E+00	-8.00E-03	2.05E-05	-2.29E-08	601.0
11	5 20 77	1720	5.64E+00	-9.94E-03	3.58E-05	-4.25E-08	612.0
12	5 20 77	1820	5.72E+00	-1.47E-03	-3.07E-05	7.32E-08	462.0
13	5 21 77	1620	1.35E+01	-1.21E-02	2.55E-05	-2.13E-09	545.0
14	5 21 77	1720	1.34E+01	-5.58E-03	1.12E-05	-1.18E-08	530.0
16	5 23 77	1015	1.40E+01	-4.82E-02	1.61E-04	-1.92E-07	492.0
17	5 23 77	1100	1.43E+01	-5.80E-02	1.79E-04	-1.95E-07	544.0
18	5 23 77	1145	1.45E+01	-5.70E-02	1.76E-04	-1.87E-07	548.0
19	5 23 77	1710	1.47E+01	-3.01E-02	1.22E-04	-1.28E-07	470.0
20	5 23 77	1740	1.44E+01	-1.18E-02	-5.69E-05	2.18E-07	456.0
21	5 23 77	1800	1.44E+01	7.74E-03	-1.34E-05	5.85E-08	466.0
22	5 24 77	2200	1.69E+01	5.05E-03	-1.90E-05	-4.03E-08	377.0
23	5 24 77	2230	1.69E+01	3.64E-03	-4.88E-05	8.95E-08	382.0
24	5 24 77	2300	1.69E+01	3.25E-03	-5.81E-05	1.12E-07	394.0
27	5 26 77	1620	1.58E+01	1.08E-02	-1.04E-04	1.56E-07	471.0
28	5 26 77	1700	1.59E+01	1.93E-02	-1.70E-04	2.83E-07	385.0

Table B-III-11 Temperature Measurement - Kite Balloon

KITE BALLOON MEASUREMENT OF TEMPERATURE

FLT	DATE	TIME	A	B	C	D	MAX ALT
29	5 26 77	2110	1.61E+01	8.14E-03	-1.09E-04	2.09E-07	323.0
30	5 26 77	2140	1.58E+01	2.57E-02	-2.49E-04	5.02E-07	299.0
31	5 26 77	2210	1.59E+01	1.06E-02	-1.02E-04	1.41E-07	390.0
32	5 31 77	1320	1.72E+01	4.47E-02	-3.76E-04	7.37E-07	272.0
33	5 31 77	1350	1.80E+01	2.26E-02	-1.47E-04	2.11E-07	450.0
34	5 31 77	1420	1.82E+01	1.75E-02	-1.11E-04	1.50E-07	466.0
35	5 31 77	1450	1.78E+01	6.22E-02	-7.21E-04	2.05E-06	222.0
36	5 31 77	2120	1.76E+01	1.85E-02	-1.62E-04	2.60E-07	383.0
37	6 1 77	1415	1.83E+01	1.73E-02	-1.40E-04	2.04E-07	407.0
38	6 1 77	1940	1.84E+01	5.32E-03	-8.67E-05	1.42E-07	387.0
39	6 1 77	2025	1.81E+01	1.49E-02	-1.37E-04	2.24E-07	364.0
40	6 2 77	810	1.81E+01	-1.78E-03	-4.31E-05	7.53E-08	387.0
41	6 2 77	900	1.85E+01	-1.08E-02	-3.30E-05	9.74E-08	381.0
42	6 2 77	940	1.89E+01	-2.88E-02	4.01E-05	-3.60E-10	385.0
43	6 2 77	1240	1.89E+01	3.44E-02	-2.95E-04	5.62E-07	283.0
44	6 2 77	1340	1.93E+01	5.68E-03	-1.04E-04	1.93E-07	341.0
45	6 2 77	1410	1.93E+01	1.26E-02	-1.43E-04	2.58E-07	333.0
46	6 2 77	2000	1.88E+01	1.82E-02	-3.04E-04	8.94E-07	219.0
47	6 3 77	1140	1.90E+01	3.24E-02	-3.32E-04	7.56E-07	278.0
48	6 4 77	610	1.96E+01	1.28E-02	-1.89E-04	4.29E-07	266.0
49	6 4 77	810	1.97E+01	1.74E-02	-1.98E-04	4.00E-07	312.0
50	6 4 77	1440	1.94E+01	4.76E-02	-4.90E-04	1.09E-06	259.0
51	6 4 77	2015	1.98E+01	-1.31E-03	-6.20E-05	1.24E-07	306.0
52	6 4 77	2115	1.99E+01	-1.31E-02	3.67E-05	-7.29E-08	339.0
53	6 5 77	830	1.85E+01	4.69E-02	-2.86E-04	3.96E-07	438.0
54	6 5 77	1220	2.01E+01	6.78E-02	-4.51E-04	7.21E-07	373.0
55	6 5 77	1300	2.02E+01	5.50E-02	-3.61E-04	5.57E-07	390.0
56	6 5 77	2140	2.03E+01	-3.59E-03	-5.13E-05	1.09E-07	348.0

Table B-III-11 Temperature Measurement - Kite Balloon (cont'd)

KITE BALLOON MEASUREMENT OF RELATIVE HUMIDITY

FLT	DATE	TIME	A	B	C	D	MAX ALT
1	5 15 77	1940	9.47E+01	-8.37E-01	4.74E-03	-7.22E-06	392.0
2	5 17 77	213	9.80E+01	-1.15E+00	2.05E-02	-1.32E-04	116.0
3	5 18 77	220	9.45E+01	-2.31E-01	2.22E-03	-4.80E-06	324.0
4	5 18 77	1620	9.61E+01	-1.19E+00	8.49E-03	-1.62E-05	310.0
5	5 18 77	1720	9.59E+01	-6.15E-01	3.20E-03	-5.34E-06	284.0
6	5 19 77	300	9.82E+01	-4.61E-01	8.70E-05	8.74E-06	174.0
7	5 19 77	1410	9.60E+01	-4.13E-01	2.34E-03	-3.69E-06	392.0
8	5 19 77	1732	8.83E+01	1.29E+00	-5.49E-03	5.63E-06	668.0
9	5 19 77	1830	9.53E+01	6.87E-02	-2.27E-04	3.03E-07	577.0
10	5 20 77	1620	8.46E+01	4.45E-01	-2.95E-03	3.99E-06	601.0
11	5 20 77	1720	9.29E+01	-1.58E-02	-2.05E-04	3.14E-07	612.0
12	5 20 77	1820	9.39E+01	-5.52E-02	5.42E-04	-1.20E-06	462.0
13	5 21 77	1620	1.24E+02	5.92E-01	-3.92E-03	4.91E-06	545.0
14	5 21 77	1720	9.09E+01	-1.98E-01	6.44E-04	-6.88E-07	530.0
16	5 23 77	1015	8.03E+01	1.78E-01	-1.56E-03	2.40E-06	492.0
17	5 23 77	1100	7.34E+01	-2.74E-01	1.32E-03	-1.55E-06	544.0
18	5 23 77	1145	7.56E+01	-2.70E-01	1.27E-03	-1.49E-06	548.0
19	5 23 77	1710	9.20E+01	-1.99E-01	7.69E-04	-1.17E-06	470.0
20	5 23 77	1740	9.56E+01	-3.59E-01	2.66E-03	-4.82E-06	456.0
21	5 23 77	1800	9.55E+01	-3.22E-01	1.25E-03	-2.06E-06	466.0
22	5 24 77	2200	9.42E+01	-2.33E-01	1.03E-03	-1.25E-06	377.0
23	5 24 77	2230	9.37E+01	-2.04E-01	1.17E-03	-2.05E-06	382.0
24	5 24 77	2300	9.29E+01	-1.52E-01	9.10E-04	-1.60E-06	394.0
27	5 26 77	1620	8.94E+01	-3.25E-01	1.80E-03	-2.58E-06	471.0
28	5 26 77	1700	8.95E+01	-3.78E-01	2.29E-03	-3.56E-06	385.0

Table B-III-12 Relative Humidity - Kite Balloon

KITE BALLOON MEASUREMENT OF RELATIVE HUMIDITY

FLT	DATE	TIME	A	B	C	D	MAX ALT
29	5 26 77	2110	1.27E+02	-6.45E-01	2.20E-02	-6.00E-05	323.0
30	5 26 77	2140	1.07E+02	2.84E+00	-2.74E-02	6.07E-05	299.0
31	5 26 77	2210	9.22E+01	-2.81E-01	1.70E-03	-2.41E-06	390.0
32	5 31 77	1320	8.97E+01	-7.46E-01	5.59E-03	-1.17E-05	272.0
33	5 31 77	1350	8.46E+01	-3.75E-01	1.71E-03	-2.38E-06	450.0
34	5 31 77	1420	8.32E+01	-3.38E-01	1.44E-03	-1.95E-06	466.0
35	5 31 77	1450	9.10E+01	-1.14E+00	1.21E-02	-3.38E-05	222.0
36	5 31 77	2120	9.16E+01	-7.12E-01	4.20E-03	-6.61E-06	383.0
37	6 1 77	1415	8.52E+01	-5.63E-01	2.82E-03	-3.94E-06	407.0
38	6 1 77	1940	9.34E+01	-2.92E-01	1.87E-03	-3.11E-06	387.0
39	6 1 77	2025	9.36E+01	-3.02E-01	1.98E-03	-3.38E-06	364.0
40	6 2 77	810	9.43E+01	-2.87E-01	1.94E-03	-3.45E-06	387.0
41	6 2 77	900	9.26E+01	-2.39E-01	1.88E-03	-3.55E-06	381.0
42	6 2 77	940	9.07E+01	-2.26E-01	1.79E-03	-3.30E-06	385.0
43	6 2 77	1240	9.33E+01	-5.92E-01	4.30E-03	-8.51E-06	283.0
44	6 2 77	1340	8.96E+01	-3.14E-01	2.09E-03	-3.63E-06	341.0
45	6 2 77	1410	9.13E+01	-3.96E-01	2.65E-03	-4.71E-06	333.0
46	6 2 77	2000	9.68E+01	-3.73E-01	4.26E-03	-1.23E-05	219.0
47	6 3 77	1140	9.48E+01	-3.44E-01	2.68E-03	-6.06E-06	278.0
48	6 4 77	610	9.14E+01	-5.77E-01	4.52E-03	-9.53E-06	266.0
49	6 4 77	810	9.07E+01	-6.00E-01	4.33E-03	-8.37E-06	312.0
50	6 4 77	1440	9.61E+01	-9.09E-01	6.95E-03	-1.40E-05	259.0
51	6 4 77	2015	9.17E+01	-5.03E-01	3.64E-03	-7.01E-06	306.0
52	6 4 77	2115	8.92E+01	-4.02E-01	2.41E-03	-3.94E-06	339.0
53	6 5 77	830	9.03E+01	-6.41E-01	3.79E-03	-5.49E-06	438.0
54	6 5 77	1220	8.53E+01	-5.60E-01	3.21E-03	-4.98E-06	373.0
55	6 5 77	1300	8.60E+01	-5.16E-01	2.87E-03	-4.34E-06	390.0
56	6 5 77	2140	9.03E+01	-4.60E-01	2.92E-03	-4.97E-06	348.0

Table B-III-12 Relative Humidity - Kite Balloon (cont'd)

k) Sea State Observations

Table B-III-13 lists the hourly visual observations of sea state that were obtained during the cruise. The coded values have the meanings found in Table B-II-1 of Section B-II-a.

SEA STATE OBSERVATIONS

HOUR	5/15/77	5/16/77	5/17/77	5/18/77	5/19/77	5/20/77	5/21/77	5/22/77
0								
1								
2								
3								
4								
5								
6								
7								
8								
9								
10								
11								
12								
13								
14								
15								
16								
17								
18								
19								
20								
21								
22								
23								

Table B-III-13 Sea State Observations

SEA STATE OBSERVATIONS

PAGE 2

HOUR 5/23/77 5/24/77 5/25/77 5/26/77 5/27/77 5/28/77 5/29/77 5/30/77

0 1 2 3 4 5 6 7 8 9 10 11 12 13 14 15 16 17 18 19 20 21 22 23

mmmmmmmmmmmmmmmmmm

4 4 3 4 3 3

3 3 2 3 3 3

nnnnnnnnnnnnnnnn

3 3 4 4 4 3 3 4 3 3

Table B-III-13 Sea State Observation (cont'd)

356

HOUR	5/31/77	6/1/77	6/2/77	6/3/77	6/4/77	6/5/77	6/6/77	6/7/77
1								
2								
3								
4								
5								
6								
7								
8								
9								
10								
11								
12								
13								
14								
15								
16								
17								
18								
19								
20								
21								
22								
23								
24								

0 1 2 3 4 5 6 7 8 9 10 11 12 13 14 15 16 17 18 19 20 21 22 23

୪୪୪୪୩୩ ୩୩୩୩

४४ ४४३ ३३३३३३

-NNNNNNNNNNMMMMMMMM

MMMMMMMMMMMMMMMM MMMMMM MM

M M M M M M M M M M

Table B-III-13 Sea State Observations (Cont'd)

B-IV AEROSOL DATA

One of the most important features of this cruise was our ability to measure various characteristics of the natural oceanic aerosols. In this section of the report we will discuss and present the data from our routine measurements of condensation nuclei density, cloud condensation nuclei density, scattering coefficients, the Royco and P.M.S. optical aerosol size analyzers and the Thermo Systems Electrical Aerosol Analyzer.

The ship itself is a prolific source of aerosols because of effluents from the stacks and galley therefore great care must be taken to eliminate from the data those times in which there is known ship influence. The data presented in this section of the report has been prescreened to eliminate as much as possible this source of self influence on the aerosols characteristics.

Even though we experienced true winds from a westerly direction during a large portion of the cruise, the forward motion of the ship helped to counteract this influence. The frequency distribution of the relative wind direction is shown in Figure B-IV-1. Here we see that the most frequent relative wind direction was from a favorable quarter. However during the times in which relative winds were from the stern of the ship (thus causing severe sampling problems) the ship stopped its forward motion and turned into the wind from time to time in order to obtain accurate aerosol measurements.

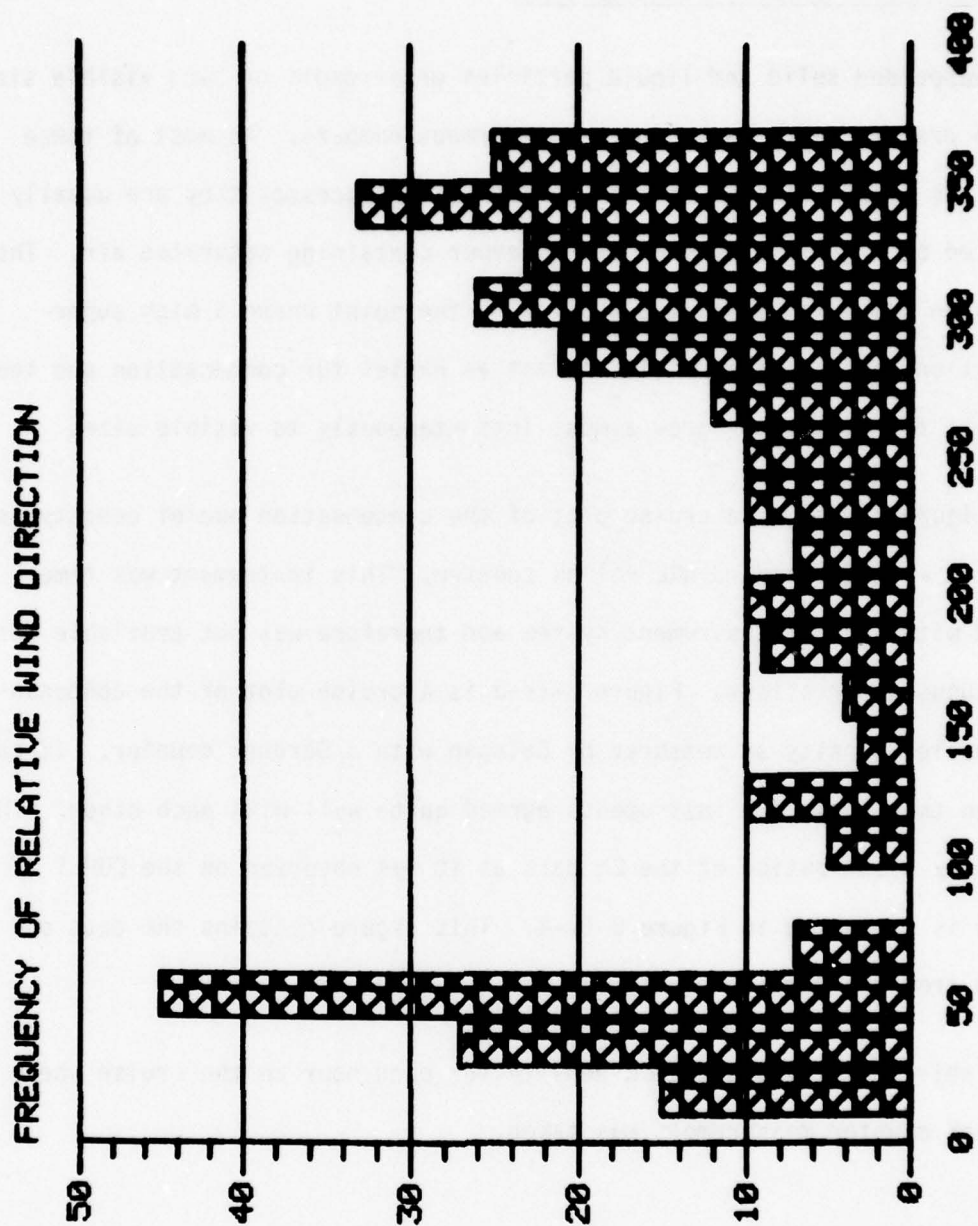


Fig. (B-IV-1) Frequency distribution of relative wind direction.

a) Condensation Nuclei Density (CN)

Suspended solid and liquid particles or aerosols of such visible size can be present in the atmosphere in enormous numbers. As most of these particles play a crucial role in condensation processes they are usually measured by a rapid expansion of a chamber containing saturated air. The expansion causes an adiabatic cooling to the point where a high supersaturation causes the particles to act as nuclei for condensation and the droplets formed thereby grow almost instantaneously to visible size.

Figure B-IV-2 is a cruise plot of the condensation nuclei density as measured with a standard NRL Pollak counter. This instrument was time shared with another instrument system and therefore was not available for continuous observations. Figure B-IV-3 is a cruise plot of the condensation nuclei density as measured by Calspan with a Gardner counter. It can be seen that these two instruments agreed quite well with each other. The frequency distribution of the CN data as it was observed on the EOMET 77 cruise is presented in Figure B-IV-4. This figure contains the data obtained from the Gardner counter.

Table B-IV-1 lists the CN density for each hour on the cruise where a Pollak counter measurement was taken.

EOMET 77 1PLOT: JULIAN DATE 135-15 MAY 1977

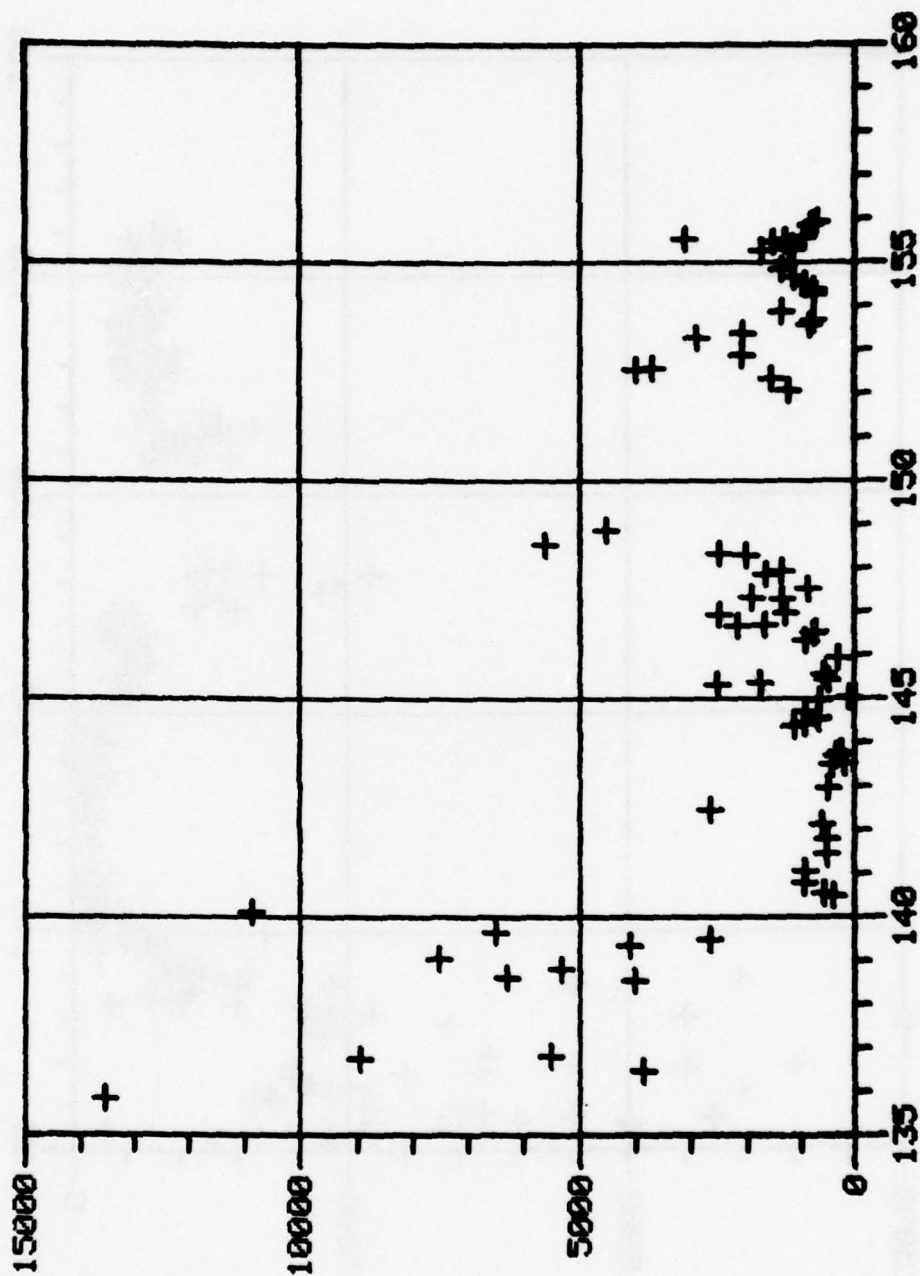


Fig. (B-IV-2) Condensation nuclei density-Pollak counter-Julian day vs. number/cc.

ECOMET 77 1PLOT: JULIAN DATE 135=15 MAY 1977

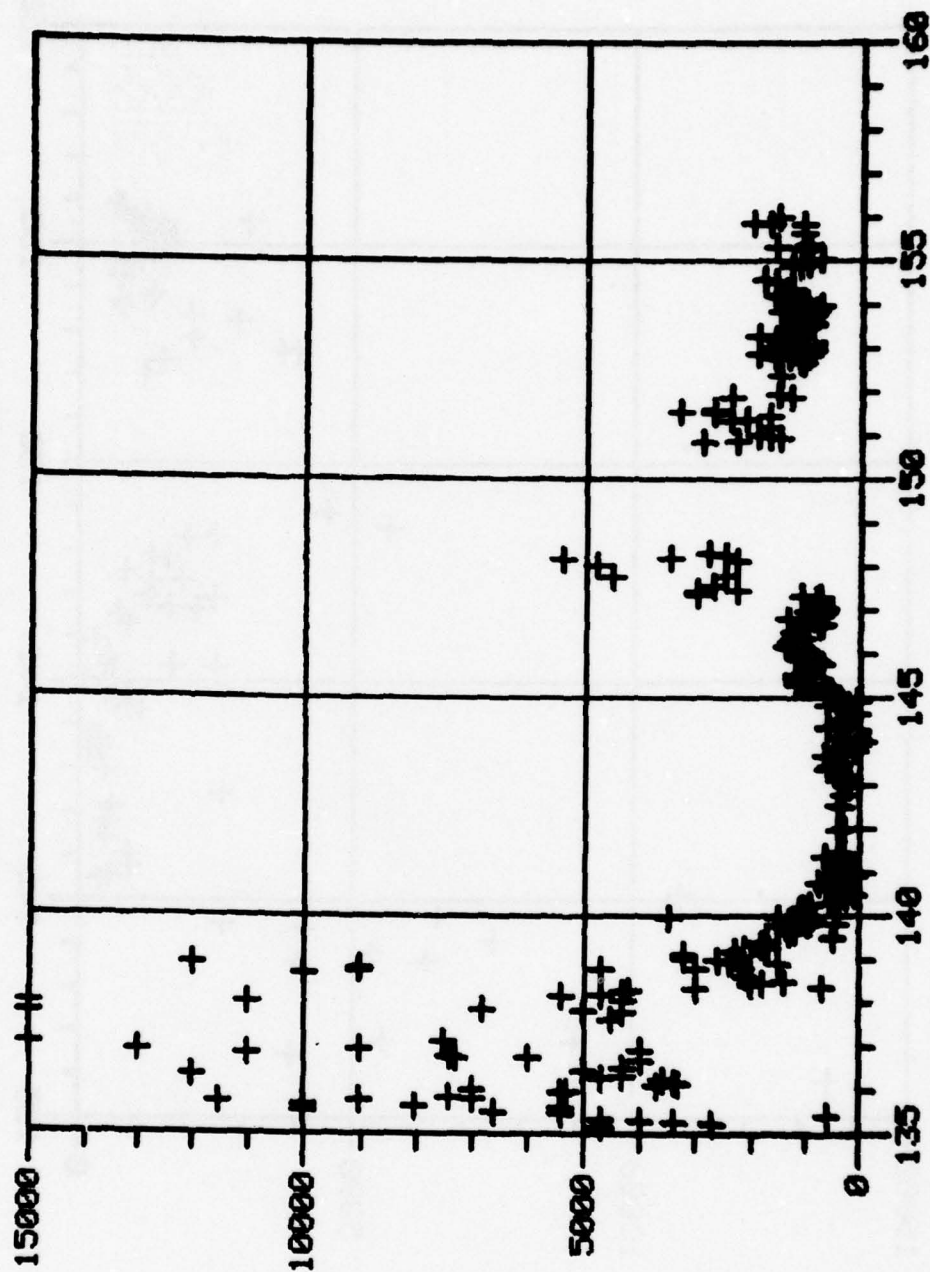


Fig. (B-IV-3) Condensation nuclei density-Gardner counter-Julian days vs. number/cc.

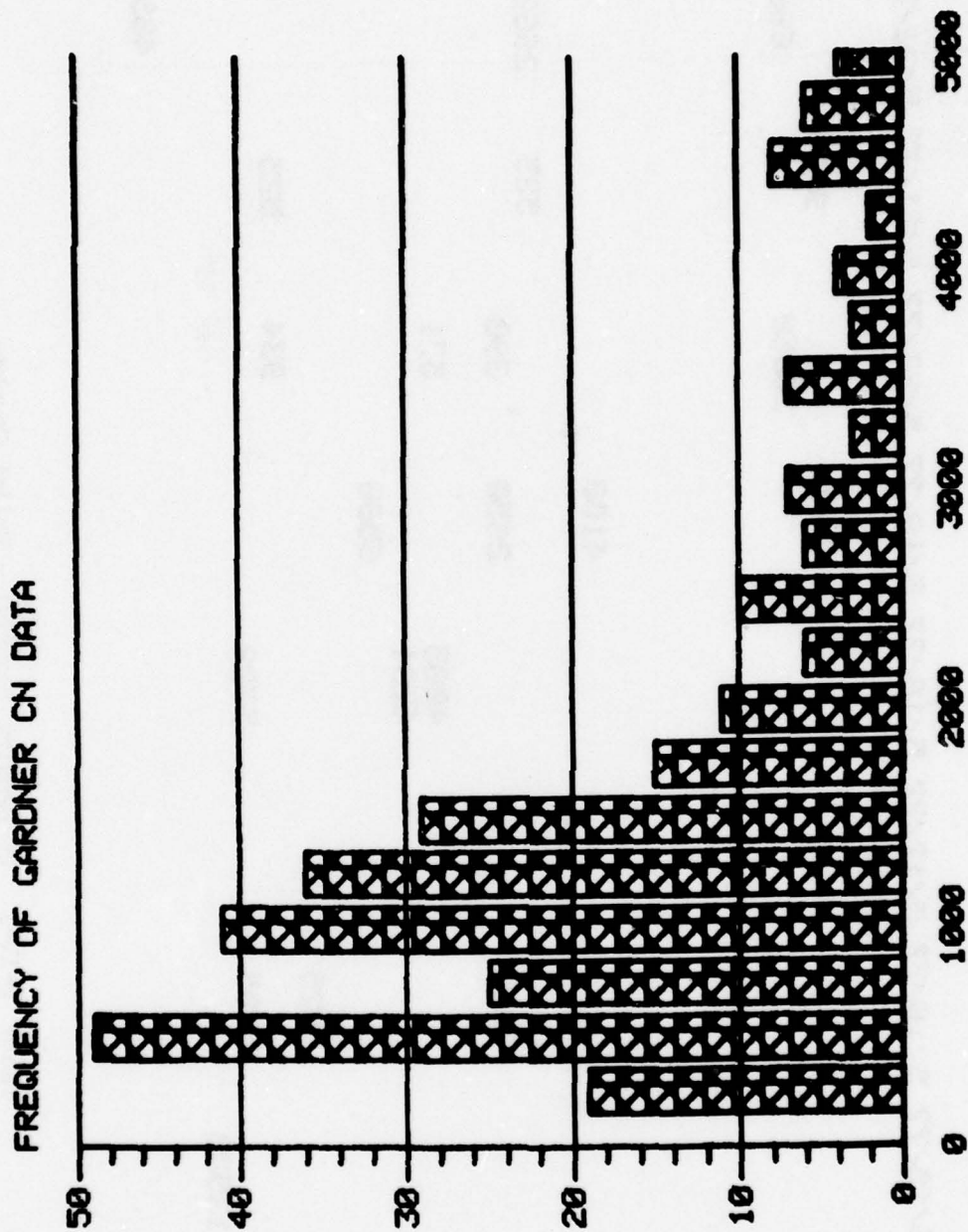


Fig. (B-IV-4) Frequency distribution of CN-Gardner counter.

* NRL CONDENSATION NUCLEI DENSITY (#/CC) POLLAK COUNTER

HOUR	5/15/77	5/16/77	5/17/77	5/18/77	5/19/77	5/20/77	5/21/77	5/22/77
0								
1								
2								
3					7500	10650	913	606
4								
5								
6								
7								
8								
9					4100			
10								
11							525	2662
12		3860			2650	390		
13						571		
14				4005				
15				6291				
16					6500			
17								
18		8925						
19		5505					525	
20				5322		934		
21	13500							
22								
23								489

Table B-IV-1 CN Density (Hourly) - Pollak Counter

NRL CONDENSATION NUCLEI DENSITY (#/CC) POLLAK COUNTER

PAGE 2

HOUR 5/23/77 5/24/77 5/25/77 5/26/77 5/27/77 5/28/77 5/29/77 5/30/77

४७

[illegible]

* NRL CONDENSATION NUCLEI DENSITY (#/CC) POLLAK COUNTER		
PAGE 3		
HOUR	5/31/77	6/1/77
0	2903	750
1	1550	1732
2		1190
3		
4		
5		
6		
7		
8		
9		
10		
11		
12		
13		
14		
15		
16		
17		
18		
19		
20		
21		
22		
23		

Table B-IV-1 CN Density (Hourly) - Pollak Counter (Cont'd)

b) Cloud Condensation Nuclei

It is generally agreed that only a small fraction of the condensation nuclei in the air are activated in natural cloud or fog condensation processes where only very small supersaturations exist. The subset of atmospheric condensation nuclei which can be activated by natural conditions are called cloud condensation nuclei. The data presented in this report were obtained by the NRL thermal gradient diffusion chamber. Figure B-IV-5 is a cruise plot of the CCN density obtained with the NRL CCN chamber for a temperature differential across the thermal gradient plates of 4.3°C . Table B-IV-2 is a listing of the hourly values of this parameter during the cruise as they were obtained.

EOMET 77 1PLOT: JULIAN DATE 135-15 MAY 1977

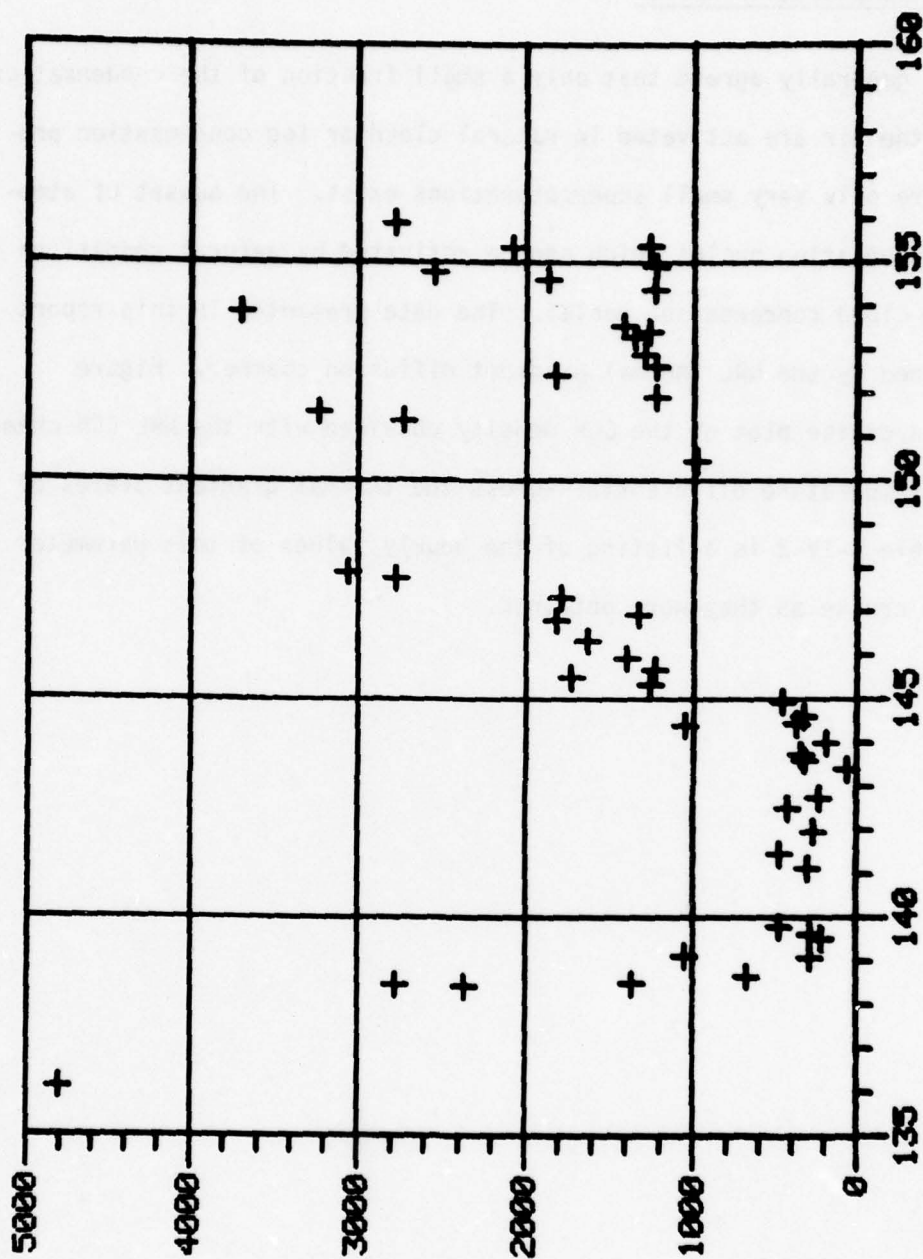


Fig. (B-IV-5) CCN density using NRL CCN chamber with 4.3°C temperature differential; number/cc vs. Julian date.

Table B-IV-2. CCN Density (hourly listing) - from NRL CCN chamber having 4.3°C Temperature Differential

CLOUD CONDENSATION NUCLEI DENSITY (#/CC @ 4.3 DEG.)

HOUR	5/15/77	5/16/77	5/17/77	5/18/77	5/19/77	5/20/77	5/21/77	5/22/77
0								
1								
2						274		
3		4020		5469	932		311	
4								
5								
6								
7								
8								
9								
10				2412				
11				2398				
12				1635				355
13	4908				281			
14			5126					
15					237			
16			5910	414				
17	5806							229
18								
19			5131		392			
20	3823							
21								
22								
23			5816				370	

CLOUD CONDENSATION NUCLEI DENSITY (#/CC @ 4.3 DEG.)

PAGE 2

HOUR	5/23/77	5/24/77	5/25/77	5/26/77	5/27/77	5/28/77	5/29/77	5/30/77
0		148						
1								
2								
3								
4								
5								
6								
7								
8			1273	1443	2013			
9		992						
10		511						755
11								
12			1399		2449			
13				1576				
14	370	348						
15								
16			1480					
17	252							
18								
19								
20								
21					2834			
22		481	1584	1184				
23								

Table B-IV-2 CCN Density - NRL CCN Chamber having
4.3°C Temperature Differential (Cont'd)

♦ CLOUD CONDENSATION NUCLEI DENSITY (#/CC @ 4.3 DEG.)
PAGE 3

HOUR	5/31/77	6/1/77	6/2/77	6/3/77	6/4/77	6/5/77	6/6/77	6/7/77
0								
1								
2								
3								
4								
5								
6			1347					
7						1628		
8				1317	1214			
9		1487	1524					
10								
11								
12			1524	2457				
13	3034							
14		1103		1709				
15								
16								
17								
18								
19								
20		1362	1450					
21	1036			1110	2775			
22								
23								

c) Scattering Coefficient

The scattering coefficient was measured simultaneously by two MRI integrating nephelometers. A high degree of reliability is attributed to these measurements because of the good correlation between these aerosol measurements. Figure B-IV-6 is a scatterplot of simultaneous measurements of the scattering coefficient from the two instruments. Values along each axis are the measured scattering coefficient multiplied by 10^4 and expressed in (meters^{-1}). The x axis represents the Calspan MRI model 2050 data and the y axis is the NRL-MRI model 1567 data.

Figure B-IV-7 is the cruise plot of the NRL measured scattering coefficient multiplied by 10^4 and expressed in meters^{-1} along the y axis and the Julian time is expressed along the x axis.

The frequency distribution of the NRL scattering coefficient ($\times 10^{-4} \text{ m}^{-1}$) is shown in Figure B-IV-8. Table B-IV-3 contains the hourly values of the NRL scattering coefficient obtained during the cruise.

SCATPLOT OF SCATTERING COEF X: CALSPAN, Y: NRL

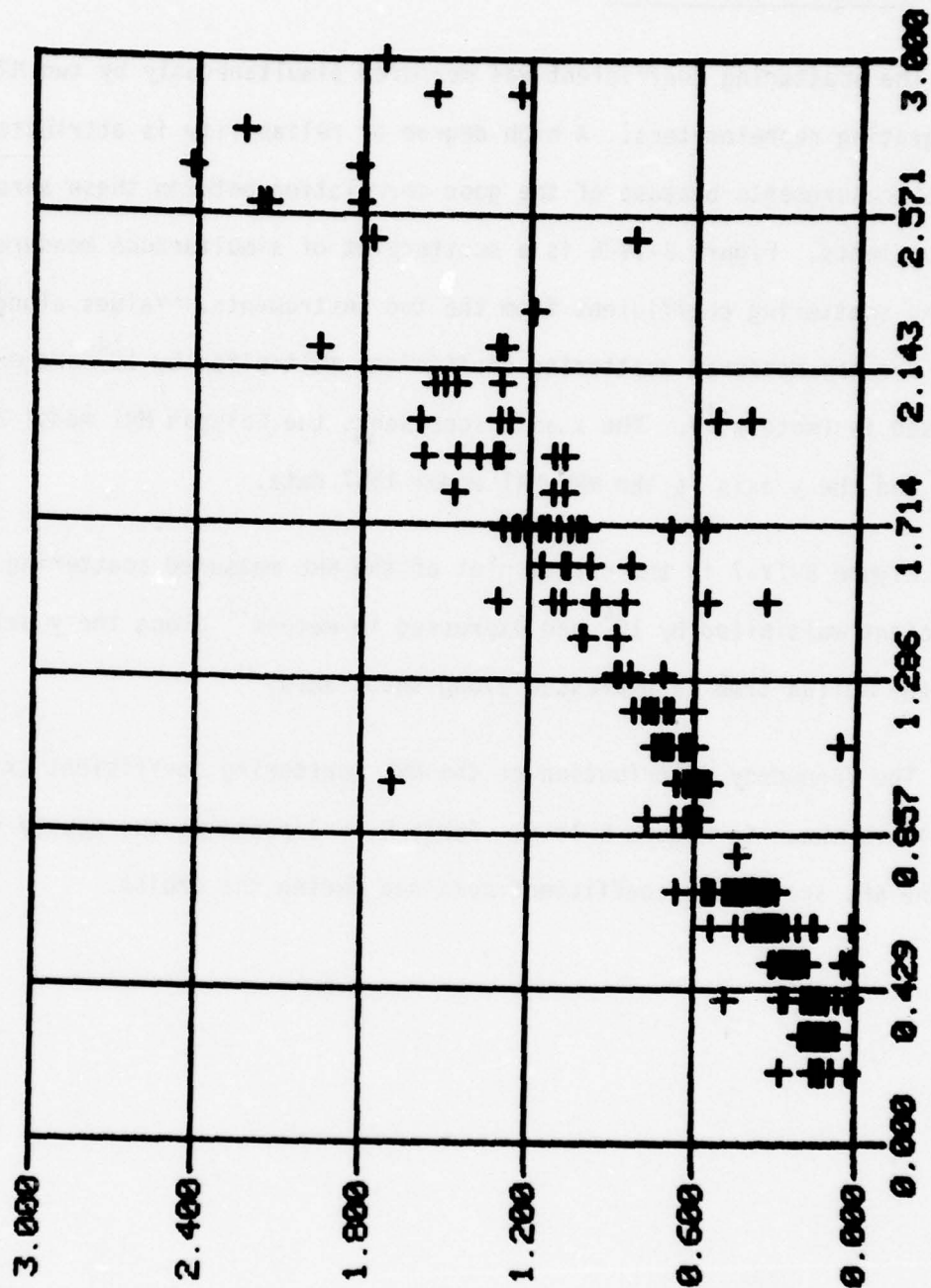


Fig. (B-IV-6) Scattering coefficient X-CALSPAN vs. Y-NRL.

EOMET 77 1PLOT: JULIAN DATE 135=15 MAY 1977

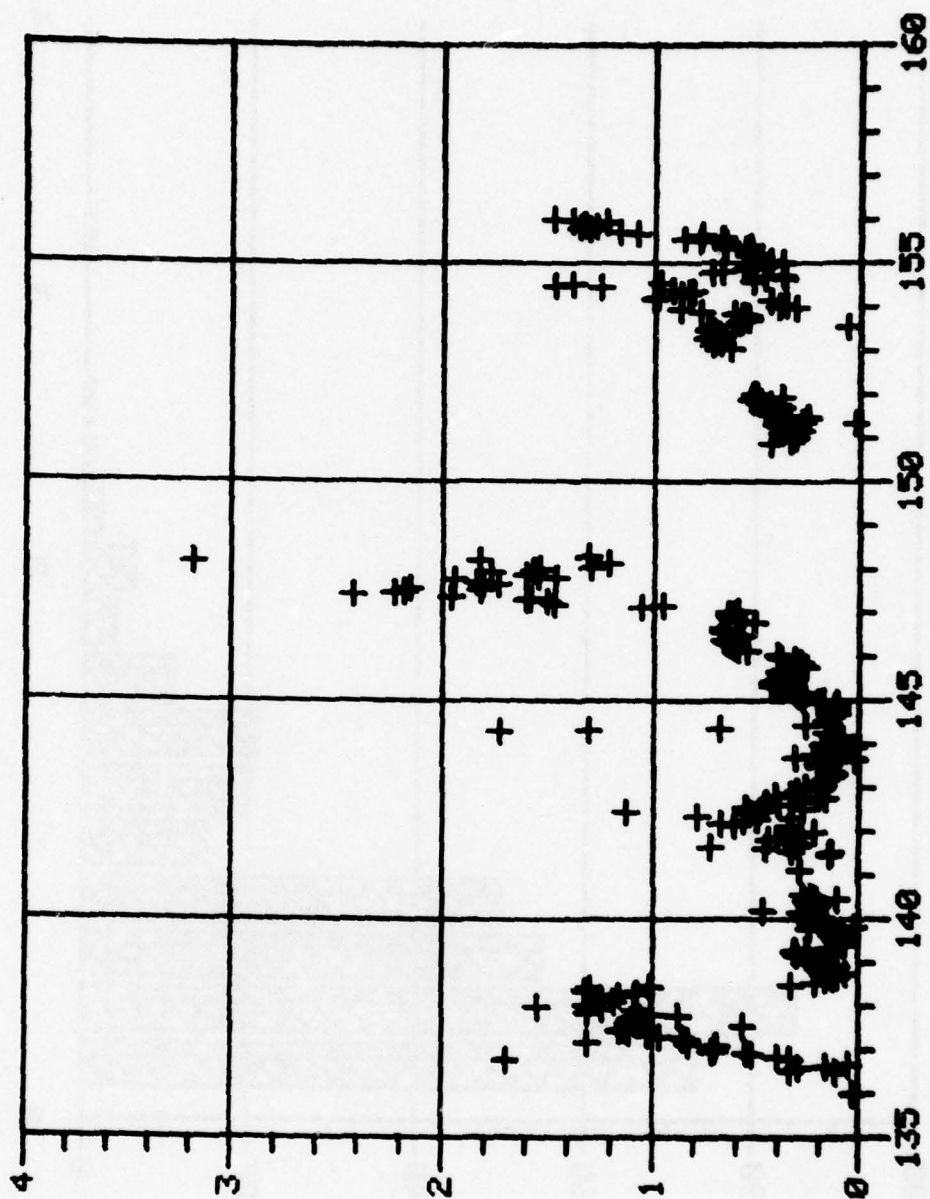


Fig. (B-IV-7) NRL scattering coefficient
 X - Julian day
 Y - Scattering coefficient multiplied by 10^4 & expressed in meters^{-1} .

FREQUENCY DISTRIBUTION OF SCATTERING MEAS

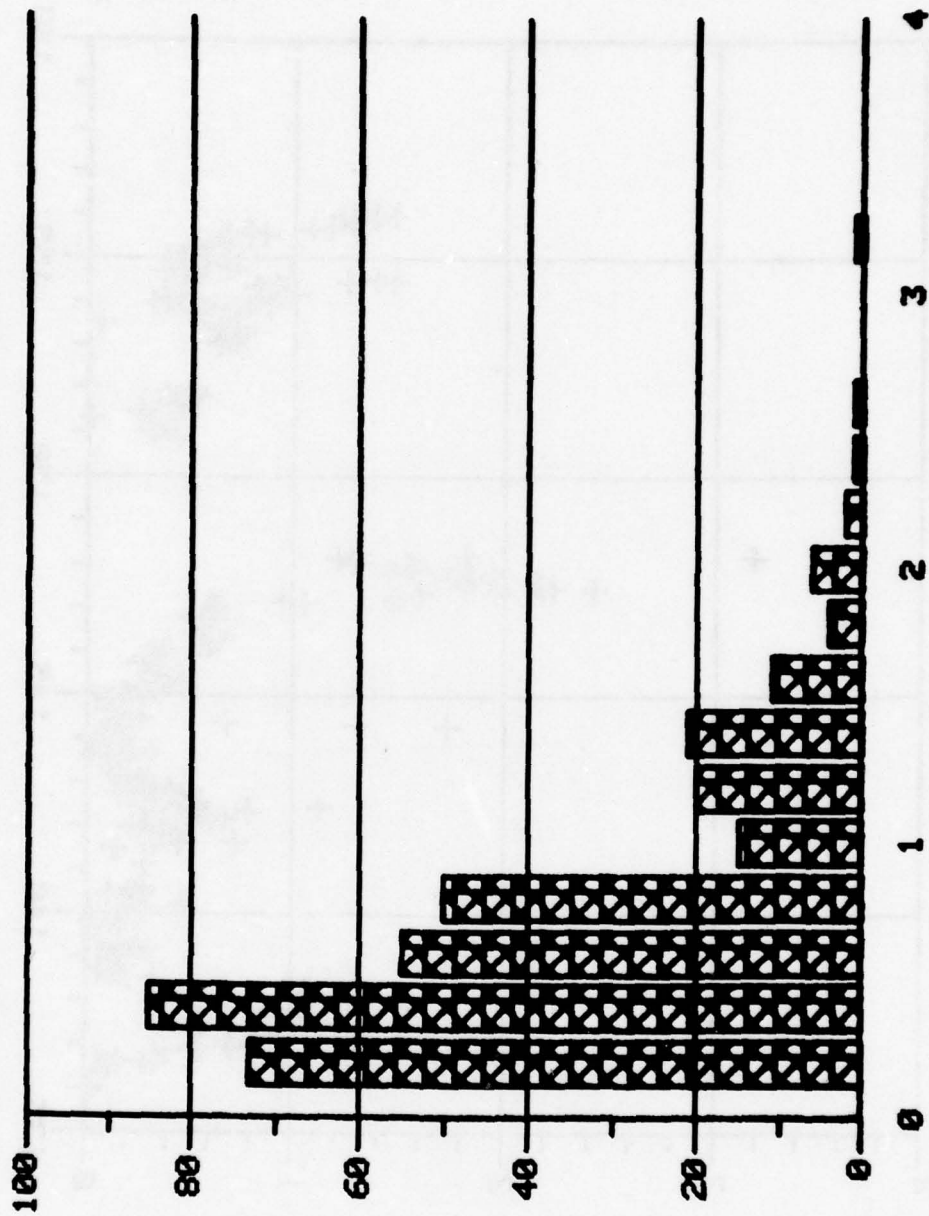


Fig. (B-IV-8) Frequency distribution - NRL scattering coefficient ($\times 10^4 \text{ (m}^{-1}\text{)}$)

* HOUR	NRL SCATTERING COEF. (* 10-4) EOMET 77									
	5/15/77	5/16/77	5/17/77	5/18/77	5/19/77	5/20/77	5/21/77	5/22/77		
0			0.716	1.547	0.194	0.196		0.222		
1		0.038	0.700	1.308	0.233	0.184		0.336		
2			0.693	1.185	0.244	0.264	0.292			
3			0.825	1.252	0.260	0.290		0.341		
4			1.306	1.241	0.308	0.473		0.614		
5			0.834	1.153	0.318	0.221		0.678		
6			0.854	1.077	0.314	0.225		0.562		
7			0.964	1.074	0.259	0.203		0.498		
8			1.023	1.313	0.130	0.251		0.335		
9			1.116	1.296	0.078	0.256		0.784		
10			1.156	1.009	0.066	0.109	0.148	0.537		
11			1.134	0.337	0.102	0.218	0.145	1.130		
12		0.115	1.114		0.109	0.233	0.137	0.484		
13		0.340	0.569	0.215	0.117	0.281	0.333	0.278		
14		0.300	1.074	0.166	0.106		0.462	0.556		
15		0.166	1.109	0.132	0.137		0.726	0.398		
16		0.054	1.095	0.110	0.082		0.298	0.462		
17			1.054	0.071	0.144		0.312	0.280		
18			0.880	0.130	0.241		0.363	0.170		
19	1.693		0.999	0.143	0.020		0.442	0.202		
20	0.342		1.311	0.137	0.176		0.407	0.411		
21	0.406		1.076	0.109	0.167		0.287	0.336		
22	0.527		1.241	0.164	0.173		0.284	0.304		
23	0.558							0.284		

Table B-IV-3. NRL Scattering Coefficient - Hourly Log

* HOUR	NRL SCATTERING COEF.		(* 10-4)		EOMET 77	
	5/23/77	5/24/77	5/25/77	5/26/77	5/27/77	5/28/77
0	0.194	0.086	0.296	0.549	1.060	1.211
1	0.180	0.103	0.269	0.601	0.955	3.179
2	0.268	0.132	0.315	0.605	1.466	1.822
3	0.168	0.161	0.385	0.620	1.506	1.308
4	0.137	1.727	0.392	0.643	1.598	1.306
5	0.129	1.303	0.431	0.645	1.580	
6	0.126	0.683	0.419	0.661	1.955	
7	0.142	0.263	0.424	0.626	2.419	
8	0.159	0.150	0.403	0.586	2.226	
9	0.167	0.150	0.375	0.602	2.176	
10	0.205	0.157	0.362	0.629	1.816	
11	0.199			0.666	2.151	
12	0.202			0.671	1.810	
13	0.020	0.139	0.394	0.631	1.733	
14	0.022	0.145	0.393	0.624	1.840	
15	0.310	0.113	0.350	0.514	1.938	
16	0.221	0.121	0.267	0.579	1.458	
17	0.096	0.120	0.289	0.616	1.546	
18	0.120	0.113	0.298	0.624	1.599	
19	0.068	0.119	0.291	0.638	1.768	
20	0.026	0.110	0.323	0.620	1.565	
21	0.093	0.201	0.387			0.436
22						0.339
23						0.336

Table B-IV-3 NRL Scattering Coefficient - Hourly Log (Cont'd)

* HOUR	NRL 5/31/77	SCATTERING COEF		(* 10-4)	EOMET 77	6/5/77 1.473	6/6/77 6/7/77
		PAGE 3	6/2/77				
0			0.525	6/3/77 0.403	6/4/77 0.382		
1	0.336	0.634		0.368	0.448		
2							
3	0.312	0.717		0.444	0.497		
4	0.295	0.685		1.002	0.549		
5	0.357	0.707		0.981	0.534		
6	0.396	0.755		0.870	0.551		
7	0.418	0.741		0.837	0.562		
8	0.018	0.704		0.817	0.664		
9	0.287	0.696		0.908	0.539		
10	0.357	0.715		1.255	0.666		
11	0.259	0.746		1.466	0.659		
12	0.358	0.735		1.383	0.782		
13	0.433	0.064		0.964	0.859		
14	0.464	0.627		0.530	0.675		
15	0.453	0.601		0.378	0.771		
16	0.442	0.585		0.470	1.076		
17	0.392	0.546		0.385	1.164		
18	0.442	0.560		0.725	1.307		
19	0.500	0.576		0.675	1.352		
20	0.491	0.620		0.568	1.273		
21	0.535	0.780		0.558	1.325		
22	0.381	0.880		0.473	1.225		
23	0.506	0.319		0.538	1.384		

Table B-IV-3 NRL Scattering Coefficient - Hourly Log (Cont'd)

d) Royco Measurements

There were two Royco aerosol spectrometers operating in a continuous monitoring mode throughout the cruise. The channel sizes of the two instruments are slightly different; nevertheless the two instruments appeared to track very well. Both sets of data are of course in the data bank and may be addressed at will by means of the archiving system described in Section D.

Figure B-IV-9 is a cumulative plot obtained with the archive system of the NRL Royco data for 0500 GMT on 18 May 1977 showing the measured number of particles/cc greater than the indicated size. Figure B-IV-10 is the plot of the Calspan Royco data for the same hour showing satisfactory agreement for experimental field data.

Figures B-IV-11 through B-IV-15 are cruise plots expressing the number of particles per cc obtained in each of the five channels of the NRL Royco as functions of time throughout the cruise.

Table B-IV-4 is a listing of the NRL Royco data where the numbers under the heading:

CH1 refers to \log_{10} [#/cc] of particles with $0.45 < d \leq 0.6$ microns

CH2 refers to \log_{10} [#/cc] of particles with $0.6 < d \leq 1.5$ microns

CH3 refers to \log_{10} [#/cc] of particles with $1.5 < d \leq 2.5$ microns

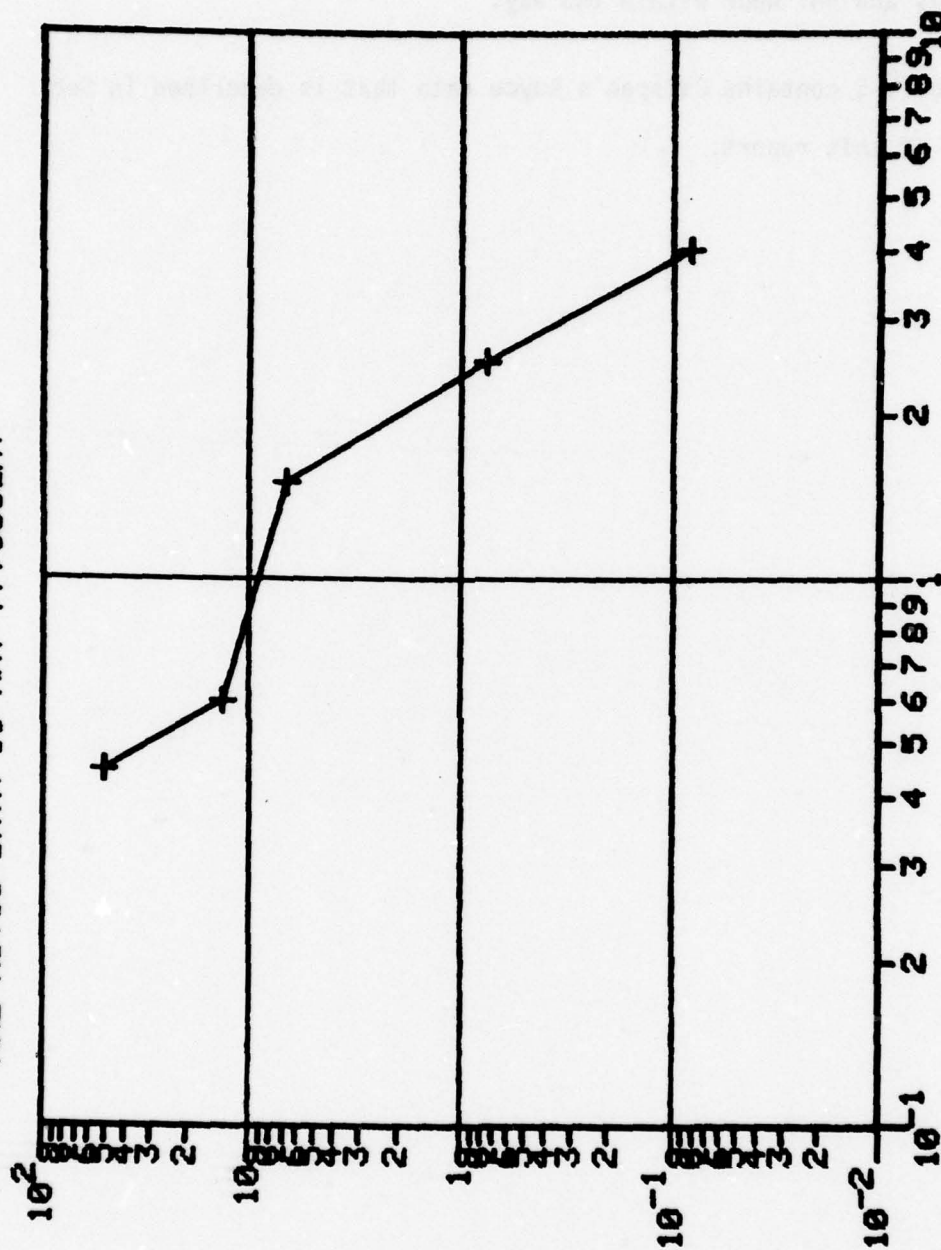
CH4 refers to \log_{10} [#/cc] of particles with $2.5 < d \leq 4.0$ microns

and CH5 refers to \log_{10} [#/cc] of particles with $d > 4.0$ microns.

Each page of the table contains two columns with each sample referred to by Julian day and GMT hour within the day.

Table B-IV-5 contains Calspan's Royco data that is described in Section B-II-b of this report.

NRL ROYCO DATA 18 MAY 77, 500GMT



DIAMETER (MICRONS)

Fig. (B-IV-9) Cumulative plot of NRL Royco data.

CALSPAN ROYCO DATA 18 MAY 77, 500 GMT

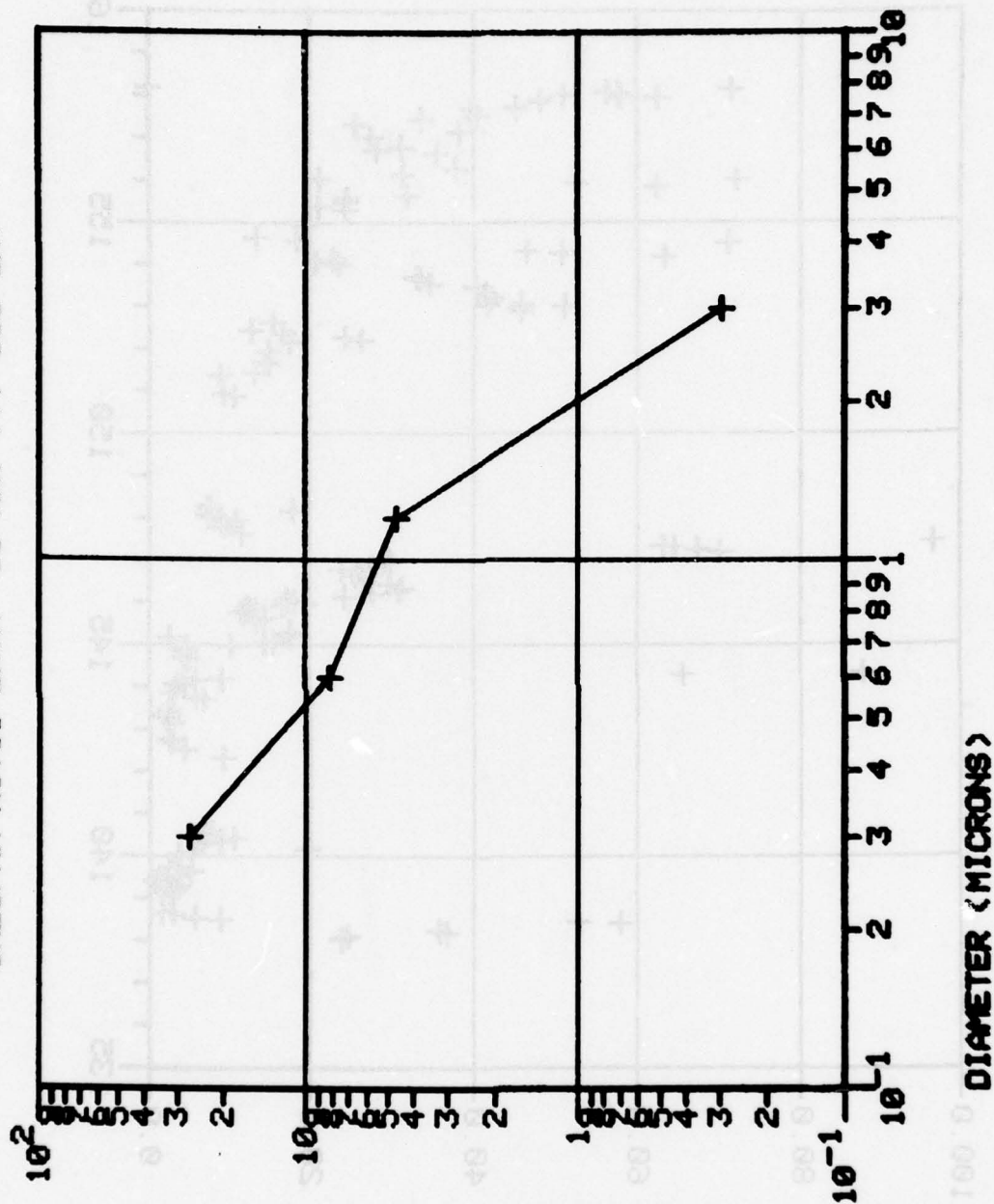


Fig. (B-IV-10) Calspan Royco data.

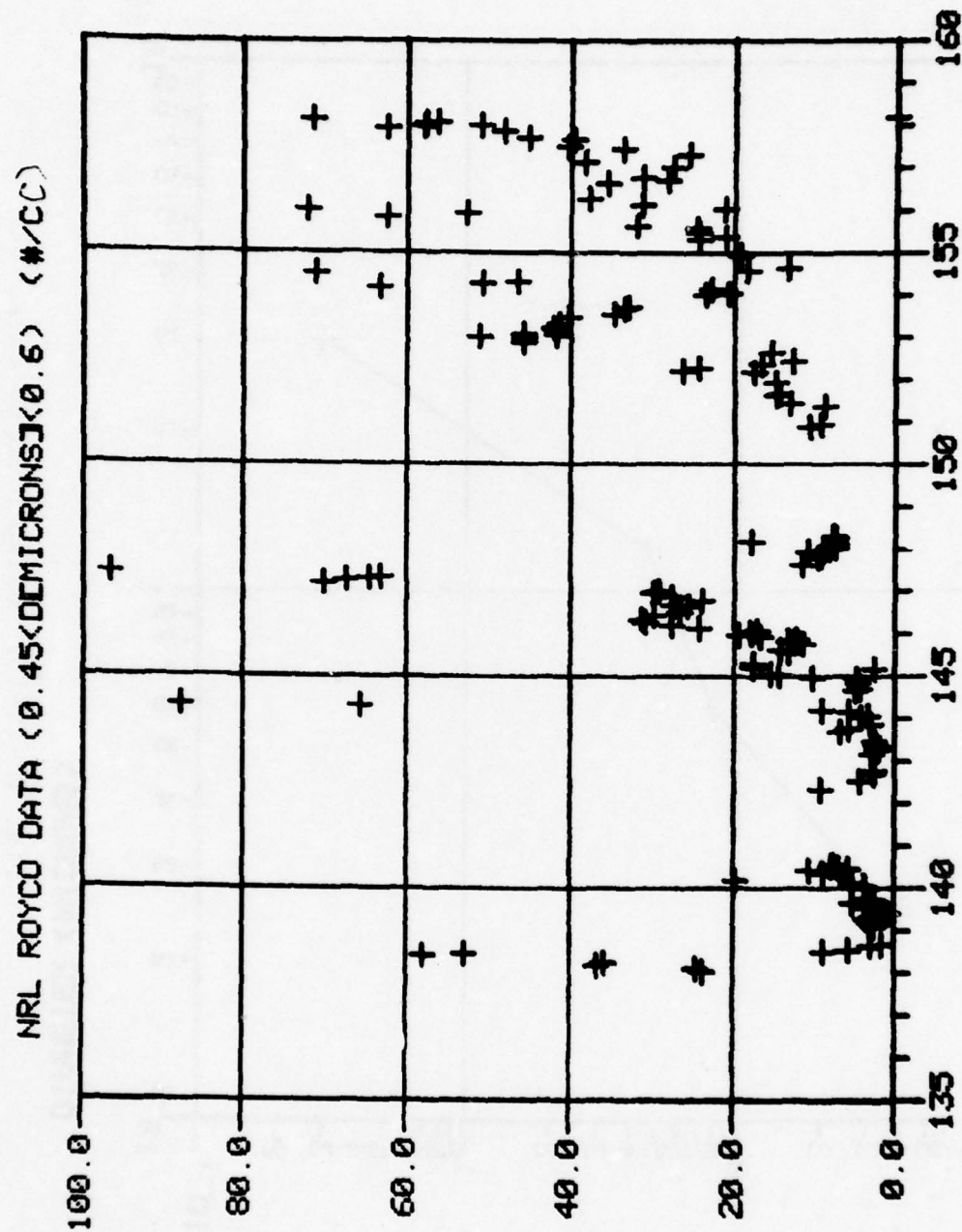


Fig. (B-IV-11) NRL Royco data channel 1.

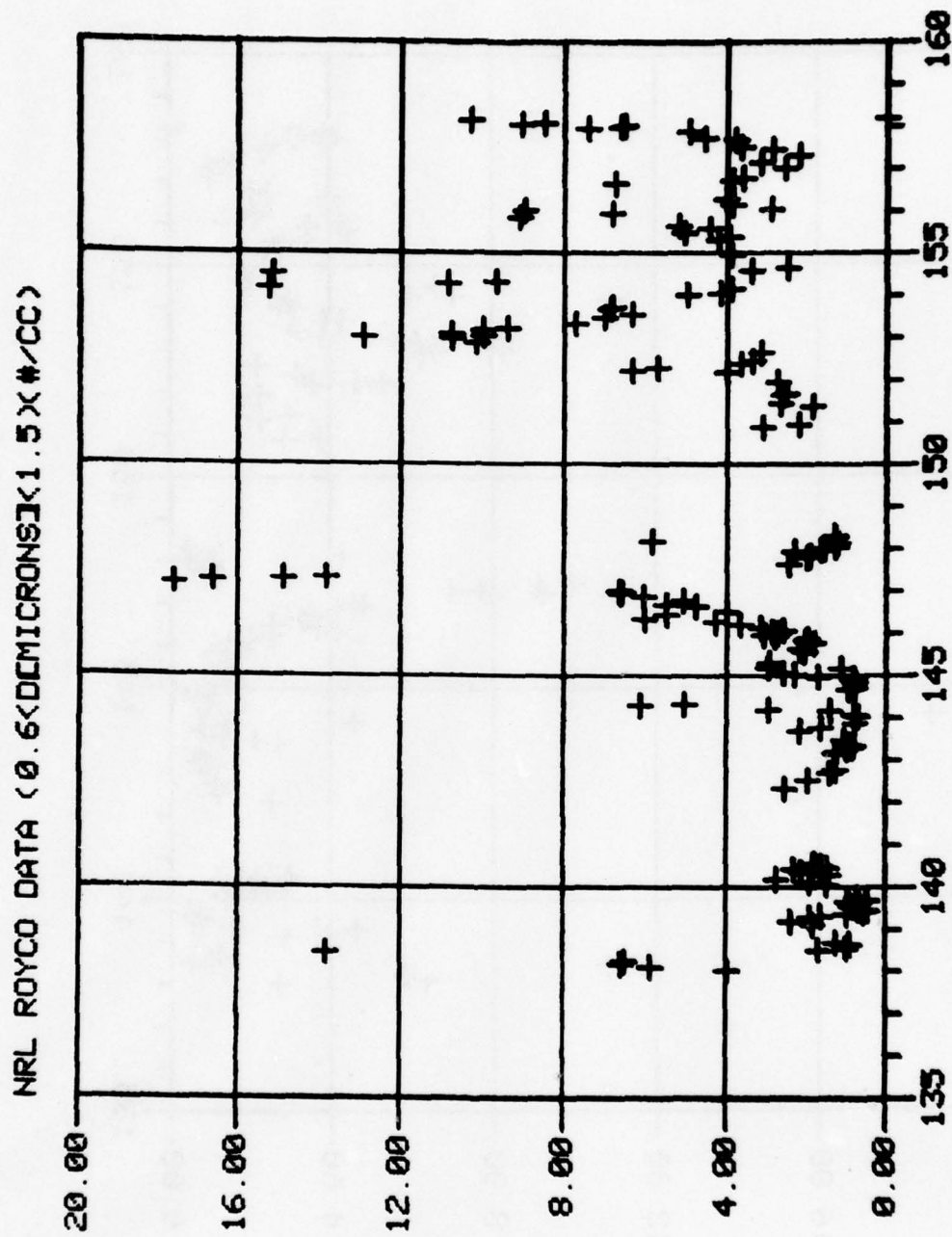


Fig. (B-IV-12) NRL Royco data channel 2.

NRL ROYCO DATA (1.5<DEMICRONS<2.5)(#/CC)

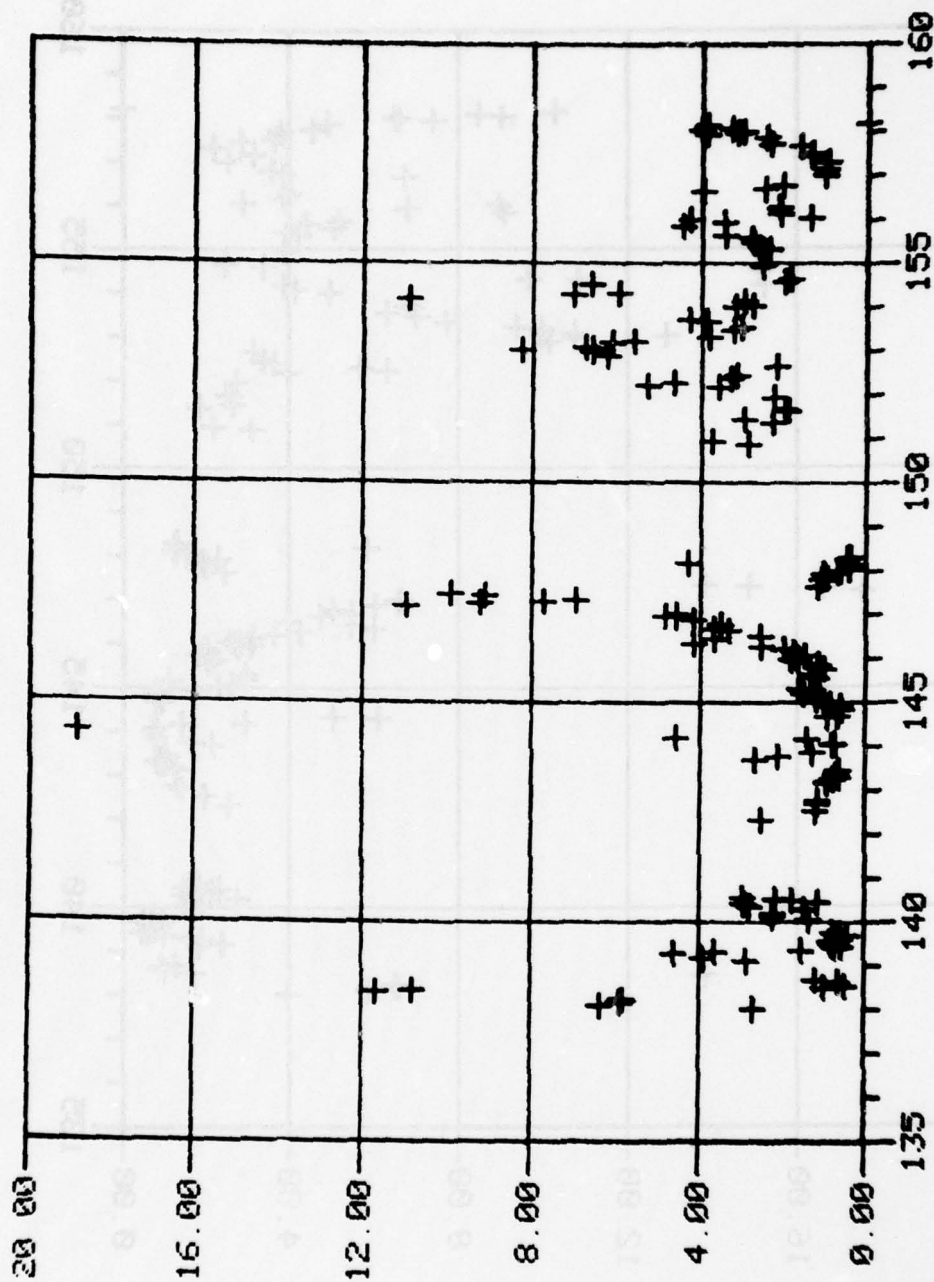


Fig. (B-IV-13) NRL Royco data channel 3.

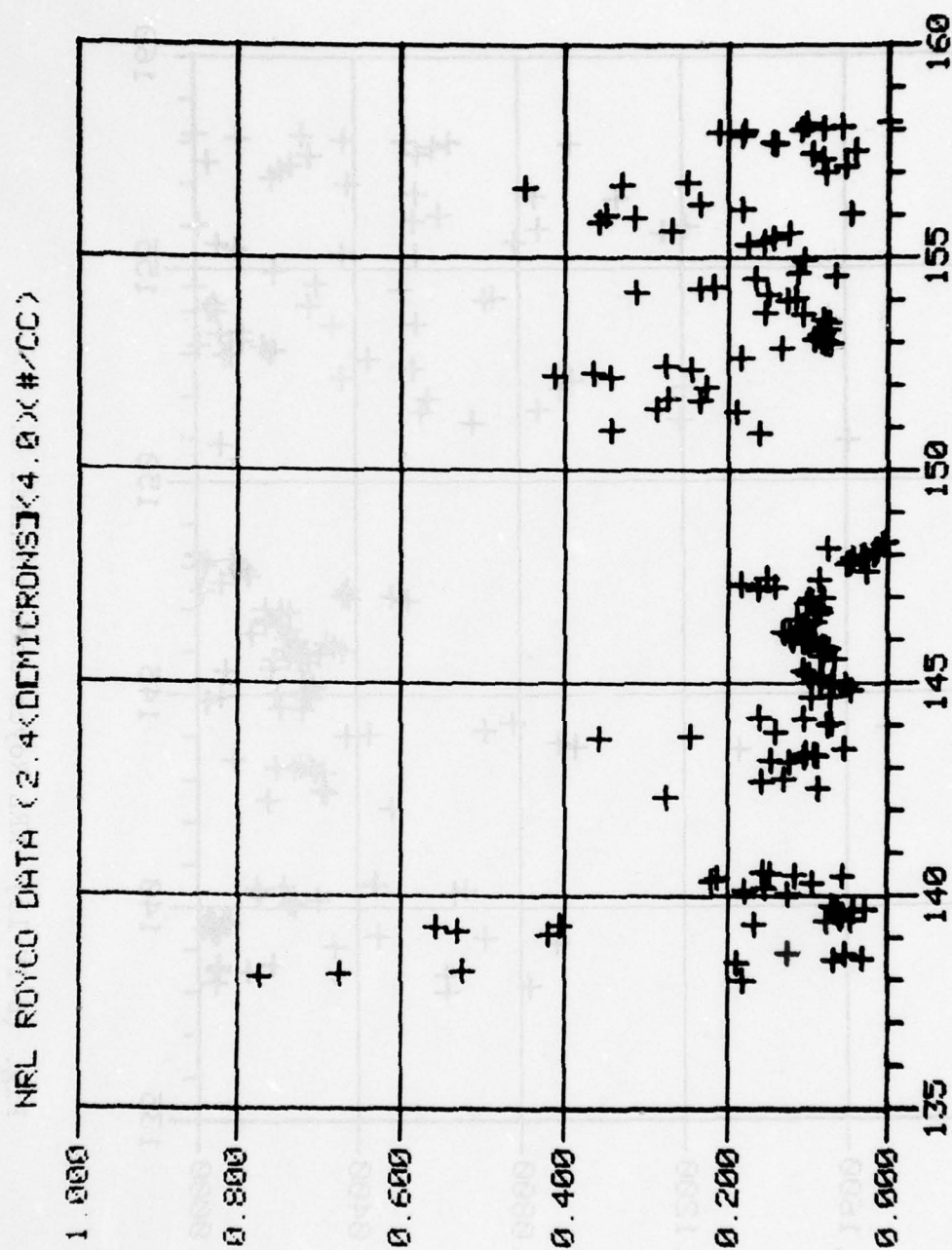


Fig. (B-IV-14) NRL Royco data channel 4.

NRL ROYCO SIZE DISTRIBUTIONS EOMET 77

DAY	HR	CH1	CH2	CH3	CH4	CH5	DAY	HR	CH1	CH2	CH3	CH4	CH5
138	2	1.38	0.60	0.44	-0.74	-1.21	140	5	1.30	0.44	0.36	-0.80	-1.51
138	3	1.39	0.77	0.80	-0.11	-0.53	140	7	0.83	0.16	0.17	-1.02	-1.79
138	5	1.57	0.82	0.77	-0.17	-1.09	140	9	0.96	0.34	0.45	-0.66	-1.19
138	6	1.55	0.81	0.77	-0.28	-2.36	140	10	1.04	0.37	0.47	-0.67	-1.18
138	10	1.76	1.40	1.07	0.92	0.07	140	11	0.77	0.18	0.07	-1.24	-1.81
138	11	1.72	1.14	1.03	-0.72	-1.21	140	12	0.85	0.21	0.26	-0.93	-1.66
138	13	0.96	0.24	0.01	-1.16	-1.89	140	13	0.90	0.27	0.34	-0.83	-1.35
138	14	0.78	0.02	-0.27	-1.49	-2.29	140	14	0.90	0.26	0.48	-0.80	-1.35
138	16	0.50	-0.03	-0.17	-1.26	-2.26	142	8	0.97	0.41	0.41	-0.56	-1.31
138	17	0.26	0.11	0.10	-0.90	-1.72	142	13	0.66	0.29	0.09	-1.05	-1.75
139	3	0.44	0.28	0.47	-0.38	-1.46	142	17	0.44	0.16	0.07	-0.80	-1.49
139	5	0.50	0.39	0.59	-0.27	-1.05	142	18	0.41	0.11	0.07	-0.88	-1.50
139	7	0.56	0.29	0.67	-0.25	-0.20	143	4	0.48	0.11	-0.03	-0.90	-1.50
139	8	0.48	0.22	0.56	-0.39	-1.15	143	5	0.34	0.09	-0.02	-0.83	-1.53
139	9	0.18	0.01	0.19	-0.77	-1.34	143	6	0.35	0.01	-0.10	-0.97	-1.61
139	10	-0.10	-0.22	-0.12	-1.11	-2.33	143	7	0.32	-0.07	-0.17	-1.05	-1.70
139	11	0.12	-0.31	-0.22	-1.32	-2.29	143	8	0.33	-0.08	-0.15	-1.03	-1.58
139	12	0.28	-0.14	-0.08	-1.22	-2.41	143	9	0.38	-0.03	-0.13	-0.98	-1.55
139	14	0.58	-0.06	-0.07	-1.22	-2.75	143	11	0.41	0.03	-0.18	-1.26	-2.01
139	15	0.48	-0.16	-0.20	-1.19	-2.36	143	17	0.85	0.34	0.43	-0.45	-0.87
139	16	0.72	-0.01	-0.16	-1.35	-2.09	143	18	0.77	0.22	0.34	-0.61	-1.03
139	17	0.42	-0.30	-0.34	-1.52	-2.15	143	21	0.51	-0.10	0.12	-0.85	-1.05
139	18	0.59	-0.15	-0.09	-1.15	-2.52	144	1	0.64	-0.13	-0.09	-1.11	-1.43
140	2	0.59	0.17	0.14	-0.89	-1.61	144	2	0.55	-0.09	-0.11	-1.15	-1.37
140	3	0.74	0.29	0.35	-0.74	-1.62	144	4	0.77	0.16	0.16	-0.98	-1.15

Table B-IV-4. NRL Royco Size Distributions - Hourly Log

NRL ROYCO SIZE DISTRIBUTIONS EOMET 77

DAY	HR	CH1	CH2	CH3	CH4	CH5	DAY	HR	CH1	CH2	CH3	CH4	CH5
144	5	0.97	0.48	0.66	-0.79	-0.77	146	5	1.44	0.57	0.31	-0.88	-1.49
144	7	1.82	0.79	1.44	0.95	-0.71	146	6	1.49	0.63	0.41	-0.95	-1.60
144	8	1.94	0.70	1.27	0.01	-1.11	146	8	1.50	0.78	0.62	-0.97	-1.65
144	16	0.70	-0.01	-0.03	-1.01	-1.57	146	10	1.47	0.74	0.57	-1.04	-1.86
144	17	0.66	-0.09	-0.16	-1.14	-1.67	146	12	1.42	0.60	0.41	-0.94	-1.62
144	20	0.68	-0.10	-0.23	-1.33	-2.58	146	15	1.41	0.68	0.52	-1.05	-1.67
144	22	0.69	-0.07	-0.22	-1.13	-1.55	146	16	1.43	0.74	0.56	-1.07	-1.75
144	23	1.02	0.24	-0.06	-1.27	-2.21	146	18	1.38	0.71	0.55	-1.06	-1.75
145	1	1.17	0.37	0.01	-1.16	-1.70	146	21	1.44	0.78	0.62	-0.99	-1.67
145	2	1.19	0.42	0.08	-1.07	-1.56	146	22	1.48	0.82	0.66	-1.01	-1.63
145	4	0.41	0.06	0.06	-1.07	-1.53	146	23	1.47	0.82	0.69	-1.00	-1.67
145	5	1.25	0.48	0.19	-0.99	-1.53	147	0	1.47	0.82	0.66	-1.08	-1.76
145	7	1.25	0.47	0.21	-0.97	-1.57	147	5	1.85	1.25	1.04	-0.79	-1.28
145	14	1.13	0.32	0.09	-1.16	-2.13	147	6	1.83	1.22	0.96	-0.85	-1.42
145	15	1.16	0.34	0.13	-1.07	-1.72	147	7	1.81	1.17	0.89	-0.73	-1.31
145	18	1.07	0.26	0.02	-1.09	-1.55	147	8	1.80	1.14	0.84	-0.73	-1.43
145	19	1.10	0.30	0.06	-1.11	-1.58	147	10	1.98	1.32	0.96	-1.06	-2.85
145	20	1.13	0.32	0.07	-1.10	-1.71	147	11	2.00	1.34	1.00	-0.82	-1.42
145	21	1.09	0.30	0.07	-1.08	-1.63	147	15	1.07	0.39	0.07	-1.58	-2.21
145	22	1.23	0.45	0.22	-0.99	-1.58	147	19	0.99	0.31	0.03	-1.28	-1.88
145	23	1.29	0.49	0.27	-0.97	-1.51	147	20	0.97	0.29	-0.02	-1.32	-2.02
146	0	1.25	0.44	0.22	-0.97	-1.56	147	22	1.04	0.37	0.02	-1.35	-1.92
146	1	1.26	0.46	0.23	-0.92	-1.44	147	23	0.96	0.22	-0.17	-1.47	-1.97
146	2	1.24	0.42	0.17	-1.01	-1.65	148	0	0.92	0.20	-0.21	-1.54	-1.97
146	3	1.39	0.50	0.25	-0.91	-1.46	148	1	0.87	0.11	-0.38	-1.76	-2.69

Table B-IV-4 NRL Royco Size Distributions - Hourly Log (Cont'd)

NRL ROYCO SIZE DISTRIBUTIONS EOMET 77													
DAY	HR	CH1	CH2	CH3	CH4	CH5	DAY	HR	CH1	CH2	CH3	CH4	CH5
148	3	0.97	0.10	-0.39	-1.84	-2.61	153	11	1.60	0.85	0.51	-1.13	-2.19
148	4	1.25	0.77	0.63	-1.12	-2.05	153	13	1.54	0.80	0.48	-1.08	-1.94
148	6	0.87	0.12	-0.35	-2.35		153	16	1.52	0.84	0.59	-0.96	-1.46
148	7	0.89	0.12	-0.41	-2.73		153	17	1.52	0.83	0.63	-0.81	-1.26
150	21	1.03	0.50	0.46	-0.79	-2.19	154	0	1.37	0.70	0.51	-0.89	-2.28
150	22	0.97	0.35	0.58	-0.46	-0.79	154	1	1.32	0.62	0.44	-0.94	-2.47
151	9	0.95	0.27	0.36	-0.72	-1.16	154	3	1.36	0.59	0.47	-0.82	-1.54
151	10	1.12	0.43	0.48	-0.54	-0.92	154	4	1.80	1.18	1.04	-0.50	-2.36
151	15	1.17	0.41	0.28	-0.63	-1.25	154	6	1.71	1.04	0.85	-0.63	-1.14
151	16	1.16	0.41	0.30	-0.56	-1.07	154	7	1.67	0.99	0.78	-0.66	-1.13
151	22	1.17	0.44	0.36	-0.64	-1.24	154	12	1.85	1.18	0.82	-0.78	-1.29
152	4	1.24	0.60	0.55	-0.46	-1.05	154	14	1.27	0.53	0.30	-1.18	
152	5	1.42	0.80	0.72	-0.38	-0.92	154	15	1.12	0.40	0.28	-0.95	-1.51
152	6	1.39	0.75	0.67	-0.44	-0.08	154	22	1.28	0.59	0.41	-0.97	-1.70
152	9	1.22	0.56	0.52	-0.61	-1.03	155	7	1.39	0.62	0.38	-0.75	-1.26
152	10	1.11	0.53	0.50	-0.56	-1.44	155	9	1.32	0.60	0.42	-0.81	-1.43
152	15	1.19	0.50	0.34	-0.73	-1.27	155	11	1.39	0.70	0.44	-0.84	-1.98
152	21	1.66	1.01	0.79	-0.87	-1.37	155	14	1.39	0.64	0.45	-0.90	-2.26
152	23	1.66	1.03	0.82	-1.14	-2.14	155	15	1.50	0.72	0.54	-0.57	-1.10
153	0	1.71	1.11	0.92	-1.11	-2.04	155	20	1.80	0.96	0.65	-0.45	-0.94
153	1	1.62	1.00	0.82	-1.08	-1.72	155	22	1.72	0.83	0.54	-0.50	-1.07
153	2	1.66	1.03	0.83	-1.03	-1.70	156	0	1.86	0.95	0.63	-0.46	-0.92
153	4	1.62	1.00	0.79	-1.06	-1.77	156	1	1.33	0.46	0.14	-1.34	-3.31
153	5	1.62	0.97	0.75	-1.08	-3.25	156	3	1.50	0.59	0.32	-0.74	-1.27
153	7	1.62	0.89	0.58	-1.12	-1.94	156	6	1.58	0.61	0.33	-0.63	-1.22

Table B-IV-4 NRL Royco Size Distributions - Hourly Log (Cont'd)

NRL ROYCO SIZE DISTRIBUTIONS EOMET 77									
DAY	HR	CH1	CH2	CH3	CH4	CH5	CH1	CH2	CH3
156	15	1.55	0.83	0.60	-0.35	-0.98	CH1	CH2	CH3
156	17	1.45	0.59	0.40	-0.48	-1.08	CH4	CH5	CH5
156	18	1.49	0.56	0.31	-0.60	-1.26			
157	0	1.44	0.41	0.03	-1.11	-1.42			
157	3	1.58	0.50	0.01	-1.27	-1.71			
157	7	1.41	0.35	-0.01	-1.09	-1.67			
157	10	1.52	0.46	0.15	-1.02	-1.61			
157	12	1.61	0.56	0.13	-1.38	-2.50			
157	16	1.60	0.58	0.21	-0.85	-1.54			
157	17	1.66	0.66	0.37	-0.83	-1.26			
157	21	1.68	0.69	0.39	-0.74	-1.23			
157	22	1.80	0.87	0.59	-0.67	-1.03			
157	23	1.76	0.82	0.50	-0.74	-1.20			
158	0	1.71	0.81	0.48	-0.96	-1.28			
158	1	1.76	0.96	0.61	-1.08	-1.43			
158	2	1.75	0.93	0.52	-1.23	-1.97			
158	3	1.85	1.01	0.59	-0.99	-1.57			

Table B-IV-4 NRL Royco Size Distributions - Hourly Log (Cont'd)

CALSPAN ROYCO SIZE DISTRIBUTIONS EOMET 77													
DAY	HR	CH1	CH2	CH3	CH4	CH5	DAY	HR	CH1	CH2	CH3	CH4	CH5
135	4	0.54	-0.19	-0.05	-1.07	-3.45	136	5	0.26	-0.43	-0.18	-1.14	
135	5	0.44	-0.23	-0.03	-0.88		136	6	0.23	-0.51	-0.29	-1.23	
135	6	0.38	-0.25	-0.04	-0.95		136	7	0.32	-0.52	-0.37	-1.34	
135	7	0.51	-0.18	0.04	-0.75		136	8	0.31	-0.49	-0.34	-1.31	
135	8	0.51	-0.24	-0.12	-1.05		136	9	0.48	-0.22	-0.08	-1.11	
135	9	0.45	-0.26	-0.07	-1.04		136	10	0.52	-0.10	0.06	-0.87	
135	10	0.45	-0.20	0.01	-0.89		136	11	0.52	-0.11	0.08	-0.87	
135	11	0.51	-0.15	0.04	-0.86		136	12	0.39	-0.23	-0.01	-0.98	
135	12	0.71		0.05	-0.81	-3.45	136	13	0.40	-0.22	0.01	-1.01	
135	13	0.55	-0.12	0.09	-0.75		136	14	0.94	0.37	0.55	-0.35	
135	14	0.46	-0.16	0.06	-0.86		136	15	0.88	0.28	0.35	-0.76	
135	15	0.50	-0.20	-0.01	-0.92		136	16	0.50	-0.06	0.15	-0.97	
135	16	0.55	-0.20	-0.11	-1.07		136	17	0.53	0.01	0.22	-0.86	
135	17	0.96	0.17	-0.01	-1.20		137	14	1.33	0.83	0.97	-0.30	
135	18	0.63	-0.16	-0.23	-1.28	-3.45	137	15	1.15	0.67	0.82	-0.44	
135	19	0.33	-0.46	-0.43	-1.45		137	20	1.10	0.54	0.69	-0.48	
135	20	0.22	-0.52	-0.46	-1.53		137	21	1.10	0.54	0.69	-0.49	
135	21	0.19	-0.52	-0.47	-1.56		138	2	1.22	0.46	0.62	-0.60	
135	22	0.21	-0.45	-0.42	-1.49		138	5	1.27	0.55	0.67	-0.53	
135	23	0.17	-0.62	-0.51	-1.56		138	6	1.22	0.55	0.65	-0.63	
136	0	0.09	-0.66	-0.48	-1.46		138	7	1.22	0.45	0.57	-0.77	
136	1	0.12	-0.61	-0.43	-1.38		138	8	1.27	0.39	0.49	-0.83	
136	2	0.16	-0.56	-0.31	-1.25		138	9	1.47	0.47	0.57	-0.76	
136	3	0.20	-0.47	-0.23	-1.17		138	11	1.39	0.57	0.63	-1.00	
136	4	0.28	-0.39	-0.11	-1.05		138	12	0.85	0.12	0.28	-1.00	

Table B-IV-5. Calspan Royco Size Distribution - Hourly Log

CALSPAN ROYCO SIZE DISTRIBUTIONS EOMET 77													
DAY	HR	CH1	CH2	CH3	CH4	CH5	DAY	HR	CH1	CH2	CH3	CH4	CH5
138	13	0.78	-0.04	0.05	-1.29		139	16	0.35	-0.34	-0.24	-1.53	
138	14	0.57	-0.23	-0.21	-1.59		139	17	0.12	-0.47	-0.40	-1.74	
138	15	0.48	-0.43	-0.47	-1.82		139	18	0.17	-0.30	-0.23	-1.52	
138	16	0.34	-0.14	-0.06	-1.30		139	19	0.53	0.08	0.20	-1.02	
138	17	0.45	-0.00	0.10	-1.05		139	20	0.46	-0.08	0.04	-1.10	
138	18	0.46	0.01	0.14	-1.03		139	21	0.40	-0.13	-0.04	-1.27	
138	19	0.47	0.05	0.15	-1.01		139	22	0.39	-0.19	-0.09	-1.29	
138	20	0.52	0.06	0.23	-0.93		139	23	0.52	-0.11	0.19	-0.97	
138	22	0.45	-0.03	0.17	-1.03		140	0	0.50	-0.17	0.19	-1.05	
138	23	0.55	0.08	0.35	-0.77		140	1	0.50	-0.08	0.24	-1.00	
139	0	0.60	0.11	0.42	-0.65		140	2	0.53	-0.05	0.26	-0.99	
139	1	0.64	0.17	0.46	-0.65		140	3	0.68	0.09	0.48	-0.74	
139	3	0.65	0.18	0.45	-0.57		140	4	0.71	0.16	0.51	-0.75	
139	4	0.70	0.25	0.52	-0.59		140	5	0.81	0.15	0.49	-0.82	
139	5	0.74	0.29	0.59	-0.48		140	6	0.57	-0.08	0.20	-1.18	
139	6	0.76	0.28	0.59	-0.47		140	7	0.57	-0.07	0.26	-1.09	
139	7	0.77	0.29	0.62	-0.38		140	8	0.52	-0.08	0.27	-1.04	
139	8	0.68	0.21	0.52	-0.54		140	9	0.66	0.05	0.47	-0.81	
139	9	0.38	-0.06	0.20	-0.93		140	10	0.60	-0.02	0.39	-0.82	
139	10	0.14	-0.29	-0.07	-1.19		140	11	0.37	-0.32	0.08	-1.25	
139	11	0.08	-0.41	-0.18	-1.25		140	12	0.63	-0.03	0.36	-0.92	
139	12	0.22	-0.26	-0.02	-1.13		140	13	0.60	-0.01	0.38	-0.90	
139	13	0.25	-0.26	-0.04	-1.17		140	14	0.62	0.05	0.46	-0.70	
139	14	0.28	-0.26	-0.12	-1.46		140	15	0.45	-0.31	0.02	-1.36	
139	15	0.23	-0.33	-0.23	-1.56		140	16	0.40	-0.32	-0.05	-1.32	

Table B-IV-5 Calspan Royco Size Distributions - Hourly Log (Cont'd)

CALSPAN ROYCO SIZE DISTRIBUTIONS EOMET 77													
DAY	HR	CH1	CH2	CH3	CH4	CH5	DAY	HR	CH1	CH2	CH3	CH4	CH5
140	17	0.51	-0.18	0.15	-1.09		143	2	0.56	0.00	0.10	-0.96	
140	18	0.57	-0.02	0.27	-0.97		143	3	0.54	-0.03	0.05	-1.07	
140	19	0.59	-0.08	0.23	-1.05		143	4	0.49	-0.09	-0.05	-1.33	
140	21	0.78	0.20	0.58	-0.58		143	5	0.48	-0.08	0.00	-1.11	
140	23	0.89	0.25	0.72	-0.38		143	6	0.39	-0.15	-0.06	-1.14	
141	0	0.94	0.30	0.76	-0.33		143	7	0.34	-0.23	-0.16	-1.36	
141	1	0.92	0.30	0.75	-0.30		143	8	0.36	-0.18	-0.02	-1.15	
141	2	0.80	0.24	0.64	-0.51		143	9	0.37	-0.18	-0.10	-1.22	
141	3	0.75	0.18	0.59	-0.57		143	10	0.44	-0.16	-0.06	-1.23	
141	4	0.83	0.24	0.66	-0.44		143	11	0.42	-0.14	-0.13	-1.46	
141	5	0.81	0.21	0.65	-0.40		143	12	0.49	-0.03	-0.03	-1.21	
141	6	0.76	0.18	0.61	-0.41		143	13	0.50	-0.02	-0.05	-1.42	
141	7	0.75	0.14	0.62	-0.42		143	15	0.50	-0.00	0.14	-0.92	
141	8	0.80	0.14	0.68	-0.32		143	16	0.64	0.14	0.33	-0.72	-3.15
141	9	0.74	0.12	0.65	-0.49		143	17	0.76	0.20	0.48	-0.52	
141	10	0.52	-0.04	0.51	-0.83		143	18	0.76	0.21	0.50	-0.50	
141	11	0.53	0.06	0.41	-1.22		143	19	0.27	-0.30	-0.02	-1.28	
141	12	0.31	-0.15	0.22	-1.08		143	22	0.10	-0.58	-0.32	-1.41	
141	23	0.66	0.17	0.46	-0.61		144	1	0.31	-0.38	-0.18	-1.22	
141	24	0.58	0.08	0.34	-0.76		144	2	0.35	-0.38	-0.14	-1.16	
142	12	0.69	0.12	0.11	-1.06		144	3	0.38	-0.35	-0.18	-1.25	
142	13	0.71	0.45	-0.79	-0.94		144	4	0.49	-0.20	-0.04	-1.11	
142	17	0.49	-0.06	-0.06	-1.26		144	5	0.55	-0.18	-0.03	-1.03	
142	18	0.51	-0.04	0.02	-1.04		144	6	0.59	-0.16	-0.07	-1.23	
142	23	0.54	-0.02	0.04	-1.07		144	7	1.75	0.93	0.87	-0.46	

Table B-IV-5 Calspan Royco Size Distributions - Hourly Log (Cont'd)

CALSPAN ROYCO SIZE DISTRIBUTIONS EOMET 77

DAY	HR	CH1	CH2	CH3	CH4	CH5	DAY	HR	CH1	CH2	CH3	CH4	CH5
144	8	1.69	0.83	0.76	-0.79		145	10	0.87	0.11	0.20	-1.04	
144	9	1.32	0.44	0.44	-0.82		145	11	0.83	0.06	0.16	-1.17	
144	10	0.60	-0.05	0.24	-0.73		145	12	0.80	0.02	0.09	-1.19	
144	11	0.48	-0.15	0.11	-1.01		145	13	0.78	0.00	0.08	-1.26	
144	12	0.45	-0.19	0.09	-0.88		145	14	0.75	-0.02	0.02	-1.32	
144	13	1.04	0.19	0.26	-0.90		145	15	0.79	0.02	0.07	-1.25	
144	14	0.37	0.12	0.06	-1.08		145	16	0.81	0.02	0.09	-1.12	
144	15	0.37	0.22	-1.55	-1.04		145	17		0.01	0.07	-1.14	
144	16	0.35	-0.27	-0.00	-1.06		145	18	0.70	-0.10	-0.04	-1.39	
144	18	0.31	-0.33	-0.08	-1.14		145	20	0.74	-0.09	-0.02	-1.36	
144	19	0.29	-0.35	-0.10	-1.13		145	21	0.78	-0.05	0.03	-1.33	
144	20	0.31	-0.40	-0.13	-1.18		145	22	0.85	0.05	0.10	-1.22	
144	21	0.30	-0.39	-0.14	-1.15		146	0	0.83	0.03	0.10	-1.24	
144	22	0.29	-0.40	-0.18	-1.22		146	2	0.82	0.02	0.07	-1.29	
144	23	0.66	-0.20	-0.09	-1.25		146	3	0.90	0.05	0.11	-1.22	
145	0	0.58	-0.26	-0.10	-1.21		146	4	0.94	0.09	0.14	-1.17	
145	1	0.80	-0.09	-0.03	-1.18		146	5	0.99	0.10	0.17	-1.23	
145	2	0.83	-0.07	-0.04	-1.24		146	6	1.04	0.17	0.23	-1.22	
145	3	0.88	-0.02	-0.01	-1.29		146	7	1.14	0.14	0.49	-1.23	
145	4	0.82	-0.09	-0.05	-1.25		146	8	1.16	0.38	0.40	-1.31	
145	5	0.82	-0.03	0.05	-1.18		146	9	1.19	0.43	0.39	-1.51	
145	6	0.91	0.11	0.21	-0.95		146	10	1.09	0.32	0.27	-1.39	
145	7	0.89	0.10	0.17	-1.08		146	11	0.99	0.21	0.16	-1.27	
145	8	0.91	0.11	0.22	-1.07		146	12	1.02	0.21	0.20	-1.42	
145	9	0.88	0.11	0.20	-1.03		146	13	1.02	0.21	0.22	-1.22	

Table B-IV-5 Calspan Royco Size Distributions - Hourly Log (Cont'd)

CALSPAN ROYCO SIZE DISTRIBUTIONS EOMET 77

DAY	HR	CH1	CH2	CH3	CH4	CH5	DAY	HR	CH1	CH2	CH3	CH4	CH5
146	14	1.04	0.23	0.22	-1.37		148	3	1.55	0.68	0.48	-1.12	
146	15	1.13	0.33	0.34	-1.35		148	4	1.91	1.16	1.04	-0.61	
146	16	1.15	0.38	0.38	-1.39		148	5	1.69	0.89	0.76	-0.92	
146	17	1.15	0.39	0.38	-1.39		148	6	1.57	0.72	0.54	-1.13	
146	19	1.15	0.41	0.40	-1.44		148	7	1.53	0.69	0.50	-1.27	
146	20	1.18	0.40	0.40	-1.41		150	20	0.77	0.21	0.41	-0.66	
146	21	1.19	0.43	0.44	-1.33		150	21	0.75	0.25	0.47	-0.72	
146	22	1.21	0.44	0.44	-1.38		150	22	0.77	0.22	0.51	-0.67	
146	23	1.20	0.44	0.44	-1.58		150	23	0.74	0.20	0.44	-0.73	
147	0	1.20	0.44	0.42	-1.41		151	0	0.49	0.16	0.42	-0.75	
147	1	1.18	0.43	0.41	-1.42		151	4	0.62	-0.06	0.37	-0.79	
147	2	1.33	0.54	0.51	-1.27		151	8	0.60	0.04	0.23	-1.09	
147	3	1.39	0.60	0.56	-1.20		151	9	0.66	0.04	0.14	-1.23	
147	4	1.39	0.60	0.58	-1.23		151	11	0.77	0.11	0.20	-1.15	
147	5		0.75	0.72	-1.16		151	12	0.76	0.11	0.20	-1.15	
147	6	1.62	0.80	0.77	-1.13		151	13	0.89	0.12	0.21	-1.10	
147	7	1.60	0.77	0.71	-1.13		151	14	0.86	0.12	0.19	-1.04	
147	8	1.57	0.73	0.65	-1.18		151	15	0.86	0.12	0.17	-1.05	
147	9	1.63	0.75	0.66	-0.91		151	16	0.89	0.13	0.20	-1.00	
147	10	1.71	0.82	0.72	-0.79		151	21	0.80	0.05	0.17	-1.06	
147	11	1.71	0.83	0.74	-0.83		151	22	0.83	0.08	0.19	-0.94	
147	12	1.66	0.82	0.75	-0.72		152	9	0.83	0.21	0.28	-0.85	
147	13	1.67	0.81	0.77	-0.71		152	14	1.01	0.20	0.13	-1.10	
147	14	1.67	0.84	0.80	-0.66		154	0	0.95	0.15	0.25	-0.97	
148	1	1.58	0.67	0.49	-1.08		154	1	0.92	0.10	0.15	-1.00	

Table B-IV-5 Calspan Royco Size Distributions - Hourly Log (Cont'd)

CALSPAN ROYCO SIZE DISTRIBUTIONS EOMET 77

DAY	HR	CH1	CH2	CH3	CH4	CH5	DAY	HR	CH1	CH2	CH3	CH4	CH5
154	2	1.18	0.33	0.30	-1.07		156	5	1.11	0.23	0.27	-0.56	
154	3	0.79	0.05	0.17	-0.89		156	6	1.11	0.22	0.21	-1.04	-2.85
154	4	1.34	0.54	0.54	-0.80		156	8	1.22	0.27	0.30	-0.84	
154	5	1.40	0.56	0.52	-0.96		156	9	1.09	0.23	0.20	-1.01	
154	6	1.28	0.52	0.41	-1.06		156	14	1.21	0.24	0.33	-0.85	
154	7	1.32	0.49	0.44	-1.00		156	15	1.17	0.28	0.35	-0.76	
154	8	1.25	0.43	0.33	-1.09		156	18	1.06	0.20	0.24	-0.95	-3.45
154	12	1.52	0.66	0.53	-0.99		156	19	1.11	0.20	0.21	-0.96	-3.45
154	14	1.02	0.25	0.29	-0.92		156	20	1.07	0.11	0.13	-1.04	
154	15	0.85	0.16	0.23	-0.94		156	21	1.16	0.20	0.21	-1.02	
154	21	0.92	0.21	0.30	-0.91		156	22	1.02	0.04	0.07	-1.12	
154	22	0.93	0.22	0.33	-0.94		156	23	0.81	0.24	0.25	-1.56	
155	1	0.92	0.21	0.31	-0.91		157	0	0.89	0.17	0.17	-1.42	
155	6	0.93	0.10	0.25	-1.16		157	1	1.00	0.05	0.10	-1.38	
155	7	1.00	0.20	0.21	-1.33		157	2	1.09	0.00	0.12	-1.52	
155	8	0.93	0.17	0.14	-1.26		157	3	1.05	0.03	0.13	-1.46	
155	9	0.97	0.26	0.26	-1.11		157	4	0.97	0.04	0.14	-1.55	
155	14	0.98	0.30	0.34	-0.94		157	5	0.96	0.04	0.14	-1.42	
155	15	1.04	0.26	0.25	-0.91		157	6	0.95	0.05	0.14	-1.42	
155	20	1.39	0.47	0.47	-0.69		157	7	0.97	0.03	0.13	-1.43	
155	21	1.34	0.45	0.46	-0.70		157	8	1.00	0.01	0.08	-1.40	
156	0	1.31	0.40	0.40	-0.75		157	9	1.03	0.03	0.01	-1.26	
156	1	1.01	0.21	0.29	-0.79		157	10	1.06	0.10	0.04	-1.27	
156	3	1.06	0.19	0.25	-1.04		157	13	1.08	0.11	0.09	-1.24	
156	4	1.07	0.18	0.27	-0.83		157	14	1.12	0.13	0.12	-1.17	

Table B-IV-5 Calspan Royco Size Distributions - Hourly Log (Cont'd)

CALSPAN ROYCO SIZE DISTRIBUTIONS EOMET 77													
DAY	HR	CH1	CH2	CH3	CH4	CH5	DAY	HR	CH1	CH2	CH3	CH4	CH5
157	16	1.12	0.13	0.11	-1.16								
157	18	1.11	0.15	0.12	-1.18								
157	19	1.24	0.31	0.30	-1.03								
157	20	1.11	0.16	0.14	-1.03								
157	21	1.05	0.10	0.06	-1.17								
157	22	1.12	0.14	0.15	-1.06								
157	23	1.13	0.14	0.10	-1.09								
158	3	1.23	0.19	-0.02	-1.34								

Table B-IV-5 Calspan Royco Size Distributions - Hourly Log (Cont'd)

e) Electrical Aerosol Analyzer Data

The data in this section was obtained with Calspan's Thermo Systems Model 3030 Electrical Aerosol Analyzer, EAA, with its sensor mounted approximately 18 meters above the sea surface. This device provides the aerosol size distribution for sizes between 0.003 micrometers and 1.0 micrometers diameter. Data in this section represents the actual size distributions in cumulative form. They were obtained after computer processing at Calspan of the raw EAA data. The archived data has been sorted to eliminate periods of adverse relative wind direction. Figure B-IV-16 is a typical plot of the results of the EAA where the particle diameter in micrometers is plotted along the x axis and the cumulative number concentrations in (cm^{-3}) is plotted along the y axis.

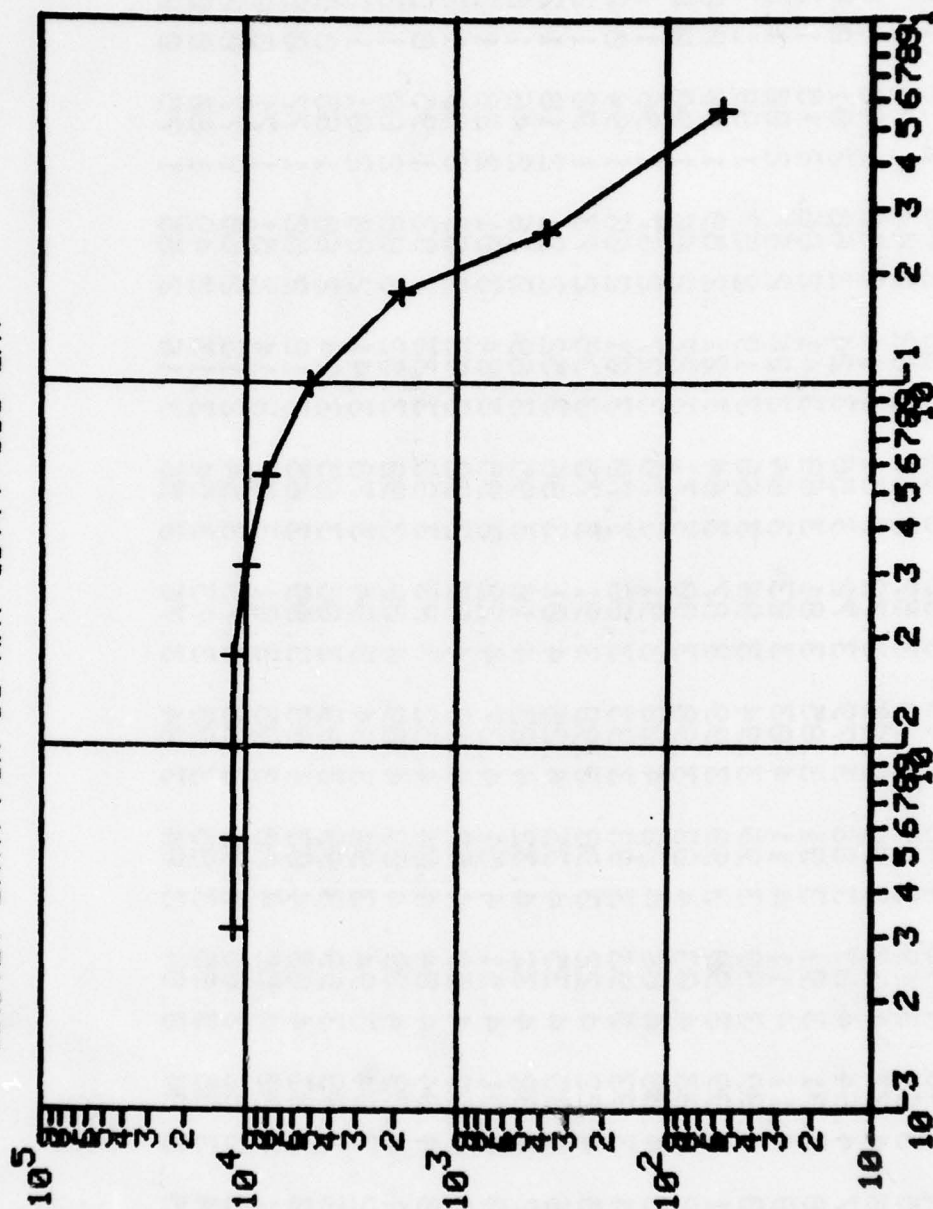
Table B-IV-7 is a listing of the archived data where for each day and hour the numbers listed are the logarithms to the base of 10 of the cumulative number densities (cm^{-3}). The corresponding channel sizes are listed in Table B-IV-6.

Table B-IV-6

Channel Number vs Aerosol Size

CH1	d > .0032 μm
CH2	d > .0056 μm
CH3	d > .01 μm
CH4	d > .0178 μm
CH5	d > .0316 μm
CH6	d > .0562 μm
CH7	d > .1 μm
CH8	d > .178 μm
CH9	d > .3160 μm
CH10	d > .562 μm

WHITBY DATA FOR 18 MAY 1977, 500 GMT



DIAMETER (MICRONS)

Fig. (B-IV-16) Whitby data
 X - particle diameter
 Y - cumulative number concentrations in (cm⁻³)

CALSPAN WHITBY SIZE DISTRIBUTIONS											EDMET 77
DAY	HR	CH1	CH2	CH3	CH4	CH5	CH6	CH7	CH8	CH9	CH10
135	4	4.45	4.45	4.45	4.19	3.90	3.68	3.39	2.88	2.16	1.43
135	5	3.69	3.69	3.69	3.69	3.57	3.37	3.02	2.44	1.78	1.13
135	6	4.37	4.37	3.96	3.85	3.72	3.51	3.11	2.52	1.80	0.00
135	7	4.64	4.03	3.86	3.79	3.72	3.56	3.24	2.68	2.01	0.00
135	8	3.91	3.91	3.91	3.85	3.81	3.68	3.41	2.86	2.15	1.24
135	9	4.11	4.11	4.11	4.03	3.83	3.64	3.26	2.67	2.00	1.35
135	10	4.99	3.99	3.99	3.94	3.86	3.60	3.19	2.57	1.89	1.35
135	11	3.99	3.99	3.99	3.99	3.87	3.64	3.21	2.59	1.90	0.00
135	12	4.03	4.03	4.03	3.98	3.90	3.71	3.27	2.66	1.90	0.00
135	13	4.08	4.08	4.08	4.08	3.91	3.70	3.27	2.67	1.96	1.13
135	14	3.93	3.93	3.93	3.93	3.88	3.70	3.01	2.66	1.94	0.00
135	15	4.22	4.22	3.98	3.98	3.91	3.75	3.35	2.73	1.98	1.25
135	16	4.35	4.35	4.35	4.25	4.01	3.86	3.52	2.91	2.18	1.23
135	17	4.32	4.32	4.32	4.23	4.10	3.95	3.64	3.16	2.46	1.69
135	18	4.51	4.51	4.51	4.37	4.22	3.95	3.53	3.01	2.28	1.25
135	19	4.59	4.59	4.59	4.18	4.03	3.92	3.53	2.89	2.09	1.35
135	20	4.84	4.84	4.84	4.32	4.03	3.80	3.33	2.83	1.95	0.00
135	21	4.09	4.09	4.09	4.09	4.09	3.92	3.52	3.88	2.00	1.35
135	22	3.94	3.94	3.94	3.94	3.94	3.78	3.41	2.80	2.01	1.25
135	23	3.99	3.99	3.99	3.99	3.86	3.65	3.24	2.60	1.85	0.00
136	0	4.03	4.03	4.03	4.03	3.89	3.65	3.18	2.50	1.77	0.00
136	1	4.00	4.00	4.00	3.95	3.81	3.57	3.14	2.51	1.71	0.00
136	3	3.86	3.86	3.86	3.86	3.75	3.54	3.13	2.50	1.77	0.00
136	4	3.85	3.85	3.85	3.85	3.73	3.54	3.13	2.49	1.80	0.00
136	5	3.84	3.84	3.84	3.84	3.76	3.56	3.16	2.55	1.75	0.00

Table B-IV-7. Hourly Listing of Whitby Aerosol Size Distributions

CALSPAN WHITBY SIZE DISTRIBUTIONS										EOMET 77	
DAY	HR	CH1	CH2	CH3	CH4	CH5	CH6	CH7	CH8	CH9	CH10
136	6	3.84	3.84	3.84	3.84	3.78	3.59	3.23	2.60	1.80	0.00
136	7	3.87	3.87	3.87	3.87	3.85	3.72	3.42	3.86	2.10	1.25
136	8	3.80	3.80	3.80	3.80	3.80	3.67	3.34	2.76	2.03	1.13
136	9	3.54	4.54	4.54	3.89	3.77	3.58	3.36	2.74	2.06	1.13
136	10	4.68	4.68	4.68	3.98	3.81	3.65	3.29	2.70	1.96	1.13
136	12	3.94	3.94	3.94	3.81	3.77	3.65	3.33	2.69	1.64	1.13
136	13	3.97	3.97	3.97	3.78	3.78	3.65	3.32	2.69	1.92	1.13
136	14	3.92	3.92	3.92	3.79	3.75	3.68	3.38	2.76	2.00	1.13
136	16	3.84	3.84	3.84	3.77	3.72	3.65	3.38	2.78	2.04	0.00
136	17	3.81	3.81	3.81	3.81	3.75	3.66	3.39	2.80	2.03	1.13
137	19	3.88	3.88	3.88	3.88	3.80	3.77	3.63	3.21	2.52	1.65
137	20	3.94	3.94	3.94	3.94	3.90	3.80	3.64	3.23	2.53	1.65
138	5	4.06	4.06	4.06	4.06	4.00	3.91	3.70	3.26	2.57	1.73
138	6	3.88	3.88	3.88	3.88	3.82	3.75	3.55	3.14	2.48	1.60
138	7	4.71	3.83	3.83	3.83	3.74	3.69	3.59	3.10	2.46	1.60
138	8	3.71	3.71	3.71	3.71	3.66	3.60	3.44	3.08	2.46	1.60
138	9	3.70	3.70	3.70	3.70	3.61	3.64	3.40	3.08	2.52	1.73
138	10	3.39	3.39	3.39	3.39	3.39	3.28	3.20	3.93	2.42	1.60
138	11	3.26	3.26	3.26	3.26	3.26	3.21	3.11	3.81	2.30	1.55
138	12	3.07	3.07	3.07	3.07	3.07	2.99	2.84	2.45	1.83	1.13
138	13	3.89	3.89	3.89	3.38	3.17	3.10	2.97	2.57	1.92	1.13
138	14	4.18	4.18	4.18	4.18	3.57	3.28	2.96	2.44	1.75	0.00
138	15	4.07	4.07	3.91	3.69	3.08	3.04	2.83	2.41	1.71	0.00
138	17	4.44	4.44	4.44	4.16	3.44	2.50	1.90	1.50	0.00	0.00
138	19	4.30	4.30	4.22	3.90	3.51	3.08	2.47	1.54	0.00	0.00

Table B-IV-7 Whitby Aerosol Size Distributions-Hourly Log (cont'd)

CALSPAN WHITBY SIZE DISTRIBUTIONS EOMET 77											
DAY	HR	CH1	CH2	CH3	CH4	CH5	CH6	CH7	CH8	CH9	CH10
138	20	3.77	3.77	3.77	3.42	2.91	2.35	1.90	1.50	0.00	0.00
138	22	3.76	3.76	3.76	3.41	2.88	2.23	1.87	1.43	0.00	0.00
138	23	3.86	3.86	3.86	3.71	3.38	2.84	2.24	1.75	1.19	0.00
139	0	3.90	3.90	3.90	3.84	3.46	3.00	2.47	1.90	1.09	0.00
139	1	3.96	3.96	3.96	3.84	3.55	3.67	2.67	1.97	1.09	0.00
139	3	3.93	3.93	3.93	3.80	3.47	3.10	2.74	2.12	1.37	0.00
139	5	3.72	3.72	3.72	3.62	3.31	2.93	2.51	1.82	1.09	0.00
139	6	3.59	3.59	3.59	3.59	3.36	3.09	2.71	2.13	0.89	0.00
139	9	3.83	3.83	3.83	3.49	3.27	3.94	2.48	1.84	1.19	0.00
139	10	3.50	3.50	3.50	3.33	3.08	2.71	2.24	1.75	1.19	0.00
139	11	3.25	3.25	3.25	2.84	2.58	2.27	1.95	1.63	1.19	0.00
139	12	2.71	2.71	2.71	2.71	2.31	2.03	1.77	1.54	0.00	0.00
139	13	3.08	3.08	3.08	2.09	2.09	2.09	1.88	1.46	1.19	0.00
139	14	2.07	2.07	2.07	2.07	2.07	2.07	1.85	1.67	1.30	0.00
139	16	2.72	2.72	2.72	2.72	2.35	2.09	1.88	1.71	1.39	0.00
139	17	4.06	4.06	4.06	3.86	3.47	2.98	2.46	1.95	0.00	0.00
139	18	3.64	3.64	3.64	3.34	3.10	2.83	2.46	2.09	1.46	1.13
139	19	3.37	3.37	3.37	3.11	2.56	2.23	1.87	1.70	1.37	0.00
139	20	3.37	3.37	3.37	2.32	2.32	2.04	1.79	1.58	1.39	0.00
139	22	2.73	2.73	2.73	2.73	2.36	2.12	1.93	1.78	1.35	0.00
140	0	3.55	3.55	3.55	3.14	2.68	2.25	1.93	1.78	1.30	0.00
140	1	3.46	3.46	3.46	3.26	2.44	2.25	1.91	1.76	1.22	0.00
140	3	3.45	3.45	3.45	3.25	2.93	2.56	2.09	1.72	1.09	0.00
140	4	3.25	3.24	3.24	3.24	2.91	2.49	2.22	1.86	1.51	0.00
140	5	3.40	3.40	3.40	3.15	2.91	2.62	2.35	2.03	1.60	0.00

Table B-IV-7 Whitby Aerosol Size Distributions-Hourly Log (cont'd)

CALSPAN WHITBY SIZE DISTRIBUTIONS EOMET 77											
DAY	HR	CH1	CH2	CH3	CH4	CH5	CH6	CH7	CH8	CH9	CH10
140	6	3.18	3.18	3.18	3.18	2.95	2.48	2.21	1.96	1.57	1.13
140	7	2.94	2.94	2.94	2.94	2.75	2.23	2.09	1.88	1.33	1.13
140	8	2.57	2.57	2.57	2.57	1.80	1.80	1.80	1.60	1.09	0.00
140	9	2.61	1.61	2.61	2.61	2.02	2.02	1.76	1.53	1.30	0.00
140	10	3.07	3.07	3.07	2.02	2.02	2.02	1.76	1.53	1.30	0.00
140	11	1.65	1.65	1.65	1.65	1.65	1.65	1.65	1.33	0.00	0.00
140	12	1.96	1.96	1.96	1.96	1.96	1.96	1.64	1.64	1.22	0.00
140	13	1.97	1.97	1.97	1.97	1.97	1.97	1.97	1.67	1.30	0.00
140	14	2.07	2.07	2.07	2.07	2.07	2.07	1.85	1.67	1.30	0.00
140	15	3.57	3.57	2.19	2.19	2.19	2.19	1.78	1.30	0.00	0.00
140	16	2.12	2.12	2.12	2.12	2.12	2.12	1.93	1.78	1.30	0.00
140	17	2.21	2.21	2.21	2.21	2.21	2.21	2.05	1.95	1.55	0.00
140	18	2.41	2.41	2.41	2.41	2.41	2.20	2.20	1.94	1.55	0.00
140	21	2.67	2.67	2.67	2.67	2.21	2.21	2.05	2.00	1.55	0.00
140	23	3.58	3.58	2.21	2.21	2.21	2.21	2.06	1.84	1.44	0.00
141	0	3.09	3.09	3.09	2.21	2.21	2.21	2.06	1.96	1.71	0.00
141	1	2.26	2.26	2.26	2.26	2.26	2.26	2.13	1.94	1.51	0.00
141	2	2.23	2.23	2.23	2.23	2.23	2.23	2.09	1.88	1.55	0.00
141	3	2.23	2.23	2.23	2.23	2.23	2.23	2.08	1.87	1.30	0.00
141	4	1.99	1.99	1.99	1.99	1.99	1.99	1.99	1.87	1.30	0.00
141	5	2.22	2.22	2.22	2.22	2.22	2.22	2.08	1.86	1.51	0.00
141	6	2.18	2.18	2.18	2.18	2.18	2.18	2.01	1.74	1.44	0.00
141	7	2.34	2.34	2.34	2.34	2.34	1.07	1.85	1.67	1.30	0.00
141	8	2.41	2.41	2.41	2.41	2.20	2.05	1.81	1.39	0.00	0.00
141	9	2.41	2.41	2.41	2.41	2.41	2.19	2.03	1.78	1.30	0.00

Table B-IV-7 Whitby Aerosol Size Distributions-Hourly Log (cont'd)

CALSPAN WHITBY SIZE DISTRIBUTIONS										EOMET 77	
DAY	HR	CH1	CH2	CH3	CH4	CH5	CH6	CH7	CH8	CH9	CH10
142	22	2.65	2.65	2.65	2.65	2.16	1.65	1.65	1.33	0.00	0.00
143	23	1.94	1.94	1.94	1.94	1.94	1.94	1.94	1.60	1.09	0.00
143	3	1.94	1.94	1.94	1.94	1.94	1.94	1.94	1.81	1.37	0.00
143	4	2.03	2.03	2.03	2.03	2.03	2.03	1.78	1.57	1.37	0.00
143	5	2.25	2.25	2.25	2.25	2.25	2.25	1.91	1.77	1.49	0.00
143	6	2.09	2.09	2.09	2.09	2.09	2.09	1.88	1.46	1.19	0.00
143	7	1.41	1.41	1.41	1.41	1.41	1.41	1.41	1.41	1.09	0.00
143	8	2.22	2.22	2.22	2.22	2.22	1.83	1.83	1.64	1.22	0.00
143	9	2.06	2.06	2.06	2.06	2.06	2.06	2.06	1.82	1.09	0.00
143	10	2.63	2.63	2.63	2.63	2.09	2.09	1.87	1.87	1.30	0.00
143	11	2.00	2.00	2.00	2.00	2.00	2.00	1.71	1.71	1.39	0.00
143	12	2.20	2.20	2.20	2.20	2.20	2.20	2.05	1.81	1.39	0.00
143	15	2.13	2.13	2.13	2.13	2.13	1.94	1.60	1.09	0.00	0.00
143	16	2.33	2.33	2.33	2.33	2.33	2.06	2.06	1.84	1.44	0.00
143	17	2.30	2.30	2.30	2.30	2.30	2.01	2.01	1.89	1.39	0.00
144	3	1.85	1.85	1.85	1.85	1.85	1.85	1.37	0.00	0.00	0.00
144	4	1.33	1.33	1.33	1.33	1.33	1.33	1.33	1.33	0.00	0.00
144	5	1.33	1.33	1.33	1.33	1.33	1.33	1.33	1.33	0.00	0.00
144	7	1.62	1.62	1.62	1.62	1.62	2.62	2.57	2.44	2.11	1.55
144	8	2.72	2.72	2.72	2.72	2.72	2.72	2.59	2.43	2.12	1.49
144	9	2.51	2.51	2.51	2.51	2.51	2.51	2.36	2.25	1.93	1.35
144	11	2.41	2.41	2.41	2.41	2.41	2.20	2.05	1.81	1.39	0.00
144	12	2.43	2.43	2.43	2.43	2.43	2.22	2.08	1.86	1.51	0.00
144	13	2.71	2.71	2.71	2.71	2.31	2.31	2.19	1.93	1.65	1.13

Table B-IV-7 Whitby Aerosol Size Distributions-Hourly Log (cont'd)

CALSPAN WHITBY SIZE DISTRIBUTIONS										EOMET 77	
DAY	HR	CH1	CH2	CH3	CH4	CH5	CH6	CH7	CH8	CH9	CH10
144	15	1.97	1.97	1.97	1.97	1.97	1.97	1.97	1.67	1.30	0.00
144	16	2.31	2.31	2.31	2.31	2.31	2.02	1.73	1.73	1.22	0.00
144	18	2.04	2.04	2.04	2.04	2.04	2.04	1.80	1.60	1.09	0.00
144	20	2.09	2.09	2.09	2.09	2.09	2.09	1.88	1.46	1.19	0.00
144	21	2.23	2.23	2.23	2.23	2.23	2.23	2.08	1.70	1.37	0.00
144	22	2.28	2.28	2.28	2.28	1.95	1.95	1.63	1.19	0.00	0.00
144	23	2.45	2.45	2.45	2.45	2.45	2.27	2.14	1.95	1.55	0.00
145	0	2.46	2.46	2.46	2.46	2.47	2.27	1.96	1.84	1.44	0.00
145	1	2.40	2.40	2.40	2.40	2.40	2.40	2.31	2.03	1.60	0.00
145	2	2.11	2.11	2.11	2.11	2.11	2.11	2.11	2.02	1.70	1.43
145	3	2.37	2.37	2.37	2.37	2.37	2.37	2.14	1.95	1.55	0.00
145	4	2.50	2.50	2.50	2.50	2.50	2.50	2.24	2.01	1.55	0.00
145	5	2.57	2.57	2.57	2.57	2.57	2.57	2.44	2.09	1.71	0.00
145	6	2.72	2.72	2.72	2.72	2.72	2.62	2.57	2.27	1.89	1.35
145	7	3.65	3.65	3.65	3.65	3.65	2.77	2.65	2.37	1.92	1.25
145	8	2.90	2.90	2.90	2.90	2.90	2.85	2.71	2.44	1.92	1.13
145	9	2.94	2.94	2.94	2.94	2.94	2.88	2.76	2.43	1.96	1.13
145	10	2.97	2.97	2.97	2.97	2.97	2.92	2.84	2.42	1.94	1.25
145	11	2.98	2.98	2.98	2.98	2.98	2.93	2.82	2.46	2.98	1.24
145	12	3.08	3.08	3.08	3.08	2.96	2.90	2.71	2.41	1.83	1.13
145	13	2.91	2.91	2.91	2.91	2.91	2.85	2.68	2.26	1.85	0.00
145	14	3.31	3.31	3.31	2.83	2.83	2.83	2.68	2.35	1.87	0.00
145	15	2.88	2.88	2.88	2.88	2.88	2.81	2.66	2.35	1.80	0.00
145	16	2.98	2.98	2.98	2.98	2.82	2.82	2.67	2.32	1.86	1.25
145	18	2.93	2.93	2.93	2.93	2.74	2.65	2.48	2.21	1.72	1.13

Table B-IV-7 Whitby Aerosol Size Distributions-Hourly Log (cont'd)

CALSPAN WHITBY SIZE DISTRIBUTIONS EOMET 77

DAY	HR	CH1	CH2	CH3	CH4	CH5	CH6	CH7	CH8	CH9	CH10
145	21	2.89	2.89	2.89	2.89	2.89	2.77	2.59	2.36	1.90	0.00
145	22	2.89	2.89	2.89	2.89	2.89	2.80	2.59	2.40	1.88	1.13
146	0	2.89	2.89	2.89	2.89	2.89	2.85	2.72	2.46	1.92	1.13
146	3	2.89	2.89	2.89	2.89	2.89	2.80	2.73	2.40	1.88	1.25
146	3	3.01	3.01	3.01	3.01	3.01	3.01	2.87	2.61	2.08	1.43
146	4	3.06	3.06	3.06	3.06	3.06	3.02	2.88	2.63	2.16	1.35
146	5	3.49	3.49	3.49	3.49	3.49	3.27	2.84	2.61	2.14	1.35
146	6	3.96	3.96	3.96	3.96	3.96	3.27	2.86	2.63	2.15	1.49
146	7	3.34	3.34	3.34	3.34	3.34	3.29	2.80	2.54	2.06	1.35
146	8	3.07	3.07	3.07	3.07	3.07	3.29	2.76	2.47	1.97	1.35
146	10	2.92	2.92	2.92	2.92	2.92	3.27	2.74	2.46	1.94	1.25
146	12	2.94	2.94	2.94	2.94	2.94	3.27	2.80	2.51	1.99	1.43
146	13	3.18	3.18	3.18	3.18	3.18	3.27	2.78	2.51	2.03	1.35
146	14	3.03	3.03	3.03	3.03	3.03	3.27	2.73	2.44	2.05	1.25
146	15	2.99	2.99	2.99	2.99	2.99	3.27	2.68	2.46	2.00	1.35
146	17	2.99	2.99	2.99	2.99	2.99	3.27	2.72	2.43	1.83	1.13
146	19	2.97	2.97	2.97	2.97	2.97	3.27	2.70	2.38	1.88	1.13
146	20	2.93	2.93	2.93	2.93	2.93	3.27	2.71	2.37	1.86	1.25
146	21	2.83	2.83	2.83	2.83	2.83	3.27	2.53	2.24	1.90	1.25
146	22	2.75	2.75	2.75	2.75	2.75	3.27	2.57	2.27	1.80	0.00
146	23	2.89	2.89	2.89	2.89	2.89	3.27	2.64	2.30	1.81	1.25
147	0	2.95	2.95	2.95	2.95	2.95	3.27	2.70	2.39	1.90	1.25
147	0	2.84	2.84	2.84	2.84	2.84	3.27	2.59	2.26	1.65	1.13
147	2	2.83	2.83	2.83	2.83	2.83	3.27	2.77	2.51	2.03	1.35
147	3	3.00	3.00	3.00	3.00	3.00	3.27	2.88	2.59	2.11	1.43

Table B-IV-7 Whitby Aerosol Size Distributions-Hourly Log (cont'd)

CALSPAN WHITBY SIZE DISTRIBUTIONS EOMET 77											
DAY	HR	CH1	CH2	CH3	CH4	CH5	CH6	CH7	CH8	CH9	CH10
147	4	2.93	2.93	2.93	2.93	2.93	2.93	2.74	2.51	2.07	1.49
147	5	3.11	3.11	3.11	3.11	2.99	2.89	2.83	2.60	2.15	1.49
147	6	3.02	3.02	3.02	3.02	3.02	2.98	2.88	2.61	2.17	1.60
147	7	3.09	3.09	3.09	3.09	2.97	2.97	2.92	2.66	2.17	1.35
147	8	3.96	3.96	3.96	3.96	2.96	2.96	2.91	2.66	2.19	1.49
147	10	3.25	3.25	3.25	3.25	3.17	3.11	2.98	2.77	2.30	1.65
147	11	3.34	3.34	3.34	3.34	3.20	3.11	2.77	2.34	1.60	0.00
147	12	3.38	3.38	3.38	3.38	3.26	3.12	2.99	2.74	2.30	1.65
147	13	3.39	3.39	3.39	3.39	3.33	3.14	2.92	2.71	2.30	1.76
148	0	3.81	3.81	3.81	3.81	3.60	3.30	3.07	2.75	2.24	1.43
148	1	3.76	3.76	3.76	3.76	3.52	3.31	3.05	2.73	2.22	1.43
148	3	3.37	3.37	3.37	3.37	3.31	3.13	2.98	2.67	2.22	1.43
148	4	3.74	3.74	3.74	3.74	3.69	3.36	3.38	2.98	2.50	1.65
148	5	3.52	3.52	3.52	3.52	3.43	3.30	3.10	2.77	2.30	1.56
148	6	3.76	3.76	3.76	3.76	3.36	3.46	2.90	2.34	1.60	0.00
148	7	3.39	3.39	3.39	3.39	3.39	3.36	3.20	2.82	2.29	1.49
150	20	3.84	3.84	3.84	3.84	2.85	2.49	2.22	1.99	1.22	0.00
150	21	3.11	3.11	3.11	3.11	2.83	2.67	2.37	1.97	1.39	0.00
150	22	3.53	3.53	3.53	3.53	2.82	2.67	2.36	1.95	1.55	0.00
150	23	3.01	3.01	3.01	3.01	2.85	2.61	2.43	2.10	1.64	0.00
151	0	3.27	3.27	3.27	3.27	3.10	2.83	2.46	2.00	1.51	0.00
151	4	2.67	2.67	2.67	2.67	2.67	2.44	2.12	1.78	1.30	0.00
151	8	3.42	3.42	3.42	3.42	2.67	2.00	2.60	2.13	1.60	0.00
151	9	3.25	3.25	3.25	3.25	2.85	2.71	2.43	2.03	1.72	1.13
151	11	3.52	3.52	3.52	3.52	3.43	3.23	2.93	2.38	1.00	0.00

Table B-IV-7 Whitby Aerosol Size Distributions-Hourly Log (cont'd)

DAY	HR	CH1	CH2	CH3	CH4	CH5	CH6	CH7	CH8	CH9	CH10
151	13	3.42	3.42	3.42	3.42	3.37	3.19	2.87	2.40	1.79	1.35
151	14	3.44	3.44	3.44	3.44	3.39	3.29	2.92	2.42	1.85	0.00
151	16	3.05	3.05	3.05	3.05	3.05	2.87	2.60	2.22	1.64	0.00
152	18	3.25	3.25	3.25	3.25	3.17	3.00	2.63	2.22	1.49	0.00
152	19	3.24	3.24	3.24	3.24	3.05	2.92	2.65	2.14	1.49	0.00
152	20	3.05	3.05	3.05	3.05	3.05	2.86	2.58	2.23	1.55	0.00
152	21	3.21	3.21	3.21	3.21	3.21	3.13	2.91	2.43	1.90	0.00
152	22	3.90	3.90	3.90	3.90	3.90	3.84	3.66	3.34	1.85	0.00
152	23	3.83	3.83	3.83	3.83	3.83	3.76	3.64	3.34	1.85	0.00
153	0	3.05	3.05	3.05	3.05	3.05	2.97	2.77	2.42	1.88	1.13
153	1	3.84	3.84	3.84	3.84	3.84	3.77	3.60	3.26	2.68	0.00
153	2	3.80	3.80	3.80	3.80	3.80	3.72	3.59	3.30	1.80	0.00
153	3	3.85	3.85	3.85	3.85	3.85	3.78	3.61	3.30	1.80	0.00
153	4	3.92	3.92	3.92	3.92	3.92	3.86	3.69	3.38	1.75	0.00
153	5	3.97	3.97	3.97	3.97	3.97	3.86	3.69	3.31	1.75	0.00
153	6	3.86	3.86	3.86	3.86	3.86	3.80	3.64	3.31	1.75	0.00
153	7	3.85	3.85	3.85	3.85	3.85	3.79	3.63	3.33	1.80	0.00
153	8	3.91	3.91	3.91	3.91	3.91	3.85	3.67	3.34	1.80	0.00
153	9	3.92	3.92	3.92	3.92	3.92	3.81	3.65	3.33	1.80	0.00
153	10	3.92	3.92	3.92	3.92	3.92	3.81	3.65	3.33	1.80	0.00
153	11	3.01	3.01	3.01	3.01	3.01	2.80	2.64	2.30	1.71	0.00
153	12	3.95	3.95	3.95	3.95	3.95	3.85	3.67	3.31	1.74	0.00
153	13	3.76	3.76	3.76	3.76	3.76	3.76	3.58	3.23	1.67	0.00
153	14	3.72	3.72	3.72	3.72	3.72	3.72	3.53	3.17	1.59	0.00
153	16	3.76	3.76	3.76	3.76	3.76	3.68	3.46	3.17	1.59	0.00

Table B-IV-7 Whitby Aerosol Size Distributions-Hourly Log (cont'd)

CALSPAN WHITBY SIZE DISTRIBUTIONS											EOMET 77
DAY	HR	CH1	CH2	CH3	CH4	CH5	CH6	CH7	CH8	CH9	CH10
153	18	2.69	2.69	2.69	2.69	2.69	2.69	2.47	2.18	1.64	0.00
153	19	2.70	2.70	2.70	2.70	2.70	2.70	2.49	2.23	1.55	0.00
153	20	2.98	2.98	2.98	2.98	2.98	2.75	2.51	2.25	1.64	0.00
153	21	2.84	2.84	2.84	2.84	2.84	2.69	2.55	2.27	1.71	0.00
153	23	2.76	2.76	2.76	2.76	2.76	2.58	2.27	1.84	1.19	0.00
154	0	2.91	2.91	2.91	2.91	2.91	2.71	2.43	2.02	1.37	0.00
154	1	2.95	2.95	2.95	2.95	2.95	2.77	2.48	2.05	1.49	0.00
154	2	2.94	2.94	2.94	2.94	2.94	2.89	2.59	2.12	1.55	0.00
154	3	3.11	3.11	3.11	3.11	2.99	2.89	2.64	2.26	1.67	0.00
154	4	3.10	3.10	3.10	3.10	2.98	2.88	2.63	2.28	1.83	1.13
154	5	3.07	3.07	3.07	3.07	2.93	2.82	2.57	2.32	1.86	1.25
154	6	2.96	2.96	2.96	2.96	2.96	2.86	2.68	2.39	1.93	1.35
154	8	3.30	3.30	3.30	2.97	2.97	2.92	2.70	2.42	1.94	1.25
154	14	3.14	3.14	3.14	3.14	2.89	2.84	2.52	2.16	1.71	0.00
156	2	3.02	3.02	3.02	3.02	3.02	2.93	2.67	2.44	2.00	1.13
156	3	3.19	3.19	3.19	3.19	3.09	2.95	2.87	2.59	2.08	1.43
156	4	3.46	3.46	3.46	3.26	3.26	3.04	2.89	2.57	2.16	1.43
156	6	3.23	3.23	3.23	3.23	3.23	3.14	3.04	2.77	2.19	1.49
156	19	3.07	3.07	3.07	3.07	3.07	3.00	2.88	2.63	2.18	1.43
156	20	3.21	3.21	3.21	3.21	3.12	3.05	2.92	2.66	2.08	1.43
156	23	3.05	3.05	3.05	3.05	3.05	2.86	2.76	2.40	1.88	1.13
157	0	2.95	2.95	2.95	2.95	2.95	2.95	2.70	2.50	1.93	1.35
157	1	3.04	3.04	3.04	3.04	3.04	2.91	2.79	2.52	1.94	1.25
157	2	3.23	3.23	3.23	3.23	3.04	2.99	2.87	2.59	2.13	1.43
157	3	3.18	3.18	3.18	3.18	3.18	3.05	2.95	2.64	2.18	1.55

Table B-IV-7 Whitby Aerosol Size Distributions-Hourly Log (cont'd)

CALSPAN WHITBY SIZE DISTRIBUTIONS EOMET 77											
DAY	HR	CH1	CH2	CH3	CH4	CH5	CH6	CH7	CH8	CH9	CH10
157	4	3.25	3.25	3.25	3.25	3.25	3.23	3.06	2.71	2.10	1.49
157	5	3.32	3.32	3.32	3.32	3.32	3.30	3.14	2.69	2.14	1.35
157	6	3.28	3.28	3.28	3.28	3.28	3.28	3.10	2.75	2.15	1.25
157	7	3.37	3.37	3.37	3.37	3.31	3.29	3.11	2.80	2.13	1.43
157	8	3.38	3.38	3.38	3.38	3.32	3.28	3.10	2.78	2.21	1.13
157	9	3.31	3.31	3.31	3.31	3.31	3.26	3.16	2.74	2.20	1.44
157	13	3.50	3.50	3.50	3.50	3.41	3.21	2.68	1.79	0.00	0.00
157	18	3.38	3.38	3.38	3.38	3.38	3.34	3.16	2.67	2.01	0.00
157	21	3.49	3.49	3.49	3.49	3.45	3.36	3.15	2.67	1.93	0.00
157	23	3.41	3.41	3.41	3.41	3.41	3.36	3.16	2.71	1.95	0.00
158	4	3.84	3.84	3.84	3.69	3.60	3.41	3.12	2.62	1.90	0.00
158	5	3.44	3.44	3.44	3.44	3.44	3.34	3.16	2.78	2.02	0.00
158	6	4.54	4.54	4.54	4.53	4.27	4.10	3.78	3.20	2.30	1.35

Table B-IV-7 Whitby Aerosol Size Distributions-Hourly Log (cont'd)

Particulate Aerosol Size Spectra
as Measured by the PMS
Axially Scattering Spectrometer Probe

Richard K. Jeck
Code 8323
Naval Research Laboratory

I. Measurement Conditions and Procedure

Aerosol particle size spectra (number of particles per cm^3 per micron radius) over the range 0.7 to 46 μm diameter were obtained from measurements aboard the USNS Hayes. The ambient aerosol particles were monitored from an elevated platform about 5m above the forward, STBD corner of the Flying Bridge (04 level). The platform was about 22 m above sea level and directly above the leading edge of the superstructure. This location placed the probe in air that was free from turbulence generated by the ship's superstructure, for relative wind directions from about 70° on the PORT side to 90° or more on the STBD side. For nearly forward relative winds the air intercepted by the probe originated at a level about 4 m below the height of the probe and is gently deflected up to the level of the probe as it nears the forward superstructure. The air trajectory is inclined about 10° upward at the location of the probe. This location also keeps the probe above the levels where the air is heated by proximity to the ship surface in daytime hours. Measurements showed that on sunny days the air temperature was as much as 2°C warmer at a level 3 m below the elevated platform than at the platform itself.

The probe referred to was an Axially Scattering Spectrometer Probe (ASSP), a single particle optical counter manufactured by Particle Measuring Systems (PMS), Inc. The ASSP has four selectable size ranges covering the interval 0.7 to 46 μm diameter and each range is subdivided into fifteen particle size categories, or channels, as listed in Table B-IV-8. The particle counts were allowed to accumulate in the size channels during successive, one minute sampling intervals and the counts were then recorded at the end of each minute. The probe was set to alternate between Ranges 4 and 3, each range being in effect for a full, one minute sampling interval.

The PMS system was not operational until May 18, the third day underway. After that, the ASSP was on-line continuously except for periods of maintenance and for situations where the wind was from the aft direction of the ship. The off-line time was about 30% of the cruise, mostly due to following winds and the resulting poor sampling conditions.

II. Explanation of Data Tables

The data table, B-IV-9, contains values of dn/dr (number of particles per cm^3 per micron radius) computed from particle counts in thirteen size channels whose threshold radii are listed in the left hand column of each page.

The data came from the 15 size channels of Range 4 and the 15 from Range 3. Since the first eight channels of Range 3 are redundant with Range 4, only the results from channels 9 through 14 of Range 3 have been listed. These latter results are the last six entries in each column.

AD-A065 267

NAVAL RESEARCH LAB WASHINGTON D C
THE EOMET CRUISE OF THE USNS HAYES: MAY - JUNE 1977.(U)
JAN 79 S G GATHMAN, B G JULIAN
NRL-MR-3924

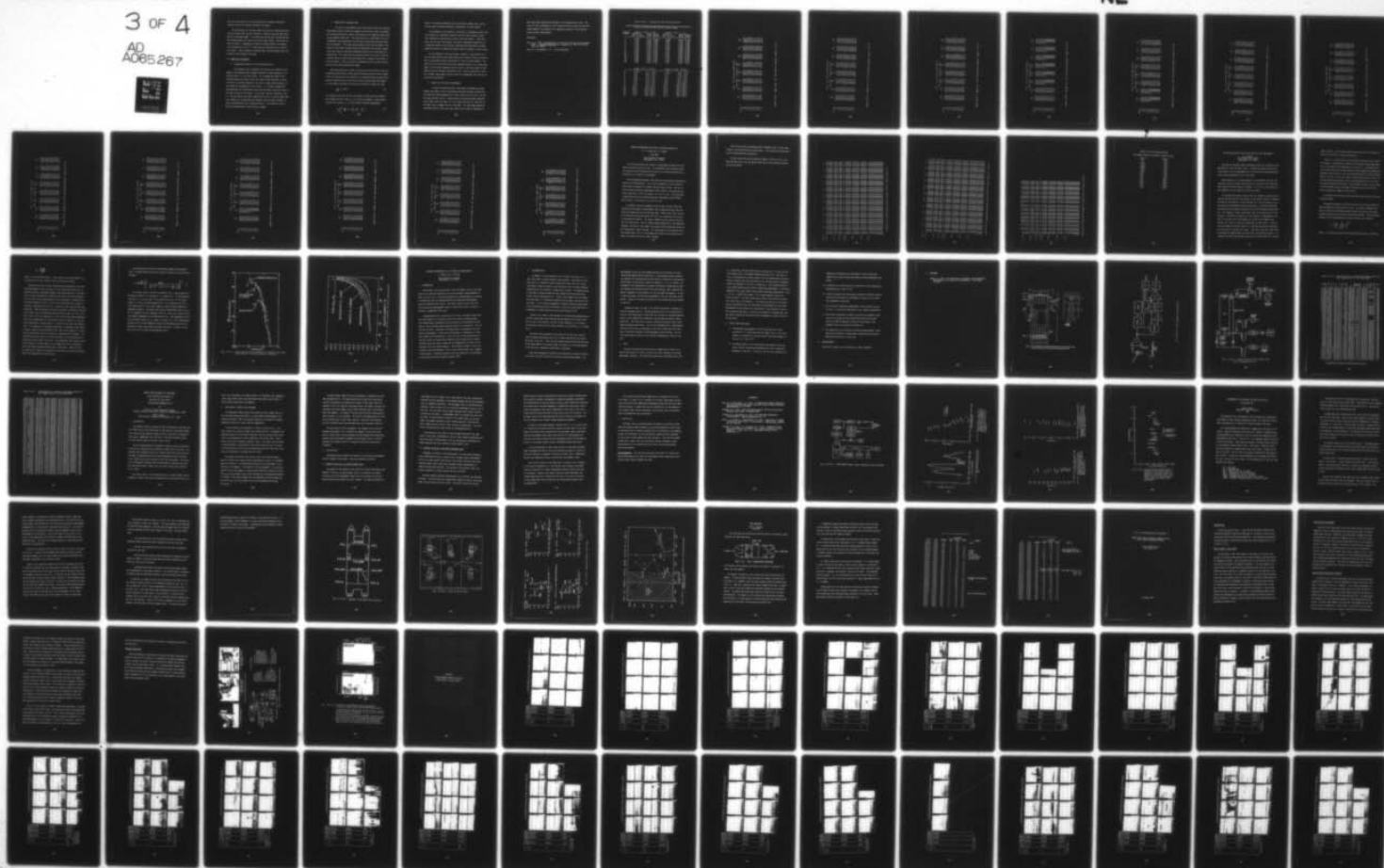
F/G 4/2

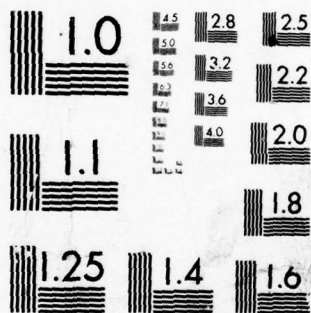
UNCLASSIFIED

NL

3 OF 4

AD
A065 267





MICROCOPY RESOLUTION TEST CHART
NATIONAL BUREAU OF STANDARDS-1963-A

The first seven entries are from alternate size channels arbitrarily selected from the 15 available channels for Range 4.

For the purposes of this data report, the particle counts were arbitrarily averaged over one hour intervals in order to keep the page count down to a tractable number. The Julian day and the hour at which the one hour average begins are given at the top of each column. The entries for dn/dr are given in computerized scientific notation where, for example, .77E-03 stands for 0.77×10^{-3} . Some data exist that were not included in this report. They correspond to periods when valid measurements were obtained for only portions of an hour.

III. Additional Information

1. Assumptions Involved in the Probe Calibration.

The threshold radii assigned to the various size channels corresponds to the expected probe response function for water droplets of refractive index $n = 1.33$ (Jeck, 1978). It is assumed that most of the maritime aerosol particles in the size range to which the ASSP is sensitive exist as solution droplets of sea salt or other soluble material at the humidities encountered on this cruise. It is further assumed that these droplets are sufficiently dilute that the actual refractive index is the same as that for pure water. In any case, realistic deviations from $n = 1.33$ are likely to be small enough that an error of no more than \pm one size channel will be made when the response curve for water droplets is used to determine the size of these particles. This amount of error is within the manufacturer's specifications anyway.

2. Method Used to Compute dn/dr

For particle spectrometers with sufficiently narrow size channels, approximate values of dn/dr are commonly arrived at for each size channel by dividing the particle count by the product of the sampling volume (cm^3) and the channel width (μm). The resultant value is then taken to be representative of the population of particles at some discrete radius within the size channel. This radius may be chosen as the lower threshold, the center, or any other location within the applicable size channel, depending on the slope or some other weighting function of the indicated size distribution. The resulting size spectrum consists of a plot or table of discrete values of dn/dr each associated with a selected, fixed value of particle radius. Values of dn/dr at intermediate radii are then inferred by the use of some interpolation scheme.

With the application in mind of using the particle data for deriving scattering coefficients or other optical properties which involve integrations over the particle size spectrum, an alternate method has been developed for computing dn/dr from the raw particle counts (Jeck and Ruhnke). In this method, continuous functions of the familiar "power law" form

$$\frac{dn}{dr} = Cr^{-(p+1)} \quad (1)$$

are assumed to describe the size distribution within each size channel. The recorded particle count, N , in a given size channel is then used to evaluate the constant, C , for that channel from the relationship

$$N = \int_a^{r_b} \frac{dn}{dr} dr = \frac{-C}{\beta} (r_b^{-\beta} - r_a^{-\beta}) , \quad (2)$$

where β is evaluated separately from an iterative scheme, and r_a and r_b are the lower and upper thresholds, respectively, for the channel.

The advantage of this method is that dn/dr is represented within each size channel by a continuous, analytic function rather than by a point value assigned to some arbitrary radius within the channel. These functions, one for each size channel, can then be integrated analytically in a piecewise fashion along with the scattering efficiency factor or other weighting function to compute the desired optical property or other result.

For the purposes of this data report, however, it was decided to retain the more familiar data format where point values of dn/dr at discrete radii are presented rather than values of C and β for each channel. The tabled values of dn/dr have still been computed from Eq. (1), as described above, for the lower threshold radius (values in left hand column of each page) of the size channels selected for use. Since no values for C and β are included, approximate values of dn/dr at intermediate radii may be obtained by interpolation.

3. Comparison with Other Measurements.

It should be mentioned that a consistent discrepancy was found between the values of dn/dr indicated by the ASSP and those indicated by two other PMS probes employed by Dr. Gary Trusty on this cruise. See the following section, B-IV-g. These Classical Scattering Aerosol Spectrometers (CSAS) cover the range 1-15 μm in radius and thus are sensitive to the same sizes as Ranges 4 and 3 of the ASSP. The CSAS probes generally indicated values of dn/dr that were smaller by an order of magnitude or

more than those indicated by the ASSP for the same particle sizes. The source of this discrepancy is still unclear at this writing, but the CSAS values appear to be unusually low compared to previous, at-sea measurements by other investigators.

References

Jeck, R. K., 1978: Performance of the PMS Axially Scattering Spectrometer Probe. In Aerosol Measurement, D. Lundgren, Ed., Univ. of Florida Press (In Press).

Jeck, R. K. and Ruhnke, L. H.: (to be published).

Table B-IV-8. Calibration Data for PMS Probes

Axially Scattering Spectrometer Probe (ASSP)				
Channel Number	Range 4 (0.37 - 4.4 μ)		Range 2 (0.4 - 7.7 μ)	
	Radius at ctr. of chan.	Range within chan. limits	Radius at ctr. of chan.	Range within chan. limits
1	0.42 μ	0.37 - 0.45 μ	0.55 μ	0.42 - 0.70 μ
2	0.52	0.45 - 0.60	0.88	0.70 - 1.05
3	0.72	0.60 - 0.82	1.25	1.05 - 1.45
4	0.95	0.82 - 1.05	1.65	1.45 - 1.85
5	1.18	1.05 - 1.30	2.10	1.85 - 2.38
6	1.40	1.30 - 1.52	2.65	2.38 - 2.92
7	1.65	1.52 - 1.75	3.20	2.92 - 3.48
8	1.88	1.75 - 2.05	3.75	3.48 - 4.02
9	2.22	2.05 - 2.38	4.30	4.02 - 4.58
10	2.55	2.38 - 2.72	4.80	4.58 - 5.10
11	2.90	2.72 - 3.08	5.35	5.10 - 5.60
12	3.22	3.08 - 3.40	5.85	5.60 - 6.15
13	3.58	3.40 - 3.75	6.40	6.15 - 6.70
14	3.90	3.75 - 4.08	7.00	6.70 - 7.25
15	4.25	4.08 - 4.42	7.50	7.25 - 7.75

Range 3 (0.7 - 15.5 μ)		Range 1 (1.05 - 23.2 μ)	
1	1.05 μ	0.7 - 1.4 μ	1.65 μ
2	1.8	1.4 - 2.2	3.0
3	2.8	2.2 - 3.3	4.5
4	3.8	3.3 - 4.3	6.0
5	4.85	4.3 - 5.3	7.5
6	5.9	5.3 - 6.4	9.0
7	7.0	6.4 - 7.5	10.5
8	8.0	7.5 - 8.5	12.0
9	9.0	8.5 - 9.5	13.5
10	10.0	9.5 - 10.5	15.0
11	11.0	10.5 - 11.5	16.5
12	12.0	11.5 - 12.5	18.0
13	13.0	12.5 - 13.5	19.5
14	14.0	13.5 - 14.5	21.0
15	15.0	14.5 - 15.5	22.5

RADIUS	dN/dR (NO. CM ⁻³ PER MICRON RADIUS)									
	START TIME - JULIAN DAY & HOUR									
	139 7	139 14	139 15	139 16	139 17	139 18	139 19	139 20		
.37	.13E+03	.65E+01	.12E+02	.42E+01	.67E+01	.60E+02	.39E+03	.32E+02		
.60	.12E+02	.25E+01	.21E+01	.20E+01	.20E+01	.45E+01	.66E+01	.50E+01		
1.05	.26E+02	.59E+01	.49E+01	.39E+01	.36E+01	.11E+02	.13E+02	.85E+01		
1.52	.12E+02	.22E+01	.17E+01	.13E+01	.15E+01	.49E+01	.51E+01	.34E+01		
2.05	.31E+01	.65E+00	.44E+00	.38E+00	.33E+00	.12E+01	.14E+01	.94E+00		
2.72	.11E+01	.29E+00	.22E+00	.14E+00	.18E+00	.46E+00	.64E+00	.41E+00		
3.40	.32E+00	.40E-01	.49E-01	.33E-01	.27E-01	.90E-01	.13E+00	.81E-01		
4.02	.17E+00	.26E-01	.18E-01	.84E-02	.16E-01	.74E-01	.57E-01	.66E-01		
4.58	.77E-01	.14E-01	.36E-02	.87E-02	.64E-02	.36E-01	.43E-01	.13E-01		
5.10	.35E-01	.69E-02	.39E-02	.59E-02	.51E-02	.20E-01	.00E+00	.15E-01		
5.60	.12E-01	.53E-02	.19E-02	.22E-02	.34E-02	.63E-02	.15E-02	.37E-02		
6.15	.94E-02	.16E-02	.19E-02	.50E-03	.00E+00	.48E-02	.45E-02	.23E-02		
6.70	.56E-02	.15E-02	.50E-03	.40E-03	.10E-03	.17E-02	.50E-03	.90E-03		

Table B-IV-9 dN/dR (no. cm⁻³ per micron radius) (page 1 of 13)

RADIUS	DN/DR (NO. CM-3 PER MICRON RADIUS)									
	START TIME - JULIAN DAY & HOUR									
	139	139	139	140	140	140	140	140	140	140
	21	22	23	0	3	4	5	6		
.37	.37E+02	.59E+02	.27E+02	.17E+02	.68E+02	.16E+02	.21E+02	.25E+02		
.60	.54E+01	.52E+01	.37E+01	.35E+01	.63E+01	.73E+01	.39E+01	.32E+01		
1.05	.80E+01	.87E+01	.77E+01	.86E+01	.15E+02	.19E+02	.10E+02	.79E+01		
1.52	.29E+01	.31E+01	.23E+01	.24E+01	.47E+01	.57E+01	.25E+01	.21E+01		
2.05	.73E+00	.78E+00	.63E+00	.73E+00	.12E+01	.15E+01	.80E+00	.61E+00		
2.72	.38E+00	.37E+00	.24E+00	.30E+00	.43E+00	.62E+00	.32E+00	.28E+00		
3.40	.61E-01	.99E-01	.53E-01	.71E-01	.90E-01	.12E+00	.39E-01	.54E-01		
4.02	.31E-01	.47E-01	.30E-01	.24E-01	.39E-01	.45E-01	.14E-01	.33E-02		
4.58	.25E-01	.11E-01	.11E-01	.12E-01	.16E-01	.16E-01	.60E-02	.62E-02		
5.10	.84E-02	.14E-01	.50E-02	.94E-02	.11E-01	.11E-01	.37E-02	.32E-02		
5.60	.36E-02	.14E-01	.46E-02	.18E-02	.44E-02	.40E-02	.00E+00	.12E-02		
6.15	.29E-02	.17E-02	.40E-02	.80E-03	.25E-02	.40E-03	.50E-03	.40E-03		
6.70	.15E-02	.18E-02	.50E-03	1.00E-03	.40E-03	.50E-03	.00E+00	.40E-03		

Table B-IV-9 dN/dr (no. cm⁻³ per micron radius) (page 2 of 13)

RADIUS	DN/DR (NO. CM-3 PER MICRON RADIUS)															
	START TIME - JULIAN DAY & HOUR															
	140	140	140	140	140	140	140	140	140	140	140	140	140	140	140	140
	7	8	9	11	12	13	14	16								
.37	.26E+02	.32E+02	.79E+02	.12E+03	.54E+02	.13E+03	.19E+03	.11E+02								
.60	.46E+01	.51E+01	.51E+01	.49E+01	.49E+01	.91E+01	.73E+01	.23E+01								
1.05	.12E+02	.13E+02	.12E+02	.90E+01	.12E+02	.13E+02	.11E+02	.55E+01								
1.52	.34E+01	.44E+01	.50E+01	.31E+01	.52E+01	.83E+01	.55E+01	.19E+01								
2.05	.97E+00	.11E+01	.12E+01	.81E+00	.14E+01	.19E+01	.14E+01	.53E+00								
2.72	.32E+00	.41E+00	.42E+00	.28E+00	.41E+00	.66E+00	.55E+00	.25E+00								
3.40	.62E-01	.85E-01	.86E-01	.74E-01	.12E+00	.21E+00	.14E+00	.61E-01								
4.02	.21E-01	.30E-01	.48E-01	.26E-01	.63E-01	.17E+00	.74E-01	.26E-01								
4.58	.14E-01	.15E-01	.22E-01	.15E-01	.42E-01	.10E+00	.43E-01	.11E-01								
5.10	.58E-02	.13E-01	.64E-02	.83E-02	.19E-01	.51E-01	.26E-01	.63E-02								
5.60	.23E-02	.11E-02	.44E-02	.28E-02	.13E-01	.83E-02	.90E-02	.52E-02								
6.15	.19E-02	.18E-02	.28E-02	1.00E-03	.78E-02	.12E-01	.66E-02	.17E-02								
6.70	.40E-03	.40E-03	.90E-03	.30E-03	.26E-02	.45E-02	.25E-02	.18E-02								

Table B-IV-9 dN/dR (no. cm⁻³ per micron radius) (page 3 of 13)

DN/DR (NO. CM-3 PER MICRON RADIUS)		START TIME - JULIAN DAY & HOUR								
RADIUS		141	142	143	143	143	143	143	143	143
		23	17	4	5	6	7	8	9	
.37		.37E+02	.29E+02	.20E+03	.12E+03	.13E+03	.13E+03	.27E+02	.17E+02	
.60		.38E+01	.36E+01	.64E+01	.58E+01	.43E+01	.43E+01	.49E+01	.57E+01	
1.05		.96E+01	.78E+01	.13E+02	.14E+02	.93E+01	.93E+01	.13E+02	.11E+02	
1.52		.36E+01	.26E+01	.44E+01	.45E+01	.27E+01	.27E+01	.47E+01	.42E+01	
2.05		.12E+01	.10E+01	.15E+01	.19E+01	.12E+01	.12E+01	.18E+01	.15E+01	
2.72		.43E+00	.28E+00	.83E+00	.83E+00	.67E+00	.67E+00	.82E+00	.77E+00	
3.40		.12E+00	.87E-01	.13E+00	.30E+00	.19E+00	.19E+00	.24E+00	.28E+00	
4.02		.58E-01	.42E-01	\$\$\$\$	\$\$\$\$	\$\$\$\$	\$\$\$\$	\$\$\$\$	\$\$\$\$	
4.58		.42E-01	.30E-01	\$\$\$\$	\$\$\$\$	\$\$\$\$	\$\$\$\$	\$\$\$\$	\$\$\$\$	
5.10		.26E-01	.24E-01	\$\$\$\$	\$\$\$\$	\$\$\$\$	\$\$\$\$	\$\$\$\$	\$\$\$\$	
5.60		.13E-01	.56E-02	\$\$\$\$	\$\$\$\$	\$\$\$\$	\$\$\$\$	\$\$\$\$	\$\$\$\$	
6.15		.96E-02	.22E-02	\$\$\$\$	\$\$\$\$	\$\$\$\$	\$\$\$\$	\$\$\$\$	\$\$\$\$	
6.70		.34E-02	.21E-02	\$\$\$\$	\$\$\$\$	\$\$\$\$	\$\$\$\$	\$\$\$\$	\$\$\$\$	

Table B-IV-9 dN/dR (no. cm⁻³ per micron radius) (page 4 of 13)

RADIUS	DN/DR (NO. CM-3 PER MICRON RADIUS)									
	START TIME - JULIAN DAY & HOUR									
	143 10	143 11	143 13	143 18	143 19	143 20	144 1	144 2	144 1	144 2
.37	.10E+03	.22E+02	.17E+02	.17E+03	.16E+03	.13E+04	.12E+04	.21E+04	.12E+04	.21E+04
.60	.59E+01	.78E+01	.48E+01	.75E+01	.47E+01	.47E+01	.21E+01	.11E+01	.21E+01	.11E+01
1.05	.13E+02	.15E+02	.88E+01	.12E+02	.68E+01	.64E+01	.27E+01	.17E+01	.27E+01	.17E+01
1.52	.42E+01	.47E+01	.29E+01	.48E+01	.25E+01	.26E+01	.94E+00	.70E+00	.94E+00	.70E+00
2.05	.17E+01	.17E+01	.11E+01	.13E+01	.85E+00	.71E+00	.31E+00	.14E+00	.31E+00	.14E+00
2.72	.70E+00	.70E+00	.45E+00	.55E+00	.24E+00	.22E+00	.74E-01	.41E-01	.74E-01	.41E-01
3.40	.16E+00	.13E+00	.89E-01	.25E+00	.99E-01	.98E-01	.74E-01	.42E-01	.74E-01	.42E-01
4.02	\$\$\$\$	\$\$\$\$.50E-01	.14E+00	.74E-01	.60E-01	.30E-01	.19E-02	.30E-01	.19E-02
4.58	\$\$\$\$	\$\$\$\$.32E-01	.96E-01	.44E-01	.43E-01	.40E-02	.45E-02	.40E-02	.45E-02
5.10	\$\$\$\$	\$\$\$\$.17E-01	.62E-01	.23E-01	.30E-01	.43E-02	.45E-02	.43E-02	.45E-02
5.60	\$\$\$\$	\$\$\$\$.86E-02	.42E-01	.13E-01	.17E-01	.23E-02	.00E+00	.23E-02	.00E+00
6.15	\$\$\$\$	\$\$\$\$.54E-02	.28E-01	1.00E-02	.46E-02	.47E-02	.20E-02	.47E-02	.20E-02
6.72	\$\$\$\$	\$\$\$\$.24E-02	.16E-01	.47E-02	.46E-02	.23E-02	.00E+00	.23E-02	.00E+00

Table B-IV-9 dn/dr (no. cm⁻³ per micron radius) (page 5 of 13)

RADIUS	DN/DR (NO. CM ⁻³ PER MICRON RADIUS)															
	START TIME - JULIAN DAY & HOUR															
	145	145	145	145	145	145	145	145	145	145	145	145	145	145	145	145
	1	2	3	4	5	6	7	8								
.37	.64E+01	.59E+01	.59E+01	.77E+01	.18E+02	.10E+02	.78E+01	.87E+01								
.60	.50E+01	.53E+01	.48E+01	.54E+01	.97E+01	.11E+02	.11E+02	.11E+02								
1.05	.44E+01	.44E+01	.46E+01	.50E+01	.85E+01	.11E+02	.11E+02	.11E+02								
1.52	.15E+01	.16E+01	.16E+01	.18E+01	.30E+01	.34E+01	.37E+01	.35E+01								
2.05	.49E+00	.52E+00	.47E+00	.51E+00	.87E+00	.11E+01	.11E+01	.11E+01								
2.72	.19E+00	.19E+00	.19E+00	.17E+00	.35E+00	.41E+00	.40E+00	.42E+00								
3.40	.80E-01	.62E-01	.64E-01	.82E-01	.13E+00	.12E+00	.15E+00	.11E+00								
4.02	.36E-01	.33E-01	.32E-01	.35E-01	.60E-01	.65E-01	.78E-01	.86E-01								
4.58	.19E-01	.14E-01	.19E-01	.19E-01	.34E-01	.40E-01	.52E-01	.49E-01								
5.10	.14E-01	.11E-01	.14E-01	.14E-01	.22E-01	.28E-01	.23E-01	.25E-01								
5.60	.56E-02	.73E-02	.56E-02	.20E-02	.52E-02	.18E-01	.13E-01	.90E-02								
6.15	.39E-02	.49E-02	.32E-02	.20E-02	.45E-02	.46E-02	.10E-01	.78E-02								
6.70	.28E-02	.11E-02	.19E-02	.12E-02	.60E-03	.45E-02	.19E-02	.41E-02								

Table B-IV-9 dn/dr (no. cm⁻³ per micron radius) (page 6 of 13)

RADIUS	DN/DR (NO. CM-3 PER MICRON RADIUS)											
	START TIME - JULIAN DAY & HOUR											
	145 9	145 10	145 11	145 12	145 16	145 17	145 18	145 19				
.37	.50E+02	.34E+02	.86E+01	.59E+01	.10E+02	.78E+01	.44E+01	.62E+01				
.60	.10E+02	.99E+01	.87E+01	.70E+01	.48E+01	.33E+01	.25E+01	.42E+01				
1.05	.11E+02	.98E+01	.92E+01	.76E+01	.55E+01	.41E+01	.33E+01	.44E+01				
1.52	.35E+01	.31E+01	.29E+01	.22E+01	.18E+01	.14E+01	.98E+00	.14E+01				
2.05	.11E+01	.93E+00	.90E+00	.74E+00	.57E+00	.40E+00	.33E+00	.39E+00				
2.72	.38E+00	.35E+00	.30E+00	.24E+00	.19E+00	.13E+00	.93E-01	.14E+00				
3.40	.16E+00	.13E+00	.92E-01	.89E-01	.57E-01	.45E-01	.54E-01	.31E-01				
4.02	.79E-01	.52E-01	.47E-01	.52E-01	.38E-01	.32E-01	.18E-01	.12E-01				
4.58	.36E-01	.31E-01	.24E-01	.29E-01	.24E-01	.20E-01	.12E-01	1.00E-02				
5.10	.26E-01	.16E-01	.16E-01	.17E-01	.14E-01	.57E-02	.66E-02	.80E-02				
5.60	.22E-01	.58E-02	.00E+00	.73E-02	.10E-01	.38E-02	.40E-02	.21E-02				
6.15	.45E-02	.51E-02	.90E-03	.25E-02	.12E-01	.28E-02	.30E-02	.16E-02				
6.70	.33E-02	.90E-03	1.00E-03	.13E-02	.13E-02	.20E-02	.17E-02	.40E-03				

Table B-IV-9 dn/dr (no. cm⁻³ per micron radius) (page 7 of 13)

RADIUS	DN/DR (NO. CM-3 PER MICRON RADIUS)												
	START TIME - JULIAN DAY & HOUR												
	145	146	146	146	146	146	146	146	146	146	146	146	146
	20	0	1	2	3	4	5	6					
.37	.79E+01	.21E+02	.23E+02	.30E+02	.40E+02	.75E+02	.11E+03	.17E+03					
.60	.52E+01	.99E+01	.85E+01	.86E+01	.11E+02	.11E+02	.13E+02	.20E+02					
1.05	.50E+01	.10E+02	.76E+01	.79E+01	.93E+01	.96E+01	.96E+01	.12E+02					
1.52	.15E+01	.30E+01	.23E+01	.22E+01	.27E+01	.26E+01	.24E+01	.24E+01					
2.05	.48E+00	.77E+00	.69E+00	.67E+00	.72E+00	.75E+00	.65E+00	.64E+00					
2.72	.13E+00	.30E+00	.22E+00	.23E+00	.28E+00	.24E+00	.20E+00	.15E+00					
3.40	.24E-01	.96E-01	.56E-01	.59E-01	.71E-01	.76E-01	.57E-01	.62E-01					
4.02	.22E-01	.28E-01	.26E-01	.19E-01	.31E-01	.41E-01	.32E-01	.18E-01					
4.58	.78E-02	.17E-01	.18E-01	.16E-01	.12E-01	.18E-01	.82E-02	.96E-02					
5.10	.85E-02	.96E-02	.12E-01	.12E-01	.11E-01	.64E-02	.89E-02	.77E-02					
5.60	.57E-02	.57E-02	.53E-02	.16E-02	.55E-02	.26E-02	.86E-02	.11E-02					
6.15	.00E+00	.00E+00	.36E-02	.16E-02	.41E-02	.20E-02	.00E+00	.11E-02					
6.70	.00E+00	.30E-03	.90E-03	.00E+00	.00E+00	.00E+00	.00E+00	1.00E-03					

Table B-IV-9 dN/dR (no. cm⁻³ per micron radius) (page 8 of 13)

RADIUS	DN/DR (NO. CM-3 PER MICRON RADIUS)									
	START TIME - JULIAN DAY & HOUR									
	146 7	146 8	146 21	146 22	146 23	147 0	147 1	147 2	147 1	147 2
.37	.22E+03	.28E+03	.13E+04	.16E+04	.15E+04	.14E+04	.22E+04	.25E+04	.22E+04	.25E+04
.60	.23E+02	.23E+02	.14E+03	.16E+03	.18E+03	.18E+03	.24E+03	.27E+03	.24E+03	.27E+03
1.05	.14E+02	.13E+02	.28E+02	.35E+02	.30E+02	.30E+02	.39E+02	.44E+02	.39E+02	.44E+02
1.52	.22E+01	.15E+01	.34E+01	.33E+01	.39E+01	.36E+01	.44E+01	.49E+01	.44E+01	.49E+01
2.05	.53E+00	.42E+00	.72E+00	.66E+00	.73E+00	.85E+00	.95E+00	.10E+01	.95E+00	.10E+01
2.72	.19E+00	.13E+00	.29E+00	.27E+00	.31E+00	.37E+00	.42E+00	.47E+00	.42E+00	.47E+00
3.40	.50E-01	.26E-01	.44E-01	.54E-01	.29E-01	.49E-01	.71E-01	.70E-01	.71E-01	.70E-01
4.02	.23E-01	.14E-01	.31E-01	.56E-01	.20E-01	.23E-01	.36E-01	.48E-01	.36E-01	.48E-01
4.58	.15E-01	.17E-02	.16E-01	.37E-01	.12E-01	.20E-01	.22E-01	.23E-01	.22E-01	.23E-01
5.10	.87E-02	.42E-02	.99E-02	.23E-01	.52E-02	.10E-01	.17E-01	.14E-01	.17E-01	.14E-01
5.60	.50E-03	.42E-02	.70E-02	.33E-02	.24E-02	.72E-02	.46E-02	.31E-02	.46E-02	.31E-02
6.15	.11E-02	.00E+00	.00E+00	.59E-02	.13E-02	.90E-02	.22E-02	.39E-02	.22E-02	.39E-02
6.70	.50E-03	.00E+00	.00E+00	.00E+00	.00E+00	.11E-02	.13E-02	.17E-02	.13E-02	.17E-02

Table B-IV-9 dN/dR (no. cm⁻³ per micron radius) (page 9 of 13)

DN/DR (NO. CM-3 PER MICRON RADIUS)		START TIME - JULIAN DAY & HOUR											
RADIUS	147 3	147			150			151			151		
		13	18	22	23	23	23	11	12	23	11	12	23
.37	.26E+04	.29E+04	.43E+01	.84E+02	.67E+02	.67E+02	.67E+02	.78E+01	.13E+02	.14E+04	.78E+01	.13E+02	.14E+04
.60	.27E+03	.39E+03	.60E+01	.13E+02	.14E+02	.14E+02	.14E+02	.30E+01	.27E+01	.15E+03	.30E+01	.27E+01	.15E+03
1.05	.43E+02	.57E+02	.69E+01	.22E+02	.23E+02	.23E+02	.23E+02	.47E+01	.37E+01	.21E+02	.47E+01	.37E+01	.21E+02
1.52	.51E+01	.94E+01	.83E+00	.61E+01	.61E+01	.61E+01	.61E+01	.12E+01	.10E+01	.20E+01	.12E+01	.10E+01	.20E+01
2.05	.11E+01	.22E+01	.20E+00	.19E+01	.19E+01	.19E+01	.19E+01	.43E+00	.33E+00	.37E+00	.43E+00	.33E+00	.37E+00
2.72	.49E+00	.92E+00	.81E-01	.64E+00	.68E+00	.68E+00	.68E+00	.14E+00	.12E+00	.10E+00	.14E+00	.12E+00	.10E+00
3.40	.79E-01	.24E+00	.25E-01	.31E+00	.33E+00	.33E+00	.33E+00	.70E-01	.61E-01	.26E-01	.70E-01	.61E-01	.26E-01
4.02	.56E-01	\$\$\$\$.14E-01	.14E+00	.17E+00	.17E+00	.17E+00	.60E-01	.45E-01	.12E-01	.60E-01	.45E-01	.12E-01
4.58	.41E-01	\$\$\$\$.60E-02	.98E-01	.95E-01	.95E-01	.95E-01	.28E-01	.15E-01	.50E-02	.28E-01	.15E-01	.50E-02
5.10	.28E-01	\$\$\$\$.71E-02	.68E-01	.66E-01	.66E-01	.66E-01	.25E-01	.17E-01	.37E-02	.25E-01	.17E-01	.37E-02
5.60	.70E-02	\$\$\$\$.32E-02	.33E-01	.44E-01	.44E-01	.44E-01	.71E-02	.22E-01	.16E-02	.71E-02	.22E-01	.16E-02
6.15	.60E-02	\$\$\$\$.26E-02	.31E-01	.23E-01	.23E-01	.23E-01	.49E-02	.43E-02	.00E+00	.49E-02	.43E-02	.00E+00
6.70	.24E-02	\$\$\$\$.50E-03	.20E-01	.17E-01	.17E-01	.17E-01	.35E-02	.33E-02	.00E+00	.35E-02	.33E-02	.00E+00

Table B-IV-9 dN/dR (no. cm⁻³ per micron radius) (page 10 of 13)

RADIUS	DN/TR (NO. CM-3 PER MICRON RADIUS)									
	START TIME - JULIAN DAY & HOUR									
	153	155	155	155	155	156	156	156	156	156
	8	20	21	22	23	2	3	5		
.37	.61E+03	.50E+02	.37E+02	.57E+02	.56E+02	.23E+02	.18E+02	.11E+02		
.60	.80E+02	.15E+02	.86E+01	.10E+02	.10E+02	.66E+01	.61E+01	.32E+01		
1.05	.16E+02	.10E+02	.74E+01	.92E+01	.99E+01	.60E+01	.53E+01	.28E+01		
1.52	.16E+01	.24E+01	.17E+01	.23E+01	.19E+01	.14E+01	.11E+01	.65E+00		
2.05	.31E+00	.81E+00	.49E+00	.53E+00	.48E+00	.46E+00	.36E+00	.21E+00		
2.72	.34E-01	.27E+00	.20E+00	.20E+00	.20E+00	.17E+00	.14E+00	.67E-01		
3.40	.90E-02	.11E+00	.64E-01	.61E-01	.72E-01	.52E-01	.50E-01	.41E-01		
4.02	.10E-01	.76E-01	.51E-01	.11E+00	.43E-01	.42E-01	.42E-01	.27E-01		
4.58	.58E-02	.46E-01	.35E-01	.65E-01	.30E-01	.25E-01	.27E-01	.13E-01		
5.10	.40E-02	.34E-01	.31E-01	.39E-01	.26E-01	.25E-01	.25E-01	.15E-01		
5.60	.22E-02	.23E-01	.19E-01	.21E-01	.16E-01	.13E-01	.53E-02	.84E-02		
6.15	.00E+00	.14E-01	.96E-02	.77E-02	.69E-02	.87E-02	.57E-02	.41E-02		
6.70	.00E+00	.70E-02	.63E-02	.83E-02	.48E-02	.25E-02	.42E-02	.22E-02		

Table B-IV-9 dn/dr (no. cm^{-3} per micron radius) (page 11 of 13)

RADIUS	DN/DR (NO. CM ⁻³ PER MICRON RADIUS)											
	START TIME - JULIAN DAY & HOUR											
	156 6	156 18	156 19	157 2	157 3	157 4	157 5	157 6	157 5	157 6	157 5	157 6
.37	.55E+01	.19E+02	.21E+02	.28E+02	.22E+02	.13E+02	.92E+01	.94E+01	.92E+01	.94E+01	.92E+01	.94E+01
.60	.27E+01	.59E+01	.80E+01	.71E+01	.65E+01	.71E+01	.85E+01	.86E+01	.85E+01	.86E+01	.85E+01	.86E+01
1.05	.20E+01	.49E+01	.57E+01	.31E+01	.33E+01	.41E+01	.41E+01	.51E+01	.41E+01	.51E+01	.41E+01	.51E+01
1.52	.49E+00	.11E+01	.14E+01	.11E+01	.11E+01	.13E+01	.15E+01	.16E+01	.15E+01	.16E+01	.15E+01	.16E+01
2.05	.16E+00	.35E+00	.46E+00	.29E+00	.34E+00	.47E+00	.48E+00	.55E+00	.48E+00	.55E+00	.48E+00	.55E+00
2.72	.58E-01	.12E+00	.19E+00	.94E-01	.10E+00	.15E+00	.15E+00	.17E+00	.15E+00	.17E+00	.15E+00	.17E+00
3.40	.21E-01	.55E-01	.50E-01	.34E-01	.25E-01	.58E-01	.58E-01	.66E-01	.58E-01	.66E-01	.58E-01	.66E-01
4.02	.34E-01	.30E-01	.41E-01	.31E-01	.28E-01	.35E-01	.35E-01	.39E-01	.35E-01	.39E-01	.35E-01	.39E-01
4.58	.23E-01	.19E-01	.26E-01	.12E-01	.14E-01	.26E-01	.26E-01	.15E-01	.22E-01	.15E-01	.22E-01	.15E-01
5.10	.44E-02	.16E-01	.21E-01	.11E-01	.13E-01	.20E-01	.14E-01	.18E-01	.14E-01	.18E-01	.14E-01	.18E-01
5.60	.40E-02	.89E-02	.48E-02	.51E-02	.69E-02	.71E-02	.29E-02	.80E-02	.29E-02	.80E-02	.29E-02	.80E-02
6.15	.56E-02	.44E-02	.69E-02	.23E-02	.39E-02	.33E-02	.29E-02	.37E-02	.29E-02	.37E-02	.29E-02	.37E-02
6.70	.21E-02	.21E-02	.51E-02	.28E-02	.17E-02	.21E-02	.16E-02	.50E-02	.16E-02	.50E-02	.16E-02	.50E-02

Table B-IV-9 dn/dr (no. cm⁻³ per micron radius) (page 12 of 13)

		DN/DR (NO. CM-3 PER MICRON RADIUS)									
RADIUS	157 7	START TIME - JULIAN DAY & HOUR									
		157 10	157 16	157 17	157 18	157 19	157 21	157 19	157 21	157 19	157 21
.37	.59E+01	.22E+01	.18E+02	.24E+02	.32E+02	.13E+03	.63E+02	.13E+03	.63E+02	.13E+03	.63E+02
.60	.64E+01	.28E+01	.62E+01	.86E+01	.95E+01	.14E+02	.81E+01	.14E+02	.81E+01	.14E+02	.81E+01
1.05	.36E+01	.14E+01	.41E+01	.61E+01	.72E+01	1.00E+01	.39E+01	1.00E+01	.39E+01	1.00E+01	.39E+01
1.52	.12E+01	.42E+00	.11E+01	.14E+01	.17E+01	.25E+01	.94E+00	.25E+01	.94E+00	.25E+01	.94E+00
2.05	.43E+00	.15E+00	.33E+00	.52E+00	.60E+00	.80E+00	.27E+00	.80E+00	.27E+00	.80E+00	.27E+00
2.72	.11E+00	.51E-01	.13E+00	.19E+00	.19E+00	.27E+00	.12E+00	.27E+00	.12E+00	.27E+00	.12E+00
3.40	.65E-01	.14E-01	.50E-01	.52E-01	.86E-01	.13E+00	.17E-01	.13E+00	.17E-01	.13E+00	.17E-01
4.02	.34E-01	.11E-01	.33E-01	.47E-01	.54E-01	.10E+00	.25E-01	.10E+00	.25E-01	.10E+00	.25E-01
4.58	.18E-01	.94E-02	.17E-01	.24E-01	.34E-01	.49E-01	.21E-01	.49E-01	.21E-01	.49E-01	.21E-01
5.10	.18E-01	.76E-02	.15E-01	.23E-01	.30E-01	.45E-01	.11E-01	.45E-01	.11E-01	.45E-01	.11E-01
5.60	.90E-02	.13E-02	.51E-02	.71E-02	.11E-01	.21E-01	.43E-02	.21E-01	.43E-02	.21E-01	.43E-02
6.15	.49E-02	.25E-02	.55E-02	.83E-02	.88E-02	.13E-01	.43E-02	.13E-01	.43E-02	.13E-01	.43E-02
6.70	.26E-02	.13E-02	.29E-02	.64E-02	.28E-02	.87E-02	.00E+00	.87E-02	.00E+00	.87E-02	.00E+00

Table B-IV-9 dn/dr (no. cm⁻³ per micron radius) (page 13 of 13)

AEROSOL MEASUREMENTS FOR OPTICAL EXTINCTION PREDICTION

G. L. Trusty and T. H. Cosden

Code 5568

Naval Research Laboratory
Washington, D.C. 20375

This section presents the results of experiments carried out by the Optical Sciences Division of NRL. The experiments were designed to measure aerosol size distributions to be used for calculating extinction coefficients as a function of wavelength.

Particle Measuring Systems' (PMS) particle spectrometers measured the aerosol size distributions. Two of the instruments sat just forward of the bridge at a height of 15 meters from the ocean surface. One was an Active Scattering Aerosol Spectrometer Probe (ASASP), which measures particles with radii in the size range of $0.1 \mu\text{m}$ to $2.0 \mu\text{m}$. The second was a High-Volume Classical Scattering Aerosol Spectrometer Probe (CSASP), which covers a size range of $1.0 \mu\text{m}$ to $15.0 \mu\text{m}$.

As examples of marine atmosphere aerosol data, we have listed the twenty-minute averages of measurements that we made during the times the ship was stopped with the bow into the wind. Table B-IV-10 gives the particle density distribution dN/dR ($\text{cm}^{-3} \mu\text{m}^{-1}$) as a function of the radius of the probe bin centers. For Probe 1 (ASASP) we give results from only the first seven bins. Due to a double-valued sensitivity in the detection response, the data for the larger size ranges of that probe have proven to be inconsistent in many instances. For the purpose of calculating extinction coefficients, we fit a line between the value for the seventh bin of Probe 1 and the first bin of Probe 2 (CSASP).

Table B-IV-11 gives the meteorological parameters and, for four wavelengths, calculated extinction coefficients. (The extinction calculations do not include molecular absorption.)

We have listed the particle probe bin edges in Table B-IV-12 to aid those who may wish to put the aerosol data into a form different from the one we have chosen.

RADIUS --->	0.12	0.15	0.19	0.22	0.26	0.29	0.33	1.22	2.17	3.12	4.07
22 MAY 77 1220	4.00E-03	7.71E-02	4.57E-02	1.17E-02	6.57E-01	5.71E-01	4.25E-01	6.95E-01	5.89E-03	2.53E-04	2.00E-04
1240	4.29E-03	9.43E-02	5.71E-02	1.54E-02	9.43E-01	6.00E-01	3.75E-01	9.58E-01	1.47E-02	5.05E-04	1.05E-04
1300	4.50E-03	1.09E-01	6.57E-02	1.57E-02	8.86E-01	6.57E-01	4.45E-01	7.79E-01	9.79E-03	5.16E-04	1.26E-04
1700	2.74E-03	4.86E-02	3.14E-02	7.43E-01	5.71E-01	3.71E-01	4.95E-01	4.95E-01	1.05E-02	3.26E-04	1.47E-04
1740	2.74E-03	5.43E-02	3.43E-02	8.29E-01	6.00E-01	2.74E-01	2.17E-01	5.37E-01	1.37E-02	5.58E-04	2.00E-04
1800	2.86E-03	5.43E-02	3.71E-02	1.00E-02	6.29E-01	4.00E-01	2.75E-01	6.63E-01	1.26E-02	4.84E-04	1.79E-04
24 MAY 77 120	1.59E-03	2.60E-02	2.11E-02	6.86E-01	4.00E-01	2.06E-01	2.02E-01	2.84E-01	1.04E-02	4.63E-04	1.79E-04
140	1.71E-03	2.43E-02	2.11E-02	8.29E-01	4.00E-01	3.14E-01	1.57E-01	2.95E-01	1.68E-02	6.21E-04	2.63E-04
1250	1.63E-03	2.17E-02	2.20E-02	7.43E-01	5.71E-01	2.83E-01	1.95E-01	3.05E-01	1.47E-02	5.58E-04	2.53E-04
1250	8.57E-03	2.51E-03	1.97E-03	6.29E-02	3.14E-02	1.80E-02	9.50E-01	4.95E-01	4.11E-02	2.11E-03	6.21E-04
26 MAY 77 2100	1.97E-03	1.26E-03	1.31E-03	4.57E-02	2.80E-02	1.40E-02	8.50E-01	4.21E-01	8.63E-04	0.00E-00	0.03E-00
2120	2.03E-03	1.34E-03	1.31E-03	4.86E-02	2.86E-02	1.29E-02	9.50E-01	4.11E-01	1.26E-03	1.16E-05	1.19E-05
2140	1.97E-03	1.29E-03	1.31E-03	4.86E-02	2.37E-02	1.49E-02	9.75E-01	4.11E-01	1.37E-03	1.79E-05	0.00E-00
31 MAY 77 2120	1.40E-03	5.14E-02	3.71E-02	1.03E-02	6.57E-01	2.86E-01	1.65E-01	4.95E-01	1.02E-02	1.05E-04	7.16E-05
1 JUN 77 900	1.97E-03	1.31E-03	1.34E-03	4.86E-02	2.63E-02	1.43E-02	9.25E-01	1.16E-00	1.03E-02	2.53E-04	1.47E-04
920	1.80E-03	1.17E-03	1.17E-03	4.00E-02	2.11E-02	1.09E-02	7.25E-01	1.16E-00	2.00E-02	4.84E-04	1.47E-04
1400	1.17E-03	7.63E-02	8.57E-02	3.14E-02	1.66E-02	9.14E-01	3.75E-01	5.37E-01	7.05E-03	2.84E-04	1.47E-04
1420	1.31E-03	8.29E-02	9.71E-02	3.43E-02	1.91E-02	9.43E-01	5.25E-01	4.42E-01	5.58E-03	8.95E-05	1.58E-04
1440	1.31E-03	8.00E-02	8.29E-02	3.14E-02	1.60E-02	8.29E-01	5.25E-01	4.63E-01	4.53E-03	1.26E-04	7.16E-05
3 JUN 77 1200	4.29E-03	4.57E-03	6.00E-03	2.86E-03	1.83E-03	1.03E-03	6.25E-02	9.16E-01	1.89E-03	5.37E-05	1.79E-05
1400	3.43E-03	2.34E-03	2.20E-03	8.86E-02	4.86E-02	2.54E-02	1.55E-02	7.68E-01	3.89E-03	1.05E-04	3.58E-05
1420	3.14E-03	2.20E-03	2.00E-03	7.14E-02	4.00E-02	1.94E-02	1.12E-02	7.58E-01	2.63E-03	1.26E-04	5.37E-05
1440	2.86E-03	2.11E-03	1.94E-03	6.29E-02	3.14E-02	1.89E-02	1.05E-02	8.63E-01	5.26E-03	1.47E-04	1.47E-04
2120	2.80E-03	1.40E-03	1.49E-03	5.14E-02	2.71E-02	1.54E-02	9.00E-01	8.63E-01	7.89E-03	1.05E-04	3.58E-05
2140	2.34E-03	1.51E-03	1.49E-03	5.43E-02	3.43E-02	1.57E-02	1.07E-02	9.47E-01	7.58E-03	1.47E-04	3.58E-05
2200	2.66E-03	1.86E-03	1.80E-03	6.57E-02	3.71E-02	2.00E-02	1.10E-02	9.16E-01	4.21E-03	7.16E-05	0.00E-00
4 JUN 77 620	1.90E-03	9.14E-02	8.86E-02	3.43E-02	1.86E-02	8.86E-01	5.25E-01	4.74E-01	6.21E-04	3.58E-05	0.00E-00
640	1.74E-03	8.00E-02	8.00E-02	2.71E-02	1.54E-02	6.86E-01	4.50E-01	4.95E-01	6.42E-04	0.00E-00	0.00E-00
700	1.83E-03	6.57E-02	5.14E-02	1.69E-02	1.09E-02	4.57E-01	1.50E-01	4.84E-01	7.47E-04	1.79E-05	0.00E-00
820	2.17E-03	1.09E-03	1.09E-03	3.71E-02	2.23E-02	1.31E-02	6.00E-01	7.89E-01	1.68E-02	5.58E-04	2.84E-04
840	2.11E-03	1.29E-03	1.40E-03	5.43E-02	2.89E-02	1.66E-02	8.50E-01	9.58E-01	1.16E-02	2.84E-04	1.79E-04
900	2.26E-03	1.40E-03	1.46E-03	5.43E-02	2.69E-02	1.57E-02	1.00E-02	9.58E-01	9.05E-03	2.00E-04	1.26E-04
5 JUN 77 20	1.06E-04	7.43E-03	6.00E-03	1.71E-03	7.71E-02	3.43E-02	1.90E-02	1.00E-00	9.16E-03	1.47E-04	5.37E-05
40	6.86E-03	4.86E-03	4.00E-03	1.20E-03	5.14E-02	2.46E-02	1.32E-02	8.63E-01	1.16E-02	2.84E-04	1.47E-04
100	4.86E-03	2.83E-03	2.29E-03	6.00E-02	3.14E-02	1.43E-02	8.75E-01	8.11E-01	1.05E-02	2.84E-04	1.26E-04
440	5.43E-03	2.86E-03	2.46E-03	5.71E-02	2.71E-02	1.14E-02	5.75E-01	7.58E-01	1.47E-02	5.37E-04	2.11E-04
500	5.71E-03	3.43E-03	2.69E-03	6.29E-02	2.54E-02	1.20E-02	7.00E-01	7.05E-01	1.04E-02	3.37E-04	2.00E-04
820	8.00E-03	5.14E-03	4.00E-03	9.71E-02	3.71E-02	1.86E-02	8.75E-01	7.37E-01	9.89E-03	2.00E-04	8.95E-05
840	7.43E-03	4.57E-03	3.71E-03	8.57E-02	3.71E-02	1.60E-02	1.00E-02	7.26E-01	3.37E-03	5.37E-05	0.00E-00
900	7.43E-03	4.57E-03	3.43E-03	8.29E-02	3.14E-02	1.37E-02	7.50E-01	6.42E-01	5.05E-03	7.16E-05	0.00E-00
1400	7.71E-03	5.43E-03	4.29E-03	1.09E-03	4.29E-02	1.89E-02	9.75E-01	7.79E-01	1.37E-02	2.00E-04	1.79E-04
1420	8.57E-03	6.00E-03	4.86E-03	1.14E-03	4.29E-02	1.89E-02	9.75E-01	8.95E-01	9.68E-03	2.84E-04	3.58E-05
1500	8.57E-03	6.00E-03	4.86E-03	1.14E-03	5.14E-02	2.03E-02	1.12E-02	8.74E-01	2.74E-03	1.79E-05	3.58E-05
2200	7.14E-03	3.14E-03	3.43E-03	8.00E-02	3.14E-02	1.34E-02	6.75E-01	4.95E-01	4.84E-03	1.05E-04	0.00E-00
2220	7.14E-03	3.14E-03	2.09E-03	4.57E-02	1.71E-02	7.71E-01	4.25E-01	3.05E-01	8.42E-03	3.37E-04	1.05E-04
2240	7.14E-03	2.83E-03	1.97E-03	4.29E-02	1.60E-02	6.57E-01	3.75E-01	2.63E-01	7.89E-03	2.34E-04	5.37E-05

Table B-IV-10 Twenty-minute averages of dN/dR ($\text{cm}^{-3} \mu\text{m}^{-1}$) versus radius (μm).

RADIUS --->	5.02	5.97	6.92	7.87	8.82	9.77	10.72	11.67	12.62	13.57	14.52	
22 MAY 77	1275	3.58E-04	2.84E-04	8.95E-05	1.79E-04	1.05E-04	7.16E-05	1.26E-04	7.16E-05	5.37E-05	7.16E-05	0.00E 00
	1240	1.58E-04	1.47E-04	8.95E-05	7.16E-05	1.47E-04	1.26E-04	7.16E-05	7.16E-05	7.16E-05	7.16E-05	0.00E 00
	1300	3.58E-05	2.32E-04	8.95E-05	5.37E-05	8.95E-05	1.05E-04	0.00E 00	5.37E-05	7.16E-05	7.16E-05	0.00E 00
	1720	1.58E-04	1.47E-04	1.47E-04	1.05E-04	1.58E-04	7.16E-05	7.16E-05	0.00E 00	3.58E-05	3.58E-05	0.00E 00
	1740	1.26E-04	1.26E-04	1.58E-04	1.47E-04	8.95E-05	5.37E-05	5.37E-05	7.16E-05	0.00E 00	3.58E-05	0.00E 00
	1800	1.58E-04	1.47E-04	7.16E-05	8.95E-05	1.47E-04	8.95E-05	1.79E-04	7.16E-05	1.05E-04	1.47E-04	0.00E 00
24 MAY 77	120	0.00E 00	8.95E-05	3.58E-05	7.16E-05	1.79E-05	1.79E-05	1.79E-05	3.58E-05	0.00E 00	1.79E-05	0.00E 00
	140	8.95E-05	8.95E-05	5.37E-05	3.58E-05	0.00E 00	1.79E-05	0.00E 00	1.79E-05	0.00E 00	0.00E 00	0.00E 00
	200	1.05E-04	5.37E-05	3.58E-05	3.58E-05	1.79E-05	3.58E-05	0.00E 00	0.00E 00	0.00E 00	0.00E 00	0.00E 00
	1220	4.11E-04	2.84E-04	1.26E-04	8.95E-05	8.95E-05	7.16E-05	1.79E-05	0.00E 00	5.37E-05	5.37E-05	0.00E 00
26 MAY 77	2100	0.00E 00	0.00E 00	0.00E 00	0.00E 00	0.00E 00	0.00E 00	0.00E 00	0.00E 00	0.00E 00	0.00E 00	0.00E 00
	2120	0.00E 00	0.00E 00	0.00E 00	0.00E 00	0.00E 00	0.00E 00	0.00E 00	0.00E 00	0.00E 00	0.00E 00	0.00E 00
	2140	0.00E 00	0.00E 00	0.00E 00	0.00E 00	0.00E 00	0.00E 00	0.00E 00	0.00E 00	0.00E 00	0.00E 00	0.00E 00
31 MAY 77	2120	7.16E-05	0.00E 00	0.00E 00	5.37E-05	3.58E-05	0.00E 00	1.79E-05	3.58E-05	0.00E 00	1.79E-05	0.00E 00
1 JUN 77	900	5.37E-05	1.05E-04	1.58E-04	1.26E-04	3.58E-05	3.58E-05	7.16E-05	3.58E-05	1.79E-05	1.79E-05	0.00E 00
	920	2.32E-04	2.00E-04	5.37E-05	5.37E-05	1.05E-04	7.16E-05	5.37E-05	7.16E-05	5.37E-05	5.37E-05	0.00E 00
	1400	1.05E-04	7.16E-05	1.05E-04	1.79E-05	3.58E-05	7.16E-05	3.58E-05	3.58E-05	0.00E 00	0.00E 00	0.00E 00
	1420	1.05E-04	1.05E-04	1.05E-04	3.58E-05	5.37E-05	5.37E-05	1.79E-05	0.00E 00	0.00E 00	0.00E 00	0.00E 00
	1440	1.47E-04	8.95E-05	8.95E-05	5.37E-05	3.58E-05	1.79E-05	0.00E 00	0.00E 00	0.00E 00	0.00E 00	0.00E 00
3 JUN 77	1200	1.79E-05	1.79E-05	0.00E 00	1.79E-05	3.58E-05	0.00E 00	0.00E 00	0.00E 00	0.00E 00	0.00E 00	0.00E 00
	1400	7.16E-05	1.05E-04	5.37E-05	7.16E-05	5.37E-05	3.58E-05	0.00E 00	3.58E-05	5.37E-05	0.00E 00	0.00E 00
	1420	1.79E-05	1.79E-05	1.79E-05	5.37E-05	5.37E-05	3.58E-05	0.00E 00	1.79E-05	0.00E 00	0.00E 00	0.00E 00
	1440	3.58E-05	1.79E-05	1.26E-04	7.16E-05	1.05E-04	5.37E-05	3.58E-05	1.79E-05	0.00E 00	0.00E 00	0.00E 00
	2120	3.58E-05	3.58E-05	0.00E 00	3.58E-05	3.58E-05	3.58E-05	0.00E 00	0.00E 00	0.00E 00	0.00E 00	0.00E 00
	2140	0.00E 00	0.00E 00	1.79E-05	1.79E-05	0.00E 00	0.00E 00	1.79E-05	0.00E 00	0.00E 00	0.00E 00	0.00E 00
	2200	0.00E 00	0.00E 00	3.58E-05	0.00E 00	0.00E 00	1.79E-05	0.00E 00	0.00E 00	0.00E 00	0.00E 00	0.00E 00
4 JUN 77	620	0.00E 00	0.00E 00	0.00E 00	0.00E 00	0.00E 00	0.00E 00	0.00E 00	0.00E 00	0.00E 00	0.00E 00	0.00E 00
	640	0.00E 00	0.00E 00	0.00E 00	0.00E 00	0.00E 00	0.00E 00	0.00E 00	0.00E 00	0.00E 00	0.00E 00	0.00E 00
	700	0.00E 00	0.00E 00	0.00E 00	0.00E 00	0.00E 00	0.00E 00	0.00E 00	0.00E 00	0.00E 00	0.00E 00	0.00E 00
	820	8.95E-05	2.11E-04	7.16E-05	1.26E-04	1.26E-04	1.79E-04	1.79E-05	7.16E-05	0.00E 00	0.00E 00	0.00E 00
	840	1.79E-05	8.95E-05	3.58E-05	5.37E-05	5.37E-05	7.16E-05	5.37E-05	5.37E-05	5.37E-05	5.37E-05	0.00E 00
	900	5.37E-05	3.58E-05	1.79E-05	5.37E-05	0.00E 00	0.00E 00	3.58E-05	1.79E-05	3.58E-05	3.58E-05	0.00E 00
5 JUN 77	20	5.37E-05	0.00E 00	1.79E-05	7.16E-05	5.37E-05	7.16E-05	3.58E-05	0.00E 00	5.37E-05	0.00E 00	0.00E 00
	40	1.79E-04	1.26E-04	1.26E-04	5.37E-05	7.16E-05	5.37E-05	5.37E-05	5.37E-05	5.37E-05	0.00E 00	0.00E 00
	100	1.26E-04	7.16E-05	3.58E-05	3.58E-05	8.95E-05	7.16E-05	5.37E-05	8.95E-05	5.37E-05	5.37E-05	0.00E 00
	440	1.58E-04	1.05E-04	8.95E-05	8.95E-05	8.95E-05	5.37E-05	8.95E-05	3.58E-05	3.58E-05	3.58E-05	0.00E 00
	500	7.16E-05	3.58E-05	3.58E-05	3.58E-05	3.58E-05	5.37E-05	5.37E-05	5.37E-05	5.37E-05	5.37E-05	0.00E 00
	820	1.05E-04	3.58E-05	7.16E-05	0.00E 00	0.00E 00	3.58E-05	3.58E-05	0.00E 00	0.00E 00	0.00E 00	0.00E 00
	840	3.58E-05	0.00E 00	0.00E 00	1.79E-05	3.58E-05	0.00E 00	0.00E 00	1.79E-05	0.00E 00	0.00E 00	0.00E 00
	900	1.79E-05	0.00E 00	0.00E 00	7.16E-05	1.79E-05	0.00E 00	0.00E 00	0.00E 00	0.00E 00	0.00E 00	0.00E 00
	1420	5.37E-05	1.79E-05	2.00E 00	7.16E-05	1.79E-05	1.79E-05	1.79E-05	5.37E-05	0.00E 00	0.00E 00	0.00E 00
	1440	7.16E-05	0.00E 00	5.37E-05	3.58E-05	5.37E-05	0.00E 00	1.79E-05	3.58E-05	1.79E-05	1.79E-05	0.00E 00
	1500	1.79E-05	3.58E-05	3.58E-05	0.00E 00	0.00E 00	0.00E 00	1.79E-05	0.00E 00	0.00E 00	0.00E 00	0.00E 00
	2200	0.00E 00	0.00E 00	0.00E 00	7.16E-05	1.79E-05	0.00E 00	1.79E-05	0.00E 00	0.00E 00	0.00E 00	0.00E 00
	2220	8.95E-05	7.16E-05	1.79E-05	0.00E 00	3.58E-05	5.37E-05	5.37E-05	5.37E-05	1.79E-05	1.79E-05	0.00E 00
	2240	3.58E-05	5.37E-05	3.58E-05	3.58E-05	0.00E 00	3.58E-05	0.00E 00	1.79E-05	0.00E 00	0.00E 00	0.00E 00

Table B-IV-10 Twenty-minute averages of dn/dr ($\text{cm}^{-3}\mu\text{m}^{-1}$) versus radius (μm). (cont'd)

	AT °C	DP °C	WS m/sec	WD deg	WVP corr	RH %	NUM cm ⁻³	VST μm	VSJ cm ⁻³	β-55 km ⁻¹	1.06-1 km ⁻¹	3.80 km ⁻¹	10.0 km ⁻¹
22 MAY 77	12.0	1.7	9.50	210	5.20	56.0	198	14.1	0.029	0.020	0.0041	0.0014	
	12.0	1.7	9.50	210	5.20	57.0	221	16.6	0.033	0.025	0.0054	0.0015	
	13.0	0.6	9.50	200	4.80	53.0	229	14.2	0.032	0.022	0.0043	0.0012	
	17.0	1.3	8.00	190	5.00	53.0	133	9.4	0.018	0.013	0.0031	0.0009	
	17.0	1.7	8.50	190	5.20	54.0	137	9.9	0.019	0.015	0.0033	0.0009	
	18.0	3.0	8.50	200	5.70	61.0	144	14.1	0.023	0.018	0.0042	0.0015	
24 MAY 77	12.0	13.0	3.50	270	11.00	88.0	83	5.7	0.013	0.009	0.0019	0.0005	
	14.0	15.0	3.45	270	11.00	88.0	84	5.6	0.013	0.009	0.0021	0.0005	
	20.0	13.0	3.50	260	11.00	88.0	81	5.8	0.014	0.009	0.0021	0.0005	
	22.0	17.0	14.0	10.50	25.0	12.00	509	21.9	0.059	0.029	0.0058	0.0018	
25 MAY 77	21.0	11.0	3.45	140	10.00	73.0	200	11.1	0.040	0.019	0.0022	0.0007	
	21.0	12.0	3.80	140	10.00	74.0	207	11.4	0.042	0.019	0.0022	0.0007	
	21.0	11.0	3.85	140	10.00	74.0	202	11.4	0.042	0.019	0.0022	0.0007	
31 MAY 77	21.0	12.0	7.50	280	10.00	69.0	90	7.5	0.017	0.013	0.0027	0.0006	
1 JUN 77	9.0	14.0	8.50	190	12.00	76.0	207	20.4	0.057	0.036	0.0060	0.0016	
	9.0	14.0	8.00	180	12.00	75.0	182	20.8	0.050	0.034	0.0065	0.0018	
	14.0	11.0	2.10	280	10.00	61.0	123	10.6	0.028	0.017	0.0030	0.0009	
	14.0	11.0	4.75	220	10.00	62.0	138	10.0	0.030	0.016	0.0025	0.0008	
	14.0	11.0	4.75	190	10.00	63.0	131	9.6	0.029	0.016	0.0025	0.0007	
3 JUN 77	12.0	19.0	7.00	190	18.00	100.0	854	49.1	0.209	0.076	0.0062	0.0030	
	14.0	15.0	10.50	180	13.00	82.0	355	22.2	0.073	0.034	0.0044	0.0017	
	14.0	15.0	10.50	180	13.00	80.0	318	18.5	0.061	0.030	0.0040	0.0013	
	14.0	15.0	10.50	180	13.00	81.0	296	19.8	0.060	0.032	0.0047	0.0015	
	21.0	19.0	9.00	170	13.00	78.0	238	16.7	0.052	0.030	0.0044	0.0012	
	21.0	15.0	8.50	170	13.00	80.0	239	18.1	0.058	0.033	0.0048	0.0012	
	22.0	19.0	9.50	170	13.00	80.0	279	18.6	0.062	0.033	0.0046	0.0012	
4 JUN 77	6.0	15.0	9.00	130	13.00	77.0	155	9.3	0.031	0.017	0.0023	0.0006	
	6.0	15.0	9.00	130	13.00	76.0	141	8.8	0.028	0.016	0.0023	0.0006	
	7.0	15.0	9.00	120	13.00	75.0	119	6.7	0.018	0.012	0.0021	0.0005	
	8.0	15.0	6.00	230	12.00	74.0	187	16.4	0.041	0.025	0.0048	0.0014	
	8.0	15.0	6.50	190	13.00	77.0	215	19.0	0.053	0.032	0.0053	0.0015	
	9.0	15.0	7.50	180	13.00	77.0	227	18.3	0.056	0.033	0.0050	0.0013	
5 JUN 77	20	14.0	10.50	180	12.00	73.0	963	35.3	0.117	0.047	0.0058	0.0023	
	40	14.0	10.50	180	12.00	70.0	636	27.0	0.084	0.037	0.0052	0.0019	
	100	14.0	9.50	190	12.00	71.0	399	20.6	0.057	0.029	0.0047	0.0016	
	440	14.0	6.50	190	12.00	73.0	418	19.0	0.050	0.026	0.0046	0.0015	
	500	14.0	6.50	190	12.00	72.0	459	19.3	0.053	0.026	0.0042	0.0015	
	820	20.0	14.0	7.00	180	12.00	666	23.2	0.069	0.030	0.0043	0.0016	
	840	20.0	14.0	7.00	180	12.00	612	21.2	0.068	0.030	0.0038	0.0014	
	900	20.0	14.0	7.00	170	12.00	595	19.0	0.059	0.025	0.0034	0.0012	
	1420	20.0	15.0	7.50	130	13.00	72.0	19.6	0.056	0.027	0.0044	0.0014	
	1440	20.0	15.0	8.00	150	13.00	684	25.3	0.077	0.034	0.0049	0.0017	
	1500	20.0	15.0	8.00	140	13.00	73.0	26.0	0.084	0.036	0.0045	0.0017	
	2200	20.0	15.0	7.50	140	12.00	72.0	17.2	0.054	0.022	0.0028	0.0011	
	2220	20.0	14.0	7.00	140	12.00	70.0	12.5	0.035	0.014	0.0021	0.0009	
	2400	20.0	14.0	140	12.00	71.0	446	10.9	0.032	0.012	0.0018	0.0007	

Table B-IV-11 Twenty-minute averages of measured and calculated parameter

Table B-IV-12 Bin Edge Locations

(Bin Edges (Radius) for Probes in Table B-IV-10)

Probe 1	Probe 2
μm	μm
0.1	0.75
0.135	1.7
0.17	2.65
0.205	3.6
0.24	4.55
0.275	5.5
0.31	6.45
0.35	7.4
0.4	8.35
0.45	9.3
0.5	10.25
0.55	11.2
0.6	12.15
0.65	13.1
0.7	14.05
0.75	15.0

Marine Observations with the NRL Mobility Size Spectrometer

W. A. Hoppel
Naval Research Laboratory
Washington, D.C. 20375

The mobility analyzer recently developed at NRL was installed on the USNS Hayes for the 1977 EOMET cruise. The mobility analyzer could function either as a size spectrometer or to strip off and transmit particles with a nearly monodisperse size to the TGDC.

When operated as a size spectrometer it could measure the size distribution in the size range from 0.006 to 0.3 μm which is well below the lower detection limit of optical counters. It is this size range which is most important in the formation of fogs and clouds.

In the mobility analyzer the particles are brought to charge equilibrium and then the mobility distribution of the charge fraction is measured. The mobility distribution is then converted to a size distribution using the equilibrium (Boltzmann) charge distribution. The aerosol detection system used with the mobility analyzer was a Pollak expansion cloud chamber. This imposed a rather severe lower limit on the sensitivity of the analyzer. The mobility resolution of the analyzer is determined by the ratio of the flow rate of the sheath air to that of the sample flow; whereas, the signal is inversely proportional to that ratio. In the marine environment the aerosol count is so low that the desired resolution was sacrificed to increase the signal. Even then in the very clean marine environment the number density was too low to give reliable results. As a general rule the total aerosol count had to be above 1000 cm^{-3} to obtain

usable results. (A new aerosol detection system which will greatly improve the sensitivity is under construction.)

Figure C-I-1 shows three size distributions obtained with the mobility analyzer. The Norfolk, VA Harbor size distribution shows many particles in the smaller size range typical of urban air. One hundred miles off the East Coast the very small particles had disappeared presumably by coagulation and the peak in the size distribution was at a radius greater than 2×10^{-6} cm. As will be evident from the CCN data given later, all of these aerosols were active as CCN at supersaturations of 1% or less. The spectrum labeled Mid-Atlantic is the average of several spectra taken in the Mid-Atlantic where the number of particles was so low that any single spectrum was judged to be unreliable.

The dotted lines represent concurrent data taken with the PMS active scattering probe.

The mobility analyzer can also be used to strip off and transmit an aerosol composed of uniform particle size. This mode of operation was used to study the relationship between aerosol size and critical supersaturation necessary for nucleation and droplet growth. The relationship between critical supersaturation S_c and dry radius r_0 is given by

$$S_c = \left(\frac{4}{27} \frac{A^3}{B_0 r_0^3} \right)^{1/2} \quad (1)$$

where A is a constant containing the surface tension and B_0 is given by

$$B_0 = \frac{i \epsilon \rho_d M}{M_s \rho_w} \quad (2)$$

where i is the vant Hoff factor, ϵ the fraction of soluble material, ρ_d the density of the dry particle, and ρ_w the density of water.

Because of the small aerosol concentrations encountered on the ship-board measurements the size interval of the transmitted aerosol was increased to obtain a detectable number of nucleated droplets in the TGDC. This of course decreased the resolution with which the relation between dry size and critical supersaturation could be measured. Knowing the relationship between dry size r_0 and critical supersaturation S_c makes it possible to determine B_0 in Eq. (1). Values of B_0 for three periods were determined. These were taken in Norfolk, VA harbor, 100 miles off the New Jersey coast, and in the Mediterranean and had the values of 0.28 ± 0.04 , 0.40 ± 0.09 , and 0.143 respectively. The first two were taken immediately after the corresponding size distributions shown in Figure C-I-1 and the stated uncertainty in these values is a result of the large size interval used. The treatment of the Mediterranean data is discussed in more detail in Hoppel, Gerber and Wojciechowski (1977) and is the average of six runs during a period when the size distribution remained nearly constant. The transmitted size was chosen to be near the peak in the distribution and hence were not the same in each case. The transmitted size intervals were $0.022-0.0318 \mu\text{m}$, $0.0318-0.0468 \mu\text{m}$, and $0.0468-0.070 \mu\text{m}$ for the Norfolk, New Jersey Coast and Mediterranean data, respectively. These values of B_0 should not be taken to be constants at any given location but variables which also depend upon air mass history.

The equation which gives the relationship between the saturation ratio S and equilibrium size can be written in terms of B_0 in the following form:

$$S = \text{Exp} \left(\frac{A}{r} \right) \cdot \left[1 + \frac{B_0 r_d^3}{\frac{\rho'}{\rho_w} \left[r^3 - r_d^3 (1 - \epsilon) - \epsilon \frac{\rho_d}{\rho'} r_d^3 \right]} \right]^{-1} \quad (3)$$

It is clear from Eq. (3) that in addition to B_0 , ϵ and ρ_d must also be known to obtain S as a function of r . However if ρ' is also expressed in terms of ϵ , ρ_w , and ρ_d and if the sensitivity of Eq. (3) to various values of ϵ and ρ_d is studied numerically, it is found that Eq. (3) is very insensitive to ϵ and ρ_d over ranges of these variables expected in atmosphere aerosols. This means that using an experimental value of B_0 in Eq. (3) together with any reasonable value of ϵ and ρ_d will give the relative humidity dependence of the equilibrium size. This dependence for the three different values of B_0 is shown in Figure C-I-2. This relationship should hold for relative humidities above the deliquescent point of the particular solute in the aerosol and thus the curves in Figure C-I-2 are only valid for R.H. above the deliquescent point.

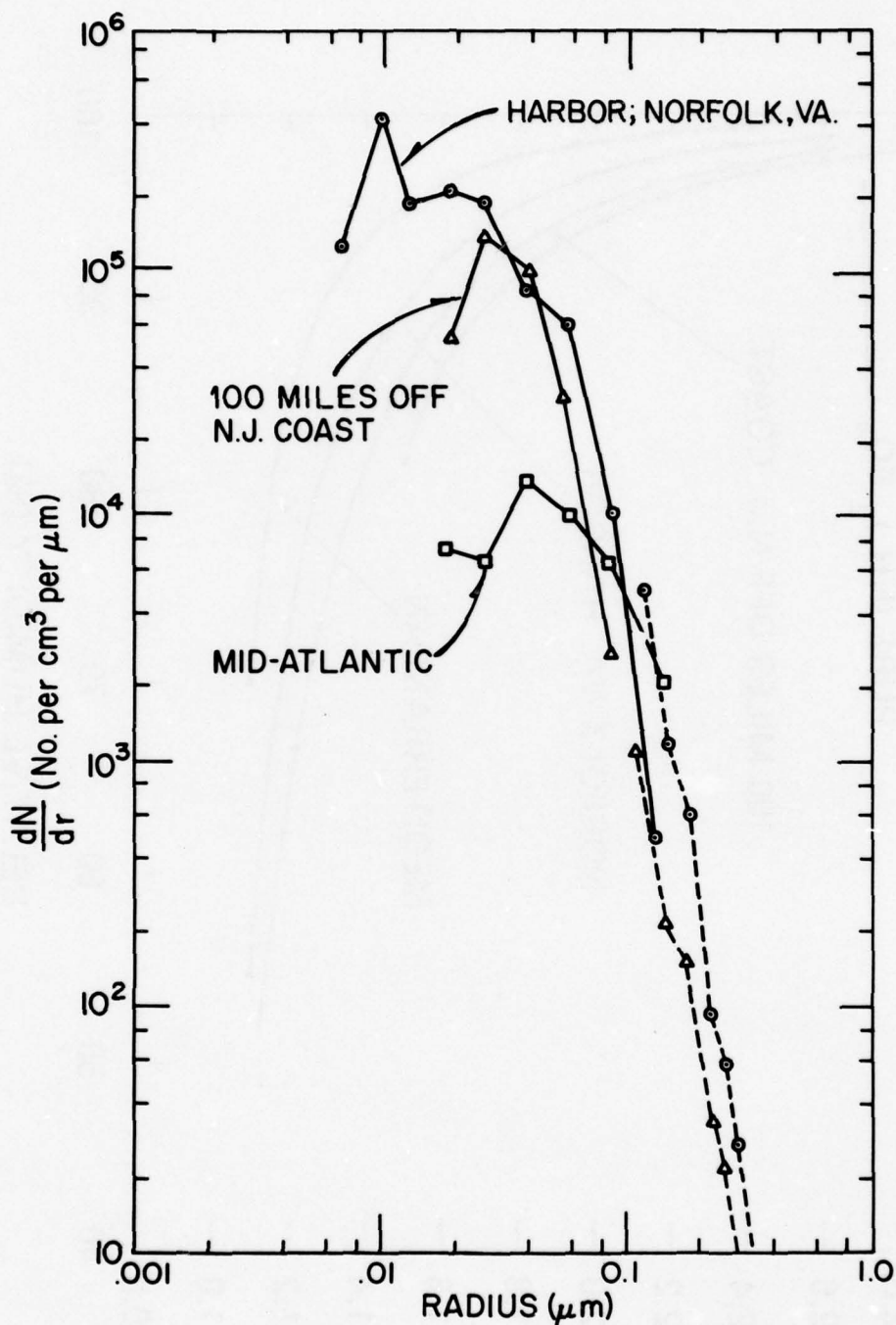


Fig. (C-I-1) Size distribution of aerosol at Norfolk, NJ coast, mid-Atlantic, using NRL mobility analyzer.

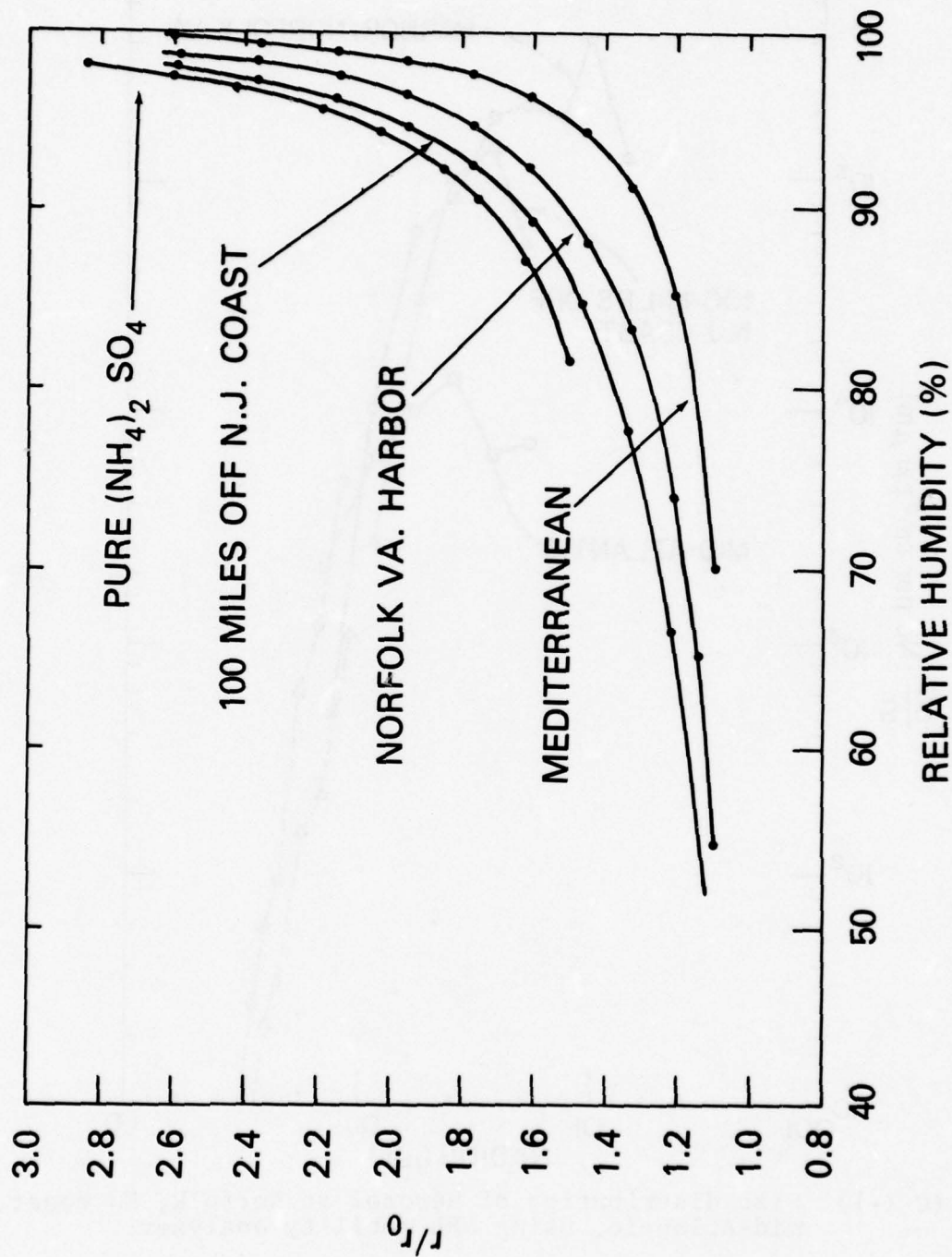


Fig. (C-I-2) $\frac{r}{r_o}$ vs. RH (%) at Norfolk, NJ coast, Mediterranean.

SHIPBOARD MEASUREMENTS WITH A PORTABLE TRANSMISSOMETER

H. Gerber and R. Stilling

Naval Research Laboratory
Washington, D.C. 20375

1. INTRODUCTION

The purpose of our participation in the 1977 EOMET cruise of the USNS Hayes was to test the feasibility of using a portable transmissometer on-board a ship at sea. If proved successful this transmissometer can become a valuable new tool for obtaining maritime transmittance measurements which are presently very scarce. This lack of data is due to the fact that existing transmissometers require a baseline of about 1 km which is obviously incompatible with ships.

Transmittances with a resolution of 0.1% over a 20 meter folded path have been measured in laboratory aerosol with the new transmissometer. This extraordinary improvement over the accuracy of long-baseline instruments is due to several unique features which will be discussed. The 0.1% accuracy reflects a laboratory environment which is amenable to precise optical measurements. Since such an environment is improbable on a ship, this accuracy will deteriorate. It was the goal of our participation on the 1977 cruise to discover the influence of wave-induced ship's motion, vibration due to the ship's machinery, and temperature variations on the accuracy of the new transmissometer. The following includes a brief discussion of the new technique, a list of the collected data, and a summary of the results. A detailed account of the new system and its performance on the cruise are given elsewhere (Gerber, 1978).

2. INSTRUMENTATION

A schematic of the transmission cell is shown in Figure C-II-1. A HeNe laser beam is passed through a beam splitter. One portion of the beam steps in a sawtooth fashion through the 2 meter cell for a total pathlength of about 20 meters, upon leaving the cell it passes through a chopper before its intensity is measured by a sensor. The second portion of the beam is routed through the same chopper and to the same sensor without passing through the cell. Holes on the chopper are so arranged that the sensor is illuminated alternately and at equal intervals by the two beams. In this unique arrangement a relative difference measurement of the light extinction due to aerosols in the cell can be made which is independent of sensor-sensitivity and laser-intensity drift.

Figure C-II-2 shows a block diagram of the phase-locked demultiplexer and pulse conditioner which provides analog outputs of the light extinction ΔI due to the aerosols, and the initial intensity I_0 of the beam. The accuracy of this circuit, which resolves ΔI to 0.01% of I_0 , is limited by A_3 .

The other sensor attached to the middle of the cell has a precise cosine response and measures the flux of light scattered by the aerosol particles in the cell. Since the two sensors provide extinction and scattering measurements in the same volume of aerosol, an in-situ measurement of the particles' absorption coefficient is provided.

Under most atmospheric conditions the extinction of light by aerosols in the cell would be insufficient to give an accurate measurement. The

measurements in the cell only became possible by filling the cell with concentrated ambient aerosol particles. A centrifugal aerosol concentrator enhances the concentration and the aerosol's extinction and scattering coefficients in the cell by a factor of about 20. It is, of course, a requirement of the concentrator to enhance the particle volume density without changing the relative particle size distribution, since otherwise the optical parameters of the aerosol will not be scaled up properly. If this is done accurately, the effective pathlength in the cell increases to 400 meters. Figure C-II-3 shows the position of the concentrator with respect to the cell.

Systems are shown in Figure C-II-3 which flow aerosol, filtered air, and Freon through the cell. During operation the cell is cycled with filtered air and concentrate in order that the influence of the beam-steering optics in the system can be subtracted from the measured aerosol optical properties. The Freon flow is used to calibrate the cosine sensor with a known scattering coefficient. The cell was suspended with a shock-mounted universal joint from a ceiling beam in the ship in order that the influence of the ship's motions on the measurements were minimized. The vertical positioning of the cell also minimized sedimentation losses in the cell.

3. DATA

The data collected during the cruise is summarized in Table C-II-1. Each of the values of ΔI and I_0 consist of 24 point averages of 5 minute measurement intervals. The extinction coefficient calculated from ΔI and

I_0 is given by b , and the coefficient of variation of b is given by $100 \times s(b)/b$ where $s(b)$ is the sample standard deviation of b . The ratio of F/F_c is the average of 24 point values of the flux measured by the cosine sensor divided by the Freon calibration flux, and the aerosol scattering coefficient measured in the cell is given by b_s . The scattering coefficient $b_s(\text{MRI})$ measured with the MRI integrating nephelometer is also given. Comparisons of b_s and $b_s(\text{MRI})$ must consider wavelength compensation, since b_s is for $\lambda = 6328 \text{ \AA}$ and $b_s(\text{MRI})$ is for a quasi-photopic source centered at 5250 \AA . The final column gives values of the aerosol's absorption coefficient b_a divided by b . The occasions during the cruise when aerosol generated by the ship influenced the measurements are not noted. Measurements of the aerosol size distribution in the ambient air and in the concentrate were made, a particle-size bandpass of somewhat more than one order of magnitude and concentration enhancement of about a factor of 20 were found.

4. RESULTS AND CONCLUSIONS

- 1) Transmittance measurements at 6328 \AA were made with a mean resolution of $\pm 0.16\%$ during the 1977 EOMET cruise. This corresponds to a resolution in aerosol-optical-depth measurements in the cell of $\pm 1.58 \times 10^{-3}$.
- 2) The deterioration of the transmittance measurements during the cruise from the laboratory measurements were due to mechanical weaknesses in the cell. Flexing of the cell due to ambient-cell

temperature differences and longitudinal stresses from wave-induced ship's motion caused beam wander on the transmitted-light sensor.

- 3) An improved cell could better the resolution of the transmittance measurements by a factor of 10.
- 4) It may be feasible with the present technique to measure infrared extinction by aerosols for wavelengths as long as $10.6 \mu\text{m}$ under hazy atmospheric conditions.
- 5) The reciprocal integrating nephelometer (cosine sensor) used on the cell is a practical alternative to the standard nephelometer.
- 6) The aerosol concentrator produces a particle-size bandpass which scales up the values of the scattering and extinction coefficients (at 6328 \AA) measured in the cell from values in the atmosphere with an uncertainty of about 10%.
- 7) The combination of extinction and scattering measurements in the same aerosol provides a unique means of measuring the particles' absorption coefficient in real time.

5. ACKNOWLEDGMENT

The data for $b_s(\text{MRI})$ was collected by Dr. James Fitzgerald.

6. REFERENCE

Gerber, H., 1978: The feasibility of shipboard laser-attenuation measurements with a portable transmissometer. NRL Report. In press.

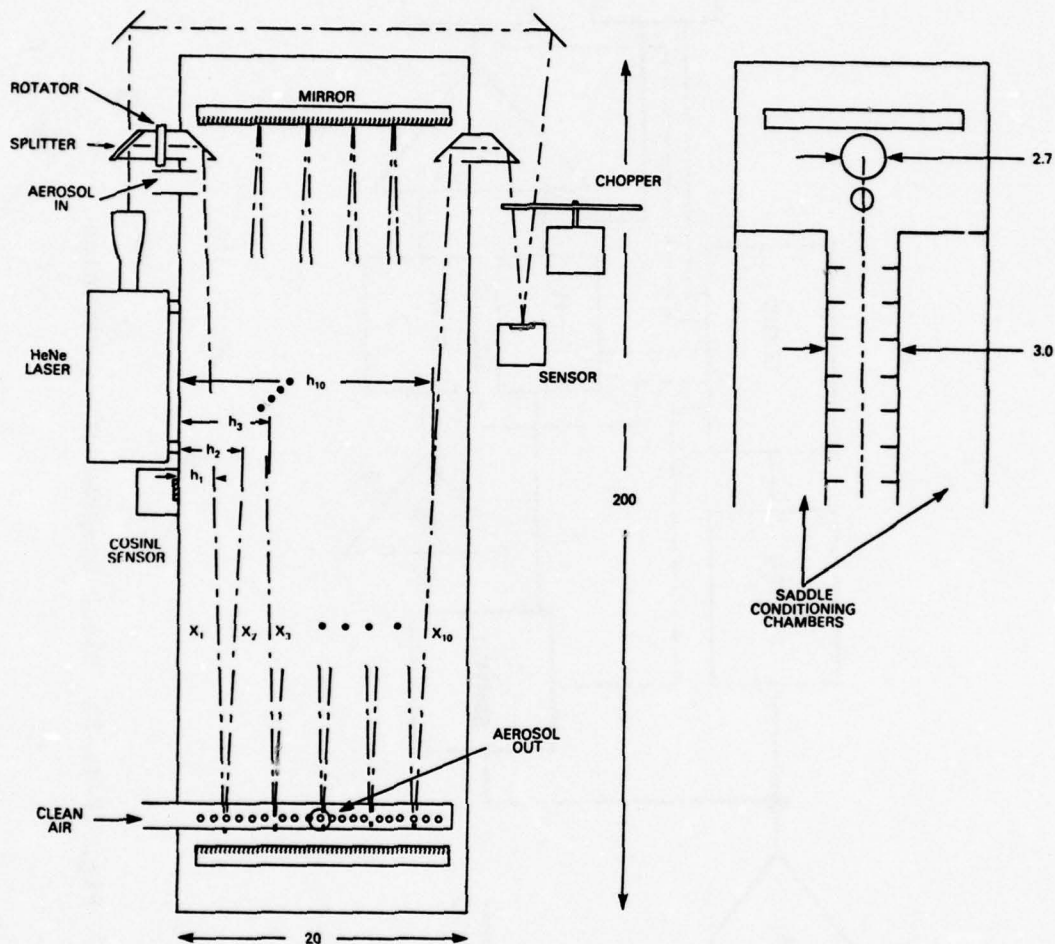


Fig. (C-II-1) Schematic of portable transmission cell, showing the laser beam path, location of the optics and dimensions (cm).

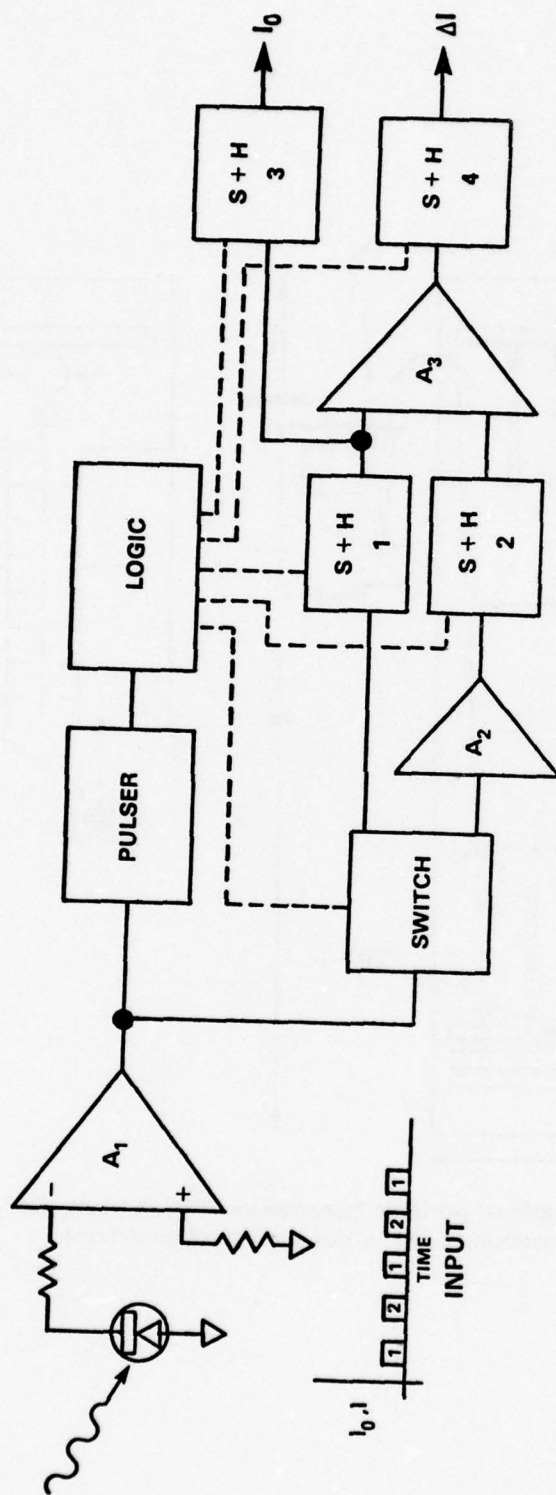


Fig. (C-II-2) Block diagram of electronics

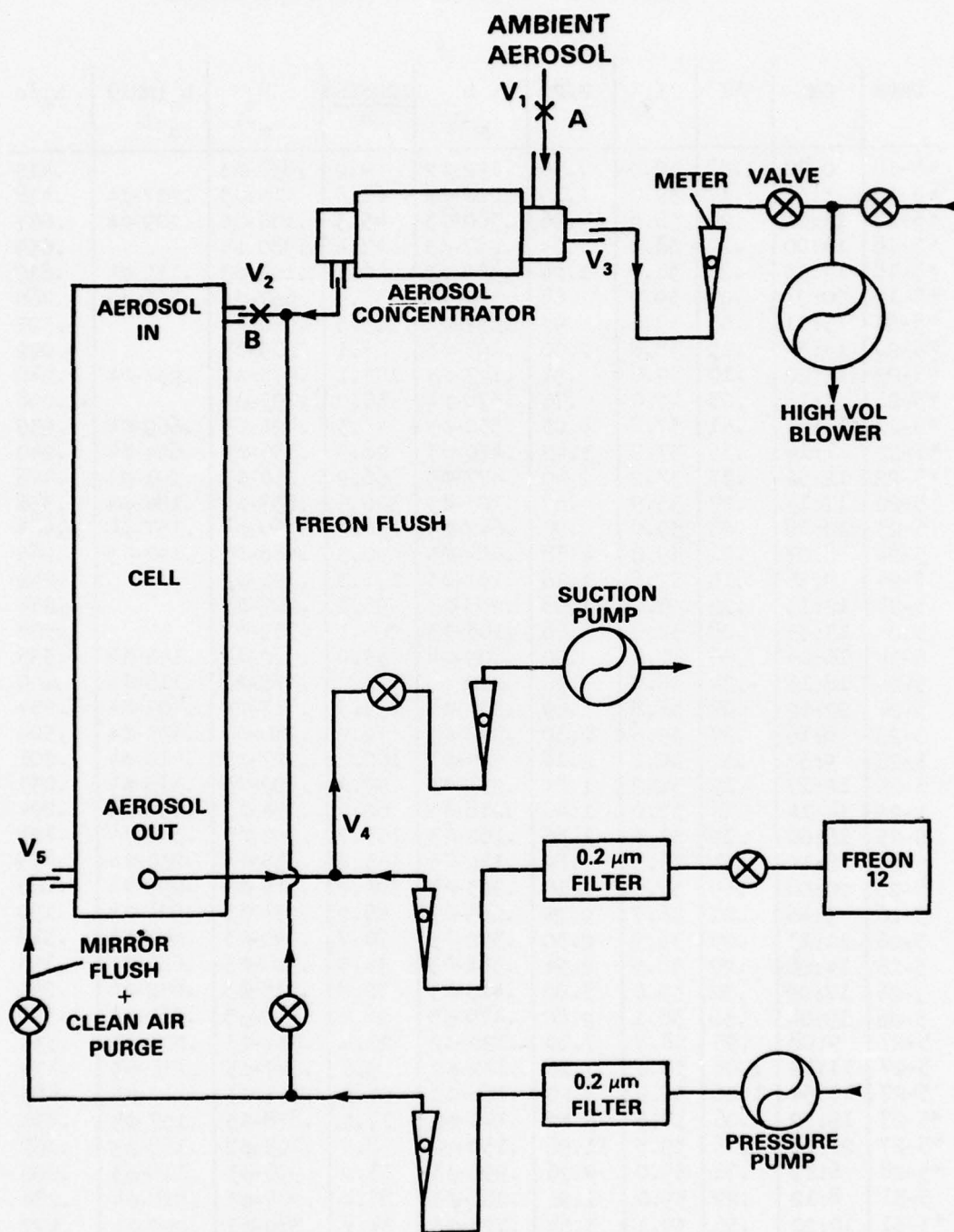


Fig. (C-II-3) Aerosol and gas-flow system used with transmission cell.

Table C-II-1. Aerosol Optical parameters Measured During the 1977 EOMET Cruise of the USNS HAYES

Date	GMT	ΔI	I_o	F/F_c	b m^{-1}	$100s(b)$ b	b_s m^{-1}	$b_s(MRI)$ m^{-1}	b_a/b
*5-18	0:30	1.08	39.0	7.96	.142- ϕ 2	9.2	.830- ϕ 3		.415
*5-18	13:51	.17	39.0	1.10	.220- ϕ 3	61.8	.115- ϕ 3	.227- ϕ 4	.478
*5-18	13:61	.23	38.8	.96	.300- ϕ 3	45.3	.100- ϕ 3	.209- ϕ 4	.667
*5-18	14:00	.22	38.8	.94	.287- ϕ 3	47.4	.980- ϕ 4		.659
*5-18	14:13	.26	38.8	1.24	.339- ϕ 3	40.1	.129- ϕ 3	.155- ϕ 4	.619
*5-19	20:21	.03	39.9	.64	.379- ϕ 4	35.9	.667- ϕ 4	.163- ϕ 4	-.760
*5-20	13:01	.05	39.6	.92	.637- ϕ 4	213.5	.960- ϕ 4		-.507
*5-20	13:34	.15	38.8	2.00	.195- ϕ 3	67.1	.209- ϕ 3		-.072
*5-20	14:20	.10	39.6	.91	.127- ϕ 3	107.1	.975- ϕ 4	.237- ϕ 4	.246
*5-21	1:16	.03	40.0	.76	.378- ϕ 4	36.0	.793- ϕ 4		-1.098
*5-22	11:03	.41	37.8	4.03	.550- ϕ 3	45.3	.421- ϕ 3	.669- ϕ 4	.235
*5-22	11:14	.35	37.7	3.42	.470- ϕ 3	28.9	.356- ϕ 3	.654- ϕ 4	.240
*5-22	12:32	.35	37.2	2.40	.477- ϕ 3	66.2	.250- ϕ 3	.291- ϕ 4	.476
5-22	17:14	.07	35.9	.67	.105- ϕ 3	300.6	.697- ϕ 4	.184- ϕ 4	.336
5-23	10:48	.05	39.0	.92	.647- ϕ 4	210.2	.960- ϕ 4	.157- ϕ 4	-.484
5-24	8:07	.51	39.0	4.68	.664- ϕ 3	20.5	.488- ϕ 3	.120- ϕ 3	.265
5-24	9:56	.13	37.6	1.16	.161- ϕ 3	170.3	.122- ϕ 3		.242
5-24	12:13	.22	39.0	1.98	.285- ϕ 3	96.2	.207- ϕ 3		.274
5-24	13:53	.08	39.0	.68	.103- ϕ 3	266.1	.709- ϕ 4		.308
5-24	16:04	-.06	37.4	.50	.809- ϕ 4	33.9	.522- ϕ 4	.140- ϕ 4	.355
5-24	18:16	-.04	36.9	.36	≈ 0		.375- ϕ 4	.118- ϕ 4	≈ 0
5-24	22:32	.07	37.8	.69	.934- ϕ 4	293.5	.715- ϕ 4	.205- ϕ 4	.234
5-25	8:16	.27	39.6	2.30	.345- ϕ 3	72.2	.240- ϕ 3	.433- ϕ 4	.304
5-25	9:57	.22	39.1	2.18	.284- ϕ 3	100.4	.227- ϕ 3	.418- ϕ 4	.201
5-25	12:17	.19	38.2	1.84	.251- ϕ 3	99.2	.192- ϕ 3	.375- ϕ 4	.235
5-25	14:14	.16	37.0	1.48	.218- ϕ 3	62.4	.154- ϕ 3	.439- ϕ 4	.294
5-25	16:00	.12	37.3	1.36	.162- ϕ 3	153.7	.142- ϕ 3	.382- ϕ 4	.123
5-25	18:19	.11	36.5	.82	.152- ϕ 3	163.8	.855- ϕ 4	.234- ϕ 4	.439
5-25	20:08	.09	37.0	1.10	.123- ϕ 3	202.4	.115- ϕ 3	.295- ϕ 4	.065
5-26	9:46	.21	36.7	2.24	.289- ϕ 3	86.2	.234- ϕ 3	.628- ϕ 4	.190
5-26	11:13	.25	35.9	2.30	.352- ϕ 3	70.7	.240- ϕ 3	.607- ϕ 4	.318
5-26	14:28	.29	38.5	2.94	.381- ϕ 3	34.3	.307- ϕ 3	.686- ϕ 4	.194
5-26	17:09	.32	39.0	3.02	.415- ϕ 3	32.8	.315- ϕ 3	.632- ϕ 4	.241
5-26	19:04	.36	38.1	2.80	.479- ϕ 3	28.4	.292- ϕ 3	.582- ϕ 4	.390
5-27	9:08	.93	38.8	7.80	.122- ϕ 2	20.4	.814- ϕ 3	.203- ϕ 3	.333
5-27	11:42	1.06	38.2	7.16	.142- ϕ 2	9.6	.747- ϕ 3	.216- ϕ 3	.474
5-27	13:54	1.26	38.9	8.20	.166- ϕ 2	28.2	.855- ϕ 3	.212- ϕ 3	.485
*5-27	19:52	1.06	37.5	8.42	.145- ϕ 2	17.2	.878- ϕ 3	.157- ϕ 3	.394
*5-27	22:21	1.16	39.5	11.96	.150- ϕ 2	8.7	.125- ϕ 2	.168- ϕ 3	.167
*5-28	6:19	.76	39.0	9.26	.992- ϕ 3	13.2	.996- ϕ 3	.116- ϕ 3	.000
5-31	8:12	.22	39.0	1.96	.285- ϕ 3	87.4	.204- ϕ 3	.918- ϕ 4	.284
*5-31	10:20	.56	39.1	3.64	.727- ϕ 3	34.2	.380- ϕ 3	.229- ϕ 4	.477
*5-31	12:01	.51	38.5	4.14	.672- ϕ 3	47.0	.432- ϕ 3	.362- ϕ 4	.357

* measurement influenced by ship-generated aerosols

Table C-II-1. Aerosol Optical parameters Measured During the 1977 EOMET Cruise of the USNS HAYES

*5-31	13:57	.38	39.0	3.60	.494- ϕ 3	50.4	.375- ϕ 3	.454- ϕ 4	.241
*5-31	16:05	.53	38.7	5.50	.695- ϕ 3	39.4	.574- ϕ 3	.380- ϕ 4	.174
*5-31	18:19	.35	38.8	4.70	.457- ϕ 3	60.0	.490- ϕ 3	.508- ϕ 4	-.072
*5-31	19:40	.42	38.6	5.20	.552- ϕ 3	49.7	.542- ϕ 3	.462- ϕ 4	.018
*5-31	21:53	.25	38.7	3.20	.327- ϕ 3	76.1	.334- ϕ 3	.389- ϕ 4	-.021
*6-1	4:11	.52	39.3	6.20	.671- ϕ 3	37.1	.647- ϕ 3	.987- ϕ 4	.065
*6-1	6:21	1.06	39.2	10.40	.138- ϕ 2	18.0	.108- ϕ 2	.101- ϕ 3	.268
*6-1	9:27	.24	38.4	3.81	.316- ϕ 3	43.0	.313- ϕ 3	.397- ϕ 4	.010
*6-1	12:04	1.00	38.4	10.20	.133- ϕ 2	20.6	.106- ϕ 2	.523- ϕ 4	.203
*6-1	14:08	.83	38.5	8.40	.110- ϕ 2	12.4	.876- ϕ 3	.504- ϕ 4	.204
*6-1	14:45	1.09	38.9	10.26	.143- ϕ 2	9.5	.107- ϕ 2	.468- ϕ 4	.252
6-1	19:45	.35	37.6	3.80	.471- ϕ 3	58.2	.396- ϕ 3	.537- ϕ 4	.159
6-2	4:19	.49	37.5	6.00	.663- ϕ 3	37.6	.626- ϕ 3	.655- ϕ 4	.056
6-2	5:23	.56	37.0	7.38	.769- ϕ 3	32.3	.759- ϕ 3	.771- ϕ 4	.013
6-2	6:25	.52	37.1	6.80	.712- ϕ 3	35.0	.709- ϕ 3	.724- ϕ 4	.000
6-2	8:12	.60	37.0	7.08	.741- ϕ 3	33.6	.738- ϕ 3	.706- ϕ 4	.004
6-2	10:07	.55	37.7	6.28	.741- ϕ 3	37.0	.655- ϕ 3	.710- ϕ 4	.116
6-2	11:58	.49	36.2	6.00	.687- ϕ 3	36.2	.626- ϕ 3	.735- ϕ 4	.089
6-2	14:04	.60	36.0	7.40	.847- ϕ 3	29.4	.772- ϕ 3	.613- ϕ 4	.089
6-2	16:25	.55	36.2	6.56	.772- ϕ 3	35.5	.684- ϕ 3	.553- ϕ 4	.114
6-2	18:04	.53	36.3	6.06	.741- ϕ 3	37.0	.632- ϕ 3	.571- ϕ 4	.147
6-2	20:33	.55	38.5	5.46	.725- ϕ 3	37.8	.569- ϕ 3	.899- ϕ 4	.215
6-2	22:22	.57	37.4	5.90	.774- ϕ 3	32.2	.615- ϕ 3	.919- ϕ 4	.205
6-2	23:11	.15	37.4	1.70	.203- ϕ 3	135.0	.177- ϕ 3	.344- ϕ 4	.128
6-3	4:10	.61	38.6	7.20	.803- ϕ 3	34.1	.751- ϕ 3	.101- ϕ 3	.065
6-3	6:13	.60	38.3	6.40	.796- ϕ 3	35.6	.668- ϕ 3	.865- ϕ 4	.161
6-3	7:56	.57	37.7	6.10	.768- ϕ 3	17.7	.636- ϕ 3	.820- ϕ 4	.171
6-3	10:02	1.10	38.3	10.76	.147- ϕ 2	16.9	.112- ϕ 2	.133- ϕ 3	.236
6-3	12:02	.92	38.1	9.40	.123- ϕ 2	10.6	.980- ϕ 3	.129- ϕ 3	.205
6-3	14:03	.31	38.1	2.72	.412- ϕ 3	33.0	.284- ϕ 3	.509- ϕ 4	.311
6-3	21:21	.25	37.4	2.96	.338- ϕ 3	73.7	.352- ϕ 3	.485- ϕ 4	-.041
6-4	8:21	.25	36.9	2.82	.343- ϕ 3	72.6	.294- ϕ 3	.550- ϕ 4	.143
6-4	14:16	.32	35.7	3.58	.454- ϕ 3	54.8	.373- ϕ 3	.697- ϕ 4	.178
6-4	20:19	.67	35.2	7.44	.696- ϕ 3	14.0	.776- ϕ 3	.140- ϕ 3	.199
6-5	0:14	.64	38.0	7.56	.856- ϕ 3	15.9	.789- ϕ 3	.140- ϕ 3	.078
6-5	4:35	.52	39.1	4.90	.675- ϕ 3	36.9	.511- ϕ 3	.970- ϕ 4	.243
6-5	8:14	.66	39.9	6.44	.841- ϕ 3	16.2	.672- ϕ 3	.125- ϕ 3	.201
6-5	14:28	.58	37.5	4.78	.786- ϕ 3	17.3	.688- ϕ 3	.109- ϕ 3	.125
6-5	18:22	.47	36.9	5.06	.646- ϕ 3	42.4	.528- ϕ 3	.970- ϕ 4	.183
6-5	20:10	.50	37.0	4.74	.686- ϕ 3	40.0	.494- ϕ 3	.987- ϕ 4	.280
6-5	20:35	.68	36.9	6.26	.938- ϕ 3	29.2	.653- ϕ 3	.123- ϕ 3	.304
6-5	20:54	.67	37.1	6.24	.919- ϕ 3	29.8	.651- ϕ 3	.118- ϕ 3	.292
6-5	23:25	.24	36.3	2.20	.334- ϕ 3	82.1	.229- ϕ 3	.491- ϕ 4	.314
6-6	4:14	.38	37.0	3.46	.520- ϕ 3	52.7	.361- ϕ 3	.808- ϕ 4	.306
6-6	6:31	.40	37.3	3.50	.544- ϕ 3	50.4	.365- ϕ 3	.817- ϕ 4	.329
6-6	10:10	.70	37.1	5.28	.960- ϕ 3	25.9	.551- ϕ 3		.426

RAMAN LIDAR MEASUREMENT OF ATMOSPHERIC
WATER VAPOR PROFILES DURING THE
MAY-JUNE 1977 USNS HAYES
ATLANTIC/MEDITERRANEAN CRUISE

by

Donald A. Leonard and Bernard Caputo
Computer Genetics Corporation, Wakefield, Massachusetts 01880

Stuart Gathman
Naval Research Laboratory, Washington, D.C. 20375

1. Introduction

The Computer Genetics Corporation (CGC) participated in the May-June 1977 EOMET cruise of the USNS Hayes for the purpose of operating a Raman lidar system to experimentally measure vertical profiles of atmospheric water vapor, temperature and visibility in the marine boundary layer. This note reports some of the water vapor results.

The basic Raman method for atmospheric humidity profile measurement has been well explored by both laboratory research and field tests. Consequently this technique requires no further feasibility testing and has also been investigated with sufficient thoroughness so that successful field systems such as that reported on here can be designed. The principles of atmospheric humidity profile measurements by Raman scatter have been described by Melfi (1969), Derr and Little (1970) and by Strauch, et al. (1972).

The primary result of this experiment was to further advance the development of remote water vapor instrumentation and provide for the first

time a well documented field demonstration of a shipboard, semi-ruggedized, single ended remote water vapor measurement tool under several weeks of typical marine operational environments.

2. Description of Raman Lidar Equipment

The atmospheric Raman spectra were obtained using a Raman lidar system originally designed and used as a single ended transmissometer (see Leonard and Caputo, 1974) and recently modified by the authors to measure atmospheric profiles of water vapor and temperature.

A block diagram of the equipment is shown in Figure C-III-1. The laser source was a pulsed nitrogen laser operating at 337.1 nanometers and producing pulses of 100 kilowatts peak power with an effective pulse duration of 10 nanoseconds at a pulse repetition rate of 500 Hertz. The nitrogen laser uses an unstable resonator cavity. The output from the laser is passed through an interference filter which passes the 337.1 nm laser line with high efficiency but blocks spontaneous emission occurring in the laser gas discharge in the Raman spectral region.

The photons collected by the receiver optics are passed through a double 1/4 meter focal length scanning spectrometer having a 0.5 nanometer spectral resolution. The wavelength scanning of the spectrometer is controlled by the computer. The function of the spectrometer is to produce a spectral scan of the Raman air spectrum with sufficient resolution so that the O_2 , N_2 and H_2O Raman lines can be resolved and the background measured. A 3-channel filter wheel assembly was also employed so that the peak signals of the O_2 , N_2 and H_2O Raman lines could be detected with higher efficiency.

The Raman photon output from the spectrometer is detected by an RCA 8850 photomultiplier. The Raman photoelectron signal and a gate pulse suitably synchronized and delayed with respect to the laser firing are combined in ten (10) separate coincidence gates, the output from which are recorded using direct memory access (DMA) techniques with a Data General NOVA 1220 computer. The number of pulses occurring during the same data taking interval is also recorded. The ratio of the Raman photons to laser pulses recorded over a given time interval is the basic data obtained. The ten coincidence gates provide Raman data at ten separate locations.

The data taking is fully automated. The computer can be directed through the teletype (TTY) to specify the number of laser pulses over which to record data at each wavelength and the maximum and minimum wavelengths and the wavelength increments of each spectral scan. The data obtained are printed on the TTY in tabular form and also recorded on cassettes.

3. Data Obtained

Experiments were performed with both the 1/4-m scanning spectrometer and the 3-channel filter wheel. Data were obtained as follows:

3.1 Spectral Scan of O_2 , N_2 and H_2O Raman Lines.

The purpose of the spectral scans with the 1/4 meter SPEX double spectrometer of the O_2 , N_2 and H_2O Raman lines is to determine the signal-to-noise ratio of the atmospheric Raman lines with respect to the background spectrum both ambient and laser induced. The spectrum plotted on a

logarithmic scale in Figure C-III-2 shows typical raw laser induced data obtained from the atmosphere at wavelengths between 345 and 390 nanometers with 1.0 nanometer resolution. The wavelength scale is uncalibrated and exhibits a bias of about 3 nm, i.e. the exact wavelength of the N_2 line is 365.8 nm. For this data set the range resolution was 10 meters and the altitude was 100 meters. A measurement time of 15 seconds per data point was used. As the spectrum of Figure C-III-2 shows the O_2 , N_2 and H_2O Raman lines appear typically as well resolved spectral lines with the basic signal-to-noise ratios of 100, 250 and 20 respectively. The noise level is essentially the dark current of the photomultiplier.

The conclusion to be drawn is that the Raman spectrum of the atmosphere in the cases investigated is free of laser induced interference and that the relative concentrations of O_2 , N_2 and H_2O may be determined by simply measuring the peak intensity at each spectral line.

3.2 Profiles of H_2O/N_2 in the Marine Boundary Layer.

Atmospheric profiles of the H_2O/N_2 Raman line ratio were obtained by using interference filters in place of the 1/4-meter double spectrometer. Due to the larger optical efficiency of the filters relative to the spectrometer higher signal levels were obtained and thus measurements at higher altitudes were possible. The results of the spectral scans, discussed in Section 3.1 above, justify the use of filters.

Data was normally obtained simultaneously at 10 distinct and separate altitudes. The Raman return was sequentially sampled at the O_2 , N_2 and H_2O Raman line positions using the filters. The ratio of the H_2O to the N_2

Raman returns was used to determine the H_2O partial pressure assuming that the N_2 partial pressure corresponded to standard atmospheric conditions. This normalization of the H_2O signal to the N_2 signal effectively cancelled out effects due to variable atmospheric transmission, laser power fluctuations and changes in the overall photoelectric efficiency of the transmitter/receiver system and gave the H_2O to N_2 mixing ratio directly. The O_2 Raman line was also monitored and the ratio of the O_2 to N_2 Raman signals was checked as an internal system redundancy procedure.

As typical of the data obtained, Figures C-III-3, -4, -5, and -6 show as a function of altitude the partial pressure of water vapor in the atmosphere in millibars (mb) as measured by the CGC Raman lidar on the Hayes. These marine boundary layer water vapor profiles are representative of both the cold Atlantic waters off the northeastern coast of North America as well as the warmer eastern Atlantic and Mediterranean type waters.

In situ measurements of water vapor profiles in the marine boundary layer throughout the entire cruise were obtained by means of a series of vertical soundings of atmospheric pressure altitude, dry air temperature and wet bulb temperature using a kite-balloon (see Gathman, 1978).

Error bars are shown for the Raman data in Figures C-III-3 through C-III-6 which correspond to a $\pm 10\%$ accuracy level based on the photon statistics obtained in a typical measurement interval usually the order of one minute. However, each typical profile plotted represents the average Raman data over a time period the order of one half to one hour so that comparisons could be made with the balloon-borne ground truth instrumentation.

Very favorable ground truth comparisons are indicated for the profiles shown in Figures C-III-3 through C-III-6 where simultaneous balloon-borne wet and dry bulb temperature measurements agree well with the remote sensing technique. Ground truth was not available for all the Raman profiles because under certain conditions, such as high winds, the balloon-borne instrumentation was not operable.

4. Conclusions

The Raman lidar was operated aboard the Hayes for a period of three weeks and produced range resolved O_2 , N_2 and H_2O atmospheric profile data in accordance with its design expectations to an altitude of 0.5 kilometer. Ground truth obtainable for the H_2O profiles showed excellent agreement in every case in which comparisons were available. This work thus demonstrated that a Raman lidar can successfully measure atmospheric water vapor profiles for an extended period of time in typical operational marine environments.

Acknowledgements. This work was sponsored by the Naval Air Systems Command and monitored by the Naval Air Development Center, Warminster, Pennsylvania under Contract N62269-76-C-0362.

REFERENCES

- Derr, V. E. and Little, C. G., 1970: "A Comparison of Remote Sensing of the Clear Atmosphere by Optical Radio and Acoustic Radar Techniques", Applied Optics, 9, 1976-1992.
- Gathman, S. G., 1978: "Real Time Meteorological Profiles Using the NRL Boundary Layer Sonde", NRL Report #8271.
- Leonard, D. A. and Caputo, B., 1974: "A Single-Ended Atmospheric Transmissometer", Optical Engineering, 13, 10.
- Melfi, S., Lawrence, J. and McCormick, M., 1969: "Observations of Raman Scattering by Water Vapor in the Atmosphere", Applied Phys. Letters, 15, (9), 295-297.
- Strauch, R. G., Derr, V. E. and Cupp, R. W., 1972: "Atmospheric Water Vapor Measurements Using Raman Lidar", Remote Sensing of the Environment (V. E. Derr, Ed.), U. S. Government Printing Office, Washington, D. C.

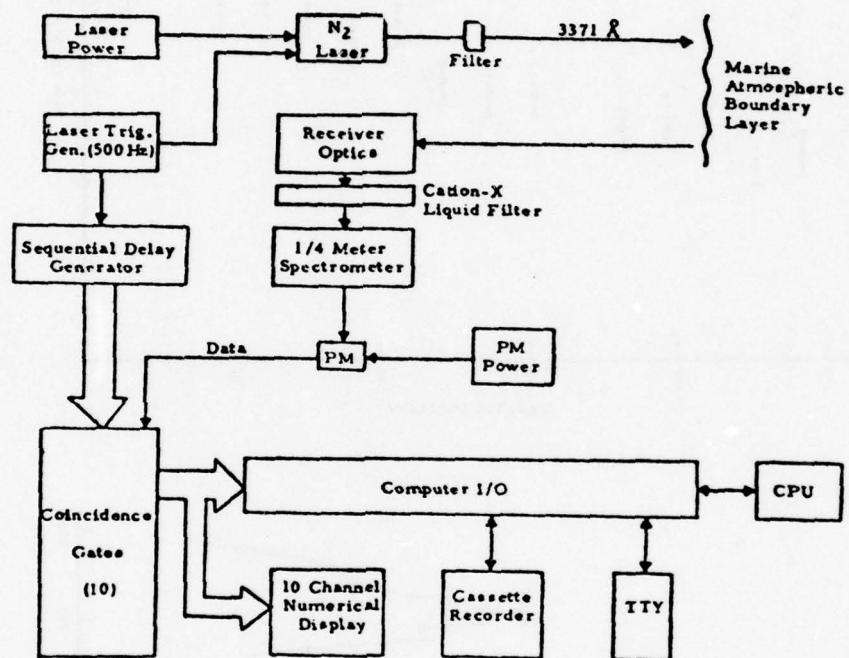


Fig. (C-III-1) USNS HAYES Raman lidar equipment block diagram.

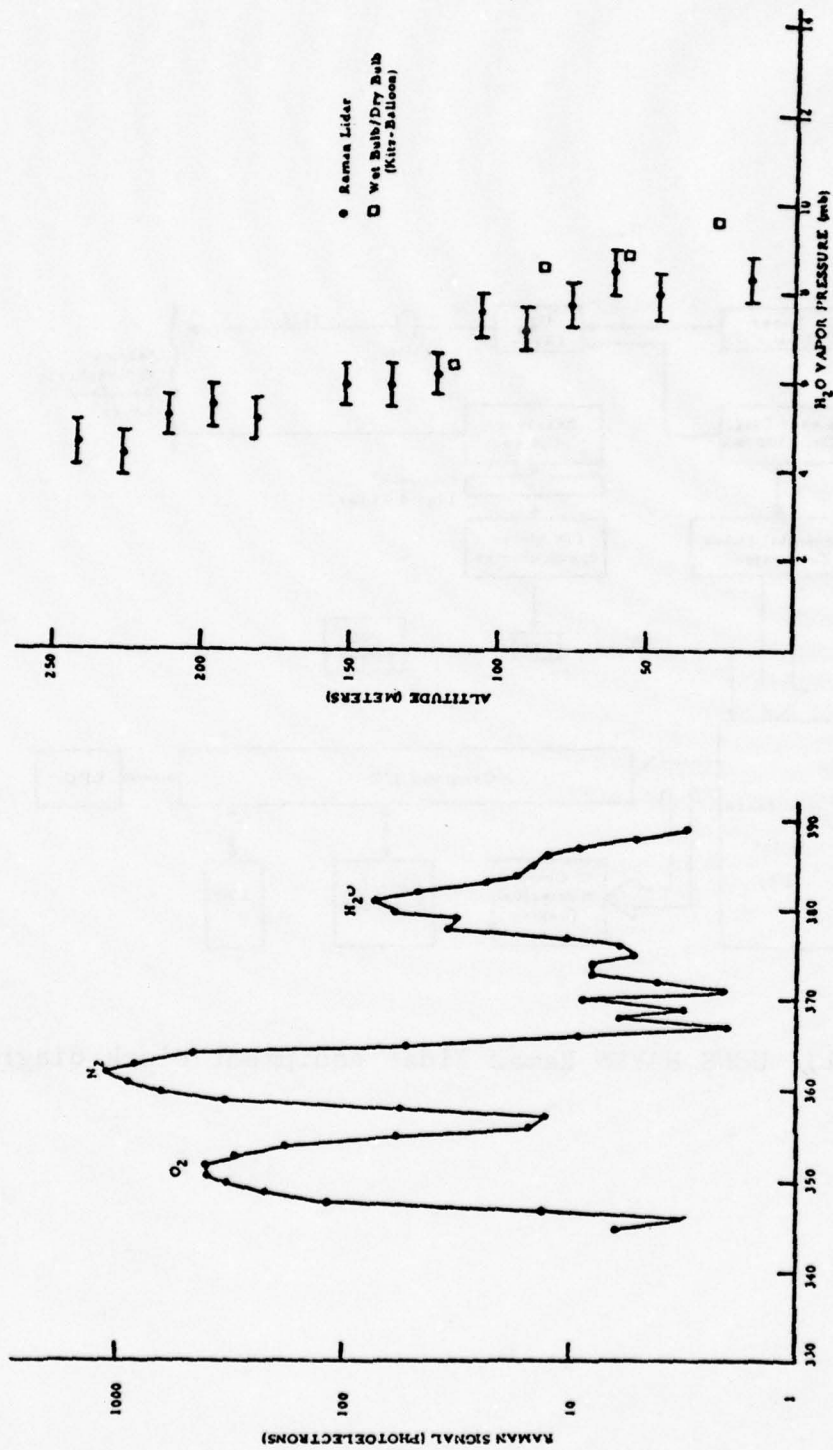


Fig. C-III-3 Partial Pressure of Water Vapor in Millibars (mb) as a Function of Altitude in Meters as Measured by the Raman Lidar on the HAYES, 16 May 1977 (4) 23° N; 67° 22' N) Calibrated by Wet Bulb/Dry Bulb Measurements.

Fig. C-III-2 Typical Raman Lidar Laser Induced Spectrum of Marine Boundary Layer Air.

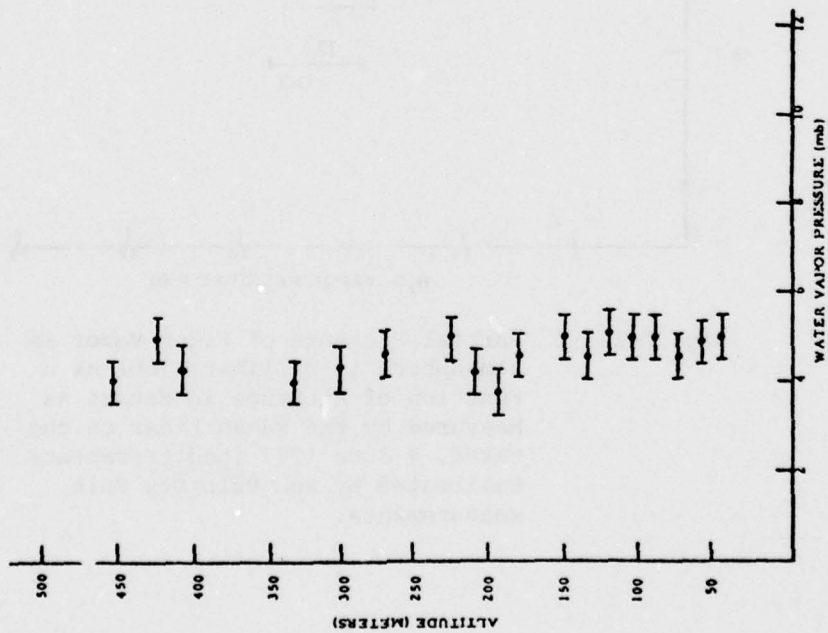


Fig. C-III-4 Partial Pressure of Water Vapor in Atmosphere in Millibars (mb) as a Function of Altitude in Meters as Measured by the Raman Lidar on the HAYES, 18 May 1977
(45° 44' N; 57° 32' W).

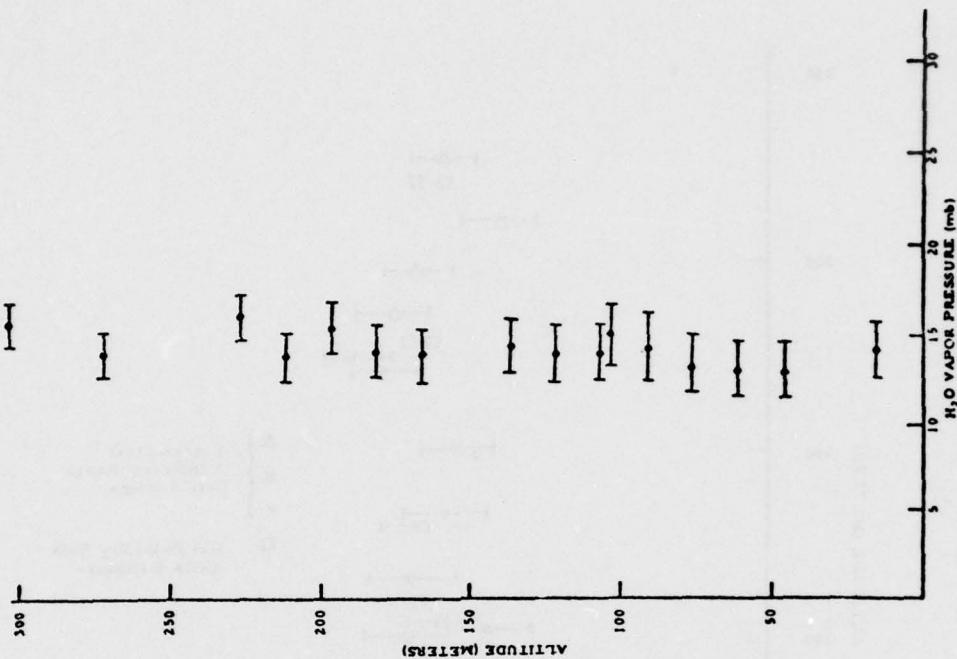


Fig C-III-5 Partial Pressure of Water Vapor in Atmosphere in Millibars (mb) as a Function of Altitude in Meters as Measured by the Raman Lidar on the HAYES, 23 May 1977

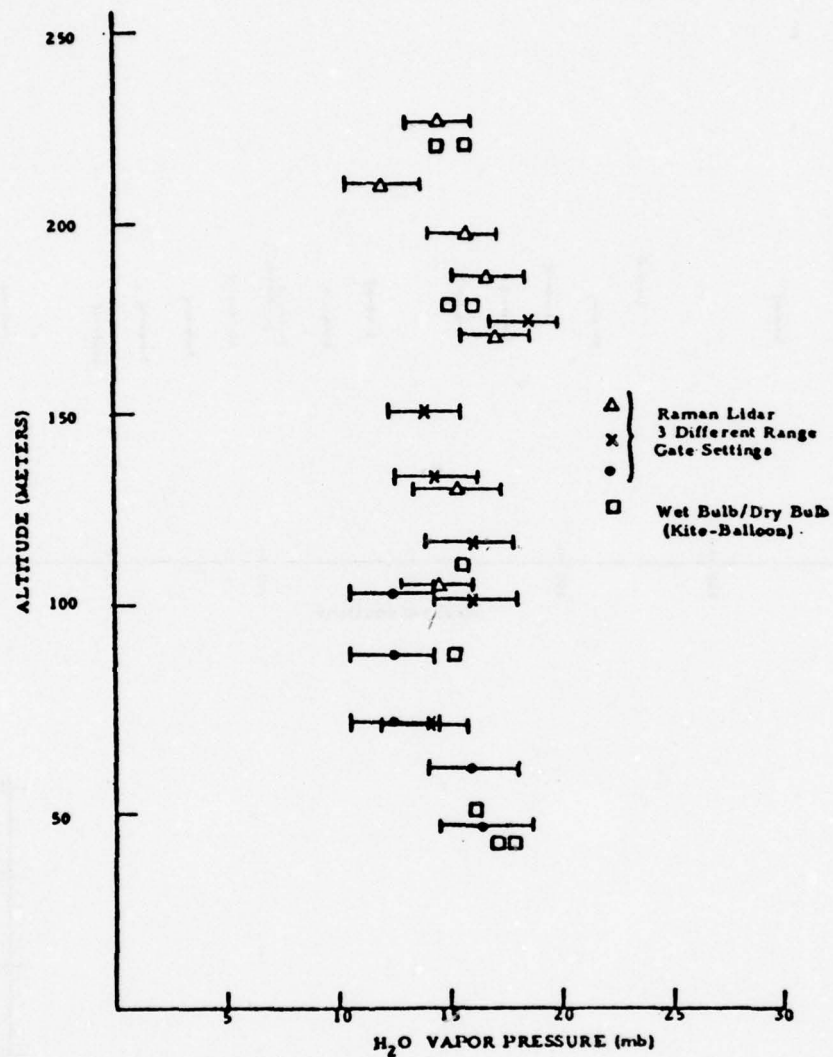


Fig. C-III-6 Partial Pressure of Water Vapor in Atmosphere in Millibars (mb) as a Function of Altitude in Meters as Measured by the Raman Lidar on the HAYES, 4 June 1977 (Mediterranean) Calibrated by Web Bulb/Dry Bulb Measurements.

MEASUREMENT OF CN ON BOARD THE USNS HAYES CRUISE
OF MAY-JUNE 1977

John N. Hayes
Atmospheric Physics Branch
NRL

The purpose of this investigation was to determine the approximate distribution of ship induced condensation nuclei, CN, about the ship and their concentration as a function of external weather conditions.

The CN measurements were made with a commercially available G.E. CN counter. About 40 locations on the ship were "staked" as standard where the measurements were repeated as often as time and the endurance of the experimenter would allow. Figure C-IV-1 is a schematic layout of the ship as seen from the top. (More detailed diagrams, including good side-views, can be obtained from NRL Report 7370.*) The letter L stands for level. Thus POLW stands for stakeouts P00W, P01W, P03W, P03W. W stands for the well of the ship. Not all levels are equally accessible at each measurement location. Forward of the area bounded by the rectangle POLW--SOLW--POL--SOL, only the 01 level exists. The following key will help the reader decipher our notation.

PB -- Port Bow
SB -- Starboard Bow
POL -- Port 01, 02, 03, 04 levels
SOL -- Starboard 01, 02, 03, 04 levels
POLW -- Port Well 01, 02, 03, 04 levels
SOLW -- Starboard Well 00, 01, 02, 03, 04 levels
FOLMW -- Middle of forward section. 00, 02, 04 levels

All positions with "A" in them imply the aft section of the ship. Not all levels were existent there either. The 04A did not exist anywhere. S03AW and S02AW, S03A, and S02 were non existent as well. X00 and Y00 were at deck level with nothing above them.

Although data were collected every day, only certain representative data sets are shown here. Not all were usable because of drastic shifts in relative wind direction during the course of measurement, instrument misbehavior, or rough seas. The plotting of the data is rather difficult because of the limited number of data points and because the plots should be represented in three dimensions. The bow data are from the 01 level; the forward contours are from the 04 level; while the aft data are from the 02 and 03 levels.

The contours shown are CN (On Board)/CN (Sea). A reasonable amount of interpolation and extrapolation was necessary because of the paucity of data stations, but will not significantly affect the conclusions to be drawn from the data.

The data taken in the Mediterranean are fewer in number than that taken in the Atlantic. Several reasons account for this: less time was spent in the Mediterranean; there was a several day instrument failure; and the operational procedures were far more lengthy there due to the loss of help.

Figure C-IV-2a shows 04 level data only and is therefore very simple. The day (135) and time of day are indicated. The exact location can be obtained from the cruise track appearing earlier in this report. The

contour numbers are the natural airborne condensation nuclei number density, divided by CN density at the measuring point. The relative wind is coming roughly from the bow with a 20° spread over the time of measurement, accompanied by a 3 knot spread in relative wind velocities. The particle densities used to generate the contours were the geometric mean of four measurements at each station. We see from Figure C-IV-2a that in the vicinity of the smokestacks the CN count is roughly 400 times that of the background level. As large as this number sounds, its associated optical effect was not discernible.

Figure C-IV-2b shows only the 03 and 02 levels in the aft of the ship for day 140. In spite of the extremely high reading, visibility, while noticeably reduced, was still good; however, the stack gas aerosols were definitely detectable by the olfactory senses.

Figure C-IV-2c shows the contours for 04 level (forward) and 03 and 02 levels aft combined for the wind conditions indicated. Because of the prevailing winds on the cruise track and the speed of the ship, these were not uncommon conditions on the trip. In order to get the relative wind to be from the bow to obtain natural aerosol samples, it was frequently necessary to reverse the course of the ship. We note the low count of CN (Sea) and the high ratio between the stacks. Such ratios often penetrated deep into the well in which the S.R.I. LIDAR was operating. Even though the aerosol sizes were of the same order as the wavelength of laser light used in the LIDAR system, they did not appear to affect its operation.

The preceding figures as well as C-IV-2d, -2e, and -2f show what was fully expected in almost all respects. The stack exhausts fully dominated the data collected downwind, as did the galley exhausts which on occasion could be separated from the stack exhaust in our data. The data showed that:

- The ship should sail into the prevailing winds to obtain uncontaminated aerosol data from centers located at the bow of the ship.
- The port and starboard bow were by far the least contaminated locations on the ship.
- Stack and galley exhaust aerosols dominated the submicron aerosol region so totally in the wind shadow that the natural airborne sea salt particles could not be discerned.
- Turbulence behind the wind screen on the flying bridge allowed for contamination of the natural aerosols. For reliable data, all gathering probes should be stationed forward of the flying bridge wind screen.

In addition, we sought vertical profile data which are shown for several levels at given stations in the remaining figures C-IV-3a, -3b, -3c, and -3d where the x axis is the CN measurement in #/cc and the y axis is the deck level. They show clearly that uncontaminated results can be obtained, especially in high winds, if the collector is situated on the windward side of the ship; but if data are collected from the leeward side, they are untrustworthy. Figure C-IV-4 tends to summarize all the results together with deviations from the average effects. The open ocean gives

uncontaminated aerosol counts of the order of 100-1000 nuclei per cc. In the wind shadow, we get (depending, in part, upon how the engines are operating) 10^5 counts/cc and higher. Intermediate results generally involve turbulent mixing or fresh air entrainment.

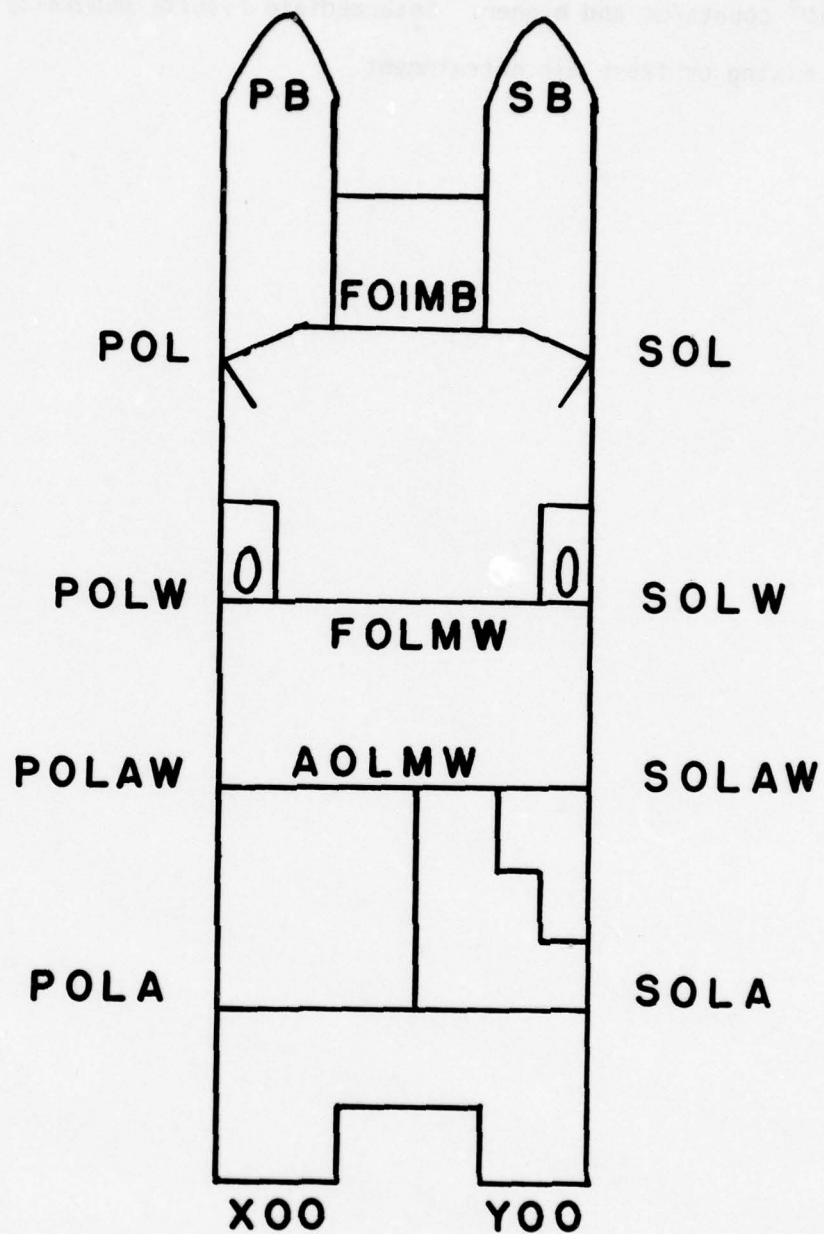


Fig. (C-IV-1) Diagram of CN measuring stations.

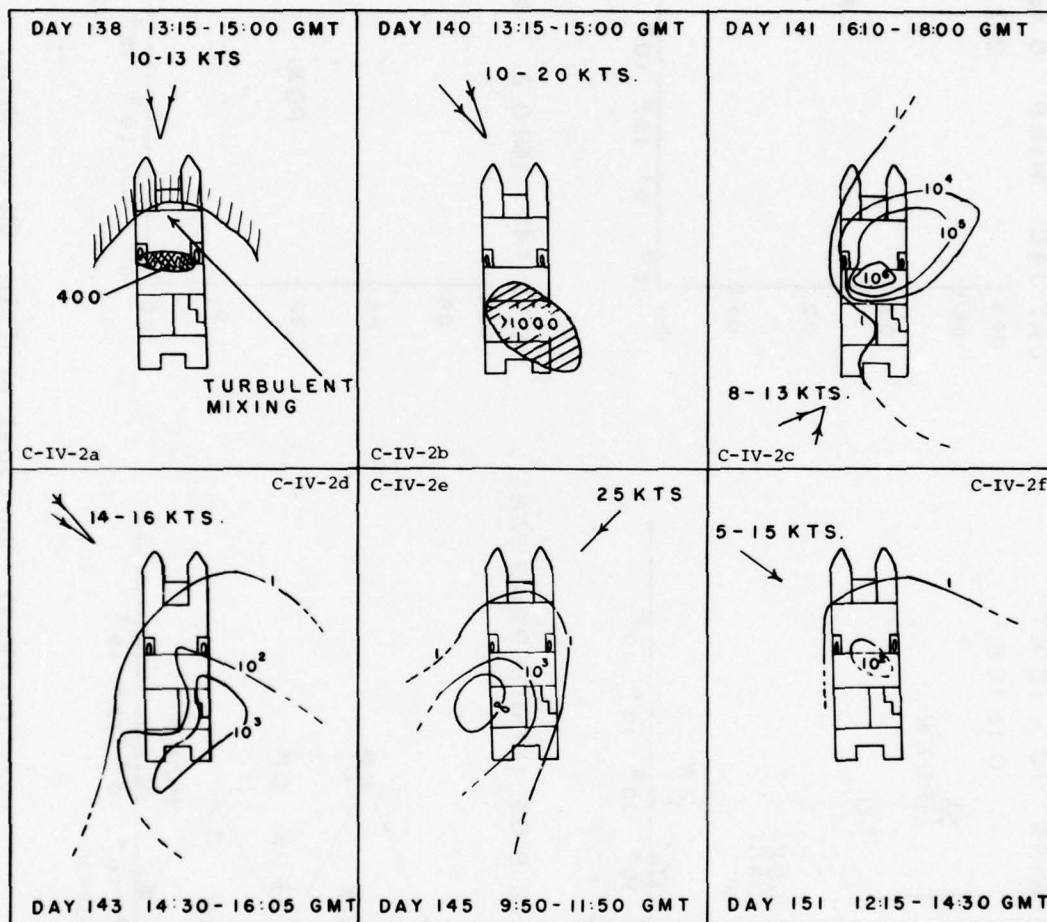


Fig. (C-IV-2) Plots of CN on ship.

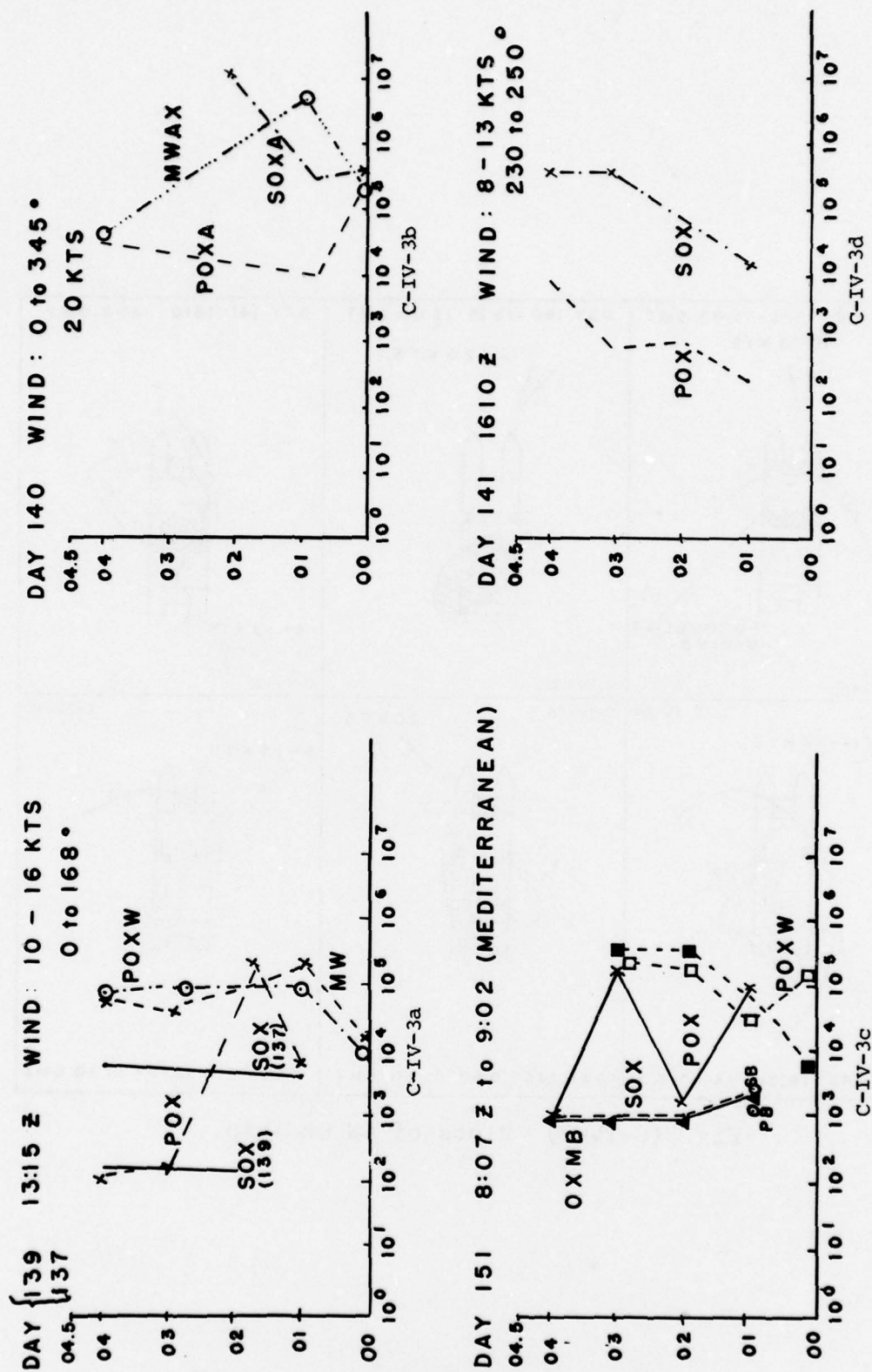


Fig. (C-IV-3) Vertical profile, CN on ship.

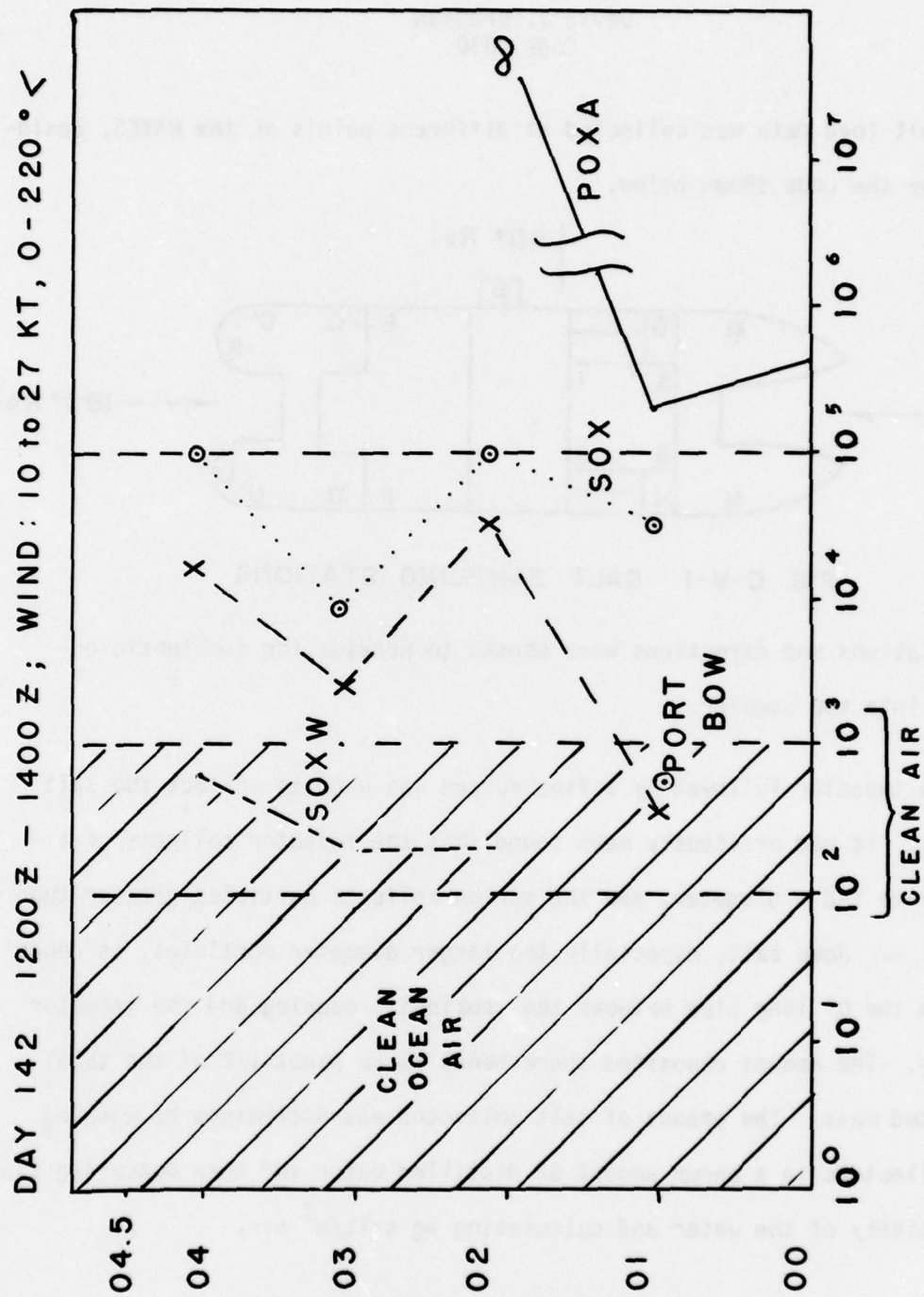


Fig. (C-IV-4) Summary of ship effects on CN, with deviation from average effects.

SALT LOAD DATA

David J. Bressan
Code 8330

Salt load data was collected at different points on the HAYES, designated by the code shown below.

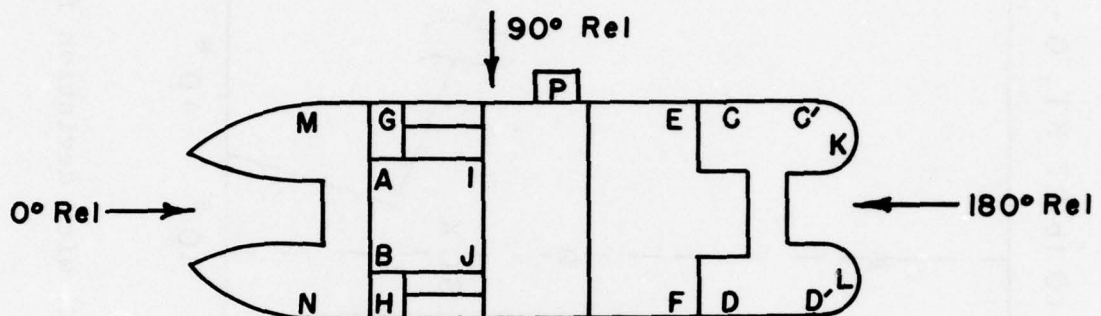


FIG. C-V-1 SALT SAMPLING STATIONS

The locations and directions were chosen to provide for isokinetic entrance into the sampler.

An impactor followed by a fine screen was used to collect the salt samples. It had previously been found that the impactor collects particles above 1-2 μ diameter, and the screen collects particles greater than 0.1-0.2 μ . Some salt, especially the larger diameter particles, is deposited in the 8" long pipe between the isokinetic opening and the impactor surface. The amount deposited there tends to be about 1/2 of the total collected mass. The amount of salt collected was determined by washing the collectors in a known amount of distilled water and then measuring the conductivity of the water and calculating $\mu\text{g salt/m}^3$ air.

A comparison between the impactor system and three of the fine mesh screens mounted in tandem showed that the total salt load computed from the sum of that on the three screens agreed to within 10-15% with the total salt retrieved from the impactor system.

The open areas of the screens are about 45% of the total, so that the screen retains about 55% of the material $\geq 0.1 \mu$ diameter which reaches it. It should be then noted that the relative humidity of the air will affect the size of the salt particles collected, as will passage through an impactor nozzle, since Bernoulli pressure changes will also affect the relative humidity.

For these reasons only the raw data is presented. It is shown simply as that collected by the screen, slide and inlet system in $\mu\text{g salt}/\text{M}^3$ of air. It is expected that the inlet system collects mostly particles larger than 30-50 μ diameter, but without a sharp cut off point. The remaining particles above $\sim 1.0 \mu$ are collected on the slide, and the screen will collect about 1/2 of the total mass reaching it, whose range should be 0.1-1.0 μ diameter.

Interpretation of this data can best be done with respect to changes in wind speed and white cap coverage, and changes in air masses with marine trajectories and turbulence being reflected in the salt load. These observations should be available in the data file.

Table C-V-1 Salt Load Data (page 1 of 2)

<u>Date</u>	<u>Time</u>	<u>Location</u>	<u>µg salt/M³</u>			<u>Remarks</u>
			<u>Inlet</u>	<u>Slide</u>	<u>Screen</u>	
05/16/77	10:30L	1-C	—	43.5		RW 170°
05/16/77	11:30L	03-E	—	11.8		
05/17/77	12:00L	04-A	—	17.5	7.9	
05/17/77	13:00L	1-D	—	30.6	5.9	
05/17/77	14:30L	03-F	—	16.5	9.6	RW 240°
05/17/77	15:45L	04-A	—	16.3	5.6	RW 000°
05/18/77	11:50L	04-A	—	1.8	2.4	No white caps
05/18/77	12:15L	01-M	—	1.8	4.3	(Air mass change?)
05/18/77	16:45L	04-A	—	5.9	3.0	Many white caps
5/18/77	17:10L	01-M	—	9.0	-	
05/19/77	11:20L	01-M	—	1.0	2.4	
05/19/77	13:50L	1-C	—	1.9	2.3	
05/19/77	16:10L	04-A	—	2.5	1.8	
05/19/77	16:30L	02-C	—	1.9	3.5	
05/21/77	15:25L	03-H	—	14.8	4.1	
05/21/77	23:15Z	04-A	—	12.2	1.1	
05/21/77	23:30Z	04-A	—	9.4	1.2	
05/21/77	23:55Z	04-A	—	11.2	-	
05/22/77	12:05Z	04-A	—	15.1	1.4	Note when wind speed changes on 22nd
05/22/77	12:20Z	04-A	—	18.3	2.1	
05/22/77	12:40Z	04-A	—	15.9	2.4	
05/22/77	17:15Z	04-A	—	10.1	1.3	
05/22/77	17:30Z	04-A	—	10.3	1.6	
05/22/77	17:45Z	04-A	—	10.3	0.9	
05/24/77	16:45Z	04-A	—	3.2	1.2	
05/25/77	10:55Z	04-A	—	3.3	2.6	
05/25/77	11:15Z	04-A	—	6-8	2.1	Quite a few small white caps
5/25/77	15:20Z	04-A	—	3.3	1.3	
5/25/77	15:50Z	04-A	—	3.8	1.3	
5/26/77	09:00Z	03-G	—	2.5	1.5	
5/26/77	09:20Z	03-G	—	1.9	1.3	
5/26/77	14:40Z	03-G	—	2.7	1.5	
5/26/77	14:50Z	03-G	—	2.1	1.8	
5/26/77	15:15Z	1-E	—	1.6	2.2	

Table C-V-1 Salt Load Data (page 2 of 2)

Date	Time	Location	ug salt/M ³			Remarks
			Inlet	Slide	Screen	
05/27/77	09:25Z	03-H	—	10.9	2.6	
05/27/77	09:45Z	03-H	—	11.2	3.7	
05/31/77	08:35Z	03-G	10.8	8.0	2.3	For this, and other runs where apparent, the Inlet is the average for 3 samples
5/31/77	08:55Z	03-G	—	7.9	2.2	
05/31/77	08:15Z	03-G	10.8	8.2	2.1	
06/01/77	08:50Z	03-G	10.9	11.7	1.5	
06/01/77	09:15Z	03-G	10.9	11.9	1.4	
06/01/77	09:30Z	03-G	10.9	13.1	1.4	
06/02/77	08:30Z	03-G	4.1	1.5	1.9	
06/02/77	08:35Z	03-G	4.1	1.3	2.5	
06/03/77	11:35Z	03-G	3.6	4.3	2.0	
06/03/77	11:55Z	03-G	3.6	4.7	2.0	
06/03/77	12:10Z	03-G	3.6	4.3	1.8	
06/04/77	06:30Z	03-H	1st 10.8	2nd 5.6	3rd 5.3	Three screen test total = 27.0
06/04/77	06:40Z	03-H	8.0	8.7	2.5	total = 22.7
06/04/77	06:55Z	03-H	9.0	10.2	4.8	total = 28.8
06/04/77	06:55Z	03-H	9.0	10.2	4.8	
06/04/77	14:10Z	03-G	12.8	11.1	2.9	
06/04/77	14:25Z	03-G	12.8	9.9	2.9	
06/05/77	08:10Z	03-G	7.8	9.4	1.5	
06/05/77	08:30Z	03-G	7.8	8.6	2.3	
06/05/77	20:30Z	03-G	5.2	7.2	1.8	
06/05/77	20:45Z	03-G	5.2	6.3	2.5	
06/16/77	11:30Z	03-H	5.2	12.3	2.0	
06/16/77	11:50Z	03-H	5.2	12.3	2.1	
06/18/77	07:05Z	1-P	6.8	9.0	1.0	
06/18/77	07:35Z	03-G	3.4	5.9	1.5	
06/28/77	14:25Z	03-H	5.8	8.4	1.7	
06/28/77	14:50Z	03-H	5.8	9.0	1.8	

S.R.I. Lidar Observations During EOMET 77

Edward Uthe, John Livingston, Raymond Endlich,
Joyce Kealoha and Norman Nielson

S.R.I. International
Menlo Park, CA

31 August 1978

INTRODUCTION

During the period 15 May - 7 June 1977 the SRI Mark IX mobile lidar system was operated on board the USNS Hayes on a scientific cruise across the Atlantic Ocean and the Mediterranean Sea. The purpose was to obtain a continuous record of the vertical aerosol and cloud structure up to an altitude of 3.5 km.

MARK IX MOBILE LIDAR SYSTEM

The SRI Mark IX ruby lidar system is the product of 14 years of experience in developing and applying laser radar systems to the observation of atmospheric aerosol, cloud, and precipitation distributions over remote areas with high spatial and temporal resolution. The lidar system is operated from a 6 m van provided with power-generating facilities to allow completely mobile operation or immediate operation at any stationary location. One of the Mark IX's principal features is a digital data recording, processing, and display system for real-time TV-viewing of controlled gray-scale presentations of atmospheric structure. These gray-scale displays are generated from backscatter data obtained from multiple laser firings while the lidar is being scanned in elevation or azimuth, or repetitively pulsed with time or distance. In addition, the minicomputer-based system permits the determination of quantitative estimates of aerosol densities. Views of the Mark IX system, a block diagram, and lidar specifications are presented in Figure C-VI-1.

DATA ACQUISITION PROGRAM

During the 1977 USNS Hayes cruise the vertical aerosol structure was sampled at a rate of approximately three profiles per minute for about twenty hours each day. Generally, each backscatter signature (profile) was digitized in real time with a sampling rate of 5×10^{-8} sec (range resolution of 7.5 m) from the lidar height aboard ship to an altitude of 3.6 km. Periodically, however, profiles were digitized with a sampling rate of 20×10^{-8} sec (range resolution of 30 m) up to an altitude of 14.4 km in order to monitor upper level clouds, primarily cirrus. Concurrent with each lidar firing, the output of an MRI (Meteorology Research, Inc.) integrating nephelometer was sampled and digitized with a low-speed analog-to-digital converter. The lidar and nephelometer data along with date and time information were recorded on nine-track magnetic tape for further analysis.

LIDAR OBSERVED ATMOSPHERIC STRUCTURE

A complete set of Polaroid photographs depicting intensity-modulated height/time TV displays of vertical atmospheric structure along the cruise route is presented in the S.R.I. appendix. Two of these photographs are shown in Figure C-VI-2 in order to explain the scale labels and types of backscatter returns observed. Tick marks equally spaced at ten minute intervals at the top of each Polaroid frame delineate time. The photographs are arranged in rows and numbered sequentially from the beginning of the cruise. The date, frame number, and times (GMT) corresponding to the first and last ticks, respectively, of each frame in a particular row are tabulated to the left of each row. Periodic time gaps due to missing data and

resulting in missing, extra, or unequally-spaced tick marks are also documented. Height above the lidar is indicated in each frame by bright horizontal lines spaced at one kilometer intervals. Gross discontinuities in the vertical aerosol structure appearing within a single frame are artificial: they are due to a reduction in the height scale resulting from an increase in the range (altitude) of the lidar beam in order to detect high altitude clouds, as noted previously. In these cases, the vertical scale has been reduced by a factor of 4, and the bright horizontal lines appear at 4 km intervals (see Figure C-VI-2b).

Picture brightness is proportional to the logarithm of observed backscatter. The TV display provides 16 gray steps, as shown by the gray scale presented beside each data frame. During data processing, the computer operator selected a signal level for each gray step to emphasize structure of the near-surface aerosol layer. This resulted in saturation of the display for very large backscatter values, principally related to clouds and precipitation. When the maximum brightness was exceeded for these data, the computer recirculated the data to the lowest brightness gray step. This technique provides digital isoecho contouring evident in the cloud and precipitation returns (see Figure C-VI-2b).

The 0 to 5 volt output of the MRI integrating nephelometer, as sampled at the time of each lidar firing, is plotted at the top of the height/time cross section (see Figure C-VI-2b). The 0-V level corresponds to the 3-km range mark and a 3.5-V calibration signal is normally inserted once for each experimental run (for example, at 1516 GMT in Frame 38). Using information provided by the manufacturer, the 3.5-V level corresponds to an

aerosol concentration of $265 \mu\text{g}/\text{m}^3$ and provides a concentration scale for the data plot.

RESEARCH OBJECTIVES

Detailed analyses of the pictorial displays and digital data which are presently under way will enable us to characterize the marine atmospheric aerosol structure in terms of aerosol mixing layer heights and relative columnar aerosol backscatter values. It is expected that planned correlative analyses between these Mark IX lidar-derived aerosol layer heights and backscatter values and the shipboard observations of various meteorological parameters will also contribute to our understanding of the atmospheric marine boundary layer.

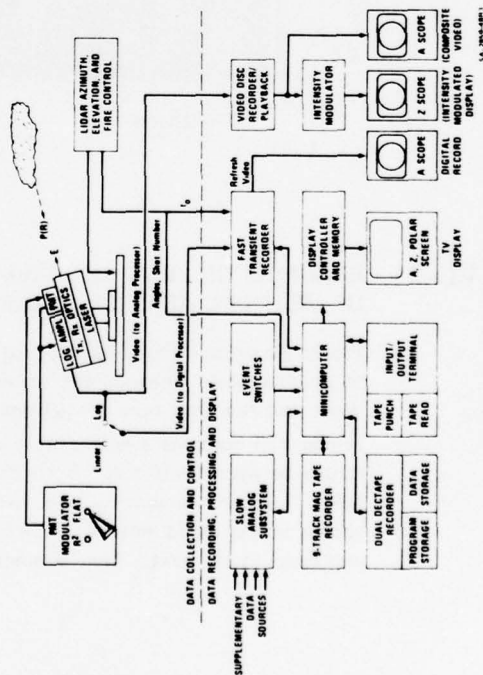


(a) MARK IX LIDAR VAN

(b) ANALOG DATA AND FIRE CONTROL ELECTRONICS

(c) DIGITAL DATA ELECTRONICS AND TV DISPLAY

EXTERIOR AND INTERIOR VIEWS OF THE LIDAR VAN



BLOCK DIAGRAM OF THE LIDAR SYSTEM

LIDAR SPECIFICATIONS

DATA SYSTEMS

Analog video disc recording (4.5 MHz) with A-scope and Z-scope real-time displays. Digital magnetic tape (data and programs) recording (25 MHz) with computer processing and real-time TV display (512 x 256 x 4 bit) of processed data.

MOUNT

Automatic azimuth and elevation fire and scan with 0.1° minimum resolution. Automatic reset. Mechanical safety stops.

TRANSMITTER

6943A Wavelength
0.5 mrad Beamwidth
1.0 J Pulse Energy
30 ns Pulse Length
60 ppm Maximum PRF

RECEIVER

6 inch Newtonian
1 to 5 mrad Field of View
5A Predetection Filter
RCA 7265 PMT Detector
4-decade, 35-MHz Logarithmic Amplifier. Inverse-range-squared or step-function PMT modulation.

Fig. (C-VI-1) SRI mobile lidar system.

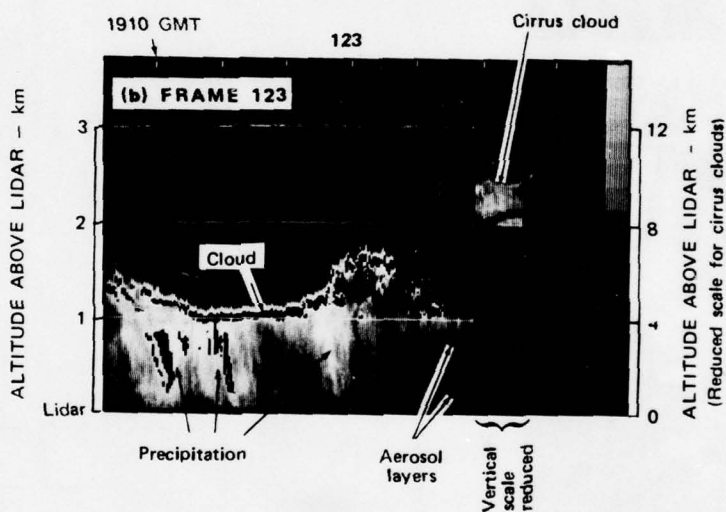
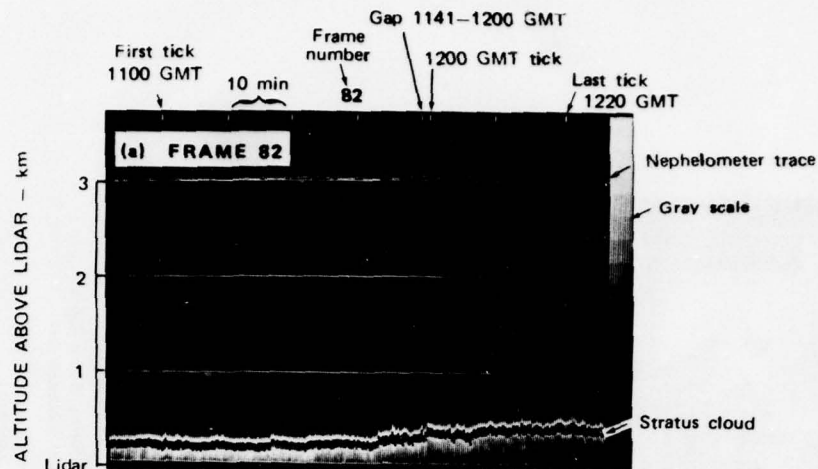


Fig. (C-VI-2) EXAMPLES OF LIDAR OBSERVED HEIGHT/TIME SECTIONS OF VERTICAL AEROSOL, CLOUD, AND PRECIPITATION STRUCTURE.

Frame 82 exemplifies a height/time display containing a time gap. In addition to detailed scale labeling, the nephelometer data trace, a low level stratus cloud deck, and the gray scale are all denoted.

Frame 123 contains a height scale change at 2000 GMT. Note the cirrus cloud return between 8-10 km. Both the bright echoes and embedded dark echoes below 1 km are caused by rain. These embedded dark echoes, which also appear in the cloud returns, are examples of the isoecho contouring effect explained in the text. Two distinct aerosol layers are also evident below 1 km.

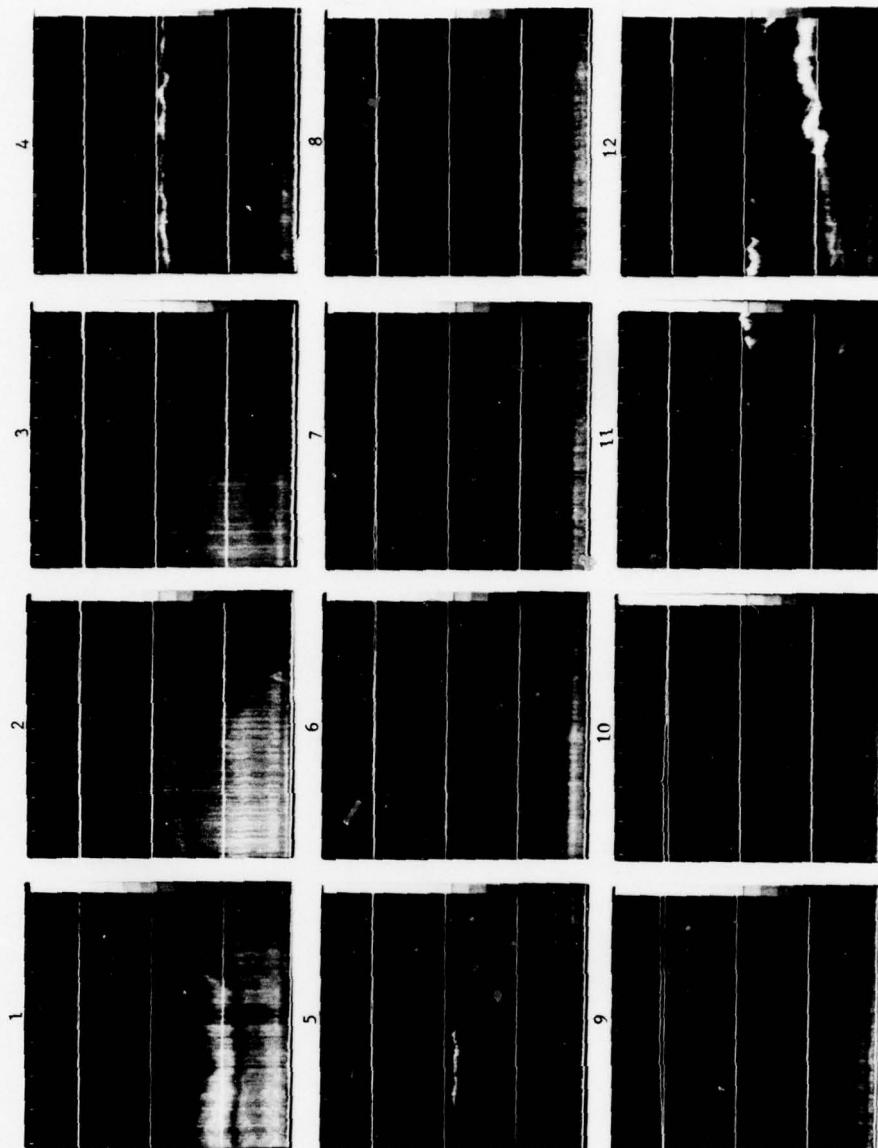
Appendix
LIDAR-OBSERVED AEROSOL STRUCTURE
ABOVE EOMET 77 CRUISE ROUTE

DATE	TIME	LOCATION	WIND	TEMP	HUMID	WAVE	WIND	TEMP	HUMID	WAVE
1968	1200	1000	1000	1000	1000	1000	1000	1000	1000	1000
1968	1200	1000	1000	1000	1000	1000	1000	1000	1000	1000
1968	1200	1000	1000	1000	1000	1000	1000	1000	1000	1000
1968	1200	1000	1000	1000	1000	1000	1000	1000	1000	1000

LIDAR BACKSCATTER HEIGHT/TIME TV DISPLAYS (1-12)

Day	Frame Number	Time (GMT)	
		First Tick	Last Tick
135 (May 15)	1	0600	0710
	2	0720	0820
	3	0830	0930
	4	0940	1050
135	5*	1100	1220
	6	1230	1330
	7	1340	1450
	8	1500	1600
135	9	1610	1710
	10	1720	1830
	11	1840	1940
	12	1950	2050

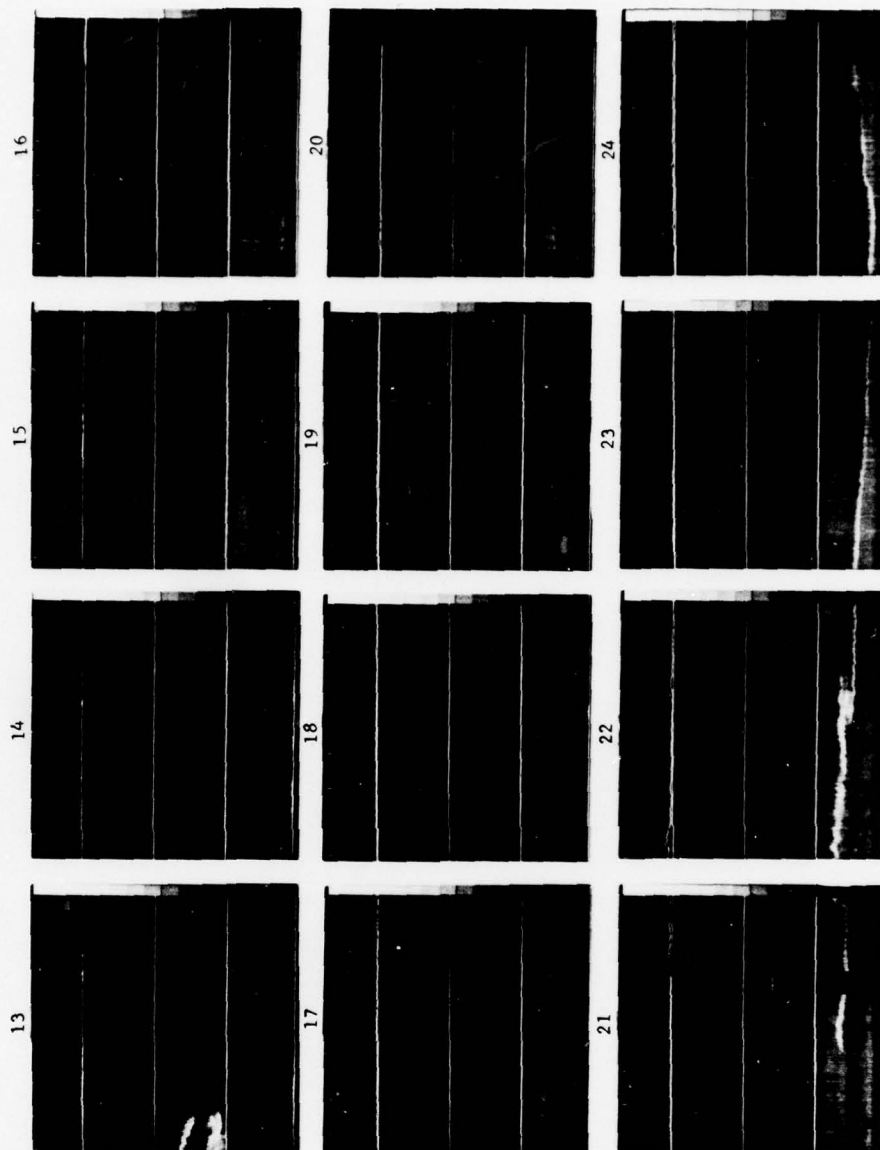
* Time gap 1159-1215.



LIDAR BACKSCATTER HEIGHT/TIME TV DISPLAYS (13-24)

Day	Frame Number	Time (GMT)	
		First Tick	Last Tick
135	13	2100	2210
	14	2220	2320
	15	2330	0040
	16	0050	0150
136 (May 16)	17	0200	0300
	18	0310	0420
	19*	0430	1050
	20	1100	1200
136	21	1250	1350
	22	1400	1510
	23	1520	1620
	24	1630	1740

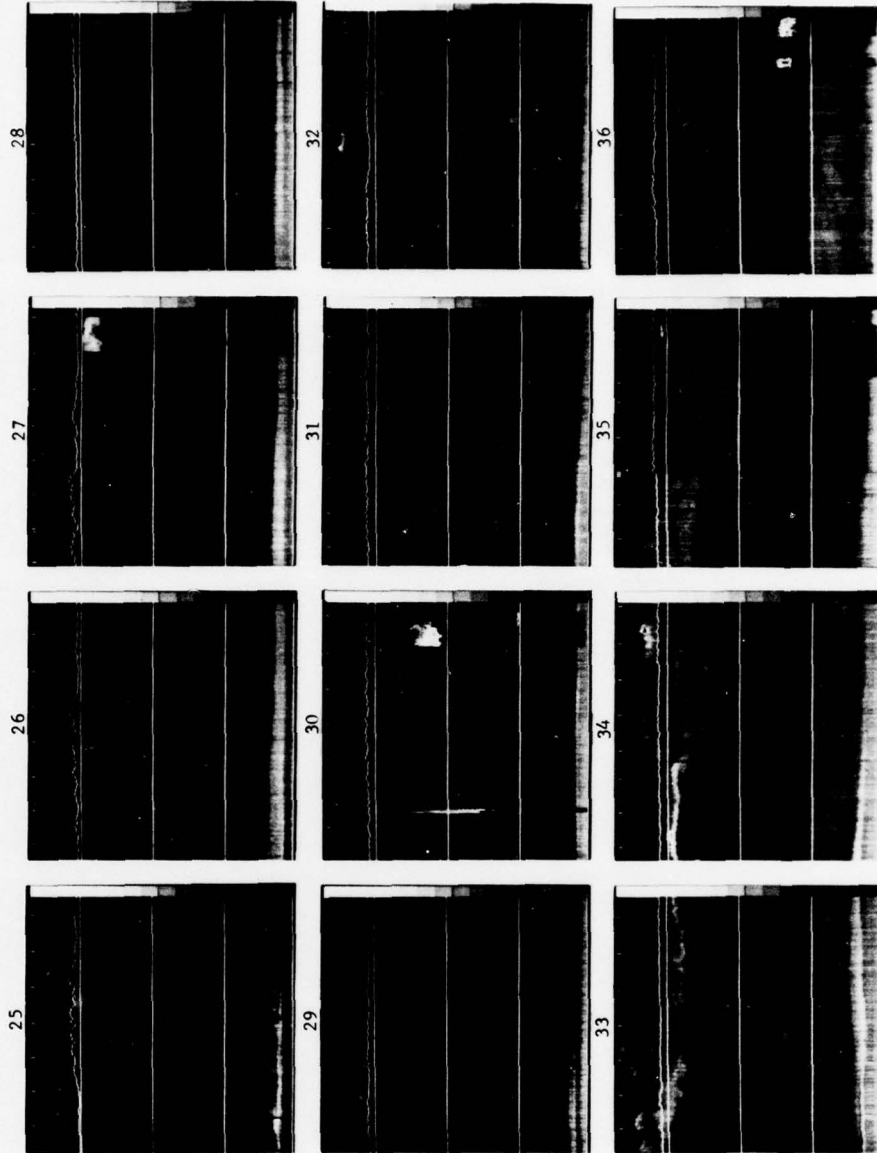
* Time gap 0525-1046



LIDAR BACKSCATTER HEIGHT/TIME TV DISPLAYS (25-36)

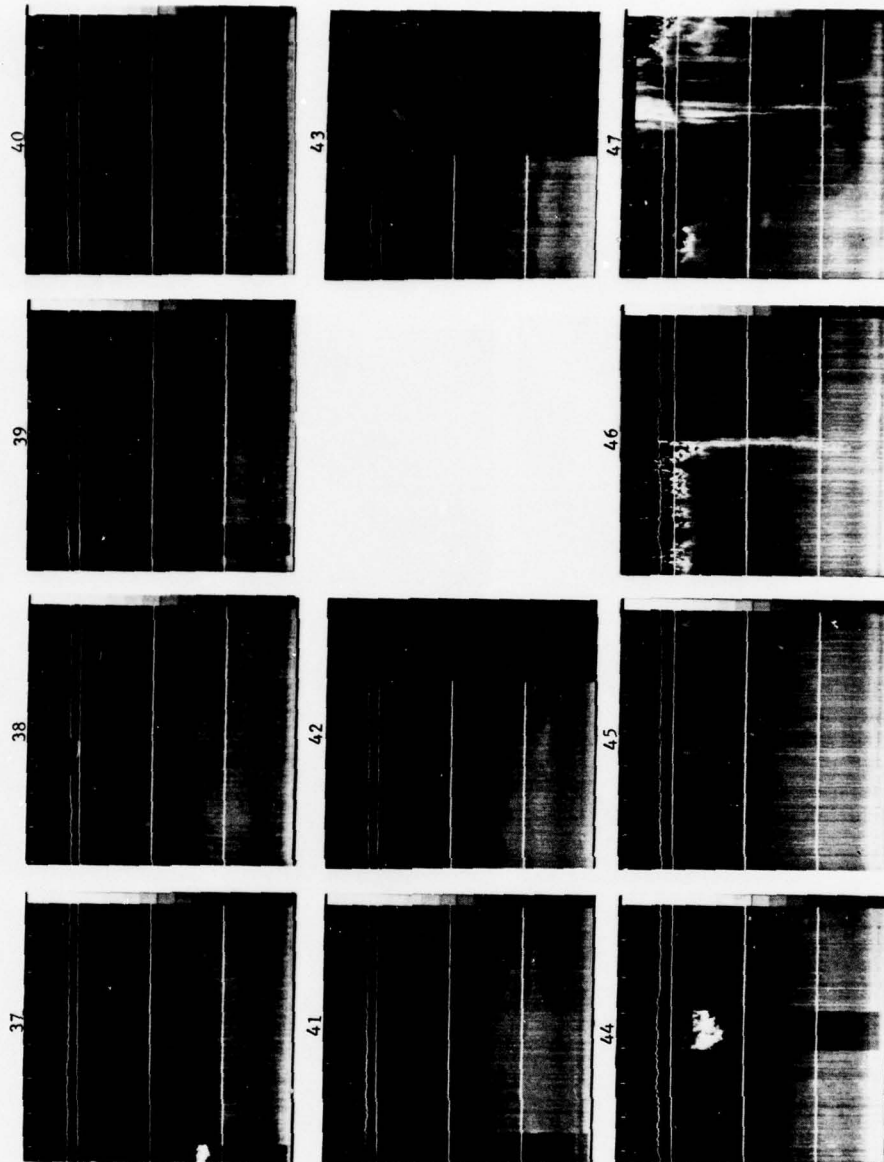
Day	Frame Number	Time (GMT)	
		First Tick	Last Tick
136	25	1750	1850
	26	1900	2000
	27	2010	2120
	28	2130	2230
136	29	2240	2350
	30	0000	0100
	31	0110	0210
	32	0220	0330
137 (May 17)	33	0340	0440
	34*	0450	0600
	35†	0610	1220
	36	1230	1330

* Time gap 0510-0520
† Time gap 0630-1121; 7th tick is 1140; Time gap 1146-1200; 8th tick is 1200.



LIDAR BACKSCATTER HEIGHT/TIME TV DISPLAYS (37-47)

Day	Frame Number	Time (GMT)	
		First Tick	Last Tick
137	37	1340	1440
	38	1450	1600
	39	1610	1710
	40	1720	1830
137	41	1840	1940
	42	1950	2030
	43	2110	2130
137	44	2200	2300
	45	2310	0020
	46	0030	0130
	47	0140	0250



LIDAR BACKSCATTER HEIGHT/TIME TV DISPLAYS (48-59)

Day	Frame Number	Time (GMT)	
		First Tick	Last Tick
138 (May 18)	48	0300	0400
	49	0410	0520
	50	0530	0630
	51*	0640	1110
138	52	1120	1220
	53	1230	1330
	54	1340	1450
	55	1500	1600
138	56	1610	1710
	57	1720	1830
	58	1840	1940
	59†	1949	2120

* Time gap 0741-1100.
† Time gap 1949-2010; 2nd tick is 2010.

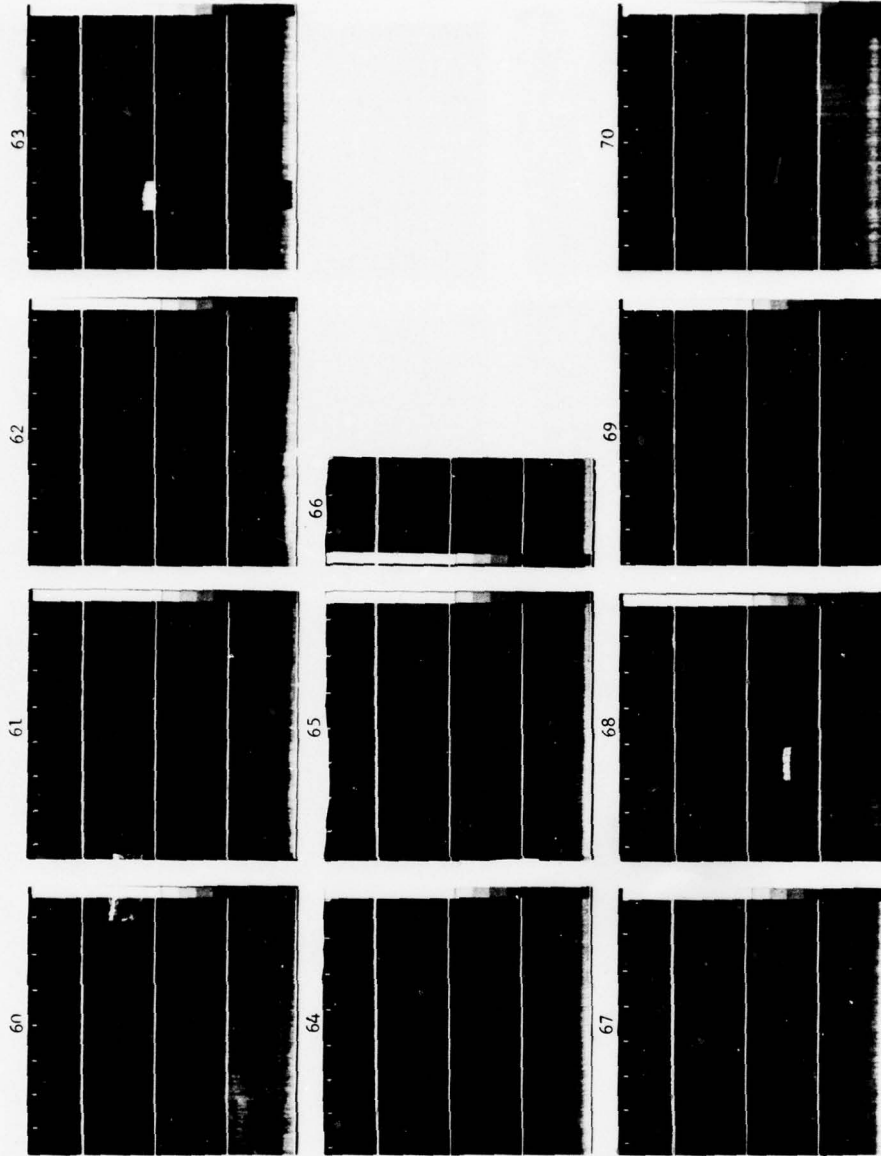


LIDAR BACKSCATTER HEIGHT/TIME TV DISPLAYS (60-70)

Day	Frame Number	Time (GMT)	
		First Tick	Last Tick
138	60	2130	2230
	61	2240	2340
	62*	0000	0100
	63	0110	0210
139 (May 19)	64	0220	0330
	65	0340	0440
	66	0450	0510
139	67	0530	0640
	68	1050	1150
	69	1200	1310
	70†	1320	1507

* No 2350 tick.

† Time gap 1419-1500; 6th tick is 1410.



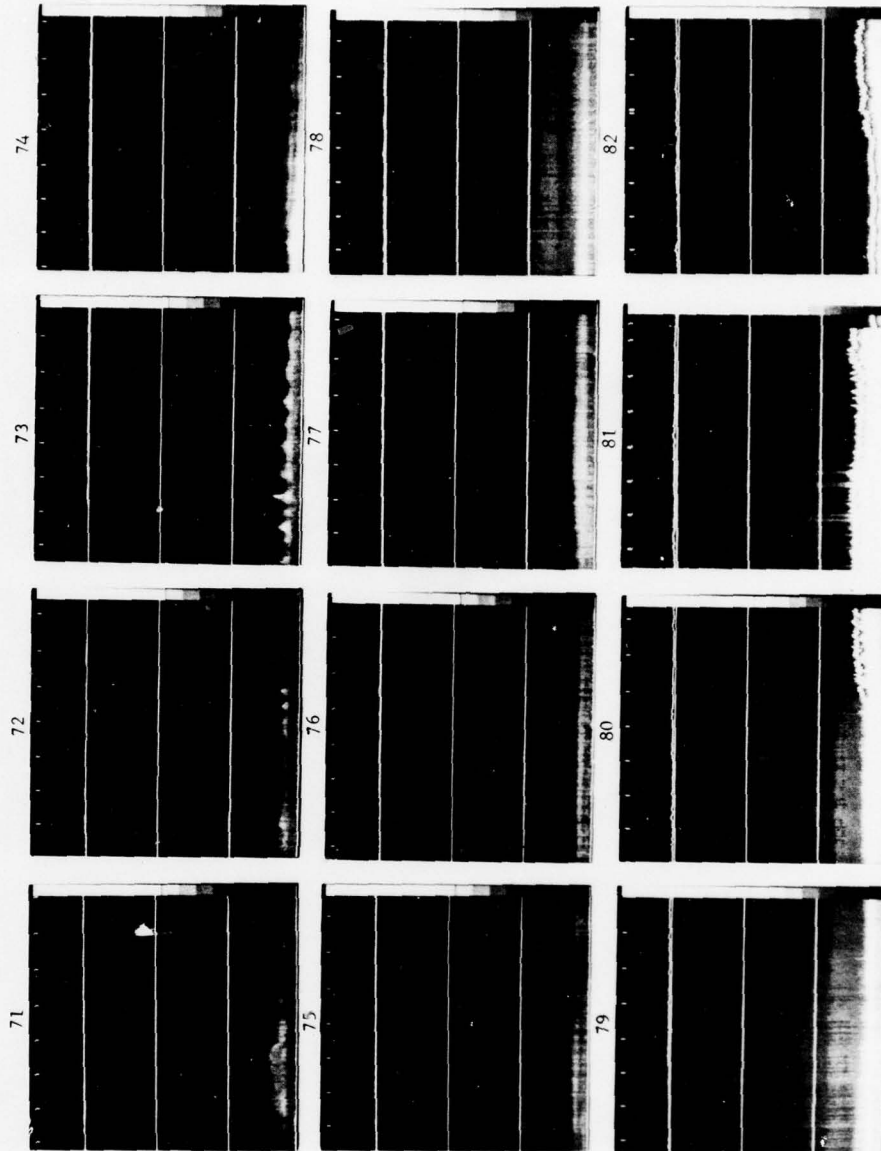
LIDAR BACKSCATTER HEIGHT/TIME TV DISPLAYS (71-82)

Day	Frame Number	Time (GMT)	
		First Tick	Last Tick
139	71	1510	1620
	72	1630	1730
	73	1740	1840
	74	1850	2000
139	75	2010	2110
	76	2120	2220
	77*	2240	0000
	78	0010	0110
140	79	0120	0220
	80	0230	0340
	81†	0350	1050
	82‡	1100	1220

* No 2230 tick; Time gap 2332-2351.

† Time gap 0454-1049.

‡ Time gap 1141-1200.



LIDAR BACKSCATTER HEIGHT/TIME TV DISPLAYS (83-93)

Day	Frame Number	Time (GMT)	
		First Tick	Last Tick
140	83	1230	1330
	84*	1350	1450
	85	1500	1600
	86	1610	1720
140	87	1730	1830
	88	1840	1940
	89	1950	2010
140	90	2030	2130
	91†	2140	2300
	92	2310	0020
	93	0030	0130

* No 1340 tick.
† Time gap 2229-2249.



LIDAR BACKSCATTER HEIGHT/TIME TV DISPLAYS (94-105)

Day	Frame Number	Time (GMT)	
		First Tick	Last Tick
141 (May 21)	94	0140	0240
	95	0250	0400
	96	0410	0510
	97	0520	0620
141	98	0630	0740
	99	0750	0850
	100*	0900	1110
	101	1120	1220
141	102	1230	1340
	103	1350	1450
	104	1500	1600
	105	1610	1650

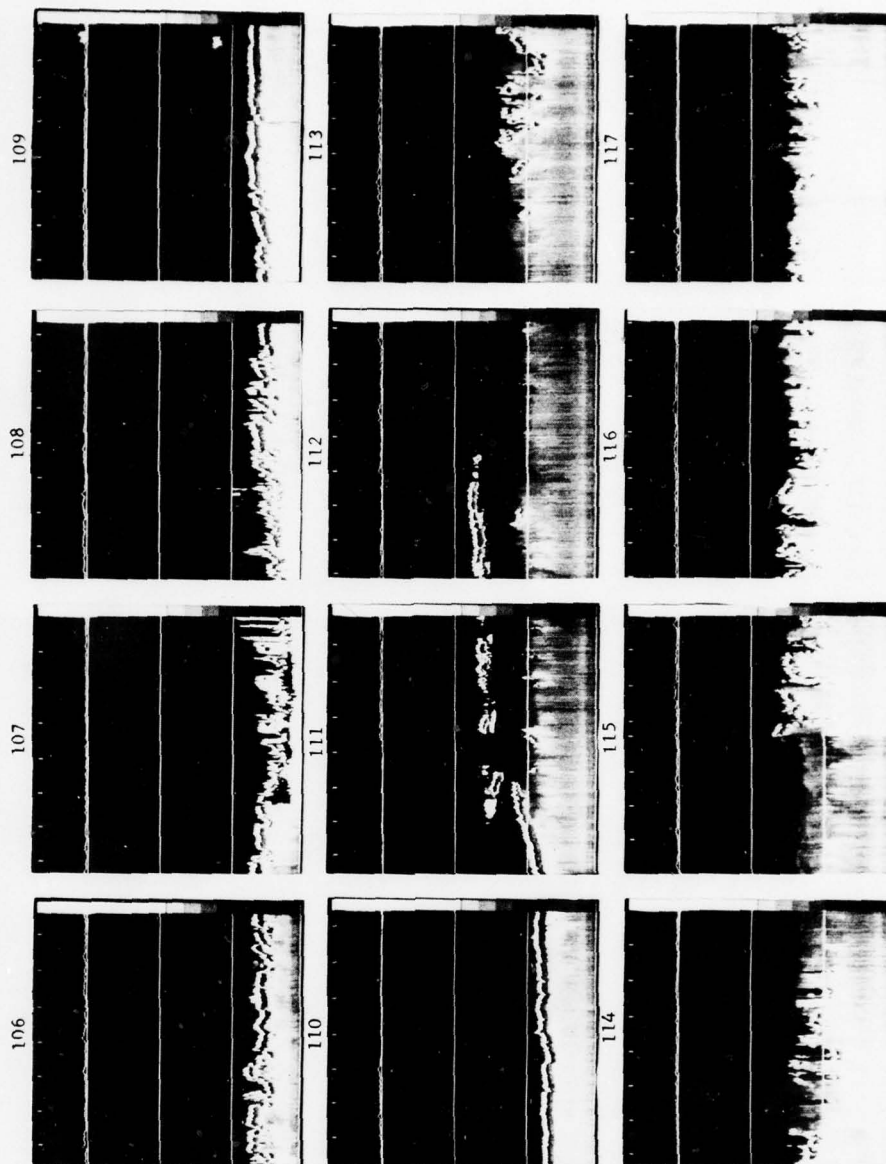
* Time gap 0945-1048.



LIDAR BACKSCATTER HEIGHT/TIME TV DISPLAYS (106-117)

Day	Frame Number	Time (GMT)	
		First Tick	Last Tick
141	106	1720	1820
	107	1830	1930
	108*	1950	2050
	109†	2100	2220
141	110	2230	2330
	111	2340	0040
	112	0050	0200
	113	0210	0310
142 (May 22)	114	0320	0420
	115†	0440	1000
	116‡	1010	1140
	117	1150	1250

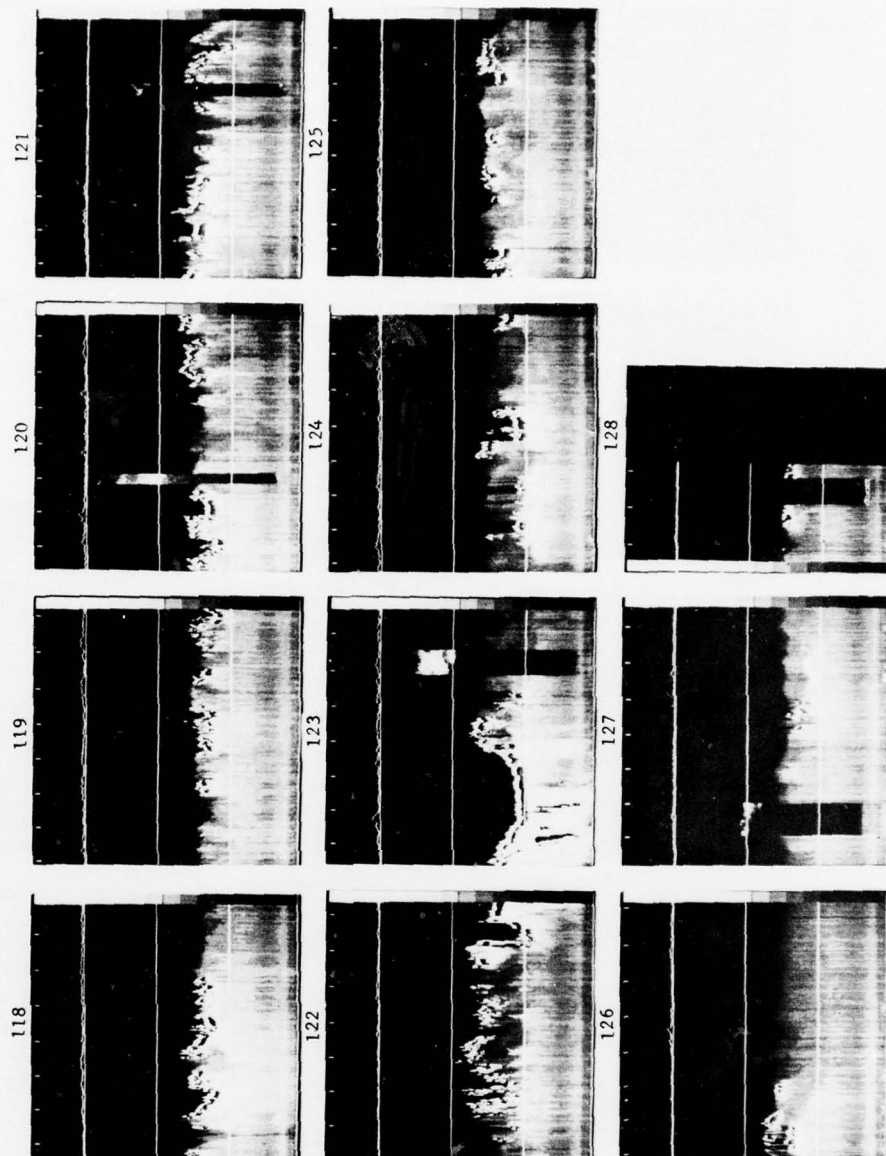
* No 1940 tick.
† Time gap 2140-2153.
‡ Time gap 0510-0936.
§ Time gap 1039-1057.



LIDAR BACKSCATTER HEIGHT/TIME TV DISPLAYS (118-128)

Day	Frame Number	Time (GMT)	
		First Tick	Last Tick
142	118	1300	1400
	119	1410	1520
	120	1530	1630
	121	1640	1740
142	122	1800	1900
	123	1910	2010
	124	2020	2130
	125*	2140	2250
142	126	2300	0010
	127	0020	0120
	128	0130	0150

* Time gap 2140-2153.



LIDAR BACKSCATTER HEIGHT/TIME TV DISPLAYS (129-140)

Day	Frame Number	Time (GMT)	
		First Tick	Last Tick
143 (May 23)	129	0230	0330
	130*	0340	1022
	131	1030	1140
	132	1150	1250
143	133	1300	1400
	134†	1420	1520
	135	1530	1630
	136	1640	1750
143	137	1800	1900
	138	1910	2010
	139‡	2020	2150
	140	2200	2310

* Time gap 0444-1022.

† No 1410 tick.

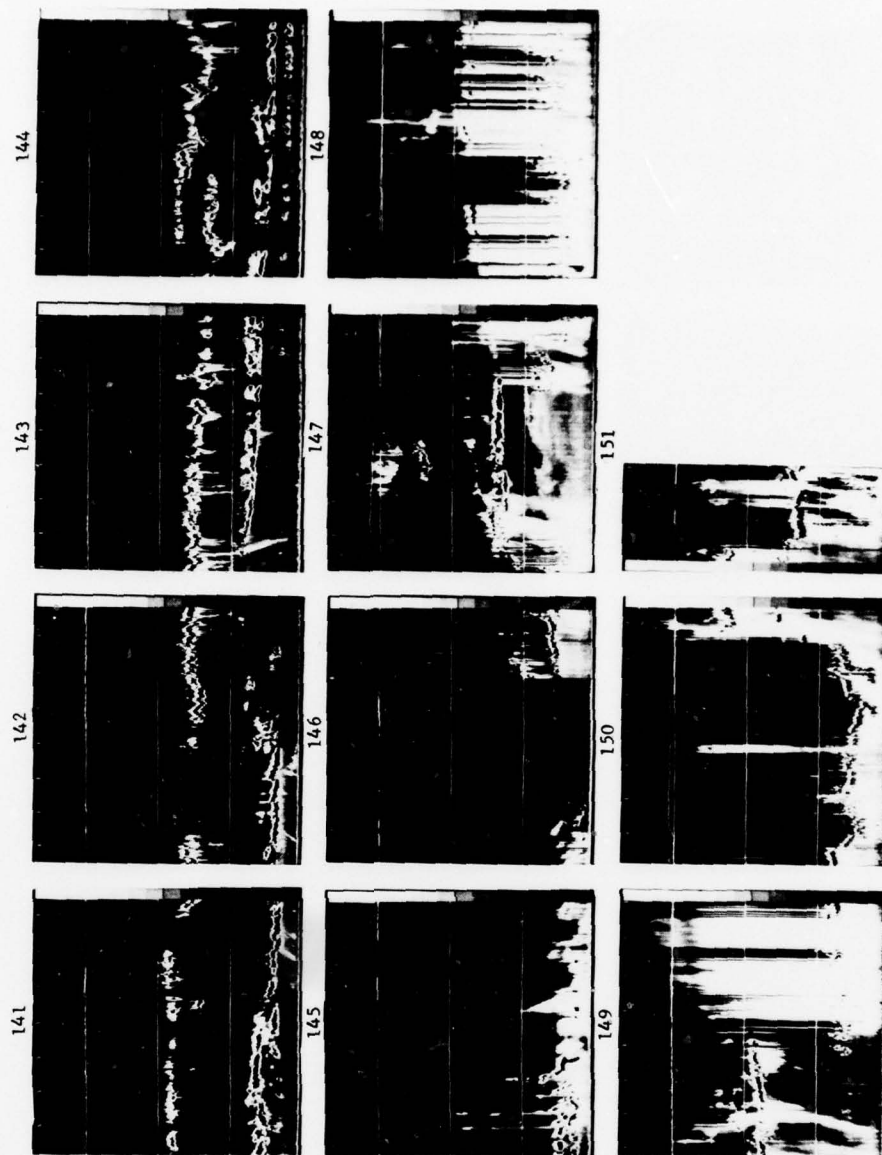
‡ Time gap 2026-2050; 3rd tick is 2050.



LIDAR BACKSCATTER HEIGHT/TIME TV DISPLAYS (141-151)

Day	Frame Number	Time (GMT)	
		First Tick	Last Tick
143	141	2320	0020
	142	0030	0130
	143	0140	0250
	144	0300	0400
144 (May 24)	145*	0410	0510
	146†	0530	0820
	147	0830	0940
	148	0950	1050
144	149	1100	1210
	150	1220	1320
	151	1330	1350

* No 0520 tick.
† Time gap 0614-0810.



LIDAR BACKSCATTER HEIGHT/TIME TV DISPLAYS (152-163)

Day	Frame Number	Time (GMT)	
		First Tick	Last Tick
144	152	1420	1520
	153	1530	1630
	154	1650	1750
	155	1800	1900
144	156	1910	2020
	157	2030	2130
	158	2140	2240
	159	2250	0000
145 (May 25)	160	0010	0110
	161	0120	0220
	162	0230	0340
	163	0350	0450



LIDAR BACKSCATTER HEIGHT/TIME TV DISPLAYS (164-174)

Day	Frame Number	Time (GMT)	
		First Tick	Last Tick
145	164*	0500	0810
	165	0820	0930
	166	0940	1040
	167	1050	1200
145	168	1210	1310
	169	1320	1420
	170	1430	1540
	171	1550	1650
145	172	1700	1810
	173	1820	1920
	174†	1930	2000

* Time gap 0601-0810.

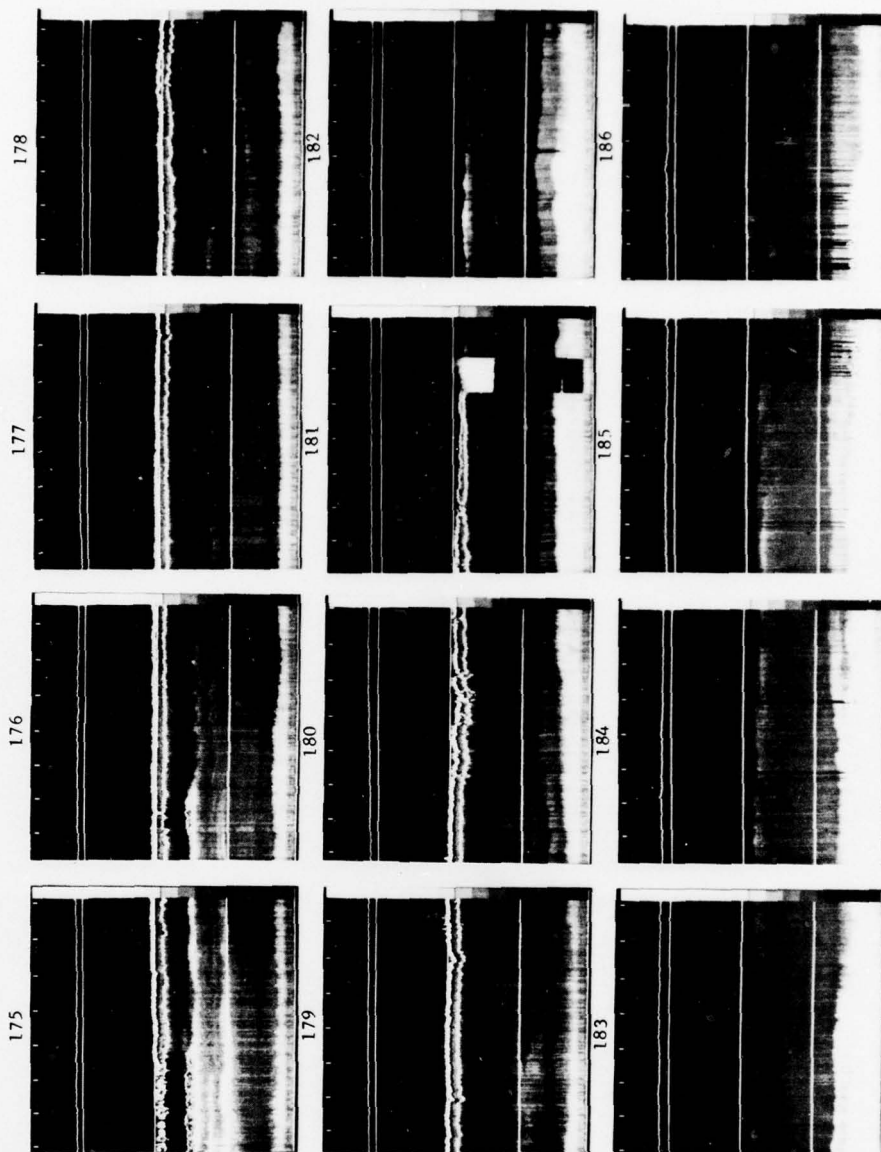
† Time gap 1937-1951.



LIDAR BACKSCATTER HEIGHT/TIME TV DISPLAYS (175-186)

Day	Frame Number	Time (GMT)	
		First Tick	Last Tick
145	175	2010	2120
	176	2130	2230
	177	2240	2340
	178	2350	0100
146 (May 26)	179	0110	0210
	180	0220	0330
	181	0340	0440
	182	0450	0550
146	183*	0600	0730
	184	0740	0840
	185	0850	0950
	186	1000	1110

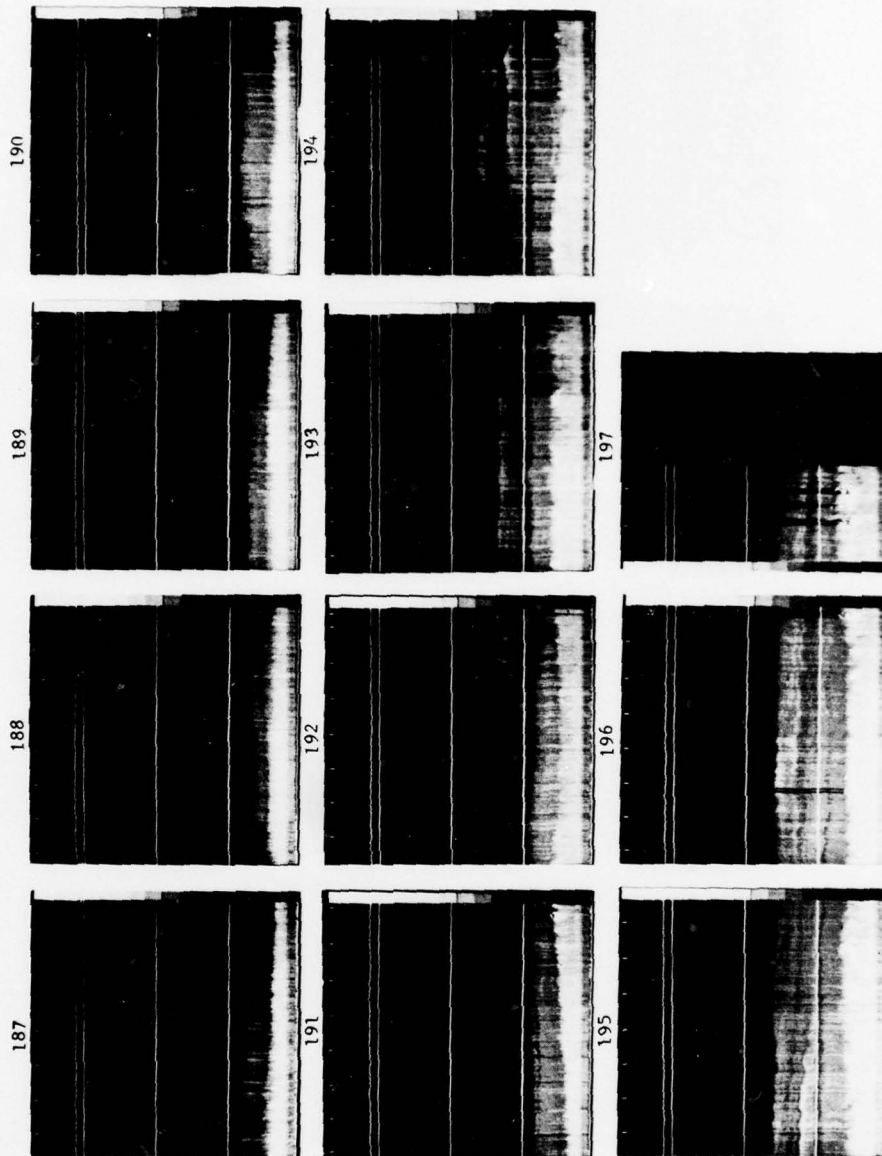
* Time gap 0654-0713.



LIDAR BACKSCATTER HEIGHT/TIME TV DISPLAYS (187-197)

Day	Frame Number	Time (GMT)	
		First Tick	Last Tick
146	187	1120	1220
	188	1230	1340
	189	1350	1450
	190	1500	1600
146	191	1610	1720
	192*	1730	1853
	193	1900	2000
	194	2010	2120
146	195	2130	2230
	196	2240	2350
	197	0000	0010

* Time gap 1833-1853.



LIDAR BACKSCATTER HEIGHT/TIME TV DISPLAYS (198-208)

Day	Frame Number	Time (GMT)	
		First Tick	Last Tick
147 (May 27)	198*	0030	0150
	199	0200	0300
	200†	0310	0410
	201	0720	0830
147	202	0840	0940
	203	0950	1100
	204	1110	1210
	205	1220	1320
147	206	1330	1440
	207	1450	1604
	208	1610	--

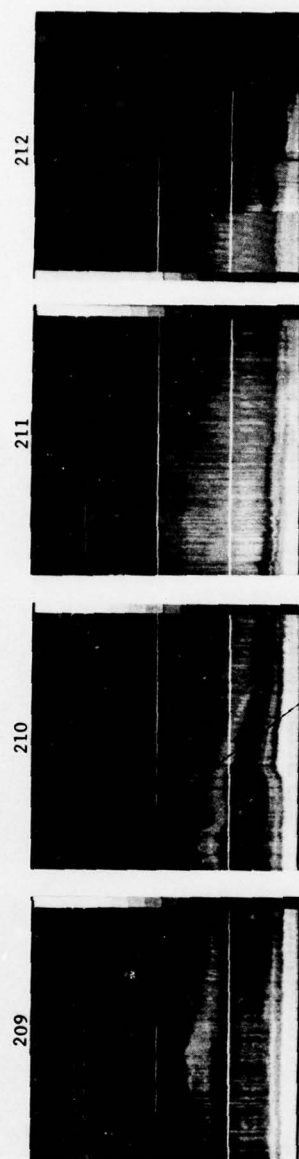
* Time gap 0130-0148.

† Time gap 0414-0713.



Day	Frame Number	Time (GMT)	
		First Tick	Last Tick
147	209	1640	1740
	210	1750	1900
	211	1910	2010
	212*	2020	0540

LIDAR BACKSCATTER HEIGHT/TIME TV DISPLAYS (209-212)



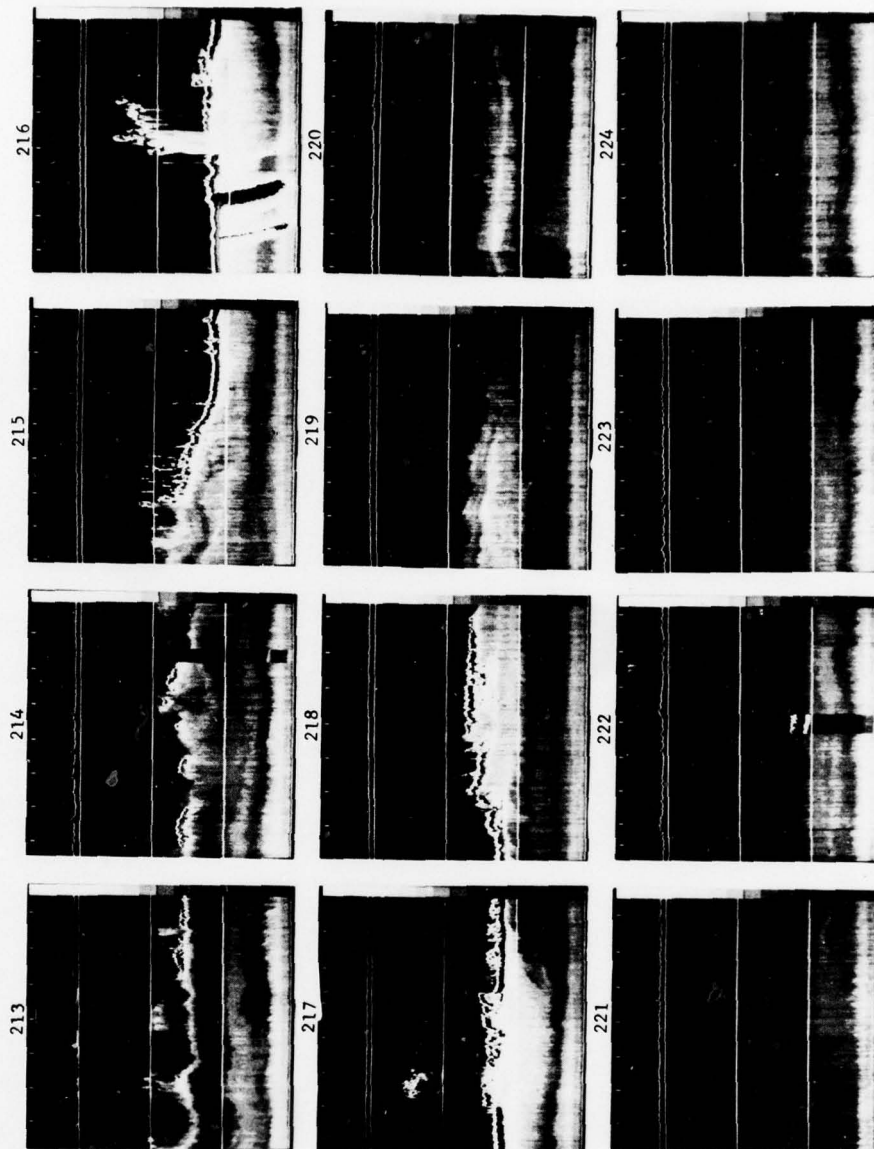
* Time gap 2033-0502.

LIDAR BACKSCATTER HEIGHT/TIME TV DISPLAYS (213-224)

Day	Frame Number	Time (GMT)	
		First Tick	Last Tick
151 (May 31)	213	0600	0700
	214	0710	0810
	215	0820	0930
	216	0940	1040
151	217	1050	1150
	218*	1210	1310
	219	1320	1420
	220	1430	1540
151	221	1550	1650
	222†	1700	1820
	223	1830	1930
	224	1940	2040

* No 1200 tick.

† Time gap 1705-1719.

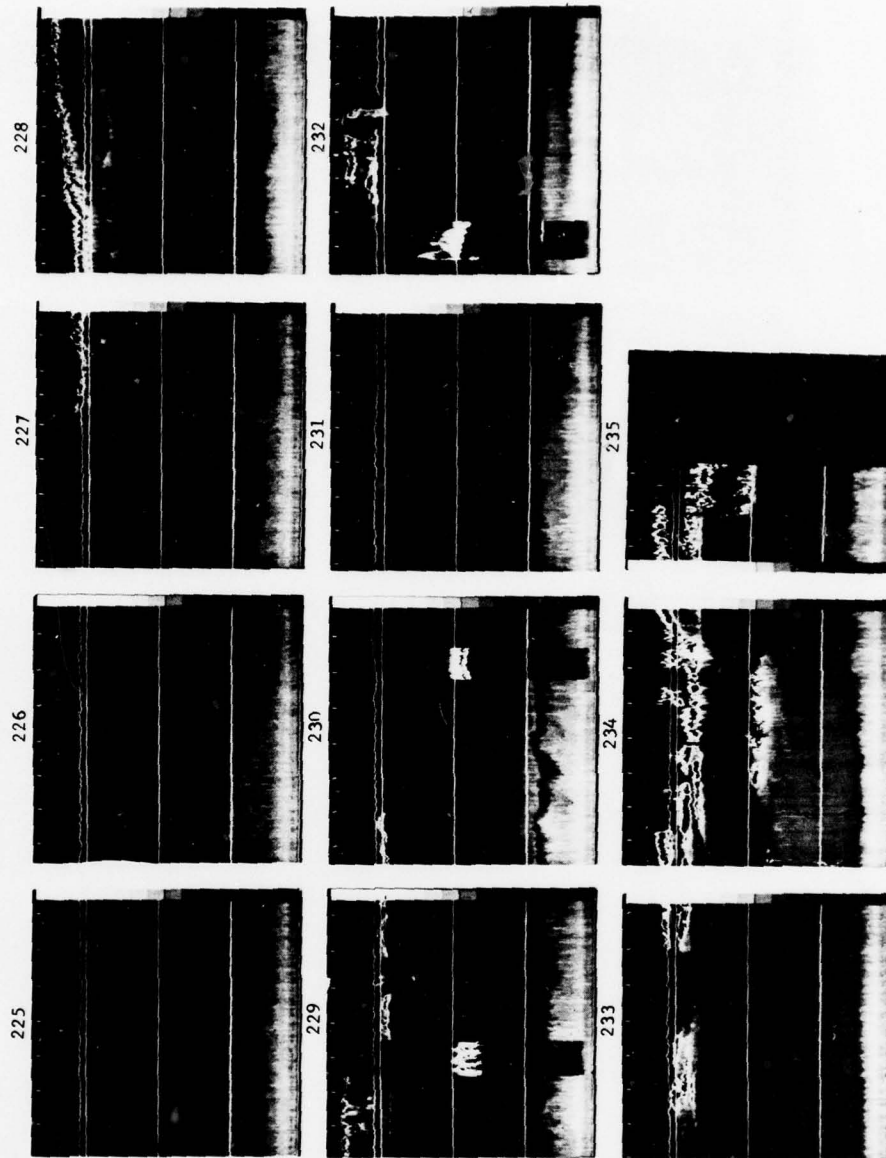


LIDAR BACKSCATTER HEIGHT/TIME TV DISPLAYS (225-235)

Day	Frame Number	Time (GMT)	
		First	Last Tick
151	225*	2100	2200
	226	2210	2310
	227	2320	0030
	228	0040	0150
152 (June 1)	229	0200	0300
	230	0310	0410
	231	0420	0530
	232†	0540	0650
	233	0700	0810
152	234	0820	0920
	235	0930	0950

* No 2050 tick.

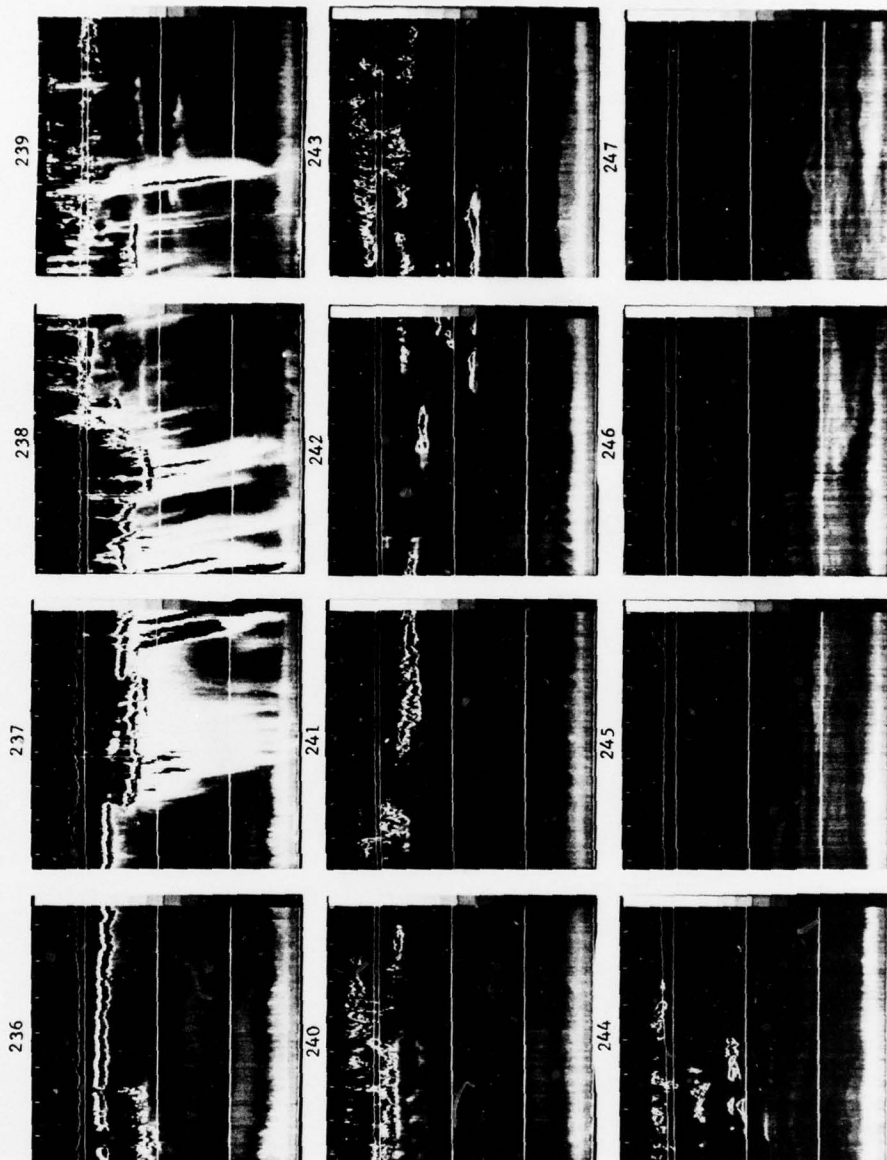
† Time gap 0607-0621.



LIDAR BACKSCATTER HEIGHT/TIME TV DISPLAYS (236-247)

Day	Frame Number	Time (GMT)	
		First Tick	Last Tick
152	236	1010	1110
	237	1120	1220
	238	1230	1340
	239	1350	1450
152	240	1500	1610
	241*	1620	1735
	242	1740	1840
	243	1850	2000
152	244	2010	2110
	245	2120	2230
	246	2240	2340
	247	2350	0050

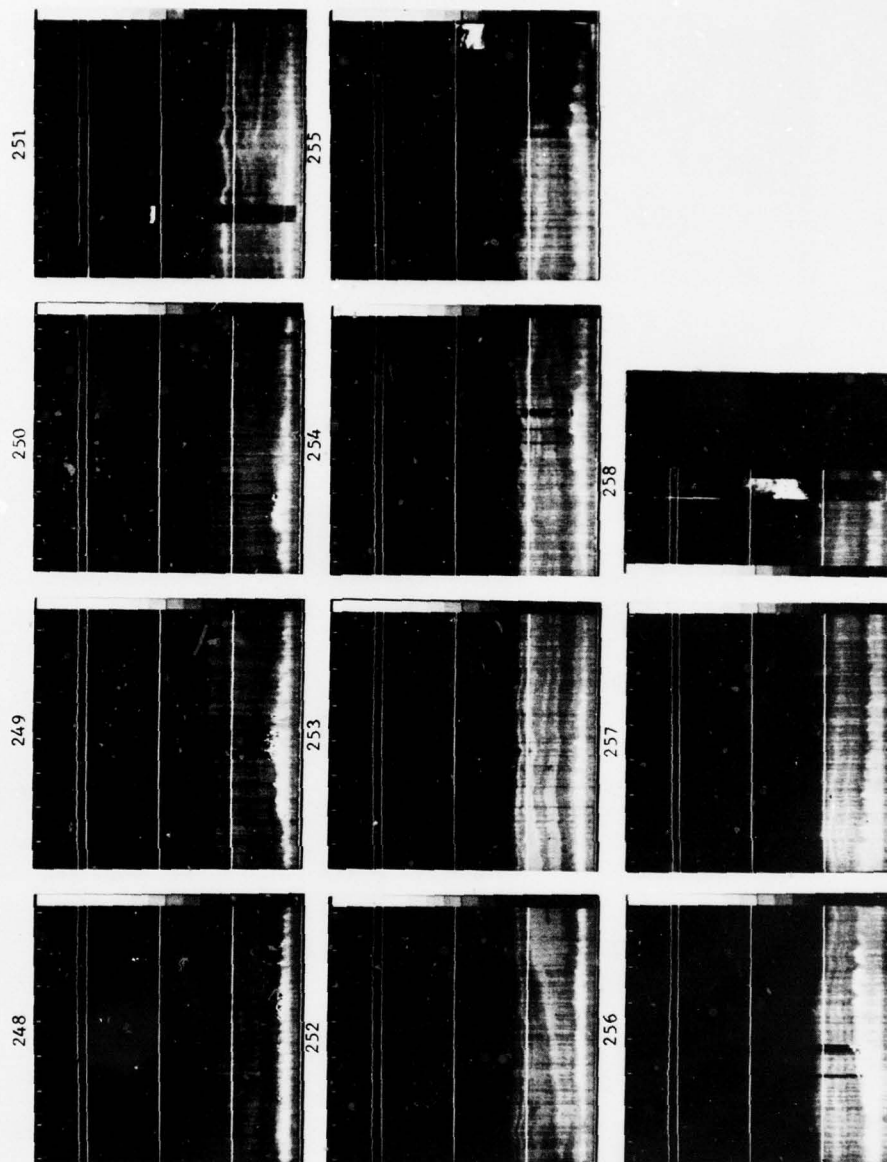
* Time gap 1722-1733.



LIDAR BACKSCATTER HEIGHT/TIME TV DISPLAYS (248-258)

Day	Frame Number	Time (GMT)	
		First Tick	Last Tick
153 (June 2)	248	0100	0210
	249	0220	0320
	250*	0330	0600
	251	0610	0710
153	252	0720	0830
	253	0840	0940
	254	0950	1050
	255	1100	1210
153	256	1220	1320
	257	1330	1440
	258	1450	1500

* Time gap 0435-0559.



AD-A065 267

NAVAL RESEARCH LAB WASHINGTON D C
THE EOMET CRUISE OF THE USNS HAYES: MAY - JUNE 1977.(U)
JAN 79 S G GATHMAN, B G JULIAN
NRL-MR-3924

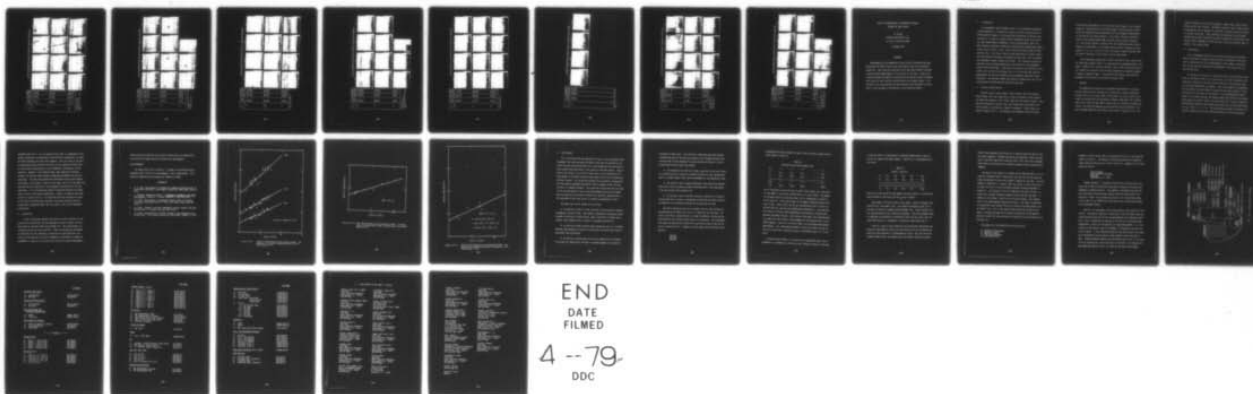
F/G 4/2

UNCLASSIFIED

NL

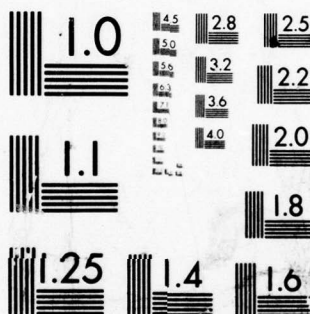
4 OF 4

AD
A065267



END
DATE
FILMED

4 -- 79
DDC

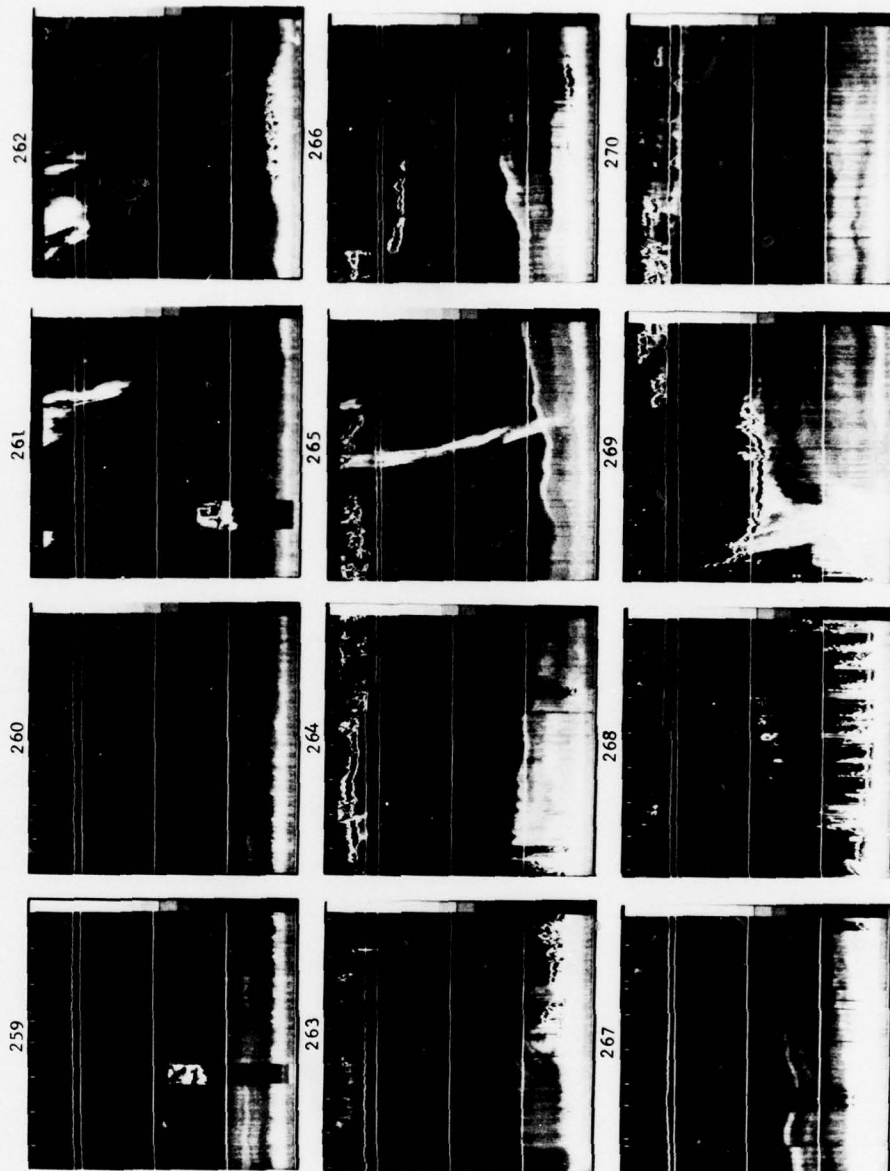


MICROCOPY RESOLUTION TEST CHART
NATIONAL BUREAU OF STANDARDS-1963-A

LIDAR BACKSCATTER HEIGHT/TIME TV DISPLAYS (259-270)

Day	Frame Number	Time (GMT)	
		First Tick	Last Tick
153	259	1520	1630
	260*	1640	1800
	261	1810	1910
	262	1920	2020
153	263	2030	2140
	264†	2150	2300
	265	2310	0010
	266	0020	0130
154 (June 3)	267‡	0140	0300
	268	0310	0420
	269	0430	0530
	270	0540	0640

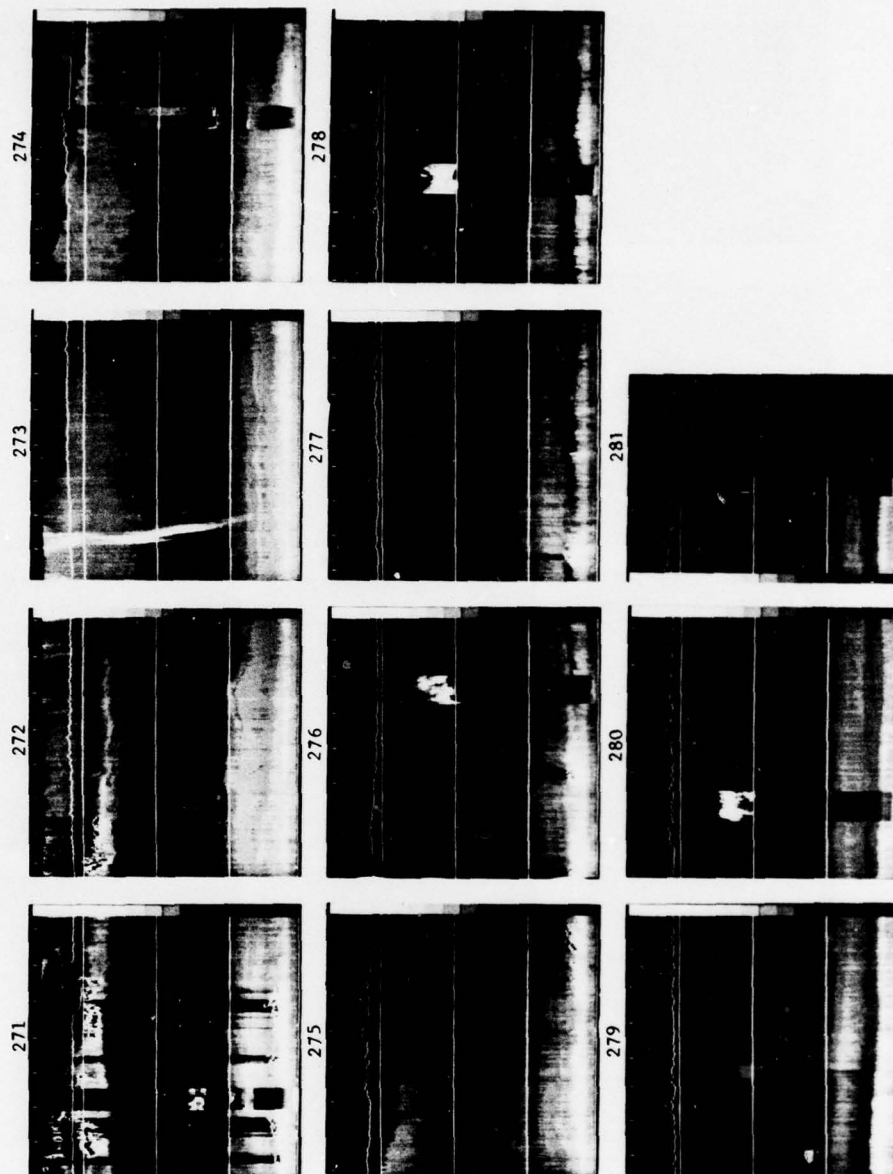
* Time gap 1705-1722.
† Time gap 2232-2237.
‡ Time gaps 0140-0150, 0240-0250.



LIDAR BACKSCATTER HEIGHT/TIME TV DISPLAYS (271-281)

Day	Frame Number	Time (GMT)	
		First Tick	Last Tick
154	271	0650	0800
	272*	0810	0930
	273	0940	1040
	274	1050	1150
154	275	1200	1310
	276	1320	1420
	277	1430	1530
	278	1540	1650
154	279†	1700	1810
	280	1820	1930
	281	1940	1950

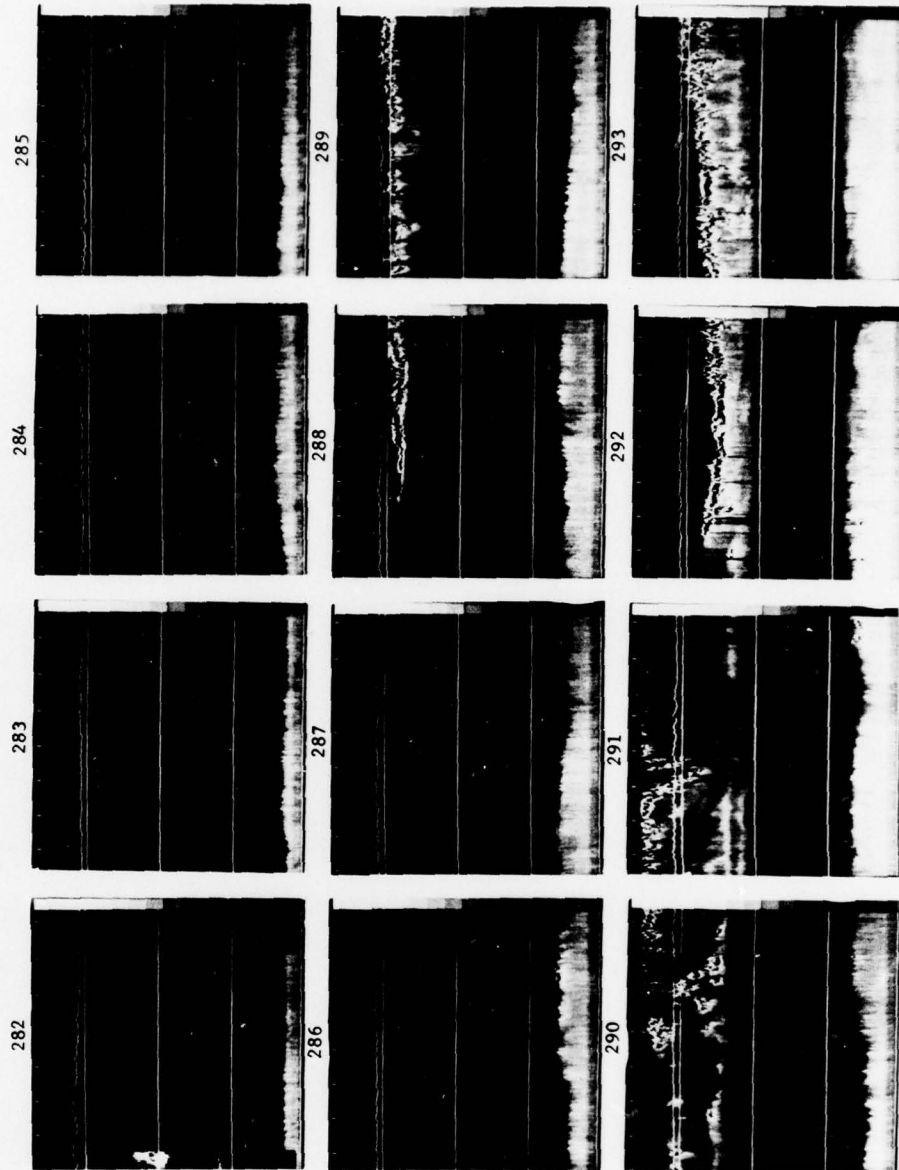
* Time gap 0807-0821; 2nd tick is 0830.
 † Time gap 1724-1736.



LIDAR BACKSCATTER HEIGHT/TIME TV DISPLAYS (282-293)

Day	Frame Number	Time (GMT)	
		First Tick	Last Tick
154	282	2020	2120
	283	2130	2230
	284	2240	2350
	285	0000	0100
155 (June 4)	286	0110	0210
	287	0220	0330
	288	0340	0440
	289	0450	0550
155	290	0600	0710
	291*	0720	0840
	292	0850	0950
	293	1000	1100

* Time gap 0809-0823.



LIDAR BACKSCATTER HEIGHT/TIME TV DISPLAYS (294-304)

Day	Frame Number	Time (GMT)	
		First Tick	Last Tick
155	294*	1120	1220
	295	1230	1330
	296	1340	1450
	297	1500	1600
155	298	1610	1710
	299†	1720	1840
	300	1850	1950
	301	2000	2110
155	302	2120	2220
	303	2230	2340
	304‡	2350	0000

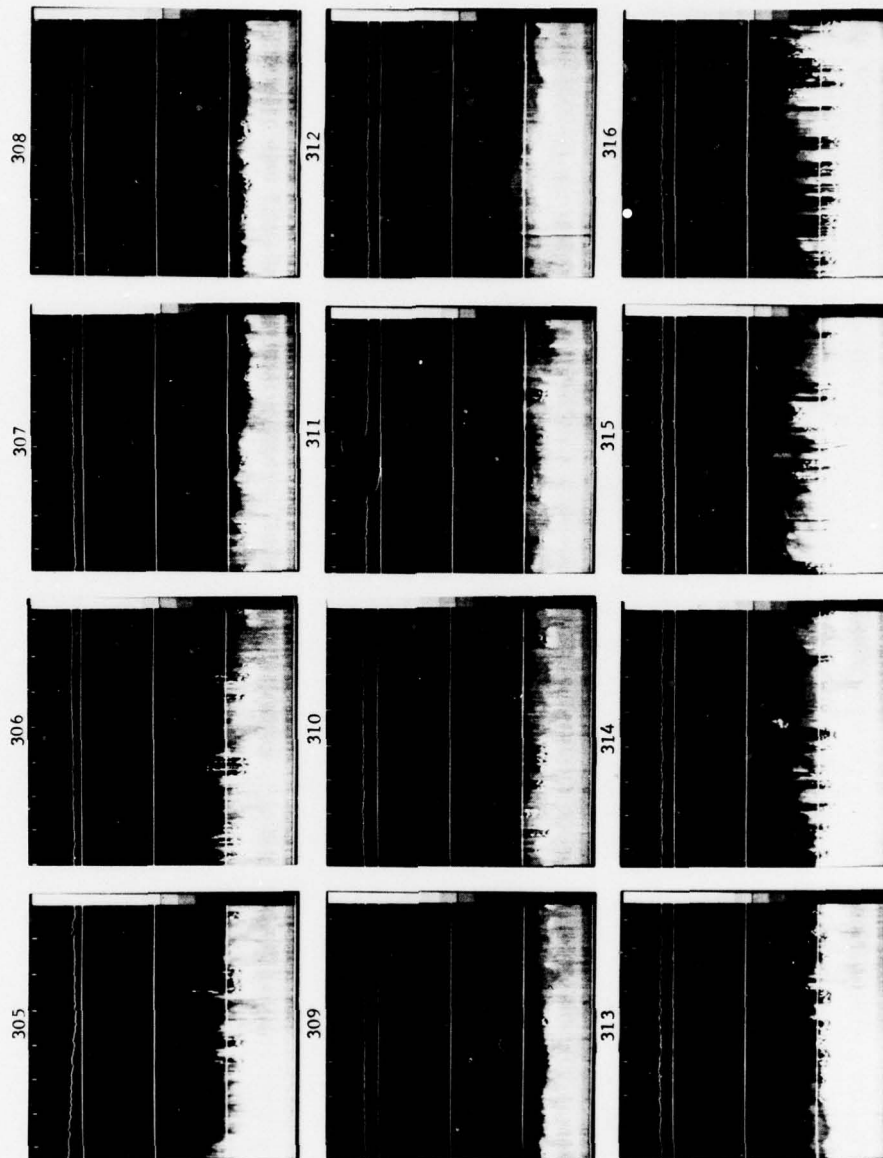
* No 1110 tick.
† Time gap 1723-1735.
‡ Time gap 0008-0016 (picture 305).



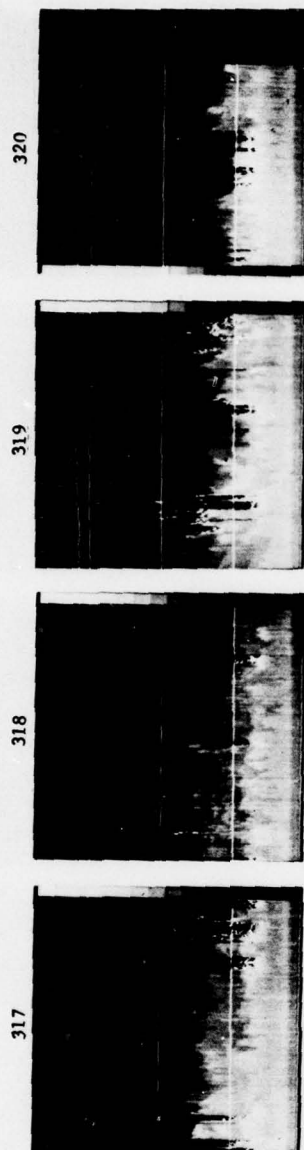
LIDAR BACKSCATTER HEIGHT/TIME TV DISPLAYS (305-316)

Day	Frame Number	Time (GMT)	
		First Tick	Last Tick
156	305	0020	0120
	306	0130	0240
	307	0250	0350
	308	0400	0510
156	309	0520	0620
	310	0630	0730
	311	0740	0850
	312*	0900	1020
156	313	1030	1130
	314	1140	1240
	315	1250	1400
	316	1410	1510

* Time gap 0904-0920.



LIDAR BACKSCATTER HEIGHT/TIME TV DISPLAYS (317-320)



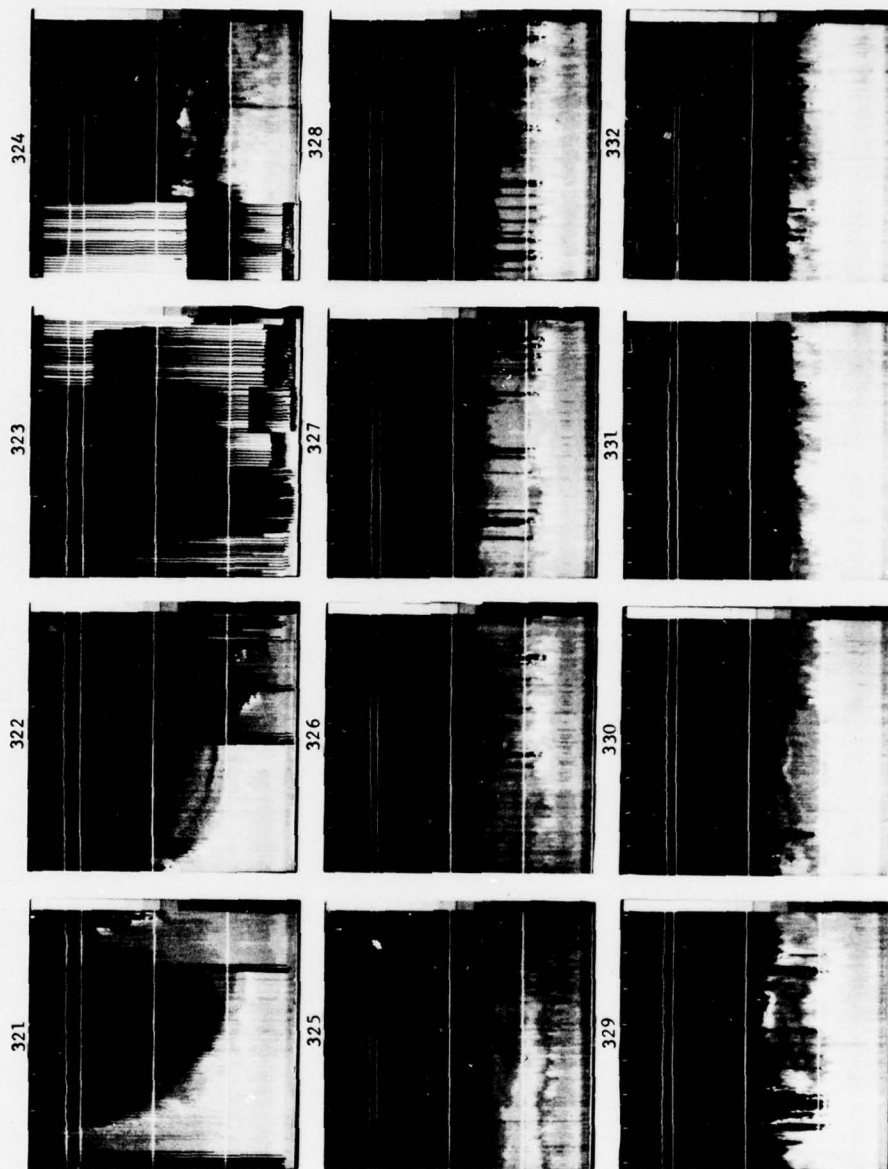
Day	Frame Number	Time (GMT)	
		First Tick	Last Tick
156	317	1520	1620
	318*	1640	1750
	319	1800	1900
	320	1910	2000

* No 1630 tick; time gap 1730-1741.

LIDAR BACKSCATTER HEIGHT/TIME TV DISPLAYS (321-332)

Day	Frame Number	Time (GMT)		
		First Tick	Last Tick	
156	321	2020	2030	
	322	2040	-	
	323	2050	-	
	324*	2100	2200	
156	325	2210	2310	
	326	2320	0020	
	327†	0040	0140	
	328	0150	0250	
157 (June 6)	329	0300	0410	
	330	0420	0520	
	331	0530	0630	
	332‡	0640	0800	

* Time gap 2103-2108
† No 0030 tick.
‡ Time gap 0714-0731.



LIDAR BACKSCATTER HEIGHT/TIME TV DISPLAYS (333-343)

Day	Frame Number	Time (GMT)	
		First Tick	Last Tick
157	333	0820	0920
	334	0930	1030
	335	1040	1150
	336	1200	1300
157	337	1310	1410
	338	1420	1530
	339	1540	1640
	340	1650	1800
157	341*	1810	2040
158	342†	2050	0510
(June 7)	343	0520	0530

* Time gap 1900-2030.

† Time gaps 2101-0324, 0400-0454. 3rd tick is 0330.



SATELLITE OBSERVATIONS OF ATMOSPHERIC AEROSOLS
DURING THE EOMET CRUISE

M. Griggs
SCIENCE APPLICATIONS, INC.
La Jolla, California 92038

28 August 1978

ABSTRACT

Measurements of the atmospheric aerosol optical thickness were made during the 1977 EOMET cruise across the Atlantic Ocean and the Mediterranean Sea. These data were obtained at the same time as NOSS-5 and GOES visible radiance measurements in the vicinity of the ship. Linear relationships between the upwelling radiance and the aerosol optical thickness were found for each satellite, confirming earlier Landsat results. Differences in the relationships for each satellite are attributed to differences in the radiometric calibrations of the satellite sensors.

1. Introduction

The atmospheric marine boundary layer is of considerable importance to Navy operations. Of particular interest, with the increasing use of electro-optical systems, is the nature and distribution of aerosols over the oceans. In order to provide further information about the aerosols, and other meteorological parameters in the marine boundary layer, the Naval Research Laboratory conducted an Electro-Optical Meteorology (EOMET) cruise, May 15 to June 6, 1977, across the North Atlantic Ocean and Mediterranean Sea. This cruise offered a good opportunity to further investigate the satellite technique, developed by Griggs (1975, 1977) to measure the atmospheric aerosol content over oceans. This technique relates the upwelling visible radiance measured by the satellite to the atmospheric aerosol optical thickness. Since 60% of the aerosols are typically in the lowest 1 km, and 90% in the lowest 3 km, it is clear that the satellite measurements can provide information of considerable importance to Navy operations. The previous studies were based on Landsat data, but for this investigation the NOAA and GOES satellites were used.

2. Previous Landsat Results

Previous results using Landsat 1 data (Griggs, 1975) and Landsat 2 data (Griggs, 1977) have shown that a linear relationship exists between the upwelling radiance in the visible region and the aerosol content. Data have been obtained at several sites, the largest data set being for the Pacific Ocean at San Diego for Landsat 2 overpasses. These results are shown in Figure C-VII-1. The radiances are determined from the Landsat

digital data (densitometry of the black and white imagery is not accurate enough for intercomparison of different images), and the aerosol content values are determined with ground-based Voiz sun photometer measurements at the time of the Landsat overpass. The aerosol content is defined in terms of the Elterman (1964) model vertical aerosol optical thickness; i.e., the aerosol content is given by the ratio (measured aerosol optical thickness at wavelength λ to the model aerosol optical thickness at wavelength λ) $\times N$; i.e., a value of $2N$ for the aerosol content indicates that the optical thickness is twice that of the Elterman model.

The relationships appear best for MSS 5 and MSS 6; this is due to the fact that the radiance in MSS 4 is affected more by suspended matter in the water. Figure C-VII-1 does not show MSS 7 data, since the digital data for this channel are uncertain owing to NASA procedures for producing Landsat 2 computer compatible types. The measured relationships show excellent agreement with theoretical calculations (Griggs, 1978).

3. Approach

Arrangements were made for sun photometer measurements of the atmospheric aerosol optical thickness to be taken daily, weather permitting, on board the U.S.N.S. Hayes (EOMET cruise vessel) at times as nearly coincident as possible with the overpasses of NOAA-5 (0800-1000 local standard time) and at 1600 GMT, when GOES-1 digital data are routinely recorded and stored. The radiances measured by the satellites must be modified in order to compare them with the Landsat values shown in Figure C-VII-1. The

Landsat radiances are for the multispectral scanner (MSS) spectral band-passes and for nadir viewing. The NOAA-5 and GOES-1 have slightly different bandpasses, and in general the radiances of interest are not obtained in the nadir direction. These radiances are normalized to the Landsat viewing and sun angle conditions by means of theoretical calculations with the Dave (1972) atmospheric scattering code, which was previously used in support of the Landsat study.

4. Data Analysis

The sun photometer data had to be carefully reviewed since measurements are difficult to make on board ship due to the motion of the ship. This is especially true for the measurement of the airmass; fortunately this can be precisely calculated from knowledge of the location of the ship and the time.

The location of the ship as a function of time, and the orbital parameters of the NOAA-5, which is in a polar orbit, are used to determine the respective locations of the ship and the satellite at the time the satellite radiance measurement is acquired. Then, using spherical trigonometry, the sun zenith (θ_0) and azimuth (ϕ) angles and the viewing angle (θ) from the satellite to the ship are calculated. For the geosynchronous GOES-1, which is at a fixed location, the required angles are similarly calculated. These angles are used as input to the Dave code which is used to normalize the measured radiance to the standard conditions used for the Landsat data, viz. $\theta_0 = 63.3^\circ$, $\phi = 0$, $\theta = 0$. The calculations are made for each pair of satellite radiance and aerosol content observations, using the measured

aerosol content as input to the code. The aerosol model used in the code is one that gave good agreement with the Landsat-2 data, i.e., a Junge size distribution with $v = 4.0$ and refractive index $n = 1.5$. Thus, the normalized radiance (I) is given by

$$I = I_m \times \frac{I_c(0, 63.3^\circ, 0, N_m)}{I_c(\theta, \theta_0, \phi, N_m)}$$

when I_m is the measured radiance
 I_c is the calculated radiance
 N_m is the measured aerosol content

The calculations are performed at $0.67 \mu\text{m}$ for the NOAA-5 Scanning Radiometer (SR) and at $0.64 \mu\text{m}$ for the GOES Visible Infrared Spin Scan Radiometer (VISSR).

The satellite data were obtained in digital form from the National Environmental Satellite Service (NESS) of NOAA. The SR data were available only in the mapped format (with 20 km resolution) for this investigation, and did not provide all the resolution elements actually measured during the satellite overpasses. Another shortcoming of the SR data is the fact that the SR output is subject to a non-random noise which cannot be readily eliminated. In an attempt to minimize these effects, each SR radiance reported here is the mean of a 5×5 block of pixels centered on the calculated ship location. The VISSR radiances (with 6 km resolution) reported here are also the means of 5×5 blocks of pixels. The radiances are given in units of $\text{mW}/\text{cm}^2/\mu\text{m}/\text{sr}$, and are based on calibration data

obtained from NESS, converting digital counts to foot-lamberts, in the case of the SR, and directly into radiance units in the case of the VISSR.

5. Results

The weather during the cruise was generally quite good, enabling coincident sun photometer and satellite measurements to be obtained on several occasions. The GOES coverage of the Atlantic Ocean is good only to about 25° W longitude, which was reached by the U.S.N.S. Hayes on May 24, 1977. In these first ten days, sets of data were obtained on six occasions for the GOES. During the same time period, six sets of data were also obtained for NOAA-5 overpasses. However, after May 24, 1977, ten more days were spent at sea, but only three more sets of data were obtained for the NOAA-5 overpasses.

The GOES VISSR data, plotted in Figure C-VII-2 show an excellent linear relationship, as anticipated from the Landsat results, and shows that normalization procedures with the Dave code are satisfactory.

The NOAA-5 data were not expected to be very useful due to their format and noise problems, as described above. However, in spite of these shortcomings, the relationship shown for the SR radiances in Figure C-VII-3 is remarkably good. A linear relationship can probably be inferred. The x-points show an enhanced radiance due to sun-glitter, and demonstrate that observations should be made away from the sun, except close to the nadir as illustrated by the o-point.

In comparing these results with those of Landsat 2, taking into account the wavelength differences, it is found that for the SR data, the

radiance value for $N = 0$ is as expected (this value is independent of the aerosol properties, and represents a pure molecular atmosphere), but that the other radiances are lower than expected. This can be due to the aerosol properties being different from those of the Landsat San Diego data, or can be due to uncertainties in the radiometric calibrations in each satellite. However, in the Landsat Study, data obtained at Adrigole, Ireland, for Atlantic Ocean aerosols showed good agreement with the San Diego data. The same study showed that differences also existed between the Landsat 1 and Landsat 2 results at San Diego, and it was concluded that they were due to differences in the radiometric calibrations of the two satellites. It is believed that similar calibration problems are responsible for the SR and Landsat differences. Indeed, in examining the VISSR results in Figure C-VII-2, it is found that both the intercept and slope of the line are significantly different from those predicted from the Landsat data, suggesting again that the reason is due to the radiometric calibrations.

6. Conclusions

A linear relationship between the upwelling visible radiance, as observed by the Landsat MSS, and the atmospheric aerosol content, has also been found for the GOES-VISSR and the NOAA-5 SR. The relationships are slightly different for each satellite. These differences are attributed to differences in the radiometric calibrations of the satellites, and points to the necessity of precise radiometric calibrations of satellite radiometers if they are to be used in the future for aerosol measurements.

Without precise calibration each satellite would have to be empirically calibrated with lengthy periods of ground truth measurements.

Acknowledgments

The author would like to thank Dr. L. Ruhnke for providing the sun photometer data, and for his encouragement in this investigation. This study was supported by ONR Contract No. N00014-77-C-0489.

REFERENCES

1. J. V. Dave, "Development of Programs for Computing Characteristics of Ultraviolet Radiation," Final Report Contract No. NAS5-21680, March 6, 1972.
2. L. Elterman, Atmospheric Optics, in Handbook of Geophysics and Space Environments, edited by S. Valley, McGraw-Hill, New York 1965.
3. M. Griggs, "Measurements of Atmospheric Aerosol Optical Thickness over Water Using ERTS-1 Data," J. Air. Poll. Contr. Assoc. 25, 622 (1975).
4. M. Griggs, "Comment on Relative Atmospheric Aerosol Content from ERTS Observations," J. Geophys. Res. 82, 4972 (1977).
5. M. Griggs, "Determination of Aerosol Content in the Atmosphere from Landsat Data," Final Report Contract No. NAS5-20899, January 17, 1978.

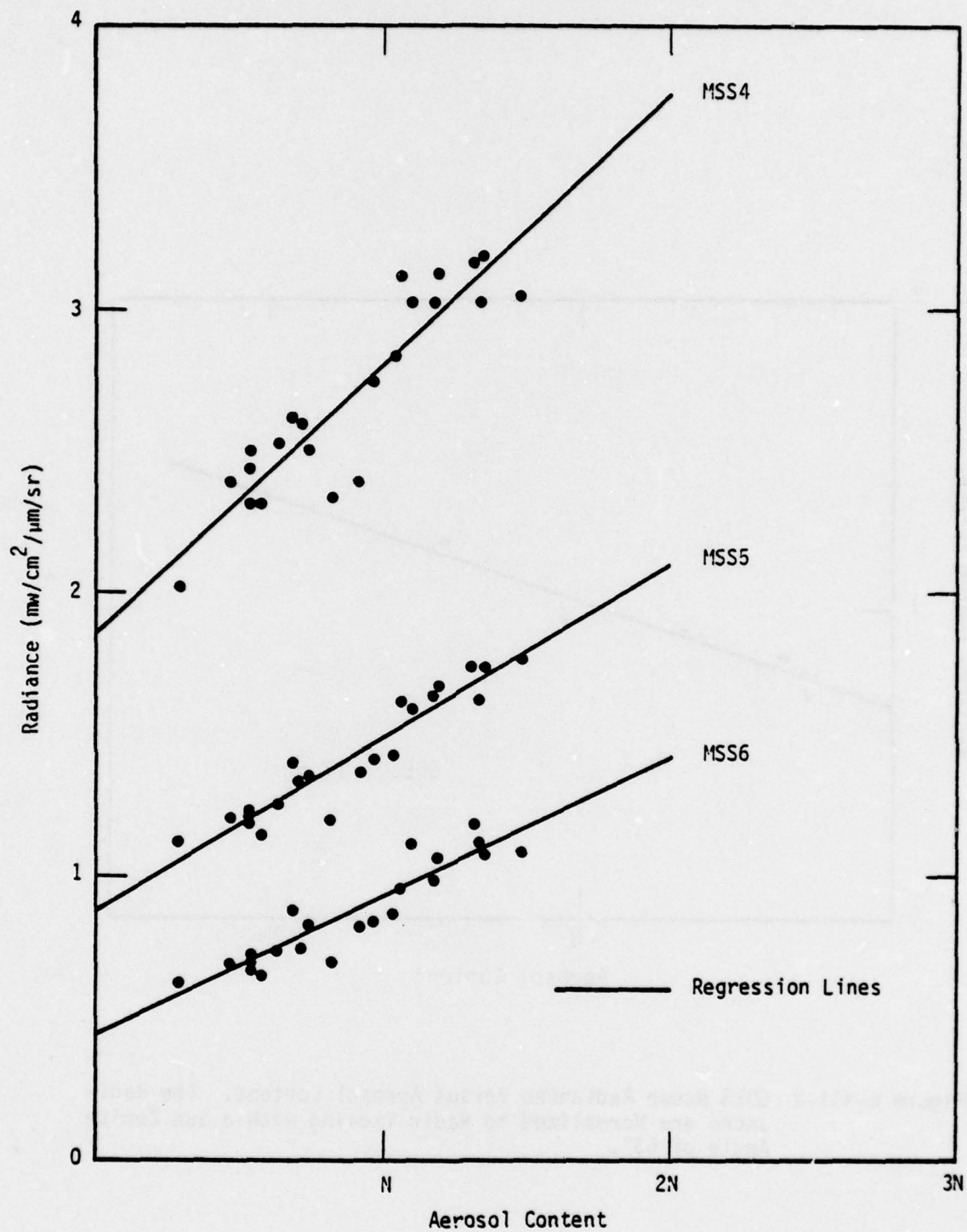


Figure C-VII-1 Landsat 2 Ocean Radiances Versus Aerosol Content. The Radiances are for Nadir Viewing Normalized to a Sun Zenith Angle of 63°.

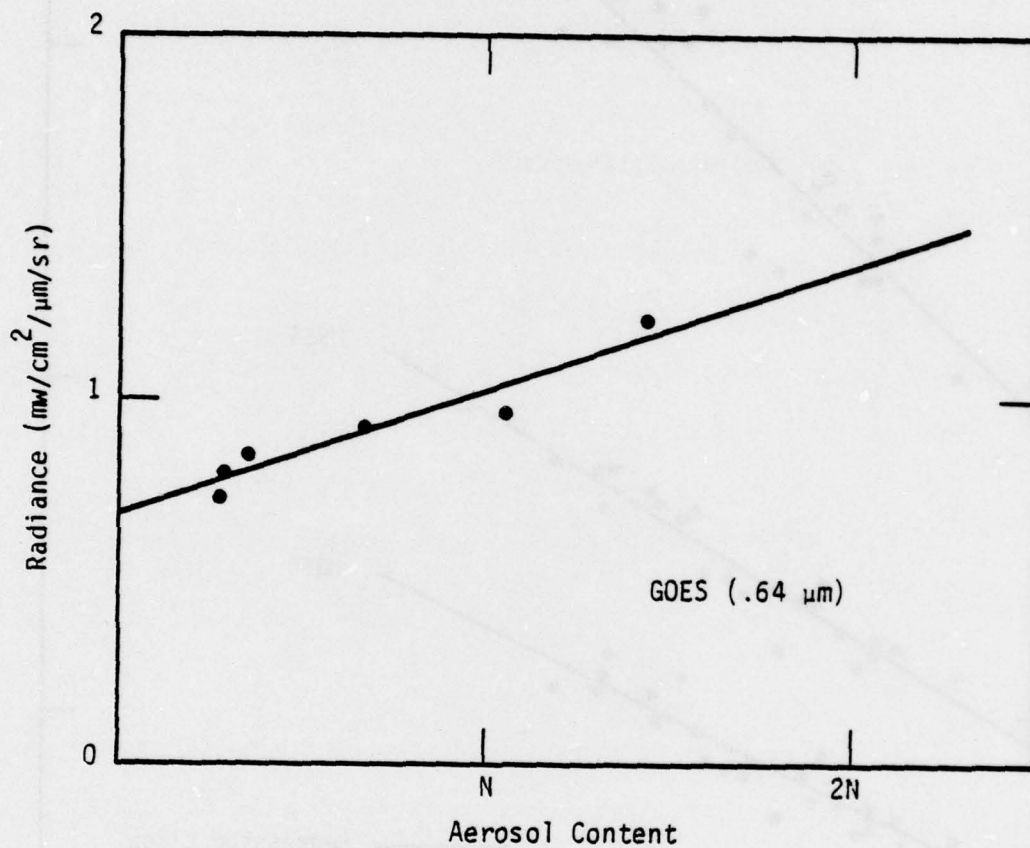


Figure C-VII-2 GOES Ocean Radiances Versus Aerosol Content. The Radiances are Normalized to Nadir Viewing with a Sun Zenith Angle of 63° .

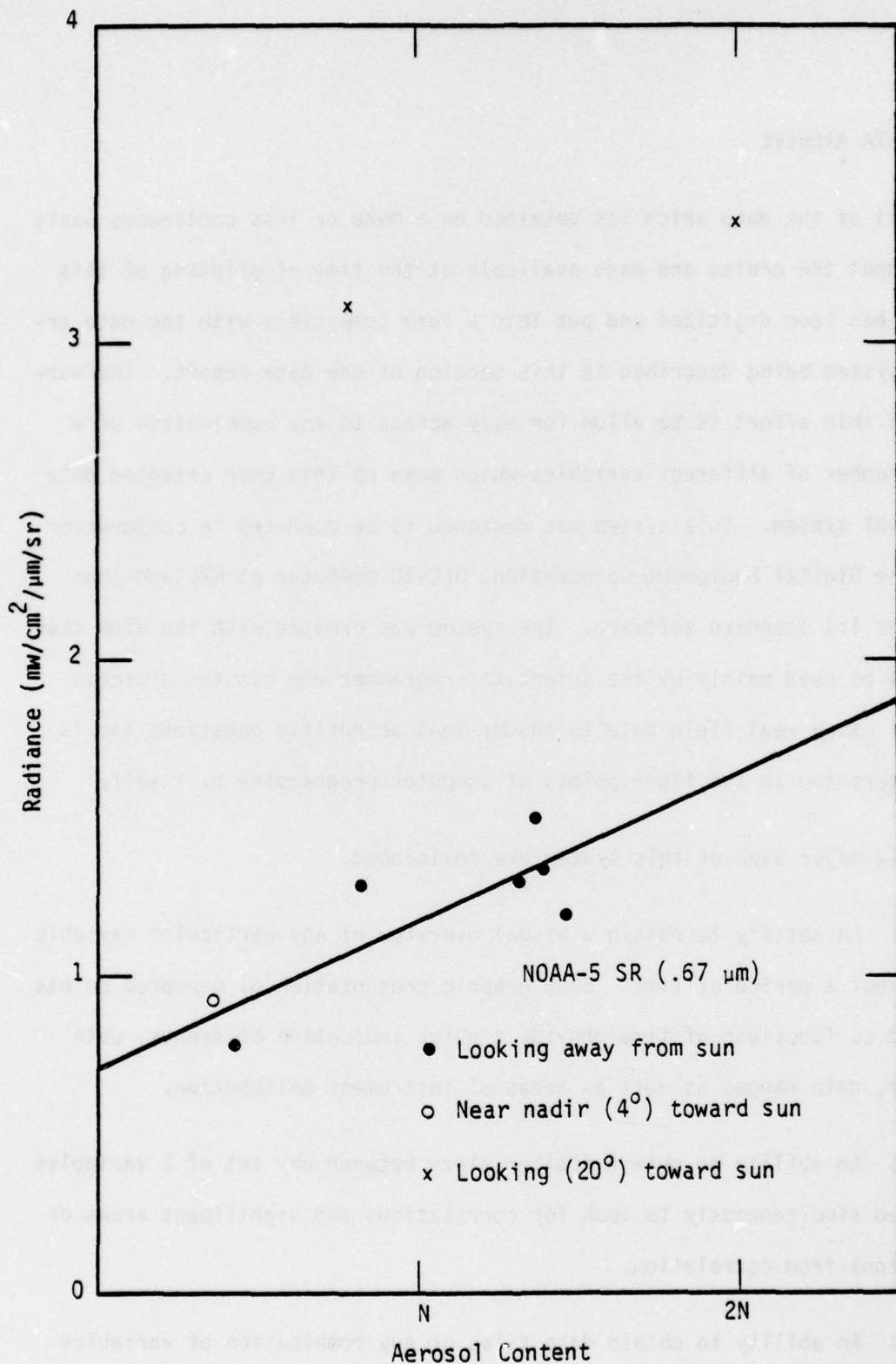


Figure C-VII-3 NOAA-5 Ocean Radiances Versus Aerosol Content. The Radiances are Normalized to Nadir Viewing with a Sun Zenith Angle of 63° .

D. DATA ARCHIVE

All of the data which was obtained on a more or less continuous basis throughout the cruise and made available at the time of printing of this report has been digitized and put into a form compatible with the data archive system being described in this section of the data report. The purpose of this effort is to allow for easy access to any combination of a large number of different variables which make up this user oriented data retrieval system. This system was designed to be operated in conjunction with the Digital Equipment Corporation, DEC-10 computer at NRL and thus utilizes its standard software. The system was created with the view that it will be used mainly by the scientist/programmer who has the ultimate goal of using real field data to answer real scientific questions and is not interested in the finer points of computer programming by itself.

Six major uses of this system are envisioned.

- 1) An ability to obtain a visual overview of any particular variable throughout a period of time. Such graphic presentation of measured points plotted as functions of time provide a quick indication of trends, data scatter, data ranges as well as areas of instrument malfunction.

- 2) An ability to obtain scatter plots between any set of 2 variables measured simultaneously to look for correlations and significant areas of deviations from correlation.

- 3) An ability to obtain data files of any combination of variables to be used for processing of the data in custom programs, and to make it

available to other users. This ability of combining and sorting should eliminate the need of the data user having to sort through and work with various forms of data presented in various formats and found in various diverse publications and/or data sheets.

4) The system has the ability to take a snap shot of any set of data at a desired period of time and it should be helpful if this system would plot in a graphic manner these various parameters in the appropriate form.

5) The system is able to make calculations from stored data measurements and is able to operate on these calculated data in the same manner as on the original data storage files.

6) The system is able to perform statistical analysis on its multi-variate data base in order to investigate correlations and other statistical measures of relationships between the various types of data.

The DEC-10 system utilizes disc resident files for data storage and the manipulation of these disc files is a simple task for the user. All files on the DEC-10 system consist of a name followed by a period and another group of up to three letters known as an extension. Thus throughout this report we describe the location of a particular piece of data as being in a particular file. Examples of files names used in the DEC-10 system are:

ASC.DAT
WHIT.DAT
CAL.DAT

Furthermore each data storage file used in this retrieval system has the format shown in Table D-1.

TABLE D-1

(Standard Format Data Storage Files)

D_1	1.	2.	3. m
T_1	$V_{1,1}$	$V_{1,2}$	$V_{1,3}$ $V_{1,m}$
T_3	V_{31}	V_{32}	V_{33} $V_{3,m}$
<hr/>				
D_{20}	1.	2.	3. m_1
T_{24}	$V_{24,1}$	$V_{24,2}$	$V_{24,3}$ V_{24,m_1}

Here D represents a date code such as 051577 which stands for 15 May 1977. For the EOMET 77 cruise the relation $51577 \leq D \leq 60777$ holds. The number of variables held in a particular data file is represented in Table D-1 by the letter m. After each D there are m numbers representing the m columns of data. Hours within the day are represented by the T's which are the GMT hours for the data code immediately preceeding it. Each date may have from 0 to 24 time values depending on how often the variables were measured throughout the day. Data stored in the matrix are represented by $V_{i,m}$ where m is the column or type parameter of the variable and i is the time parameter. Thus all V's with the same i are considered simultaneous measurements. This representation makes it easy to put data into the array and to search for a particular piece of information once it is in the array.

A second format (Format 1) is used by this system where each line of parameters is preceeded by a Julian day and a decimal fraction of that day.

In this way time is a monotonically increasing number which is easy to plot or to compare with other numbers. Table D-2 is a representation of this form.

TABLE D-2

Format 1 Type File

T_1	V_{11}	V_{12}	V_{13}	V_{14}	$\dots V_{1m}$
T_2	V_{21}	V_{22}	V_{23}	V_{24}	$\dots V_{2m}$

T_n	V_{n1}	V_{n2}	V_{n3}	V_{n4}	$\dots V_{nm}$

where the T_n are the Julian time numbers for which there is at least some data available in the array and the V_{nm} are as before.

Three types of files are used in the system. They are storage files, working files, and output files. The system is designed so that all of the data is stored in standard format storage files. These storage files are accessed mainly by two interactive programs. These two programs known as LOOK9.BAS and FIND.BAS are the means by which the user tells the computer which data he is interested in and what he wants done with it.

Figure D-1 shows a block diagram of the system where operational programs are represented by blocks and files which carry the information between the block operators are represented by lines. The solid lines are standard format files, the dashed lines are format 1 type files and the

dotted lines represent files which are of various types and used for output and/or graphing. Programs containing the extensions ".BAS" are operated in the BASIC mode while extensions with ".FTN" are Fortran programs. Blocks where the program has no extension represent DEC-10 system monitor commands.

The heart of the system is a program called LOOK9.BAS which is an interactive program written in BASIC which asks the user various questions about the working file which the program is making for the user. The final product of LOOK9.BAS is a format 1 type file which is itself then used as an input file for all of the different programs following LOOK9.BAS in Figure D-1. The contents of this file depend on the user's desires. In essence this program interfaces between the user and the data bank. It combines in one format 1 type file up to 8 data columns of any combinations of the simultaneously measured variables. The inputs to LOOK9.BAS are essentially data storage files but a provision has been added to use an "EXTRA" file. This is the feature which allows the system to test models, to manipulate data and to perform calculations on the measured data and to have this data available for further use on the system such as plotting, etc.

The output file from LOOK9.BAS has four main uses:

- 1) Graphical Presentation
- 2) Numerical Output
- 3) Statistical Analysis
- 4) Data manipulation

Examples of these various types of programs which exist in the system are shown in Figure D-1. The methods of obtaining analytical and numerical output from the data bank are listed in Table D-3. Requests for this data should be sent to:

Stuart Gathman
Naval Research Laboratory
Code 8327
Washington, D.C. 20375

Program FIND.BAS is a snapshot routine which is used to obtain displays and listing of multivariate data such as aerosol size spectra and atmospheric sounding profiles. The program is interactive and asks the user what data he wants and what specific date and time he would like plotted or listed. This program has access to all of the Data Storage files as well as to "EXTRA" type files which can be constructed by means of the LOOK9.BAS routine.

Table D-4 is a catalogue of the various types of data that are in the archive. The physical quantity is underlined in the left hand column and listed directly below are the various measurements of the physical quantities. Each is identified in some way by the initials of the performing organization. Details on the specifics of these measurements, i.e., the location of the sensors, type of instrument, is discussed in Section B-11 of this report. In the right hand column are the data storage files names and in parenthesis are the specific data columns in which the data is kept. Program FIND.BAS requires just the name of the file as it will work on all of the data at a particular time in a particular file whereas program LOOK9.BAS requires both a file name and the data column number.

DATA ARCHIVES SYSTEM

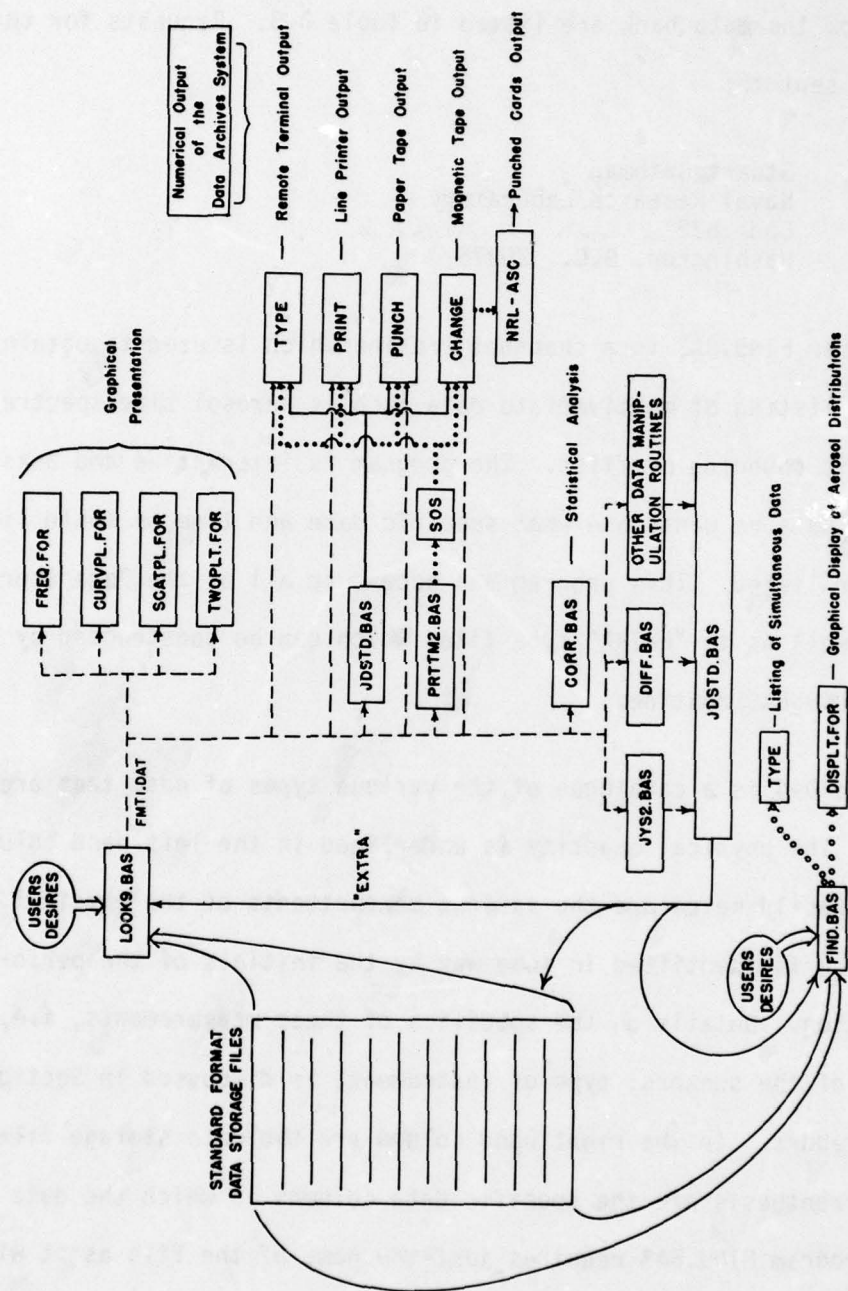


Fig. (D-1) Data archives system.

TABLE D-3

Methods of Obtaining Numerical Data From the Archive

- 1) Files may be typed by a teletype or other type of hard copy device.
- 2) Files may be printed on the system line printer and mailed to user.
- 3) Graphical reproductions are available in Polaroid reproduction of plot-10 programs. This includes a time plot of any variable in the archive or a scatter plot of any two variables in the archive.
- 4) Facilities are also available to obtain hard copies of all graphics utilizing the Tektronix 4631 hard copy unit.
- 5) Mag tapes may be made with a variety of modes using the program CHANGE on the DEC-10. These will be 9 track 800 bpi tapes in the following modes:
 - ASCII
 - G. E. ASCII
 - H. P. ASCII
 - HONBCD
 - BOD
 - BOL
 - G. E. BOD
 - FIXSIX
 - EBCDIC
 - SIXBIT
- 6) ASCII paper tapes can be punched on the system paper tape punch.
- 7) Punched card decks can be made on the NRL Advanced Scientific Computer.

TABLE D-4
DATA ARCHIVE

	<u>File Name</u>
<u>Sea Surface Temperature</u>	
1) NRL Keel Level Probe	THERM.DAT(2)
2) Calspan Fish	CALTMP.DAT(5)
3) NPS Fish	NAVPGS.DAT(2)
4) NRL PRT-5(IR)	FILE.DAT(4)
5) NRL PRT-10(IR)	PRT10.DAT(2)
6) Average SST	AVE.DAT(2)
<u>Air Temperature</u>	
1) NPS Bow	NAVPGS.DAT(3)
2) Calspan Bow - 9 m	CALTMP.DAT(4)
3) NRL 8330 Rear Deck	THERM.DAT(5)
4) NRL 8327 Tower	THERM.DAT(3)
5) Calspan Tower - 15 m	CALTMP.DAT(3)
6) NRL 8323 Tower	FILE.DAT(2)
7) NPS Mast	NAVPGS.DAT(4)
8) Calspan Mast - 27 m	CALTMP.DAT(2)
9) NRL Kytoon System Profiles	DATA.DAT(2,3,4,5)
10) Average Air Temp.	AVE.DAT(3)
<u>Temperature Fluctuations</u>	
1) NPS C^2_{T1} Bow	NAVPGS.DAT(7)
2) NPS C^2_{T2} Mast	NAVPGS.DAT(8)
3) NPS ϵ Bow	NAVPGS.DAT(9)
4) NPS ϵ Mast	NAVPGS.DAT(10)
<u>Humidity</u>	
1) NPS Bow	NAVPGS.DAT(5)
2) NRL 8330 Rear Deck	THERM.DAT(4,5)
3) NRL 8323 Tower (Dewpoint)	FILE.DAT(3)
4) Calspan Tower - 15 m	CALTMP.DAT(7)
5) Calspan Sling, Tower	CALVIS.DAT(6,7)
6) NPS Mast	NAVPGS.DAT(6)
7) Calspan Mast - 27 m	CALTMP.DAT(6)
8) Kytoon System Profiles	DATA2.DAT(2,3,4,5)
9) Best Relative Humidity (%)	AVE.DAT(4)

File Name

Relative Wind Speed

1) Calspan Mast	CALVIS.DAT(3)
2) NRL Mast	ASC.DAT(2)

Relative Wind Direction

1) Calspan Mast	CALVIS.DAT(2)
2) NRL Mast	ASC.DAT(3)

Real Wind Speed and
Direction Calculations

1) Speed	WDREAL.DAT(3)
2) Direction	WDREAL.DAT(2)

Ship Speed and Heading

1) Heading, magnetic, Calspan	CALTMP.DAT(8)
2) Course Made Good	NAV.DAT(6)
3) Ship Speed	NAV.DAT(7)

* * * * * AEROSOLS * * * * *

Calspan Royco

a) Royco > .3/2.8 liter	OUT.AER(3)
b) Royco > .6/2.8 liter	OUT.AER(4)
c) Royco > 1.2/2.8 liter	OUT.AER(5)
d) Royco > 3.0/2.8 liter	OUT.AER(6)
e) Royco > 5.0/2.8 liter	OUT.AER(7)

NRL Royco #/cc

a) $0.45 \mu\text{m} < d < 0.60 \mu\text{m}$	ROY.DAT(2)
b) $0.60 \mu\text{m} < d < 1.50 \mu\text{m}$	ROY.DAT(3)
c) $1.50 \mu\text{m} < d < 2.5 \mu\text{m}$	ROY.DAT(4)
d) $2.50 \mu\text{m} < d < 4.0 \mu\text{m}$	ROY.DAT(5)
e) $d \geq 4.0 \mu\text{m}$	ROY.DAT(6)

File Name

Thermo Systems - E.A.A.

a)	$\log_{10} N (r > .0032 \mu)$	WHIT2.DAT(2)
b)	$\log_{10} N (r > .0056 \mu)$	WHIT2.DAT(3)
c)	$\log_{10} N (r > .01 \mu)$	WHIT2.DAT(4)
d)	$\log_{10} N (r > .0178 \mu)$	WHIT2.DAT(5)
e)	$\log_{10} N (r > .0316 \mu)$	WHIT2.DAT(6)
f)	$\log_{10} N (r > .0562 \mu)$	WHIT2.DAT(7)
g)	$\log_{10} N (r > .1 \mu)$	WHIT2.DAT(8)
h)	$\log_{10} N (r > .178 \mu)$	WHIT2.DAT(9)
i)	$\log_{10} N (r > .360 \mu)$	WHIT2.DAT(10)
j)	$\log_{10} N (r > .560 \mu)$	WHIT2.DAT(11)

Visibility

1)	MRI Nephelometer (NRL)	ASC.DAT(5)
2)	MRI Nephelometer (Calspan)	CALVIS.DAT(5)
3)	EG&G Foward Scattering (Calspan)	CALVIS.DAT(4)
4)	MRI Fog Visibility (NRL 8323)	ASC.DAT(6)
5)	Observer Estimates	CLOUD.DAT(4)

Inversion Height

1)	SRI Lidar	SRI.DAT(2)
----	-----------	------------

Radon

1)	A.R.C. (NRL 8326)	RADON2.DAT(2)
----	-------------------	---------------

CN

1)	Calspan - Gardner Counter, Aiken Nuclei	OUT.AER(2)
2)	NRL Hoppel - Pollak Counter	CN.DAT(2)
3)	E 1 Data NRL Hoppel $\log_{10}(\#/cc)$	ASC.DAT(7)

CCN (NRL Code 8326)

1)	$\#/cc$ at 2°C	CCN.DAT(2)
2)	$\#/cc$ at 3°C	CCN.DAT(3)
3)	$\#/cc$ at 4.3°C	CCN.DAT(4)
4)	$\#/cc$ at 5°C	CCN.DAT(5)
5)	$\#/cc$ % Involatile at 4.3°C	CCN.DAT(6)

Scattering Coefficient

1)	MRI Nephelometer Calspan	OUT.AER(8)
2)	MRI Nephelometer NRL	ASC.DAT(4)

File Name

Meteorological Observations

1) Sea State	CLOUD.DAT(2)
2) % White Caps	CLOUD.DAT(3)
3) % Cloud Cover	CLOUD.DAT(5)
4) Cloud Type - Low Cloud	CLOUD.DAT(6)
Middle Cloud	CLOUD.DAT(7)
High Cloud	CLOUD.DAT(8)
5) PRT-10	
i) Sea Surface Temp.	PRT10.DAT(2)
ii) Sky Temp.	PRT10.DAT(3)
iii) -10 deg.	PRT10.DAT(4)
iv) +10 deg.	PRT10.DAT(5)
v) +30 deg.	PRT10.DAT(6)
vi) +60 deg.	PRT10.DAT(7)
vii) Cloud Base	PRT10.DAT(8)

Stability

1) U _s NPS	NAVPGS.DAT(11)
2) R _j NPS	NAVPGS.DAT(12)
3) NRL Lapse Rate Kytoon System	TKITE.DAT(3)

Volz. Sun Photometer Readings

1) Air Mass	VOLTZ.DAT(2)
2) 0.88 μ VSP Reading	VOLTZ.DAT(3)
3) 0.50 μ VSP Reading	VOLTZ.DAT(4)
4) 0.94 μ VSP Reading	VOLTZ.DAT(5)
5) Turbidity (0.88 μ)	TURBID.DAT(2)
6) Turbidity (0.50 μ)	TURBID.DAT(3)
7) Turbidity (0.94 μ)	TURBID.DAT(4)

<u>8323 Tower Positions (Up or Down)</u>	UPDOWN.DAT(2)
--	---------------

Ship Position

1) Latitude (deg)	NAV.DAT(2)
2) Latitude [min. (decimal)]	NAV.DAT(3)
3) Longitude (deg)	NAV.DAT(4)
4) Longitude [min. (decimal)]	NAV.DAT(5)

E -- PARTICIPANTS OF NRL EOMET 77 CRUISE

Ruhnke, Lothar (Dr.) (SSOB)
Code 8320
Naval Research Laboratory
Washington, D.C. 20375
202-767-2951

Gathman, Stuart (deputy SSOB)
Code 8327
Naval Research Laboratory
Washington, D.C. 20375
202-767-2022

Anderson, R. V.
Code 8325
Naval Research Laboratory
Washington, D.C. 20375
202-767-3350

Bressan, David S.
Code 8330
Naval Research Laboratory
Washington, D.C. 20375
202-767-2667

Caputo, Bernard (Dr.)
Computer Genetics Corp.
4 Lakeside Office Park
Wakefield, Mass 01880
617-246-2838

Clamons, Dean
Code 8003
Naval Research Laboratory
Washington, D.C. 20375
202-767-2384

Cosden, Thomas
Code 5568
Naval Research Laboratory
Washington, D.C. 20375
202-767-3224

Fairall, Christopher (Dr.)
Naval Postgraduate School
Monterey, Calif 93940
408-646-2219

Fitzgerald, James (Dr.)
Code 8326
Naval Research Laboratory
Washington, D.C. 20375
202-767-2362

Fraser, Alistair (Dr.)
Penn State Univ.
507 Deike Blvd
University Park, Penna 16802
814-865-0478

Gerber, Hermann (Dr.)
Code 8322
Naval Research Laboratory
Washington, D.C. 20375
202-767-2780

Hayes, John N. (Dr.)
Code 8326
Naval Research Laboratory
Washington, D.C. 20375
202-767-3589

Hoppel, William A. (Dr.)
Code 8326
Naval Research Laboratory
Washington, D.C. 20375
202-767-2362

Jeck, Richard K. (Dr.)
Code 8323
Naval Research Laboratory
Washington, D.C. 20375
202-767-2437

Julian, Ben G.
Code 8327
Naval Research Laboratory
Washington, D.C. 20375
202-767-2022

Katz, Ulrich (Dr.)
Calspan Corp.
P. O. Box 235
Buffalo, N. Y. 14221

Kidwell, Raymond
Code 8323
Naval Research Laboratory
Washington, D.C. 20375
202-767-2437

Larson, Reginald E.
Code 8326
Naval Research Laboratory
Washington, D.C. 20375
202-767-3589

Leonard, Donald (Dr.)
Computer Genetics Corp.
4 Lakeside Office Park
Wakefield, Mass 01880
617-246-2838

Mack, Eugene
Calspan Corp
Environmental Sup. Dept
P. O. Box 235 (or)
4455 Genessee Street
Buffalo, N. Y. 14221
716-632-7500, x643

May, Lenwood
Naval Postgraduate School
Monterey, Calif 93940
408-646-2219

Nielson, Norman
Atmospheric Sciences Laboratory
Stanford Research Institute
Menlo Park, Calif 94025
415-326-6200 x2838

Rosenwasser, Bruce
Code 8320
Naval Research Laboratory
Washington, D.C. 20375
202-767-2022

Schefer, Murray
NavAir-Code 370

Spalding, Glenn
NavMat

Stilling, Robert
Code 8322
Naval Research Laboratory
Washington, D.C. 20375
202-767-3317

Trusty, Gary (Dr.)
Code 5568
Naval Research Laboratory
Washington, D.C. 20375
202-767-3224

Twomey, Sean (Dr.)
Institute of Atmospheric Physics
University of Ariz.
Tucson, Ariz 85721
602-626-1327

Uthe, Edward (Dr.)
Atmospheric Sciences Laboratory
Stanford Research Institute
Menlo Park, Calif 94025
415-326-6200 x 4667

Wojciechowski, T. A.
Code 8326
Naval Research Laboratory
Washington, D.C. 20375
202-767-3589

Zuccaro, Anthony
Code 8004
Naval Research Laboratory
Washington, D.C. 20375
202-767-2731